UNIVERSIDADE DE SÃO PAULO
INSTITUTO DE CIENCIAS BIOMÉDICAS

Jéssica Aparecida da Silva Pereira

RECEPTORES LXR E SEU PAPEL NA MODULAÇÃO DO METABOLISMO E FUNÇÃO DE MACRÓFAGOS RESIDENTES DO TECIDO ADIPOSO: UMA NOVA FERRAMENTA PARA O TRATAMENTO DE DOENÇAS METABÓLICAS

São Paulo, SP
2021

UNIVERSIDADE DE SÃO PAULO
INSTITUTO DE CIENCIAS BIOMÉDICAS

Jéssica Aparecida da Silva Pereira

RECEPTORES LXR E SEU PAPEL NA MODULAÇÃO DO METABOLISMO E FUNÇÃO DE MACRÓFAGOS RESIDENTES DO TECIDO ADIPOSO: UMA NOVA FERRAMENTA PARA O TRATAMENTO DE DOENÇAS METABÓLICAS

Tese apresentada ao Programa de Pós Graduação em Imunologia como parte dos requisitos para obtenção do título de Doutor em Ciências.
Área de concentração: Imunologia
Orientador: Pedro M. M. de Moraes Vieira

São Paulo, SP
2021

Pereira, Jéssica Aparecida da Silva

Receptores LXR e seu papel na modulação do metabolismo e função de macrófagos residentes do tecido adiposo: uma nova ferramenta para o tratamento de doenças metabólicas/ Jéssica Aparecida da Silva Pereira – São Paulo: 2021.

Orientador: Pedro Manoel Mendes de Moraes Vieira

88 p.; il.

Tese (Doutorado) – Universidade de São Paulo. Instituto de Ciências Biomédicas. Departamento de Imunologia. Área de concentração: Imunologia. Linha de pesquisa: Imunometabolismo., 2021.

Versão do título para o inglês: Liver X receptors and its role in macrophage metabolism and function: a new approach to treat metabolic diseases.

Descritores: 1. LXR 2. Resistência à insulina 3. Obesidade 4. Macrófagos I. Moraes-Vieira, Pedro M.M. II. Universidade de São Paulo. Instituto de Ciências Biomédicas. Programa de Pós-Graduação em Imunologia III. Título.

UNIVERSIDADE DE SÃO PAULO

INSTITUTO DE CIENCIAS BIOMÉDICAS

Candidato (a): Jéssica Aparecida da Silva Pereira

Título da tese: Receptores LXR e seu papel na modulação do metabolismo e função de macrófagos residentes do tecido adiposo: uma nova ferramenta para o tratamento de doenças metabólicas

Orientador (a): Pedro Manoel Mendes de Moraes Vieira

A Comissão Julgadora dos trabalhos de Defesa da Tese de Doutorado, em sessão pública realizada a ...../...../....., considerou

( ) Aprovado(a) **( ) Reprovado(a)**

Examinador (a): ……

Instituição: ……

Examinador (a): ……

Instituição: ……

Examinador (a): ……

Instituição: ……

Examinador (a): ……

Instituição: ……

Presidente: ……

Instituição: ……

ICB USP

COMISSÃO DE ÉTICA NO USO DE ANIMAIS
INSTITUTO DE CIÊNCIAS BIOMÉDICAS
UNIVERSIDADE DE SÃO PAULO

Cidade Universitária "Armando de Salles Oliveira", Butantã, São Paulo, SP Av. Professor Lineu Prestes, 2415 - ICB III - 05508 000
CEUA-ICB/USP - Telefone (11) 3091-7733 - e-mail: cep@icb.usp.br

CERTIFICADO

Certificamos que o projeto intitulado "***Efeitos da ativação dos receptores LXRs sobre parâmetros metabólicos sistêmicos e na modulação do metabolismo de macrófagos teciduais residentes do tecido adiposo***", registrado sob o protocolo nº ***51/2017***, que envolve a produção, manutenção e/ou utilização de animais pertencentes ao filo Chordata, subfilo Vertebrata (exceto o homem), para fins de *Pesquisa Científica*, encontra-se de acordo com os preceitos da Lei nº 11.794, de 8 de outubro de 2008, do Decreto nº 6.899, de 15 de julho de 2009, e com as normas editadas pelo Conselho Nacional de Controle e Experimentação Animal (CONCEA). Ante esta conformidade, o referido projeto foi avaliado e aprovado em ***09/05/2017*** pela COMISSÃO DE ÉTICA NO USO DE ANIMAIS do Instituto de Ciências Biomédicas da Universidade de São Paulo (CEUA-ICB/USP), outorgando esta licença de uso de animais com validade de **4 ano(s)** a partir da data de aprovação.

- Investigador Principal: **Dr.(a.) *Pedro Manoel Mendes de Moraes Vieira***
- Departamento: *Imunologia*
- Membros da Equipe: *Jéssica Aparecida da Silva Pereira (Pós-graduando)*

Ao final do período outorgado por esta licença, o pesquisador responsável deverá encaminhar a esta comissão, até o último dia de validade da atual proposta, *relatório final* de acordo com a Resolução Normativa CONCEA nº 30/2016 - Diretriz Brasileira para o Cuidado e a Utilização de Animais em Atividades de Ensino ou de Pesquisa Científica (DBCA), conforme modelo constante no endereço eletrônico www.icb.usp.br/ceua. Havendo interesse na renovação do projeto, a solicitação deverá ser protocolada pela Secretaria da CEUA-ICB/USP até o último dia de validade da atual proposta. Após esta data uma nova proposta deverá ser encaminhada.

CERTIFICATE

We hereby certify that the project entitled "***Effects of LXRs receptor activation on systemic metabolic parameters and on the metabolic modulation of resident tissue macrophages of adipose tissue***", protocol nº ***51/2017***, which involves the production, maintenance and/or use of animals belonging to the phylum Chordata, subphylum Vertebrata (except human), for *Scientific Research Purposes*, is in accordance with the provisions of the Law nº 11.794 passed on October 8th, 2008, Decree nº 6899 passed on July 15th, 2009, and the rules issued by the National Council for Control and Animal Experimentation (CONCEA). According to this legislation, the project was evaluated and approved on ***5/9/2017*** by the ETHICS COMMITTEE ON ANIMAL USE, Institute of Biomedical Sciences, University of Sao Paulo (CEUA-ICB/USP), and the license for animal use is valid for **4 year(s)** from the date of approval.

- Principal Investigator: **Dr.(a.) *Pedro Manoel Mendes de Moraes Vieira***
- Team members: *Jéssica Aparecida da Silva Pereira (Graduate Student).*

At the end of the period granted by this license, the Principal Investigator must submit a final report of the project to this committee, according to the Rule nº 30 and the Diretriz Brasileira para o Cuidado e a Utilização de Animais em Atividades de Ensino ou de Pesquisa Científica (DBCA) issued by the CONCEA. If a renewal of the project is intended, the request must be submitted to the CEUA-ICB/USP secretary before the expiration of the current proposal. After this date, a new proposal must be prepared.

Espécie/Species	Linhagem/Strain	Sexo/Gender	Idade-Peso/ Age-Weight	Total
Mus musculus	*C57BL/6*	*Macho/male*	*18-20 g*	*318*
	C57BL/6 LXRαKO	*Macho/male*	*18-20 g*	*78*
	C57BL/6 LXRβKO	*Macho/male*	*18-20 g*	*78*

São Paulo, 11 de maio de 2017.

Prof. Dr. **Anderson de Sá Nunes**
Coordenador CEUA-ICB/USP

Eliane Aparecida Gomes de M. Nascimento
Secretário CEUA-ICB/USP

UNICAMP

CEUA/UNICAMP

CERTIFICADO

Certificamos que a proposta intitulada **Efeitos da ativação dos receptores LXRs sobre parâmetros metabólicos sistêmicos e na modulação do metabolismo de macrófagos teciduais residentes do tecido adiposo**, registrada com o nº **4562-1/2017**, sob a responsabilidade de **Prof. Dr. Pedro Vieira e Jéssica Aparecida da Silva Pereira**, que envolve a produção, manutenção ou utilização de animais pertencentes ao filo *Chordata*, subfilo *Vertebrata* (exceto o homem) para fins de pesquisa científica (ou ensino), encontra-se de acordo com os preceitos da **LEI Nº 11.794, DE 8 DE OUTUBRO DE 2008**, que estabelece procedimentos para o uso científico de animais, do **DECRETO Nº 6.899, DE 15 DE JULHO DE 2009**, e com as normas editadas pelo **Conselho Nacional de Controle da Experimentação Animal (CONCEA)**, **tendo sido** aprovada pela **Comissão de Ética no Uso de Animais** da **Universidade Estadual de Campinas - CEUA/UNICAMP**, em **22 de maio de 2017**.

Finalidade:	**( ) Ensino (X) Pesquisa Científica**
Vigência do projeto:	**15/05/2017-15/05/2021**
Vigência da autorização para manipulação animal:	**15/05/2017-15/05/2021**
Espécie / linhagem/ raça:	**Camundongo isogênico / C57BL/6J**
No. de animais:	**286**
Peso / Idade:	**05 semanas / 20g**
Sexo:	**246 machos / 40 fêmeas**
Origem:	**CEMIB/UNICAMP**
Espécie / linhagem/ raça:	**Camundongo Knockout / B6.129S6-Nr1h3 (LXRa KO)**
No. de animais:	**66**
Peso / Idade:	**05 semanas / 20g**
Sexo:	**machos**
Espécie / linhagem/ raça:	**Camundongo Knockout / B6.129S6-Nr1h2 (LXRb KO)**
No. de animais:	**66**
Peso / Idade:	**05 semanas / 20g**
Sexo:	**machos**
Espécie / linhagem/ raça:	**Camundongo transgênico / B6.129P2-Lyztm1(cre)Ifo/J**
No. de animais:	**04**
Peso / Idade:	**05 semanas / 20g**
Sexo:	**02 machos / 02 fêmeas**
Espécie / linhagem/ raça:	**Camundongo transgênico / B6.129S4(C) - VHLtm1jae/J**
No. de animais:	**04**
Peso / Idade:	**05 semanas / 20g**
Sexo:	**02 machos / 02 fêmeas**
Origem:	**The Jackson Laboratory**

A aprovação pela CEUA/UNICAMP não dispensa autorização prévia junto ao **IBAMA**, **SISBIO** ou **CIBio** e é **restrita** a protocolos desenvolvidos em biotérios e laboratórios da Universidade Estadual de Campinas.

Campinas, 11 de maio de 2017.

Profa. Dra. Liana Maria Cardoso Verinaud
Presidente

Fátima Alonso
Secretária Executiva

IMPORTANTE: Pedimos atenção ao prazo para envio do relatório final de atividades referente a este protocolo: até 30 dias após o encerramento de sua vigência. O formulário encontra-se disponível na página da CEUA/UNICAMP, área do pesquisador responsável. A não apresentação de relatório no prazo estabelecido impedirá que novos protocolos sejam submetidos.

CEUA/UNICAMP

UNICAMP

CERTIFICADO

Certificamos que a proposta intitulada **Efeitos da ativação dos receptores LXRs sobre parâmetros metabólicos sistêmicos e na modulação do metabolismo de macrófagos teciduais residentes do tecido adiposo**, registrada com o nº **4562-1(A)/2018**, sob a responsabilidade de **Prof. Dr. Pedro Vieira e Jéssica Aparecida da Silva Pereira**, que envolve a produção, manutenção ou utilização de animais pertencentes ao filo *Chordata*, subfilo *Vertebrata* (exceto o homem) para fins de pesquisa científica (ou ensino), encontra-se de acordo com os preceitos da **LEI Nº 11.794, DE 8 DE OUTUBRO DE 2008**, que estabelece procedimentos para o uso científico de animais, do **DECRETO Nº 6.899, DE 15 DE JULHO DE 2009**, e com as normas editadas pelo **Conselho Nacional de Controle da Experimentação Animal (CONCEA), tendo sido** aprovada pela **Comissão de Ética no Uso de Animais** da **Universidade Estadual de Campinas - CEUA/UNICAMP**, em reunião de **14/12/2018**.

Finalidade:	**( ) Ensino (X) Pesquisa Científica**
Vigência do projeto:	15/05/2017 a 15/05/2021
Vigência da autorização para manipulação animal:	14/12/2018 a 15/05/2021
Espécie / linhagem/ raça:	Camundongo isogênico / C57BL/6J
No. de animais:	30
Idade/Peso:	5.00 Semanas / 20.00 Gramas
Sexo:	30 Machos
Espécie / linhagem/ raça:	Camundongo Knockout / LXR duplo knock out
No. de animais:	30
Idade/Peso:	5.00 Semanas / 20.00 Gramas
Sexo:	30 Machos
Espécie / linhagem/ raça:	Camundongo isogênico / C57BL/6J
No. de animais:	30
Idade/Peso:	5.00 Semanas / 20.00 Gramas
Sexo:	30 Machos
Espécie / linhagem/ raça:	Camundongo Knockout / LXR duplo knock out
No. de animais:	30
Idade/Peso:	5.00 Semanas / 20.00 Gramas
Sexo:	30 Machos
Espécie / linhagem/ raça:	Camundongo Knockout / LXR duplo knock out
No. de animais:	30
Idade/Peso:	5.00 Semanas / 20.00 Gramas
Sexo:	30 Machos
Espécie / linhagem/ raça:	Camundongo Knockout / LXR duplo knock out
No. de animais:	30
Idade/Peso:	5.00 Semanas / 20.00 Gramas
Sexo:	30 Machos
Espécie / linhagem/ raça:	Camundongo isogênico / C57BL/6J
No. de animais:	30
Idade/Peso:	5.00 Semanas / 20.00 Gramas
Sexo:	30 Machos

UNICAMP

CEUA/UNICAMP

CERTIFICADO

Certificamos que a proposta intitulada **Estudo dos efeitos da modulação dos fatores de transcrição LXR sobre o metabolismo sistêmico e inflamação do tecido adiposo em modelo de obesidade**, registrada com o nº **5205-1/2019**, sob a responsabilidade de **Prof. Dr. Pedro Manoel Mendes de Moraes Vieira e Jessica Aparecida da Silva Pereira**, que envolve a produção, manutenção ou utilização de animais pertencentes ao filo *Chordata*, subfilo *Vertebrata* (exceto o homem) para fins de pesquisa científica (ou ensino), encontra-se de acordo com os preceitos da **LEI Nº 11.794, DE 8 DE OUTUBRO DE 2008**, que estabelece procedimentos para o uso científico de animais, do **DECRETO Nº 6.899, DE 15 DE JULHO DE 2009**, e com as normas editadas pelo **Conselho Nacional de Controle da Experimentação Animal (CONCEA), tendo sido** aprovada pela **Comissão de Ética no Uso de Animais** da **Universidade Estadual de Campinas - CEUA/UNICAMP,** em reunião de **11/04/2019**.

Finalidade:	**( ) Ensino (X) Pesquisa Científica**
Vigência do projeto:	01/04/2019 a 01/04/2023
Vigência da autorização para manipulação animal:	11/04/2019 a 01/04/2023
Espécie / linhagem/ raça:	Camundongo isogênico / C57BL/6J
No. de animais:	33
Idade/Peso:	5.00 Semanas / 20.00 Gramas
Sexo:	33 Machos
Espécie / linhagem/ raça:	Camundongo isogênico / C57BL/6J
No. de animais:	33
Idade/Peso:	5.00 Dias / 20.00 Gramas
Sexo:	33 Machos
Espécie / linhagem/ raça:	Camundongo Knockout / LXRduploKO
No. de animais:	33
Idade/Peso:	5.00 Dias / 20.00 Gramas
Sexo:	33 Machos
Espécie / linhagem/ raça:	Camundongo Knockout / LXRduploKO
No. de animais:	33
Idade/Peso:	5.00 Dias / 20.00 Gramas
Sexo:	33 Machos
Origem:	Biotério, CEMIB, The Jackson Laboratory
Biotério onde serão mantidos os animais:	Biotério de Animais SPF, Área de Imunolo[illegible] DGE[illegible] /UNICAMP

A aprovação pela CEUA/UNICAMP não dispensa autorização a junto ao **IBAMA**, **SISBIO** ou **CIBio** e é **restrita** a protocolos desenvolvidos em biotérios e laboratórios da Universidade Estadual de Campinas.

Ao meu companheiro de vida e de bancada, por todo apoio,
amor e compreensão mesmo nos momentos mais difíceis

AGRADECIMENTOS

Ao meu orientador e amigo Dr. Pedro M. M. Moraes Vieira, por ter me recebido em seu laboratório, pela total liberdade e confiança depositada em mim no desenvolvimento desse trabalho que sem sombra de dúvidas me deu a oportunidade de crescer profissionalmente.

Aos queridos João e Juliana, por serem excelentes alunos e grandes amigos. Vocês me incentivaram a sempre querer aprender mais e me mostraram o quão gratificante é ver a evolução profissional dos nossos pupilos. Espero ter atendido as expectativa de vocês.

Aos meus colegas de laboratório pelas discussões científicas e auxílio nos experimentos que contribuíram para o desenvolvimento desse trabalho.

Ao meu marido, companheiro e colaborador Gerson. Sou muito grata por nossa evolução pessoal e profissional e sinto muito orgulho do caminho que trilhamos juntos. Obrigada por ser tão incrível.

Aos amigos Henver e Tati que em tão pouco tempo de convívio se tornaram tão especiais. A conexão que temos é impressionante, eu simplesmente sinto que conheço vocês minha vida toda. Obrigada por serem amigos tão queridos. Vocês são família!

Á minha grande amiga e profissional exemplar Elzira, você teve e tem um papel essencial na nossa jornada. Obrigada por ser essa grande amiga, que se preocupa, acolhe e cuida, mas que também dá broncas e puxões de orelha quando necessário. Amo você!

Aos queridos Felippe, João, Nati, André e André Santiago, com quem pude dividir momentos importantes profissionais e pessoais. Obrigada por todo carinho e apoio.

Às queridas Carol (Gremlin e tantos outros apelidos) e Lari por todas as experiências que compartilhamos durante nosso período em Boston.

Aos amigos Ju e Bozi, pessoas incríveis que me acolheram sempre. Muito obrigada pela amizade e incentivo profissional.

Ao Dr. Francisco Quintana e aos amigos do departamento de neurologia do BWH pelas discussões científicas e por toda ajuda durante o período em que estive em seu laboratório.

Aos amigos e agora padrinhos Fernando e Marisa por todo exemplo de integridade, pelo suporte incondicional e por sempre torcer pelo nosso sucesso

Aos meus familiares que sempre torceram pelo meu sucesso. Em especial aos queridos Joice e Wilian que nos deram amor e o apoio necessário em cada nova etapa dessa jornada. E ao Bailey, que chegou para completar nossa família.

Aos queridos Maria Eni e João, que sempre foram muito solicitos e ao Programa de Pós Graduação em Imunologia. Obrigada por toda ajuda ao longo desses anos.

Ao bioterista Marcos, que me auxiliou muito durante esse período e por seu trabalho essencial que possibilitou a realização de todos os experimentos desse trabalho.

Aos colaboradores que possibilitaram a realização de lindos experimentos que tornaram possível a realização desse trabalho, em especial ao Dr. Niels Olsen pelos reagentes, discussões e cafés, ao Dr. Alexandre Basso pela grande ajuda na aquisição dos animais e transplante de medula óssea e ao Dr. Marcelo Mori pelos reagentes, discussões e por me tornar uma quase integrante de seu laboratório.

Minha gratidão e respeito a todos os animais usados nesse trabalho, sem eles essa tese não existiria.

À Fundação de Amparo à Pesquisa do Estado de São Paulo (FAPESP) que através de seu financiamento (processos 2017/00079-7 e 2019/04780-7) me proporcionou não somente a possibilidade de me dedicar a este trabalho, como também possibilitou a participação em diversos eventos e o network necessário para meu amadurecimento científico.

Às agências de fomento CAPES, CNPq e FUNCAMP pelo financiamento deste trabalho.

À todos que de algum modo participaram da realização deste trabalho, muito obrigada.

"Devo ater-me a meu próprio estilo e seguir meu próprio caminho. E apesar de eu poder nunca mais ter sucesso deste modo, estou convencida de que falharia totalmente de qualquer outro"
Jane Austen

RESUMO

PEREIRA, JAS. **Receptores LXR e seu papel na modulação do metabolismo e função de macrófagos residentes do tecido adiposo: uma nova ferramenta para o tratamento de doenças metabólicas**. 2021. 88 f. Tese (Doutorado em Imunologia). São Paulo: Instituto de Ciências Biomédicas, Universidade de São Paulo, São Paulo, 2020.

Receptores hepáticos X (LXRs) são fatores de transcrição ativados por moléculas derivadas do metabolismo de colesterol. Os níveis de colesterol são frequentemente aumentados em indivíduos obesos e contribuem para a ativação de diversas vias inflamatórias. Obesidade é caracterizada pelo acúmulo de lipídeos nos adipócitos, favorecendo a expansão do tecido adiposo (AT) branco e o desenvolvimento de inflamação crônica sistêmica de baixo grau, a qual contribui para o desenvolvimento de outras doenças metabólicas, como a resistencia à insulina. LXRs são envolvidos na manutenção da homeostase de colesterol, além disso, LXRs atuam na regulação das respostas imunes. No entanto, o papel de LXRs na patologia da obesidade e sua contribuição para o fenótipo de macrófagos residentes do tecido adiposo (ATM) permanece desconhecido. Nós mostramos que a deleção de LXR prejudica o ganho de peso e acúmulo de gordura em camundongos. Animais LXRαβKO apresentam elevada sensibilidade à insulina e o uso preferencial de carboidratos como fonte de energia. Animais LXRαKO, apresentam maior sensibilidade à insulina, o que não foi observado em animais LXRβKO. ATMs de animais obesos apresentam um enriquecimento da via de colesterol, e a deleção de LXR potencializa o acúmulo de lipídeos em macrófagos, bem como agrava a inflamação do AT por promover o aumento da expressão de IL-1β e TNF-α nos ATMs em resposta a alimentação com dieta hiperlipídica, o que ocorreu de maneira dependente de LXRβ. Na ausência de estresse metabólico, a deleção de uma única isoforma de LXR foi capaz de induzir inflamação no AT, marcada pelo aumento de macrófagos $CD11c^{+}$. Além disso, a deleção de LXR especificamente em células imunes contribuiu para o rompimento balanço imune no AT, o qual foi marcado pelo aumento de macrófagos $CD11c^{+}$, pela maior expressão de IL-1β, bem como pelo maior infiltrado de monócitos. Em adição, a deleção de LXR em células imunes agravou a inflamação do AT induzida por dieta hiperlipídica, sem, no entanto, promover alterações na homeostase de glicose. Nós encontramos que o composto naringenin (NAR) atua como um agonista de LXR em macrófagos. NAR induziu a expressão de genes alvo de LXR e reduziu a secreção de citocinas pró-inflamatórias em macrófagos ativados com LPS ou polarizados para o perfil pró-inflamatório. O tratamento de animais obesos com NAR reduziu a inflamação do AT, marcada pelo menor acúmulo de macrófagos $CD11c^{+}$, menor infiltrado de monócitos e reduzida expressão de IL-1β+ e TNF-α+ nos ATMs. Tal efeito favoreceu o aumento da sensibilidade à insulina nos animais tratados com NAR, o que não foi visto em animais tratados com veículo. Nós exploramos como a ativação de LXR com NAR poderia afetar o metabolismo de macrófagos, sendo observada redução da via glicolítica e menor disfunção mitocondrial em células estimuladas, tratadas com NAR. Adicionalmente, nós observamos que os efeitos anti-inflamatórios induzidos por NAR ocorrem de maneira dependente de LXRβ. Juntos, nossos dados revelaram um papel diferenciado para as isoformas de LXR no que compete à regulação do metabolismo sistêmico e imunidade. A expressão de LXRβ em células imunes é essencial para o balanço pro/anti-inflamatório no AT. LXRβ é um potencial alvo terapêutico para o tratamento de inflamação do AT e resistência à insulina.

SUMMARY

PEREIRA, JAS. **Liver X receptors and its role in macrophage metabolism and function: a new approach to treat metabolic diseases.** 2021. 88 f. Thesis (PhD in Immunology). São Paulo: Instituto de Ciências Biomédicas, Universidade de São Paulo, São Paulo, 2020.

Liver X receptors (LXRs) are nuclear receptors activated by molecules derived from cholesterol metabolism. Cholesterol levels are commonly increased in obesity and contribute for the activation of pro-inflammatory responses. Obesity is characterized by increased lipid accumulation in white adipocytes and systemic chronic low-grade inflammation. LXRs are involved in the maintenance of cholesterol homeostasis, and also have a role in the regulation of immune response. The role of LXRs in obesity and how these receptors contribute to adipose tissue macrophage (ATM) phenotype and metabolic programming remains to be elucidated. Here, we show that LXR deletion impairs body weight gain and fat accumulation in mice. LXRαβKO mice has increased insulin sensitivity and a preferential usage of carbohydrates as fuel to energy production. LXRα-depleted but not LXRβ-depleted animals display increased insulin sensitivity with no changes in the energy fuel usage preference compared to WT mice. ATMs from obese animals have enriched cholesterol pathway, and LXR deletion boost the lipid accumulation in macrophages, while increase the adipose tissue inflammation by inducing IL-1β and TNF-α in ATMs in a LXRβ-dependent manner. In the absence of metabolic stress, the lack of any LXR isoform leads to adipose tissue inflammation with increased $CD11c^+$ ATMs. Also the LXR deletion specifically in immune cells contribute for the disruption of adipose tissue immune balance, marked by the increase in $CD11c^+$ and $IL\text{-}1\beta^+$ ATMs as enhanced monocyte infiltration on AT. Moreover, the deletion of LXR in immune cells aggravates obesity-induced adipose tissue inflammation without promote changes in glucose homeostasis. We found that naringenin (NAR) is an LXR agonist in macrophages. NAR induces LXR-target genes expression and reduces the secretion of pro-inflammatory cytokines in LPS-activated and LPS+IFNγ-activated macrophages by reducing glycolysis and mitochondrial dysfunction. In addition, obese mice treated with NAR display increased insulin sensitivity and reduced AT inflammation, as observed by the reduction on $CD11c^+$, $IL\text{-}1\beta^+$ and $TNF\text{-}\alpha^+$ ATMs and reduced monocyte infiltration compared to obese control group. Together our results show that each LXR isoform displays a distinct role in the regulation of systemic glucose homeostasis and adipose tissue inflammation. LXRβ expression in immune cells is essential for the pro/anti-inflammatory balance of the adipose tissue. LXRβ has the potential to become a novel therapeutic target to treat adipose tissue inflammation and insulin resistance.

LISTA DE ABREVIATURAS

ABCA1 - *ATP-binding cassete sub-family A member 1*

ABCG1 - *ATP-binding cassete sub-family G member 1*

AF-1 - Domínio função de ativação-1

AP1 - Proteína ativador 1, do inglês *activator protein 1*

APOE - Apolipoproteína e

ARG-1 - Arginase-1

AT - Tecido adiposo

ATMs - Macrófagos residentes do tecido adiposo, do inglês *adipose tissue macrophages*

BAT - Tecido adiposo marrom, do inglês *brown adipose tissue*

BMCs - Células da medula óssea, do inglês *bone marrow cells*

BMDMs - Macrófagos derivados da medula óssea, do inglês *bone marrow-derived macrophages*

BMT - Transplante de células da medula óssea, do inglês *bone marrow transplant*

CCL-2/MCP1 - *Chemokine ligand 2/Monocyte chemoattractant protein-1*

DBD - domínio de ligação ao DNA, do inglês *DNA-binding domain*

DNA - Ácido deoxiribonucleico, do inglês *deoxyribonucleic acid*

DRs - Sequências de repetições diretas

DR-4 - Bases espaçadoras

ECAR - Taxa de acidificação do meio extracelular, do inglês extracellular acidification rate

ELISA - do inglês *Enzyme Linked ImmunonoSorbent Assay*

FASN - Ácido graxo sintase, do inglês *fatty acid synthase*

FIZZ1 - *Resistin-like molecule alpha 1*

FXRs - Receptor ácidos biliares, do inglês *farnesoid X receptor*

GLUT4 - Transportador de glicose tipo 4, do inglês *glucose transporter type 4*

GTT - Teste de tolerância à glicose, do inglês *glucose tolerance test*

HFD - Dieta hiperlipídica, do inglês *high fat diet*

IFN-γ - Interferon gama

IL-1β - Interleucina 1 beta

IL-12 - Interleucina 12

IL-4 - Interleucina 4

IL-13 - Interleucina 4

IL-10 - Interleucina 10

IL-6 - Interleucina 6

iNOS/NOS2 - Óxido nítrico sintase indutível, do inglês *inducible nitric oxide synthase*

IRF - Fator regulatório de interferon 1, do inglês *interferon regulatory factor 1*

IRS-1 - Substrato do receptor de insulina, do inglês *insulin receptor substrate-1*

ITT - Teste de tolerância à insulina, do inglês *insulin tolerance test*

LBD - Domínio de associação ao ligante, do inglês *ligand-binding domain*

LDHA - Lactato desidrogenase isoforma a

LPL - Lipoproteína lipase

LPS - Lipopolissacarídeo

LXR - Receptores hepáticos X, do ingles *liver X receptors*

LXRα - Receptor hepático X isoforma alfa, do inglês *liver X receptor α*

LXRβ - Receptor hepático X isoforma beta, do inglês *liver X receptor β*

LXRαKO - Camundongos deficientes de LXRα

LXRβKO - Camundongos deficientes de LXRβ

LXREs - Elementos de resposta ao LXR

M1 - Macrófagos classicamente ativados

M2 - Macrófagos alternativamente ativados

NAR - Naringenin

NCoR - Co-repressor de receptores nucleares, do ingles *NR co-repressor*

NFκB - Fator nuclear kappa B, do inglês *nuclear factor kappa B*

NRs - Receptores nucleares, do inglês *nuclear receptors*

Nr1h3 - gene codificador de LXRα, do inglês *nuclear receptor subfamily 1 group H member 3*

Nr1h2 - gene codificador de LXRβ, do inglês *nuclear receptor subfamily 1 group H member 2*

ORO - *Oil Red O*

OXPHOS - Fosforilação oxidativa, do inglês *oxidative phosphorylation*

PFKFB3 - 6-fosfofruto-2-quinase/frutose-2,6-bifosfatase

PgAT - Tecido adiposo perigonadal

PPAR-γ - Receptor ativado por proliferares de pejoxissoma gama, do inglês *peroxisome proliferator-activated receptor gamma*

REs - Elementos de resposta

RNA - Ácido ribonucleico, do inglês *ribonucleic acid*

RT-qPCR - Reação em cadeia da polimerase quantitativa em tempo real, do inglês *real time quantitative polimerase chain reaction*

RXR - Receptores de retinóide X, do inglês *retinoid X receptor*

SMRT - Mediador de silenciamento dos receptores retinóicos e de hormônio tireoidiano, do inglês *silencing mediator of retinoic acid and thyroid hormone receptors*

STAT6 - Trasdutor de sinal e ativador de transcrição 6, do inglês *signal transducer and activator of transcription 6*

SVF - Fração vascular estromal, do inglês *stromal vascular fraction*

TCA - Ciclo do ácido cítrico, do inglês *tricarboxylic acid cycle*

TGF-β - Fator de crescimento transformador beta, do inglês *transforming groth fator β*

TLR4 - Receptor do tipo toll 4, do inglês *toll like receptor 4*

TNF-α - Fator de necrose tumoral alfa

VCO2 - Volume de gás carbônico

VO2 - Volume de oxigênio

WAT - Tecido adiposo branco, do inglês *white adipose tissue*

WT - Camundongos selvagens, do inglês *wild type*

YM1 - Chitinase-like protein 3

LISTA DE FIGURAS

LISTA DE TABELAS

SUMÁRIO

1. INTRODUÇÃO

Obesidade é uma doença de etiologia complexa, marcada por um desequilíbrio energético causado pelo excessivo consumo alimentar associado a um gasto energético insuficiente (1, 2). Estima-se que cerca de 650 milhões indivíduos no mundo todo são obesos (3), o que faz com que a obesidade seja considerada uma das principais epidemias do século XXI (3, 4).

O tecido adiposo (AT) é um órgão amplamente distribuído pelo corpo humano (5), que apresenta um importante papel não somente de armazenamento, mas também na regulação de diversos processos metabólicos (6, 7). De maneira simplificada o tecido adiposo pode dividido em tecido adiposo marrom (BAT, do inglês *brown adipose tissue*) e tecido adiposo branco (WAT, do inglês *white adipose tissue*) (8).

O WAT é constituído por diversos tipos celulares, sendo os adipócitos a população majoritária, responsável por armazenar energia na forma de triacilgliceróis, proporcionar a disponibilidade de substratos energéticos, bem como pela secreção de adipocinas que contribuem de modo importante para a maturação de adipócitos, comunicação do status nutricional e na regulação do metabolismo de diversos outros tipos celulares (9-12). Além dos adipócitos maduros, o WAT é constituído por células da fração vascular estromal (SVF), a qual contém uma população celular heterogênea constituída por pré-adipócitos, fibroblastos e células imunes como macrófagos, eosinófilos e linfócitos T, dentre outros tipos celulares que desempenham um papel fundamental na regulação da homeostase tecidual (13, 14).

Alterações na demanda nutricional, como na obesidade, favorecem a expansão do WAT por promover o acúmulo excessivo de lipídeos (15), levando ao surgimento de uma inflamação crônica de baixo grau, caracterizada por alterações na população de macrófagos residentes do tecido adiposo (ATMs, do inglês *adipose tissue macrophages*) (4, 8, 16), bem como a um desequilíbrio imune caracterizado pela redução de citocinas anti-inflamatórias e pelo aumento na secreção de citocinas pró-inflamatórias como o fator de necrose tumoral alfa (TNF-α) (17) e a interleucina 1 beta (IL-1β), os quais tem sido fortemente associados ao desenvolvimento de resistência à insulina devido a sua capacidade em promover a redução da autofosforilação do receptor de insulina e subsequente redução da expressão e fosforilação do substrato do receptor de insulina (IRS-1, do inglês *insulin receptor substrate-1*) (18, 19).

Além disso, uma elevada concentração de ácidos graxos livres e colesterol é observada em indivíduos obesos, os quais podem promover alterações na expressão e ativação de diversos receptores nucleares que atuam como sensores de alterações metabólicas e controlam a programação transcricional, participando assim, na regulação do metabolismo e função celular (20).

1.1. Receptores Nucleares

Receptores nucleares (NRs, do inglês *nuclear receptors*) correspondem a um dos maiores grupos de fatores de transcrição que desempenham papel fundamental na regulação de diversos processos fisiológicos, tais como desenvolvimento, reprodução, metabolismo e imunidade (21-23), e em muitos processos patológicos como câncer, diabetes e desordens metabólicas (24).

Os NRs são proteínas que regulam a expressão gênica através de sua associação a porções específicas do DNA, denominados elementos de resposta (REs), em decorrência de sua ativação mediada por ligantes (25). Ligantes de NRs geralmente correspondem à pequenas moléculas lipofílicas que transpõem facilmente as membranas biológicas, podendo variar entre hormônios e metabólitos tais como ácidos biliares, ácidos graxos e oxisteróis, dentre outras moléculas (26, 27).

A associação de ligantes à NRs leva a numerosas modificações, destacando-se as alterações estruturais no receptor, que possibilitam sua ligação ao DNA e moléculas co-regulatórias essenciais para a regulação da programação transcricional (28). É importante destacar que embora a função melhor documentada dos NRs esteja associada a sua capacidade em regular a transcrição gênica, diversos trabalhos tem reportado que alguns NRs podem modular o funcionamento celular ainda no citoplasma (25).

De maneira geral, os NRs podem ser divididos em três principais grupos baseando-se em sua associação a ligantes (22). O primeiro grupo é constituído por NRs de esteroides, os quais são ativados mediante associação com hormônios esteróides, hormônios da tireóide e a algumas formas ativas de vitamina A e D (29, 30). O segundo grupo consiste em NRs órfãos, os quais não apresentam ligantes endógenos conhecidos (24, 31), e por fim, o terceiro grupo é constituído por NRs adotados, que correspondem a receptores previamente descritos e caracterizados como NRs órfãos e que, posteriormente, tiveram seu ligante endógeno

identificado (28). Dentre os receptores pertencentes ao grupo de NRs adotados destacam-se os PPARs, FXRs e LXRs (23, 32).

1.1.1. Características estruturais dos receptores nucleares

Assim como a maior parte dos NRs, os receptores hepáticos X (LXR, do ingles *liver X receptors*) apresentam domínios estruturais bem estabelecidos (28). De maneira simplificada, sua estrutura é composta por domínios A/B, C, D, E. O domínio A/B, também denominado domínio função de ativação-1 (AF-1) devido sua alta propriedade de ativação transcricional, compreende a um domínio amino-terminal altamente variado em tamanho e sequencia. O domínio central C consiste em uma porção altamente conservada que possibilita a associação do receptor ao DNA, denominado DBD (do inglês, *DNA-binding domain*). O domínio D corresponde a uma curta porção responsável pela localização nuclear. O domínio carboxi-terminal E ou LBD (do inglês, *ligand-binding domain*), é fundamental para a associação de ligantes e contribui para interações de receptores nucleares que formam heterodímeros. Alguns NRs possuem ainda um domínio F altamente variável próximo à porção carboxi-terminal, no entanto, a função deste domínio ainda não está bem estabelecida (Figura 1) (21).

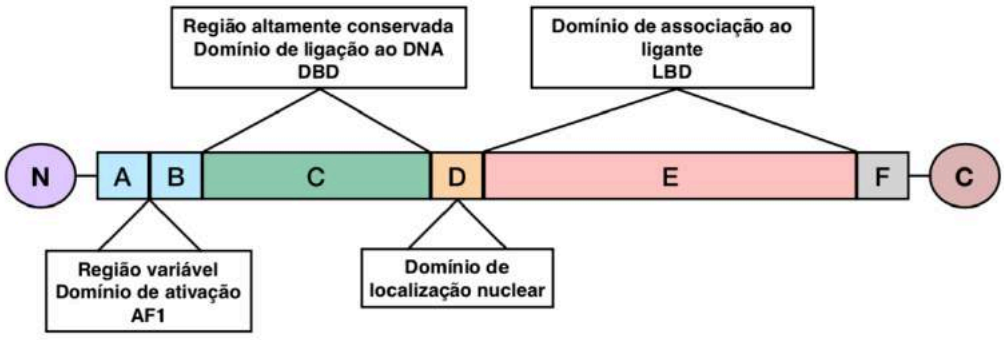

Figura 1 - *Representação esquemática da composição estrutural dos receptores nucleares.* NRs são constituídos por 6 domínios, os quais correspondem a uma porção N-terminal, um domínio de ativação (A/B), um domínio central de associação ao DNA (C), um domínio de localização nuclear (D), um domínio de associação ao ligante (E), e um domínio altamente variável (F) situado próximo à porção carboxi-terminal.

1.2. Receptores hepáticos X (LXR)

Os receptores hepáticos X (LXR, do ingles *liver X receptors*) são fatores de transcrição/receptores nucleares envolvidos na regulação de genes associados ao metabolismo de lipídeos e carboidratos (33-35). O modelo clássico proposto como mecanismo de ação de LXR baseia-se na formação de heterodímeros com receptores de retinóide X (RXR, do inglês *retinoid X receptor*), seguida da associação do complexo LXR-RXR a elementos de resposta

ao LXR (LXREs) (20). LXREs consistem em duas sequências de repetições diretas (DRs) de AGGTCA, separadas por quatro bases espaçadoras (DR-4) situadas em regiões promotoras de genes cuja transcrição é modulada por LXR (36).

A regulação da transcrição gênica promovida por LXR pode ocorrer de maneira dependente ou independente de ligantes (37). Na ausência de ligantes, a regulação transcricional ocorre através da formação de um complexo entre as moléculas co-repressoras NCoR (do ingles, *NR co-repressor*) e SMRT (do ingles, *silencing mediator of retinoic acid and thyroid hormone receptors*) com o heterodímero LXR-RXR que encontra-se ligado ao DNA, impedindo, dessa forma, a transcrição gênica (Figura 2A) (38). Ao passo que em resposta à associação com ligantes, a regulação gênica ocorre por meio de alterações conformacionais no receptor, as quais favorecem o desligamento das moléculas co-repressoras, e induz o recrutamento de moléculas co-ativadoras que facilitam a modificação das histonas e o remodelamento da cromatina, induzindo, desta forma, a transcrição gênica (Figura 2B) (24).

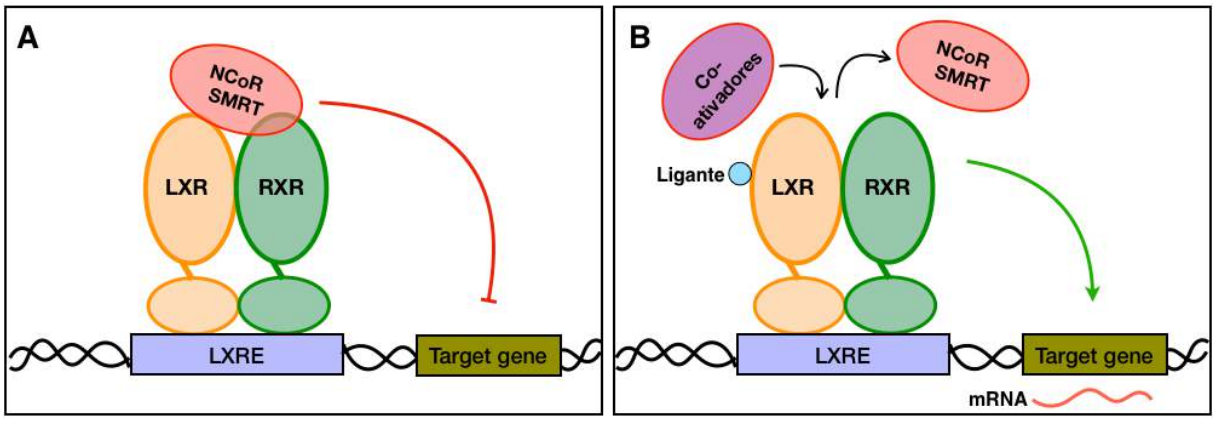

Figura 2 - *Representação esquemática do mecanismo de ação clássico dos receptores hepáticos X.* **A -** Mecanismo inibitório independente de ligantes: Na ausência de ligantes moléculas co-repressoras impedem a transcrição gênica. **B -** Mecanismo de ativação dependente de ligantes: A associação de um ligante na porção LBD promove alterações estruturais no receptor que levam ao desligamento de moléculas co-inibitórias e subsequente aumento da afinidade por moléculas co-estimulatórias, resultando na ativação da transcrição gênica.

LXRs são ativados por moléculas oxidadas derivadas do metabolismo de colesterol, tais como oxisterol (37), e assim, atuam como sensores dos níveis de colesterol e exercem papel fundamental na regulação da transcrição de genes associados ao metabolismo, transporte e efluxo do colesterol (38).

Os receptores LXR apresentam duas isoformas, LXRα e LXRβ, codificadas pelos genes Nr1h3 e Nr1h2, respectivamente, que possuem distinto padrão de expressão e um alto grau de homologia (35, 39). A expressão de LXRα encontra-se restrita a órgãos com alta

atividade metabólica (35) e células da linhagem mielóide, como macrófagos (40), ao passo que a isoforma LXRβ encontra-se expressa de maneira constante, em todos os tipos celulares (39).

Além de sua importante participação na regulação do metabolismo de colesterol, LXRs desempenham um papel na manutenção da homeostase de glicose. De fato, dados da literatura mostram que LXRs podem ser ativados diretamente pela glicose ou seu derivados (41), bem como participar da regulação da expressão gênica de GLUT4 (42). Também tem sido reportado um importante papel para LXRs no que se refere a regulação das respostas imunes (43).

1.3. LXRs na regulação da função de macrófagos e inflamação do tecido adiposo

Macrófagos são células da imunidade inata, altamente plásticas, que contribuem para a manutenção da homeostase em diversos processos biológicos (44). Em resposta a alterações em seu microambiente, essas células são capazes de apresentar um perfil de ativação diferenciado, o qual é frequentemente caracterizado por alterações em suas moléculas de superfície, bem como em seu perfil de secreção de citocinas, o que faz com que essas células exerçam uma participação direta na regulação de vias metabólicas distintas, bem como um grande envolvimento em diversas patologias (16, 45, 46).

Embora macrófagos apresentem um amplo espectro de fenótipos, de maneira simplificada essas células podem ser classificadas em dois subtipos opostos, caracterizados por sua capacidade em gerar uma resposta reparadora (M2) ou pró-inflamatórias (M1) (47-50).

Macrófagos classicamente ativados (M1), são induzidos *in vitro* em resposta ao estímulo pró-inflamatório mediado por LPS e IFN-γ (51). *In vivo*, macrófagos M1 desempenham papel essencial na eliminação de patógenos, e são caracterizadas pela expressão de citocinas pró-inflamatórias como TNFα, IL-1β e IL-12, além de proteínas como a óxido nítrico sintase indutível (iNOS, do inglês *inducible nitric oxide synthase*) e no caso de macrófagos residentes do tecido adiposo (ATMs) a molécula de superfície CD11c (47, 52, 53).

A polarização de macrófagos alternativamente ativados (M2) *in vitro* ocorre em resposta ao estímulo com citocinas do padrão Th2 de resposta, como IL-4 e IL-13 (51). *In*

vivo, contrariamente às funções exercidas por macrófagos M1, macrófagos M2 apresentam um importante envolvimento na angiogênese, reparo e remodelação tecidual (47, 49, 54, 55), desencadeando uma resposta com características anti-inflamatórias e marcada pela secreção de IL-10 e TGF-β, bem como pela expressão de Arginase-1 (Arg-1), CD206, CD301 e o fator de transcrição PPAR-γ (47, 52).

Além de suas funções distintas, macrófagos M1 e M2 apresentam características únicas no que se refere ao metabolismo celular (56), sendo observado em macrófagos M1 o aumento da atividade glicolítica, a qual é acompanhada de duas "quebras" no ciclo do ácido cítrico (TCA), levando ao acúmulo de metabólitos como citrato e succinato na mitocôndria (57), possibilitando o emprego de tais intermediários do TCA na geração de macromoléculas essenciais para a resposta efetora de macrófagos M1 (58).

Macrófagos M2 são caracterizados por um maior metabolismo oxidativo, apresentando TCA intacto o qual é acoplado a fosforilação oxidativa (59). Além disso, macrófagos M2 apresentam maior dependência da oxidação de ácidos graxos, a qual tem sido demonstrada ocorrer em resposta à programação celular mediada por STAT6, apresentado assim um importante papel na produção de citocinas envolvidas na resposta anti-inflamatória (Figura 3) (60, 61).

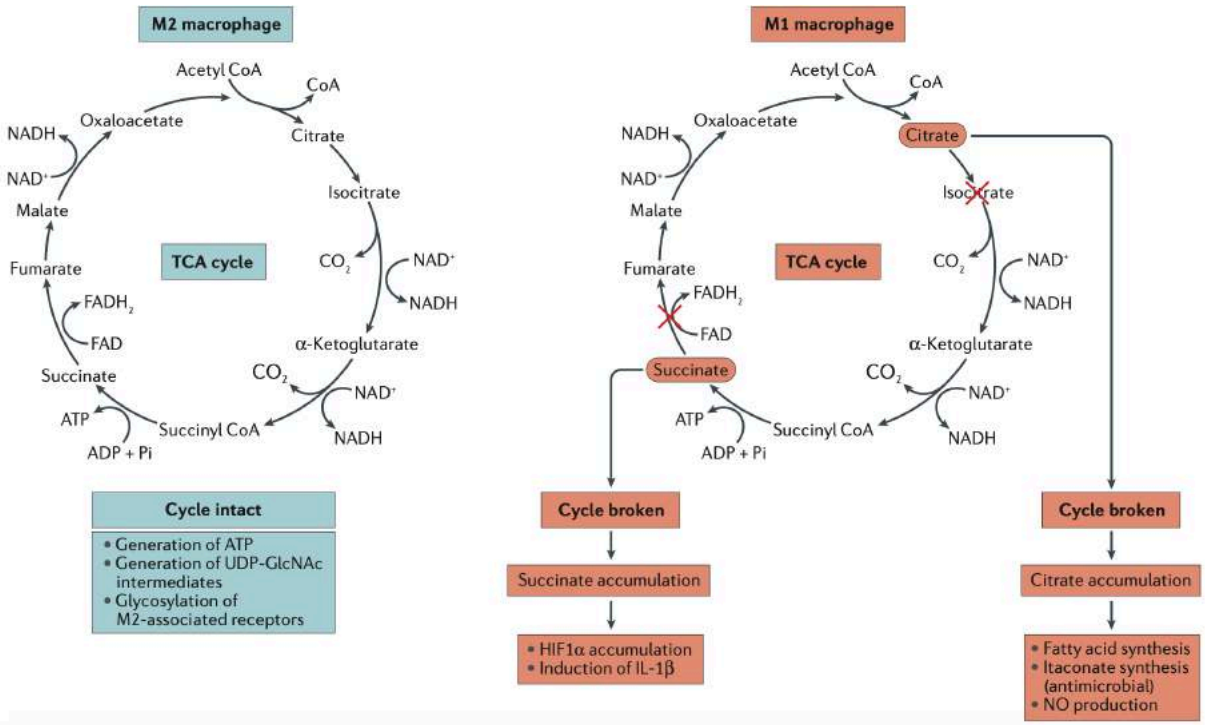

Figura 3 - *Representação esquemática do perfil metabólico em macrófagos polarizados para o perfil M1 (classicamente ativados) ou M2 (alternativamente ativados).* A ativação de macrófagos com LPS e IFN-γ induz

o fenótipo M1, caracterizado por duas quebras no TCA gerando o acúmulo de succinato e citrato, favorecendo a secreção de mediadores pró-inflamatórios e aumentado metabolismo glicolítico. A ativação de macrófagos com IL-4 e IL-13 induz o fenótipo M2, caracterizado pela secreção de mediadores anti-inflamatórios e pelo aumento da fosforilação oxidativa - OXPHOS (57).

Estudos têm reportado que alterações na população de macrófagos residentes do tecido adiposo (ATMs) e a produção excessiva de citocinas pró-inflamatórias estão diretamente relacionadas com o desenvolvimento de resistência à insulina, diabetes e aterosclerose em indivíduos obesos (48, 50, 62-64). Em condições de obesidade um acúmulo excessivo de macrófagos M1 no tecido adiposo é observado, os quais secretam citocinas pró-inflamatórias, como TNF-α e a quimiocina CCL-2 resultando na inibição da via da insulina, o que contribui para o quadro de síndrome metabólica (16, 17, 65). Nessa condição também se observa uma elevada concentração de ácidos graxos livres e colesterol, que podem promover alterações na expressão e ativação de LXRs e, consequentemente, no metabolismo e função dos ATMs (66).

Diversos trabalhos tem sido desenvolvidos com intuito de compreender a maneira pela qual LXRs contribuem para a ativação e função de células imunes (67-71). Dados na literatura mostram que o tratamento de células da imunidade inata com agonistas de LXR promovem um efeito anti-inflamatório devido sua capacidade em reprimir a expressão de genes pró-inflamatórios como *Nos2* e *Tnf-α* (72). Em resposta a um estímulo pró-inflamatório, fatores de transcrição como NFκB (do inglês, *nuclear factor kappa B*), AP1 (do inglês, *activator protein 1*) e IRF (do inglês, *interferon regulatory factor 1*) induzem a expressão de diversos genes pró-inflamatórios (73). Frente a sua associação com ligantes, LXRs são capazes de inibir expressão de genes pró-inflamatórios em macrófagos através da indução da expressão de genes associados ao efluxo de lipídeos em células imunes ou por um mecanismo de transrepressão de genes alvo de fatores de transcrição associados a resposta pró-inflamatória, a qual consiste na SUMOilação de LXR por SUMO2/3 (LXRα) e SUMO1 (LXRβ) e sua subsequente associação com NCoR, impedindo, desta forma, a associação de fatores de transcrição como NFκB, AP1 e IRF a região promotora de seus genes alvo (36, 73-79). Em adição a ativação de LXR promove maior expressão de marcadores anti-inflamatórios como a arginase I e arginase II, efeito não observados em macrófagos deficientes de LXR (80, 81), indicando que LXRs atuam como reguladores do elo entre resposta imune e metabolismo.

Embora muitos trabalhos tenham discutido as ações anti-inflamatórias de LXRs e seu papel na regulação do metabolismo lipídico, a maneira pela qual estes receptores modulam a função e o metabolismo de macrófagos *in vivo* ainda é pouco conhecida e estudos abrangendo a regulação do metabolismo de ATMs pelos LXRs e seu papel na resistência à insulina induzida pela obesidade ainda são escassos. Desta forma, temos como objetivo determinar como LXRs modulam a função de macrófagos residentes do tecido adiposo bem como sua contribuição para o desenvolvimento do quadro inflamatório e resistência à insulina induzida pela obesidade. Assim, nossa hipótese é que a ativação de LXRs irá inibir a ativação de macrófagos e a polarização para um perfil M1, sem alterar ou mesmo favorecendo a polarização para um perfil M2, resultando em menor inflamação no tecido adiposo e na consequente melhora da sensibilidade à insulina e da síndrome metabólica. Ainda, nós acreditamos que a ativação de LXR possa promover alterações no metabolismo celular e na função de macrófagos, levando estas células a um perfil menos glicolítico bem como a uma menor secreção de citocinas pró-inflamatórias.

2. JUSTIFICATIVA

Obesidade é uma doença crônica multifatorial, que acomete cerca de 600 milhões de pessoas no mundo todo sendo observado um aumento considerável no número de indivíduos com sobrepeso nos últimos anos. Estima-se que até o ano de 2025 cerca de 2,3 bilhões de pessoas estejam acima do peso, dentre as quais 700 milhões serão obesas (3). Associada com a resistência à insulina, a obesidade contribui para o desenvolvimento de outras desordens como dislipidemias, doenças cardiovasculares e diabetes mellitus tipo II, sendo considerada um dos principais fatores de risco para o desenvolvimento de síndrome metabólica (3, 82). Essa junção de transtornos cardiometabólicos acomete mais da metade da população de indivíduos adultos, sendo uma das principais causas de morbidade e mortalidade nos países desenvolvidos, tornando-se assim um dos grandes problemas de saúde pública da atualidade (83, 84).

Estudos têm reportado que alterações na população de macrófagos residentes do tecido adiposo e a produção excessiva de citocinas pró-inflamatórias estão diretamente relacionadas com o desenvolvimento de resistência à insulina, diabetes e aterosclerose em indivíduos obesos (16, 17, 65). Nesta condição também se observa uma elevada concentração de ácidos graxos livres e colesterol, que podem promover alterações na expressão de LXRs e consequentemente no metabolismo e função dos ATMs (62). Em adição, a administração de agonistas sintéticos de LXRs promovem melhora no quadro de resistência à insulina e intolerância a glicose em diversos tipos celulares, suportando a hipótese de que a modulação de LXR em macrófagos exerce grande participação no desenvolvimento de doenças metabólicas (62). Contudo, a maneira pela qual alterações metabólicas sistêmicas modulam a função e o metabolismo de macrófagos e como a ativação de LXRs em ATMs contribuem para o desenvolvimento de resistência a insulina ainda é pouco conhecida. Baseado nisso, nós hipotetizamos que a ativação de LXR em macrófagos irá inibir a ativação e a polarização para um perfil M1, resultando em menor inflamação do tecido adiposo e na consequente melhora na sensibilidade à insulina e síndrome metabólica

3. OBJETIVOS

3.1. Geral

Analisar como os fatores de transcrição LXR modulam a função e o metabolismo de macrófagos.

3.2. Específicos

3.2.1. Determinar os efeitos da ativação de LXRs na polarização de macrófagos;

3.2.1.1. Avaliar a resposta de macrófagos frente a ativação de LXR in vitro;

3.2.1.2. Determinar os efeitos da ativação de LXR sobre a polarização (M{LPS+IFNγ} ou M{IL-4}) e ativação (M{LPS}) de macrófagos;

3.2.1.3. Encontrar novos moduladores de LXR em macrófagos para subsequente aplicação in vivo;

3.2.1.4. Determinar os efeitos da ativação de LXRs in vivo, avaliando parâmetros metabólicos sistêmicos bem como a modulação da polarização de ATMs de animais obesos;

3.2.2. Determinar os efeitos da deleção (knockout) de Lxr sobre a polarização de macrófagos;

3.2.2.1. Avaliar o impacto da deleção de Lxrα, Lxrβ ou de ambos sobre perfil de ativação de macrófagos residentes do tecido adiposo ($F4/80^+$ $CD11b^+$ $CD11c^+$ e $F4/80^+$ $CD11b^+$ $CD206^+$) de animais magros e obesos;

3.2.2.2. Investigar os efeitos da deleção de LXR sobre parâmetros metabólicos sistêmicos em animais submetidos ao modelo de obesidade;

3.2.2.3. Avaliar os efeitos da deleção de LXR especificamente em células imunes sobre a inflamação do tecido adiposo em animais magros e obesos.

4. MATERIAIS E MÉTODOS

4.1. Animais

Para realização dos experimentos, foram empregados animais machos, adultos pesando cerca de 20 g, com idade aproximada de 5 semanas, das linhagens C57BL/6J (WT), B6.129S6-Nr1h3tm1Djm/J (LXRαKO) e B6.129S6-Nr1h2tm1Djm/J (LxrβKO). Animais WT foram fornecidos pelo Centro Multidisciplinar para Investigação Biológica na Área da Ciência em Animais de Laboratório (CEMIB/UNICAMP), e animais LXRαKO e LxrβKO foram adquiridos da Jackson Laboratory. Animais LXRαβKO foram originados a partir do cruzamento das linhagens de animais LXRαKO e LxrβKO, empregando nos estudos apenas animais genotipados que apresentaram homozigose para ambas isoformas.

Para indução de obesidade, os animais foram alimentados ração hiperlipídica Envigo TD.93075, a qual apresenta teor calórico de 4,8 kcal/g, dos quais 55% são provenientes de gordura. O grupo não obeso foi alimentado com ração controle Nuvilab CR1, a qual apresenta 3,8 kcal/g, sendo 10% das calorias totais provenientes de gordura. Os animais forma monitorados durante o período de 14 a 16 semanas, e o ganho de peso e consumo alimentar avaliado semanalmente.

O tratamento com o agonista de LXR, naringenin (cat num. 14173 - Cayman Chemical), foi iniciado após confirmação do quadro de resistência à insulina em animais obesos, sendo administrados 10 mg/kg da droga pela via intraperitoneal. A administração de naringenin foi realizada diariamente durante 4 semanas, seguida da avaliação da sensibilidade à insulina. Como controle, animais magros e obesos foram tratados com o volume equivalente de veículo, o qual é composto por 50% PEG 400 (Sigma), 0,5% de Tween 80 (Sigma) e 49,5% de água destilada estéril. Após eutanásia dos animais, foi realizada coleta de soro para mensuração do níveis de colesterol e triglicerídeos, bem como obtenção de diferentes tecidos para avaliação dos efeitos promovidos pela obesidade.

Todos os experimentos empregando animais foram aprovados pela CEUA: CEUA/ UNICAMP no 4562-1/2017, 4562-1A/2018 e CEUA-ICB/USP no 51/2017. Os animais foram mantidos no biotério de experimentação animal do departamento de Imunologia, situado no Bloco F do Instituto de Biologia da UNICAMP, sob as condições de temperatura entre 20-22 ± 2ºC e umidade de 75-80%, tendo ciclo de luz/escuro de 12 horas durante todo o período de experimentação.

4.2. Teste de Tolerância à Glicose e Insulina

A avaliação da sensibilidade à insulina (ITT, do inglês *insulin tolerance test*) e tolerância à glicose (GTT, do inglês *glucose tolerance test*) foi realizada através da mensuração dos níveis de glicose presente na corrente sanguínea dos animais. Para realização do ITT, os animais foram submetidos a 5 horas de privação alimentar, e a glicemia foi avaliada, sendo este o tempo zero, seguida da administração intraperitoneal de 0,75 U/kg de insulina humulin R (Eli Lilly). Para realização do GTT, os animais foram submetidos a 12 horas de jejum, e os níveis glicêmicos foram avaliados para obtenção do tempo zero. Em seguida os animais foram submetidos a administração intraperitoneal de 1g/kg de D-Glucose (cat. num. G8270 - Sigma). O acompanhamento das alterações nos níveis glicêmicos em resposta aos diferentes estímulos foi realizado 15, 30, 60, 90 e 120 minutos após a injeção intraperitoneal de insulina ou glicose.

4.3. Avaliação metabólica

A avaliação do metabolismo dos animais foi realizada através de calorimetria indireta em circuito aberto. Para isso, animais WT, LxrαKO, LxrβKO ou LxrαβKO foram mantidos em gaiolas metabólicas individuais no Oxymax/CLAMS (Columbus Instruments) durante 48 horas com ração hiperlipídica e água *ad libitum*. Foi realizado um período de aclimatação de 24 horas seguido de um período de medida da atividade metabólica (VO2, VCO2) por 24 horas, mantendo-se um ciclo de luz de 12h de maneira a determinar a atividade dos mesmos nos ciclos claro e escuro.

4.4. Mensuração da gordura corporal

A mensuração da composição corporal dos animais foi avaliada através do *Dual-energy X-ray absorptiometry* (DEXA scan) *In Vivo* Imaging System FX PRO (Carestream) situado no Centro de Facilidades para a Pesquisa (CEFAP) do Instituto de Ciências Biomédicas da USP. Para realização do procedimento, os animais foram anestesiados com solução composta por 100 mg/kg de quetamina e 10 mg/kg de xilazina, administrada por via intraperitoneal. Os animais anestesiados foram então posicionados no scaner de maneira ventral, com os membros e a cauda afastados do corpo. Posteriormente, foram adquiridas

imagens empregando dois níveis de energia de modo a possibilitar a avaliação do conteúdo de gordura corporal presente na região de interesse (ROI).

4.5. Transferência adotiva de células imunes

A deleção de LXR especificamente em células imunes foi obtida pela irradiação e subsequente transplante de células da medula óssea deficientes de LXR em animais WT seguindo o seguinte protocolo:

4.5.1. Irradiação

Animais "aceptores" do transplante de medula óssea, entre 6 a 8 semanas de idade, foram acondicionados em um container de acrílico com fluxo de ar contínuo (28 cm diâmetro x 8 cm profundidade), situado entre duas fontes de raios γ. Os animais foram expostos a sessões de irradiação de modo a depletar todas as células imunes.

4.5.2. Transplante de medula óssea

Células da medula óssea (BMCs) foram coletadas das tíbias e fêmurs de animais doadores LXRαβKO e WT, entre 6 a 8 semanas de idade. BMCs foram ressuspendidas em PBS acrescido de 2% de soro fetal bovino inativado (Gibco®). Um dia após a irradiação, os animais aceptores receberam injeção intravenosa pela veia caudal, utilizando uma agulha de 27 gauge, contendo $3x10^6$ BMCs provenientes dos doadores, sendo as combinações doador/ aceptor LXRαβKO→WT e WT→WT. A fim de prevenir possíveis infecções, os animais foram tratados com sulfametoxazol + trimetoprima por via oral durante 7 dias e a repopulação das células imunes foi avaliada após 7 semanas do transplante. Após confirmada a eficácia do transplante, os animais foram submetidos a dieta hiperlipídica ou normolipídica durante 16 semanas e posteriormente a resistência à insulina e inflamação do tecido adiposo foram avaliados conforme descrito.

4.6. Cultura de Células

4.6.1. Macrófagos - Bone marrow-derived macrophages (BMDMs)

Células da medula óssea proveniente do fêmur e tíbia de camundongos C57BL/6J wild type (WT), LXRαKO, LxrβKO e LXRαβKO foram obtidas e submetidas à lise de hemácias e

posterior centrifugação. O pellet celular foi ressuspendido em 1 mL de meio RPMI e a contagem celular foi realizada. Após determinação do número de células obtido, $1x10^6$ células/poço foram adicionadas em placas de 12 poços em meio RPMI 1640 contendo 10% de soro fetal bovino (FBS), 1% de penicilina/streptomicina (P/S), 1% de aminoácidos não essenciais, 1% de piruvato de sódio, 1% de glutamina, 1% de Minimum Essential Medium, 0,125% de β-mercaptoetanol e 5% de sobrenadante proveniente do cultivo de células da linhagem L929. As células foram cultivadas durante 7 dias, sendo a troca de meio realizada no dia 5 e o estímulo com os moduladores de LXR, naringenin ou GW3965 (cat num.10054 - Cayman Chemical) e LPS ou a polarização com LPS+IFNγ ou IL-4 realizada no dia 6 após o plaqueamento. A confirmação do perfil celular foi realizada através de citometria de fluxo, pela marcação de F4/80 e CD11b. E os efeitos da ativação de LXR sobre a função e metabolismo de macrófagos avaliados 24 horas após o estímulo.

4.6.2. Adipócitos

Após obtenção do tecido adiposo perigonadal de animais WT e LXRαβKO realizou-se a obtenção de células presentes na fração vascular estromal através da digestão tecidual com solução constituída por 2 mg/mL de colagenase II (Sigma) em meio RPMI1640 contendo 3,5% de FBS durante 1 hora. Após completa digestão, foi adicionado ao tubo contendo a suspensão celular 10% de FBS para inativação da colagenase. A suspensão foi centrifugada a 1200 rpm, a 4℃ durante 10 minutos. O sobrenadante contendo adipócitos maduros foi descartado e ao pellet celular contendo a fração vascular estromal adicionou-se 2 mL de tampão para promover a lise de hemácias, seguindo com uma nova etapa de centrifugação. O pellet celular foi ressuspendido em 1 mL de meio DMEM e a contagem celular foi realizada. Após determinação do número de células obtido, $1x10^6$ células/poço foram adicionadas em placas de 6 poços em meio de crescimento constituído por DMEM high glucose, 10% FBS, 1% Ciprofloxacino a 1 mg/mL, 0,1% de biotina a 33 mM (Sigma) e 0,1% de ácido pantotênico a 17 mM (Sigma). As células foram mantidas em estufa a 37℃ com 5% de CO_2, sendo a troca de meio realizada no dia seguinte ao plaqueamento, para remoção de artefatos. Posteriormente, o meio de cultivo foi trocado a cada 2 dias até que as células entrarem em confluência. A diferenciação das células provenientes da fração vascular estromal foi realizada empregando o meio de indução composto por DMEM high glucose, 10% FBS, 1%

Ciprofloxacino a 1 mg/mL, 0,1% de biotina a 33 mM (Sigma) e 0,1% de ácido pantotênico a 17 mM (Sigma), rosiglitazona 1 μM, insulina 850 nM, IBMX 250 μM e dexametasona 1 μM, o qual foi empregado por 3 dias, e posteriormente pelo emprego do meio de diferenciação composto por DMEM high glucose, 10% FBS, 1% Ciprofloxacino a 1 mg/mL, 0,1% de biotina a 33 mM (Sigma) e 0,1% de ácido pantotênico a 17 mM (Sigma) e rosiglitazona 1 μM, o qual foi substituído a cada 2 dias durante o período de 15 dias. Após completa diferenciação dos adipócitos brancos, as células foram lavadas com PBS e mantidas em meio sem FBS durante 8 horas, e posteriormente estimuladas com 100 nM de insulina durante 15 minutos. Após esse período, as células foram lavadas com PBS, coletadas e empregadas na avaliação da fosforilação de Akt por western blot ou na avaliação da expressão genes envolvidos na adipogênese por qPCR.

4.7. Citometria de Fluxo

Alterações no potencial de membrana mitocondrial de macrófagos foram avaliadas por citometria de fluxo, empregando os marcadores MitoTracker™ Green (M7514 - Invitrogen™) FM e MitoTracker™ Red CMXRos (M7512 - Invitrogen™). Para os experimentos *in vivo*, a distinção da população de leucócitos presentes no tecido adiposo visceral dos animais foi realizada através da marcação de CD45 (Pacific Blue - clone 30-F11), F4/80 (FITC - clone BM8), CD11b (APC-Cy7 - clone M1/70), CD206 (APC - clone C069C2), CD11c (BV421 - clone N418), Ly6C (PE-Cy7 - clone HK1.4), Ly6G (PercP - clone 1A8) e Siglec F (PE - clone E50-2440) (BD Pharmingen™) e pela avaliação do tamanho e complexidade de cada tipo celular. Em todos os casos foi realizada marcação com Zombie Aqua™ Fixable Viability Kit (Biolegend) para exclusão de células mortas nas análises posteriores, bem como o emprego de células não marcadas como controle. Para avaliação da expressão de citocinas, as células foram fixadas com Cytofix® (BD Biosciences) após a marcação das moléculas de superfície e permeabilizadas com o PermWash® (BD Biosciences). A marcação intracelular foi realizada para as citocinas IL-12 (APC - clone C15.6), IL-1β (PE - clone NJTEN3) e TNF-α (PE-Cy7 - clone MP6-XT22). Os eventos foram adquiridos em citômetro de fluxo BD FACSVerse (BD Biosciences) após compensação apropriada das cores. Todas as aquisições foram analisadas através do software *FlowJo*®.

4.8. Quantificação de citocinas secretadas

Possíveis alterações no perfil de citocinas secretadas por BMDMs foram verificadas através da técnica de ELISA (*Enzyme Linked ImmunonoSorbent Assay*), utilizando amostras do sobrenadante proveniente da cultura celular. As dosagens foram realizadas utilizando os kits para quantificação de TNF-α (Biolegend), IL-6 (BD), IL-12 (BD), IL-1β (Biolegend), MCP-1 (BD) e IL-10 (BD) segundo instruções do fabricante. As amostras foram diluídas 10 vezes para a dosagem de TNF-α e IL-12, 20 vezes para IL-6 e MCP-1, 2 vezes para IL-10 e amostras não diluídas para quantificação de IL-1β . A leitura das absorbâncias foi realizada em espectrofotômetro SPECTRA max M3 (Molecular Devices) em comprimento de onda de 450 nm com correção em 570 nm.

4.9. Extração de RNA e Síntese de cDNA

A expressão dos genes alvo de LXR e genes associados ao metabolismo e ativação de macrófagos em BMDMs e no tecido adiposo foi analisada por RT-qPCR. Para realização destas análises, o RNA total foi extraído utilizando o reagente a base de fenol TRI Reagent® (Sigma-Aldrich). As concentrações do RNA obtido foram avaliadas através do uso de Nanodrop® (Thermo Scientific) apresentando uma relação 260 nm /230 nm e 260 nm /280 nm próxima de 2. Após a extração e quantificação do RNA foi realizada a síntese de cDNA empregando o kit GoScriptTM Reverse Transcription Mix (Oligo dT) (Promega) de acordo com as instruções do fabricante e o cDNA obtido empregado em análises de expressão gênica.

4.10. Análises de expressão gênica por PCR quantitativo

As reações de RT-qPCR foram realizadas empregando SYBR® Green Supermix (Biorad). Para cada reação de qPCR foram utilizados 3 µL de SYBR® Green Supermix 2x, 0,25 µL de iniciador foward 10 µM, 0,25 µL de iniciador reverse 10 µM e 3 µL de cDNA 10 ng/µL. Após incubação por 10 minutos a 95℃, a amostra foi submetida a 40 ciclos de 20s a 95℃, 30s a 95℃ e 30s a 60℃. Os valores de ΔΔCT obtidos foram utilizados para quantificação da expressão de cada gene, sendo empregados como normalizadores o gene ribossomal 18S e como controle negativo a ausência de cDNA. A sequencia dos primers empregados nos ensaios e na genotipagem dos animais encontra-se disponível na tabela 01.

Tabela 1 - Iniciadores utilizados para análise do padrão de expressão gênica de marcadores de ativação de macrófagos e genes alvo de LXR.

Descrição		Sequência 5'- 3'
Retnlα (Fizz1)	*Foward*	TACTTGCAACTGCCTGTGCTTACT
Retnlα (Fizz1)	*Reverse*	TATCAAAGCTGGGTTCTCCACCTC
Chil3 (Ym1)	*Foward*	TCTCTACTCCTCAGAACCGTCAGA
Chil3 (Ym1)	*Reverse*	GATGTTTGTCCTTAGGAGGGCTTC
Clec10α (Mgl1/CD301)	*Foward*	TGAGAAAGGCTTTAAGAACTGGG
Clec10α (Mgl1/CD301)	*Reverse*	GACCACCTGTAGTGATGTGGG
Tnf-α	*Foward*	TAGCCCACGTCGTAGCAAAC
Tnf-α	*Reverse*	TGTCTTTGAGATCCATGCCGT
Il-1β	*Foward*	GGCAGCTACCTGTGTGTCTTTCCC
Il-1β	*Reverse*	ATATGGGTCCGACAGCACGAG
Nos2	*Foward*	TGGTGAAGGGACTGAGCTGT
Nos3	*Reverse*	CCAACGTTCTCCGTTCTCTTG
Pfkfb3	*Foward*	GTCGCCGAATACAGCTACGA
Pfkfb3	*Reverse*	CCCACAGGATCTGGGC
Abca1	*Foward*	AACAGTTTGTGGCCCTTTTG
Abca1	*Reverse*	AGTTCCAGGCTGGGGTACTT
Abcg1	*Foward*	GGTCCTGACACATCTGCGAA
Abcg1	*Reverse*	CAGGACCTTCTTGGCTTCGT
Lpl	*Foward*	TGCCCGAGGTTTCCACAAAT
Lpl	*Reverse*	GCCAGCTGAAGTAGGAGTCG
Fasn	*Foward*	GCATAACGGTCTCTGGTGGT
Fans	*Reverse*	CGAACTTTTCCAAGGTGGGG
Apoe	*Foward*	ACAGATCAGCTCGAGTGGCAAA
Apoe	*Reverse*	ATCTTGCGCAGGTGTGTGGAGA
Nr1h3 (LXRα)	*Foward*	TCAGTGGAGGGAAGGAAATG
Nr1h3 WT (LXRα)	*Reverse*	TTCCTGCCCTGGACACTTAC

Nr1h3 Mutante (LXRα)	*Reverse*	TTGTGCCCAGTCATAGCCGAAT
Nr1h2 (LXRβ)	*Foward*	CTGTCTTTTGGTCCGCTTTC
Nr1h2 WT (LXRβ)	*Reverse*	CACCCCTTGCTTACACTGCT
Nr1h2 Mutante (LXRβ)	*Reverse*	CCAGTCATAGCCGAATAGCC
18S	*Foward*	CTCAACACGGGAAACCTCAC
18S	*Reverse*	CGCTCCACCAACTAAGAACG

4.11. Avaliação do metabolismo celular

A determinação dos efeitos da modulação de LXR sobre o metabolismo de macrófagos foi avaliada através do SeaHorse XFe24 Analyzer (Agilent). Para isso, $0,5x10^6$ células/poço foram cultivadas e diferenciadas na microplaca XF 24 compatíveis com o equipamento, empregando meio de cultura RPMI 1640 contendo 10% de soro fetal bovino, 1% de penicilina/streptomicina, 1% de aminoácidos não essenciais, 1% de piruvato de sódio, 1% de glutamina, 1% de Minimum Essential Medium, 0,125% de β-mercaptoetanol e 5% de sobrenadante proveniente do cultivo de células da linhagem L929. No sétimo dia de diferenciação, o meio de cultura das BMDMs foi substituído por meio DMEM (Agilent) suplementado com 25 mM de glicose (Sigma), 2 mM de piruvato (Sigma) e 1 mM de glutamina (Lonza) e mantidas por 1 hora em estufa a 37°C sem CO_2. Nas 12 horas que antecederam a realização do experimento, o cartucho de sensores XF24-3 (Agilent) foi hidratado com solução calibrante XF (Agilent) e acondicionado em estufa a 37°C sem CO_2. A calibração do equipamento foi realizada de acordo com instruções do fabricante. Cada cartucho possui 4 canais, permitindo a injeção de até 4 diferentes moduladores por poço. O canal 1 foi preenchido com 75 µL de naringenin 3,84 µM de modo a ficar em uma concentração final de 0,5 µM na placa, após a injeção pelo equipamento. O canal 2 foi preenchido com 867 ng/mL de LPS, sendo a concentração final de LPS 100 ng/mL. Como controle os canais foram preenchidos com 75 µL de PBS. Após a calibração, a placa contendo a solução calibrante foi substituída pela placa contendo as células. A injeção de naringenin ou PBS foi realizada após 30 minutos decorridos do início do experimento, e a adição de LPS ou PBS foi realizada 30 minutos após a injeção de naringenin. A avaliação da taxa de glicólise

foi acompanhada através do ECAR (taxa de acidificação do meio extracelular) durante 6 horas.

Para realização do MitoStress Test o canal 1 foi preenchido com 56 µL de oligomicina 9,93 µM de modo a ficar em uma concentração final de 1 µM na placa, após a injeção pelo equipamento. O canal 2 foi preenchido com 62 µL de FCCP 14,95 µM, sendo a concentração final variando entre 1,5 µM. O canal 3 foi preenchido com 69 µL de solução composta de antimicina e rotenona, sendo a concentração final de 1 µM de ambas as drogas. Após a calibração, a placa contendo a solução calibrante foi substituída pela placa contendo as células. A injeção de oligomicina foi realizada após 20 minutos decorridos do início do experimento, a adição de FCCP foi realizada após 45 minutos do início da corrida, e a última injeção, com antimicina/rotenona ocorreu após 70 minutos do início da corrida. A avaliação da respiração mitocondrial dos macrófagos foi acompanhada através do OCR (*oxygen consumption rate*), sendo o tempo total da corrida de 100 minutos.

4.12. Marcação de corpúsculos lipídicos com Oil Red O

Após os estímulos com LPS ou tratamento com moduladores de LXR, BMDMs e macrófagos peritoneais foram submetidos à marcação com Oil Red O para avaliação da presença de corpúsculos lipídicos no interior destas células. Para tanto, macrófagos foram fixados em formalina 3,7 % por 30 minutos e posteriormente corados com Oil Red O 60%. A visualização de lipídeos neutros foi efetuada através de microscópio óptico de campo claro e fluorescência, sendo neste caso, a marcação de núcleos realizada com DAPI.

4.13. Western Blotting

Após a lise celular e quantificação de proteínas através do kit Pierce BCA Protein Assay Kit (Thermo Fisher Scientific), as amostras foram preparadas de modo a obter 40 µg de proteínas totais e acrescidas de tampão de amostra, posteriormente amostras foram aquecidas a 95℃ durante 5 minutos e aplicadas em gel de poliacrilamida a 12%, tendo como padrão o marcador de peso molecular TrueColor High Range Protein Marker (cat num S2600 - Sinapse Inc). A corrida foi realizada empregando 100V até que as amostras saíssem do gel de empilhamento e alcançassem o gel de separação, e então elevada para 120V até o termino da corrida. A transferência foi realizada em membrana de nitrocelulose Amersham Protran 0,45

NC (cat. num. 10600003 - GE Healthcare), em tampão Tris 25 mM, Glicina 190 mM, SDS 0,1% , a 200 mA, durante 4 horas em banho de gelo. Após transferência as membranas foram lavadas com tampão TBS-T e incubadas por 1 hora com solução de bloqueio constituída por leite desnatado 5% ou BSA 3% em diluídos em TBS-T.

Para as amostras de adipócitos, posterior a este período, a solução de bloqueio foi descartada e adicionou-se a membrana o anticorpo policlonal produzido em coelho anti-phospho-Akt (Ser473) (cat. num. 9271 - CellSignaling) na proporção 1:1000 diluído em solução de bloqueio, e seguiu-se sob incubação overnight a 4℃. Para as amostras de macrófagos, empregou-se anticorpo policlonal produzido em coelho anti-IκBα (cat. num. 9242 - CellSignaling) na proporção 1:1000 ou o anticorpo policlonal produzido em coelho anti-phospho-p38 MAPK (Thr180/Tyr182) (cat. num. 9211 - CellSignaling) na proporção 1:1000. Ambos anticorpos foram diluídos em solução de bloqueio, e incubados overnight a 4℃. Posteriormente, a membrana foi submetida a 5 ciclos de lavagem com duração de 2 minutos em tampão TBS-T e adicionou-se anticorpo secundário Rabbit IgG HRP (cat. num. NA934V – GE Healthcare) na proporção 1:10000 diluído em solução de bloqueio, seguindo incubação a temperatura ambiente durante uma hora. Após este período a membrana foi lavada novamente e adicionou-se a esta o substrato quimioluminescente SuperSignal™ West Pico PLUS (Thermo Fisher Scientific). A membrana foi então revelada no sistema de imagem ChemiDocTM Gel Imaging System (Biorad). Como controle a membrana foi incubada com o anticorpo policlonal produzido em coelho anti-Akt (cat. num. 9272 - CellSignaling) ou com o anticorpo monoclonal feito em camundongo anti-α-Tubulin (cat. num. T5168 - Sigma), na proporção 1:1000 pelo período de uma hora, para adipócitos e macrófagos, respectivamente. A revelação da membrana seguiu conforme descrito anteriormente.

A análise do nível de expressão das proteínas de interesse foi realizada através do programa Image J, empregando a densitometria das bandas apresentadas para as proteínas alvo e normalizadas pela expressão de α-Tubulin ou Akt da amostra correspondente, sendo os valores expressos através da razão proteína de interesse/proteína controle.

4.14. Análises estatísticas

As análises estatísticas de todos os dados obtidos foram realizadas com o programa GraphPad Prism® versão 9.0, empregando oneway ANOVA para análise de variância e

posthoc de Bonferroni ou *t-test* para verificação da diferença em uma variável entre os grupos experimentais. O mesmo programa foi utilizado para construção dos gráficos.

5. RESULTADOS

5.1. A deleção de LXR exacerba a resposta pró-inflamatória em macrófagos

Com intuito de avaliar a participação de LXRs na regulação da resposta de macrófagos, BMDMs de camundongos WT e LXR duplo *knockout* (LXRαβKO) foram estimulados com o agonista de TLR4, LPS. Nossos dados revelaram que a deleção de LXR reduz a expressão dos marcadores anti-inflamatórios *Clec10a*, *Chil3* e *Retnla* (Figura 4A), bem como apresentam uma maior secreção das citocinas pró-inflamatórias IL-12 e TNF-α (Figura 4B). Em adição, ao avaliarmos se diferentes isoformas de LXR poderiam exercer um papel diferenciado sobre a modulação da resposta de macrófagos uma maior participação de LXRβ foi encontrada, uma vez que células deficientes de LXRβ apresentaram níveis mais elevados dessas citocinas quando comparados a macrófagos WT e LXRαKO (Figura 4B).

Tais resultados nos fizeram questionar se um efeito similar poderia ser observado em macrófagos residentes. Assim, macrófagos residentes da cavidade peritoneal foram obtidos de animais naive WT e LXRαβKO e a marcação de corpúsculos lipídicos foi realizada. Nossos dados revelaram que a deleção de LXR leva ao aumento de corpúsculos lipídicos em macrófagos peritoneais (Figura 4C), indicando uma maior ativação dessas células (85).

5.2. Efeitos da ativação de receptores LXR sobre a ativação de macrófagos

Tendo em vista o direcionamento de macrófagos para um perfil pró-inflamatório em resposta a deleção de LXR, nosso próximo passo foi avaliar como a ativação de LXR poderia afetar a resposta de macrófagos. Assim, BMDMs derivadas de animais WT e LXRαβKO foram tratadas com o agonista sintético de LXR, GW3965.

LXRs controlam a expressão de diversos genes associados ao metabolismo lipídico (86), sendo assim, com intuito de confirmar os efeitos de GW3965 sobre a ativação de LXR, a expressão de alguns de seus genes alvo foi avaliada. Nós observamos que o tratamento de macrófagos com GW3965 levou ao aumento da expressão dos genes associados ao efluxo e transporte de lipídeos, *Abca1* e *Abcg1* em macrófagos provenientes de animais WT, não sendo observada uma resposta similar em macrófagos LXRαβKO (Figura 4D). De maneira interessante, também encontramos em macrófagos WT um aumento na expressão de *Fasn*, o qual apresenta envolvimento na síntese de lipídeos e *Nh1r2*, o qual corresponde ao receptor LXRβ, sem, no entanto, encontrar alterações na expressão de *Nh1r3* (LXRα) (Figura 4D).

Considerando os efeitos observados frente ao estímulo com LPS, nós decidimos investigar se a ação de GW3965 poderia ser dependente de uma isoforma específica do receptor. Assim, BMDMs de LXRαKO e LXRβKO foram tratados com GW3965. Nossos resultados mostram que em resposta ao tratamento com o agonista GW3965 a expressão de *Abca1*, *Abcg1* e *Fasn* em macrófagos sofre uma maior regulação exercida pela isoforma LXRβ (Figura 4E). Em adição, nós encontramos um aumento significativo na expressão de LXRβ em macrófagos depletados de LXRα (Figura 4E), indicando que macrófagos apresentam um mecanismo compensatório para a ausência de LXRα. Contudo tal efeito não foi observado em macrófagos LXRβKO (Figura 4E).

5.3. O tratamento com agonistas de LXR reduz a resposta pró-inflamatória em macrófagos ativados

A ativação de LXR tem sido mostrada capaz de inibir a translocação de NFκB (75, 76). Assim, nós avaliamos se ativação de LXR poderia promover efeitos anti-inflamatórios em células estimuladas com LPS. De maneira interessante, nós observamos que em resposta a ativação com LPS macrófagos apresentam redução significativa na expressão de genes alvos de LXR, como observado pela menor expressão de *Abca1*, *Abcg1*, *Fasn*, *Apoe* e *Lpl* (Figura 4F), sendo que a ativação de LXR promovida pelo tratamento com GW3965 foi capaz de restaurar a expressão de *Abcg1* e *Abca1*, esta última de maneira dependente de LXRβ (Figura 4F). Ainda, juntamente com a redução na expressão de moléculas responsáveis pelo efluxo de lipídios, o estímulo com LPS promoveu o acúmulo de corpúsculos lipídicos, organelas responsáveis pela compartimentalização e transporte de lipídeos neutros, com um importante papel na geração de mediadores inflamatórios lipídicos (85), o qual foi reduzido quando o tratamento com GW3965 foi realizado (Figura 4G).

Para melhor compreender o envolvimento de cada uma das isoformas de LXR na regulação da resposta imune, nós avaliamos a expressão de *Nos2* e a secreção de IL-1β em macrófagos estimulados com LPS e tratados com o agonista de LXR. Nossos dados revelaram uma forte participação da isoforma β na inibição da resposta pró-inflamatória, observada pela redução desses marcadores pró-inflamatórios em macrófagos WT e LXRαKO, mas não em LXRβKO (Figuras 4H-I). Tais dados sugerem uma participação importante do efluxo de

lipídios na regulação do perfil inflamatório de macrófagos, bem como um papel distinto para as isoformas de LXR na regulação da resposta imune.

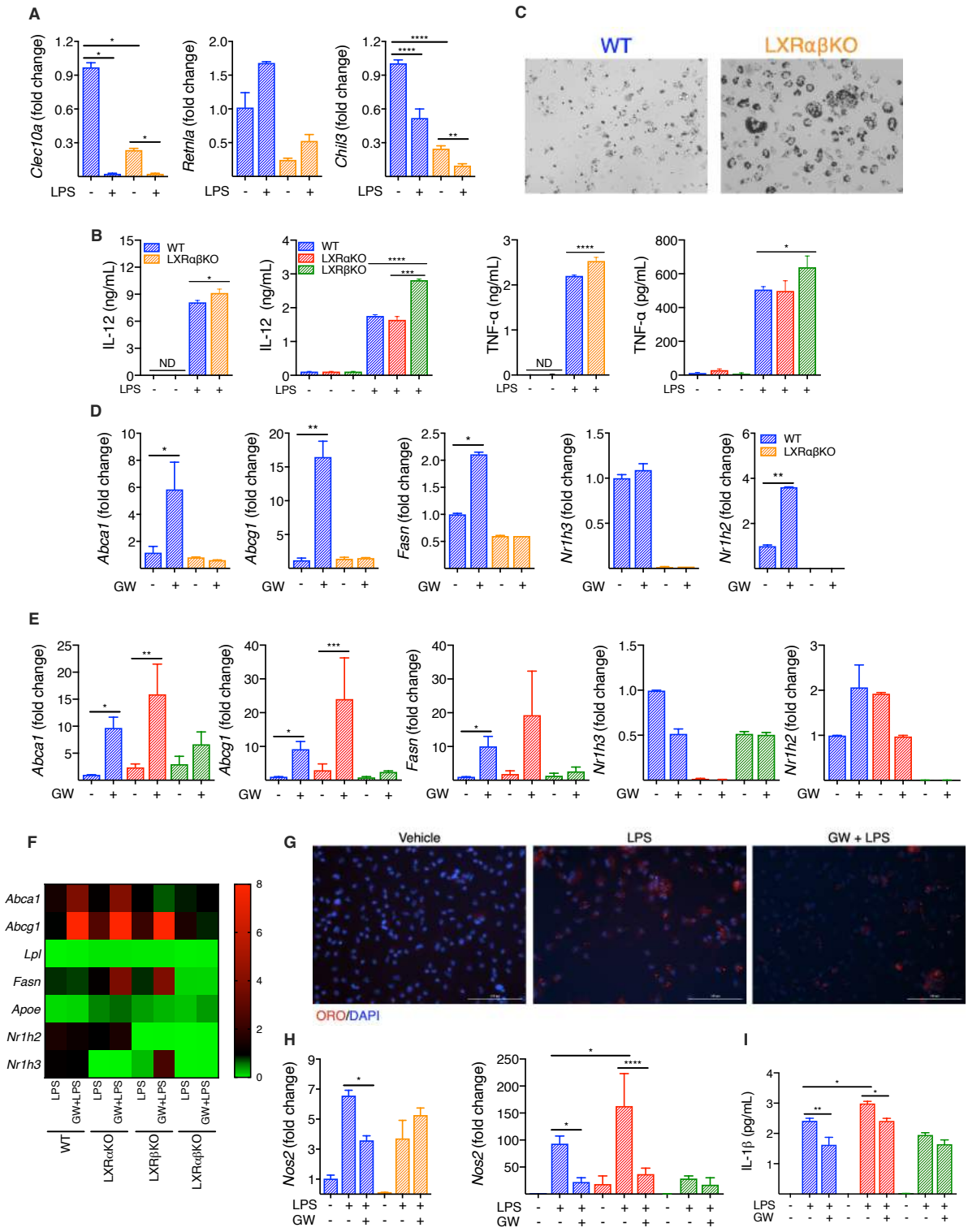

Figura 4 - *GW3965 induz a expressão de genes alvo de LXRs e reduz a expressão de marcadores pró-inflamatórios em macrófagos.*
A - Avaliação da expressão de marcadores antiinflamatórios em macrófagos WT e LXRαβKO estimulados com 100 ng/mL LPS por 24 horas. **B -** Avaliação do perfil de citocinas secretadas por BMDMs derivadas de animais WT, LXRαKO, LXRβKO ou LXRαβKO, 24 horas após o estímulo com LPS. **C -** Marcação de corpúsculos lipídicos em macrófagos peritoneais de animais WT e LXRαβKO. **D -** Avaliação da expressão de genes alvo de

LXR em BMDMs derivadas de camundongos WT e LXRαβKO, 24 horas após o tratamento com 1 μM GW3965. **E -** Avaliação da expressão de genes alvo de LXR em BMDMs derivadas de camundongos WT, LXRαKO, LXRβKO, 24 horas após o tratamento com 1 μM GW3965. **F -** Heat map de genes alvo de LXRs em BMDMs derivadas de camundongos WT, LXRαKO, LXRβKO ou LXRαβKO pré-tratados com 1 μM GW3965 e estimulados com 100 ng/mL LPS durante 24 horas. **G -** Avaliação da presença de corpúsculos lipídicos em células WT pré-tratados com 1 μM GW3965 e estimulados com 100 ng/mL LPS durante 24 horas. Corpúsculos lipídios foram marcados com *Oil Red O* (ORO) e os corpúsculos lipídicos foram avaliados por microscopia de fluorescência. **H -** Avaliação da expressão de marcadores pró-inflamatórios em BMDMs derivadas de animais WT, LXRαKO, LXRβKO ou LXRαβKO pré-tratados com 1 μM GW3965 e estimulados com 100 ng/mL LPS durante 24 horas. Dados representam a média ± SEM, sendo (*) $p \leq 0.05$, (**) $p \leq 0.01$, (***) $p \leq 0.001$ (****) $p \leq 0.0001$.

5.4. A ativação de LXR promove efeito anti-inflamatório em macrófagos polarizados

Uma vez observado que a ativação de LXR promove a redução na secreção de citocinas pró-inflamatórias em macrófagos ativados com LPS, nós decidimos avaliar se a expressão de LXR poderia ser diferenciada em macrófagos polarizados para os perfis M1 (LPS+IFNγ) ou M2 (IL-4). Nossos dados mostram que macrófagos M2 apresentam uma maior expressão de ambas as isoformas de LXR, sendo a expressão de *Nr1h3* (LXRα) mais acentuada nessas células (Figura 5A). Em adição, o tratamento com GW3965 levou ao aumento da expressão de genes alvo de LXR em macrófagos não polarizados (MØ) e polarizados para o perfil M2 (Figura 5B).

De maneira interessante, nós encontramos que em resposta ao tratamento com GW3965, macrófagos MØ expressam níveis similares aos encontrado em macrófagos M2, dos marcadores anti-inflamatórios *Retnla* e *Clec10a* (Figura 5C). No entanto, o tratamento de macrófagos M2 com o agonista de LXR não potencializou a expressão desses marcadores (Figura 5C). Ao avaliarmos os efeitos da ativação de LXR sobre a modulação da resposta de macrófagos M1 nós encontramos que o tratamento com GW3965 reduziu a expressão das citocinas pró-inflamatórias *Tnf-α* e *Il-1β* (Figura 5D). Frente a um estímulo pró-inflamatório, um desvio no metabolismo de células imunes é observado, direcionando tais células para um perfil glicolítico e favorecendo a utilização de intermediários do metabolismo na síntese de outras moléculas bioativas necessárias para proliferação e diferenciação celular (87). Assim, nós avaliamos a expressão das enzimas da via glicolítica *Pfkfb3* e *Ldha*, nossos dados revelaram que a ativação de LXR é capaz de reduzir a expressão de ambas enzimas, alcançando níveis similares aos observados em macrófagos MØ (Figura 5E), sugerindo uma participação importante de LXR na regulação do metabolismo e função de células imunes.

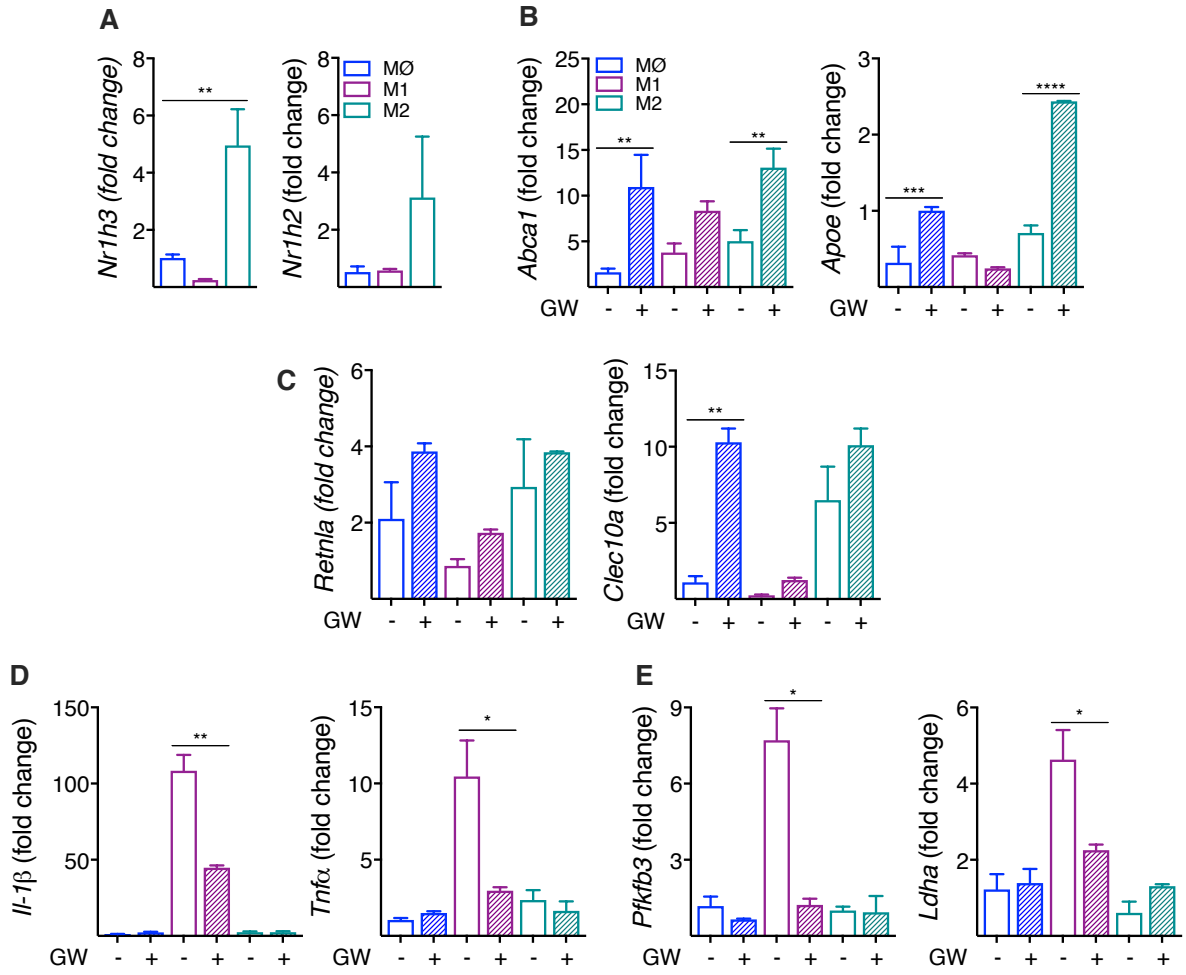

Figura 5 - *GW3965 modula a resposta de macrófagos polarizados.*
A - Avaliação da expressão de LXRα e LXRβ em macrófagos polarizados para o perfil M2 (IL-4) ou M1 (LPS+IFNγ). **B -** Avaliação da expressão de genes alvo de LXR em macrófagos M1 e M2 frente ao tratamento com o agonista de LXR. **C -** Avaliação dos efeitos de GW3965 sobre a expressão de marcadores anti-inflamatórios. **D -** Determinação dos efeitos de GW3965 sobre a expressão de marcadores pró-inflamatórios em macrófagos M1. **E -** Avaliação dos efeitos do tratamento com 1 μM GW3965 sobre a expressão de enzimas da via glicolítica. Dados representam a média ± SEM, sendo (*) p≤0.05, (**) p≤0.01, (***) p≤0.001 (****) p≤0.0001.

5.5. A deleção de LXR afeta o ganho de peso e sensibilidade à insulina em resposta à dieta hiperlipídica

LXRs atuam como sensores do metabolismo lipídico (88) e, baseado nos dados obtidos por nós e outros grupos (43, 67, 89), foi possível observar que LXRs exercem um papel fundamental na regulação do metabolismo e função de macrófagos.

Tendo em vista que a deleção de LXR promoveu um aumento na reposta pró-inflamatória de macrófagos, nosso próximo passo foi avaliar se animais deficientes em LXR poderiam responder de maneira diferenciada ao estresse metabólico. Assim, animais WT e

LXRαβKO foram alimentados com dieta hiperlipídica contendo 60% de gordura. Nossos dados mostram que camundongos LXRαβKO são resistentes ao ganho de peso induzido em resposta a alimentação rica em lipídeos (Figura 6A), bem como ao acúmulo de gordura corporal (Figura 6B), sendo que esse fenótipo não foi associado com alterações no consumo alimentar (Figura 6C).

Uma vez que obesidade é uma das causas para o desenvolvimento de doenças como diabetes e resistência à insulina (90), nós avaliamos como a deleção de LXR poderia impactar nos níveis glicêmicos dos animais em jejum. Nossos dados revelaram que animais LXRαβKO apresentaram níveis glicêmicos similares aos observados em animais WT (Figura 6D). Ao realizarmos o GTT nós encontramos que animais LXRαβKO apresentam menor tolerância à glicose, visto pelos elevados níveis de glicose circulante 30 minutos após a administração intraperitoneal de glicose (Figura 6E). No entanto, estes animais apresentaram maior captação da glicose, visto pelo retorno da glicemia aos níveis basais após 120 minutos da administração de glicose, o que não foi observado em animais WT (Figura 6F).

De maneira interessante nós encontramos elevada sensibilidade à insulina em animais LXRαβKO quando comparado à animais WT, visto pela redução de cerca de 50% nos níveis glicêmicos após 60 minutos da administração de insulina quando comparado com o nível de glicemia basal do mesmo grupo (Figura 6F). Tal dado é consistente com o reduzido ganho de peso em animais LXRαβKO frente à dieta hiperlipídica (Figura 6A).

Com intuito de avaliar se a deleção de LXR poderia afetar de alguma forma o consumo metabólico dos animais, camundongos LXRαβKO e WT foram submetidos à gaiola metabólica e os níveis de VO_2 e VCO_2 foram avaliados (Figura 6G-K). Nossas análises revelaram animais LXRαβKO apresentam reduzido consumo de oxigênio comparado a animais WT alimentados com a mesma dieta (Figura 6G-H). Nós então exploramos se a deleção de LXR poderia promover alterações no uso de macromoléculas empregadas na produção de energia. Nossos dados mostraram que animais LXRαβKO apresentam maior utilização de glicose como fonte energética, ao passo que animais WT apresentaram elevada oxidação de lipídios para produção de energia em resposta a alimentação hiperlipídica (Figura 6I). Em adição, o gasto energético foi reduzido em animais LXRαβKO (Figura 6J), sem, no entanto, prover alterações na atividade dos animais (Figura 6K). Juntos, esses dados indicam

que LXRs são importantes reguladores do balanço energético e contribuem para a manutenção da homeostase de glicose.

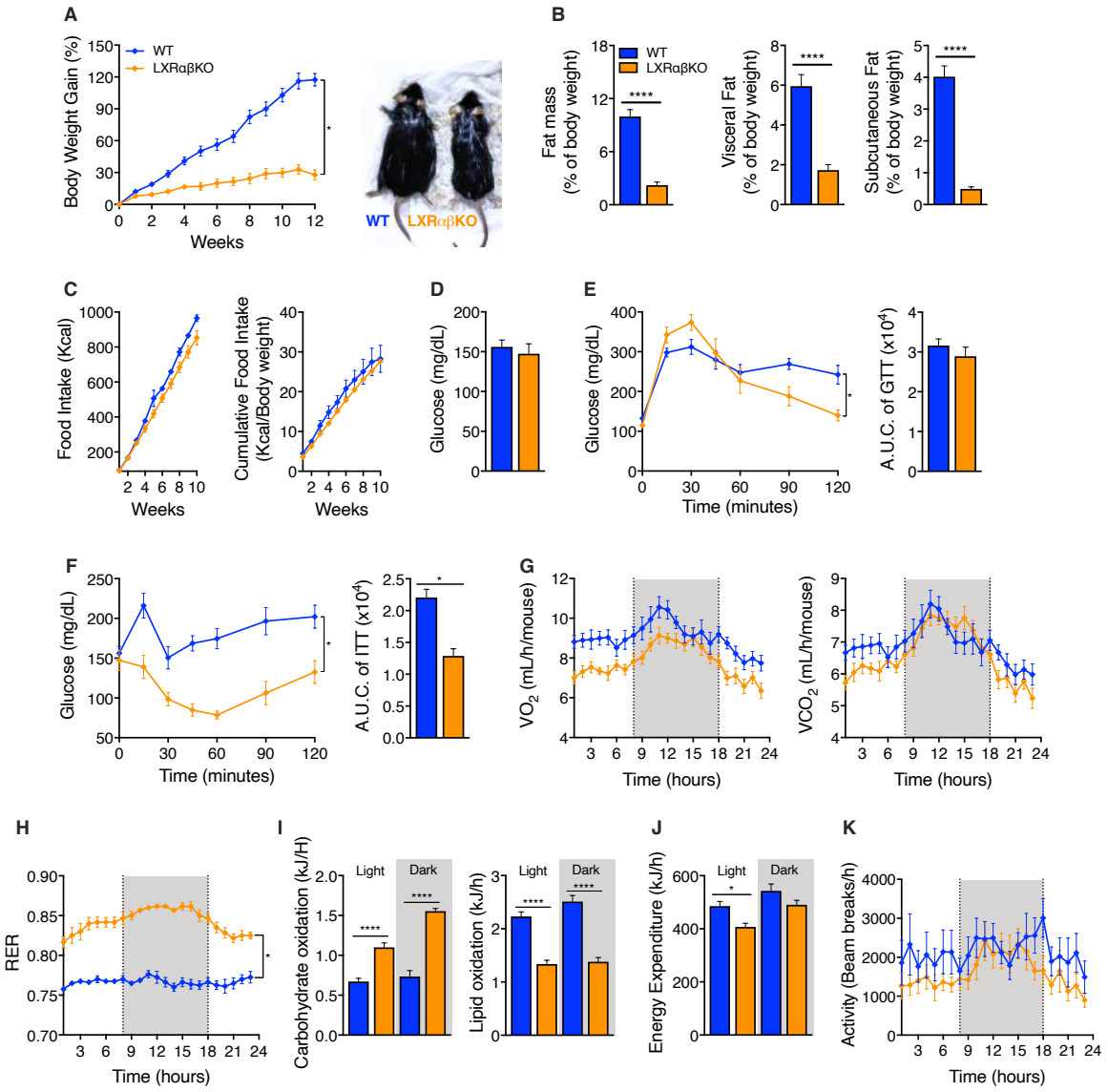

Figura 6 – *LXR é essencial para o ganho de peso em resposta à dieta hiperlipídica.*
Animais WT e LXRαβKO foram alimentados com dieta hiperlipídica e os parâmetros metabólicos foram avaliados. **A -** Ganho de peso de animais WT e LXRαβKO em resposta a HFD (esquerda). Imagem representativa de animais WT e LXRαβKO após 14 semanas de HFD (direita). **B -** Determinação do acúmulo de gordura corporal no tecido adiposo visceral e subcutâneo. **C -** Consumo alimentar em animais WT e LXRαβKO alimentados com HFD. **D -** Avaliação da glicemia dos animais em jejum. **E -** Teste de tolerância à glicose. **F -** Teste de tolerância à insulina. **G -** Consumo de O_2 e CO_2 avaliado em gaiolas metabólicas. **H -** Determinação de RER em animais WT e LXRαβKO. **I -** Determinação da fonte energética utilizada por animais WT e LXRαβKO. **J -** Gasto energético nos animais WT ou deficientes de LXR alimentados com dieta hiperlipídica. **K -** Determinação da atividade dos animais em gaiola metabólica. Valores apresentados no gráfico correspondem a media ± SEM, sendo (*) p≤0.05, (**) p≤0.01, (***) p≤0.001 (****) p≤0.0001. n=8 animais/grupo.

5.6. A deleção de LXRα mas não de LXRβ leva ao aumento da sensibilidade à insulina em animais obesos

Tendo em vista as alterações metabólicas encontradas em animais deficientes de ambas isoformas de LXR, nosso próximo passo foi avaliar o impacto que a deleção de cada uma das isoformas de LXR poderia exercer sobre o metabolismo. Assim, nós investigamos os efeitos da deleção de uma única isoforma de LXR sobre a patologia da obesidade. Para tanto, LXRαKO e LXRβKO foram submetidos ao modelo de obesidade induzida por dieta hiperlipídica. Nossos dados revelaram que animais LXRαKO apresentam rápido ganho de peso comparados a animais LXRβKO e WT, a qual não foi observada 10 semanas após o início da alimentação com a dieta hiperlipídica (Figura 7A). Em adição, nós não encontramos alterações no percentual de gordura corporal ou no consumo alimentar, independente do genótipo dos animais (Figura 7B-C).

LXRs são importantes reguladores do metabolismo de glicose (41, 42), no entanto, pouco se sabe sobre o papel de cada uma de suas isoformas na regulação do metabolismo de carboidratos. Nós encontramos que embora animais deficientes de uma única isoforma não apresentem alterações na glicemia frente a privação alimentar (Figura 7D), a deleção de LXRβ são intolerantes à glicose, visto pelo aumento nos níveis glicêmicos já nos primeiros 15 minutos após a administração de glicose exógena quando comparado a animais WT (Figura 7E). De maneira interessante, o teste de tolerância à insulina revelou que, similar ao observado em animais LXRαβKO, a deleção de LXRα promove maior sensibilidade à insulina quando comparados a animais WT e LXRβKO (Figura 7F).

Com intuito de avaliar se a deleção de LXRα ou LXRβ poderia afetar o consumo energético do animais frente ao estimulo obesogênico, nós realizamos o ensaio de calorimetria indireta. Nós encontramos que animais LXRαKO e LXRβKO apresentam similar consumo de oxigênio ao observado em animais WT (Figura 7G-H). Além disso, animais de ambos genótipos apresentaram preferencia pelo uso de lipídeos para produção de energia, similar ao observado em em animais WT (Figura 7I). Juntos, nossos dados revelaram que embora exista grande similaridade estrutural e uma sobreposição entre as funções desempenhadas pelas isoformas de LXR (39, 91), LXRα e LXRβ apresentam distinto papel na regulação da homeostase sistêmica de glicose.

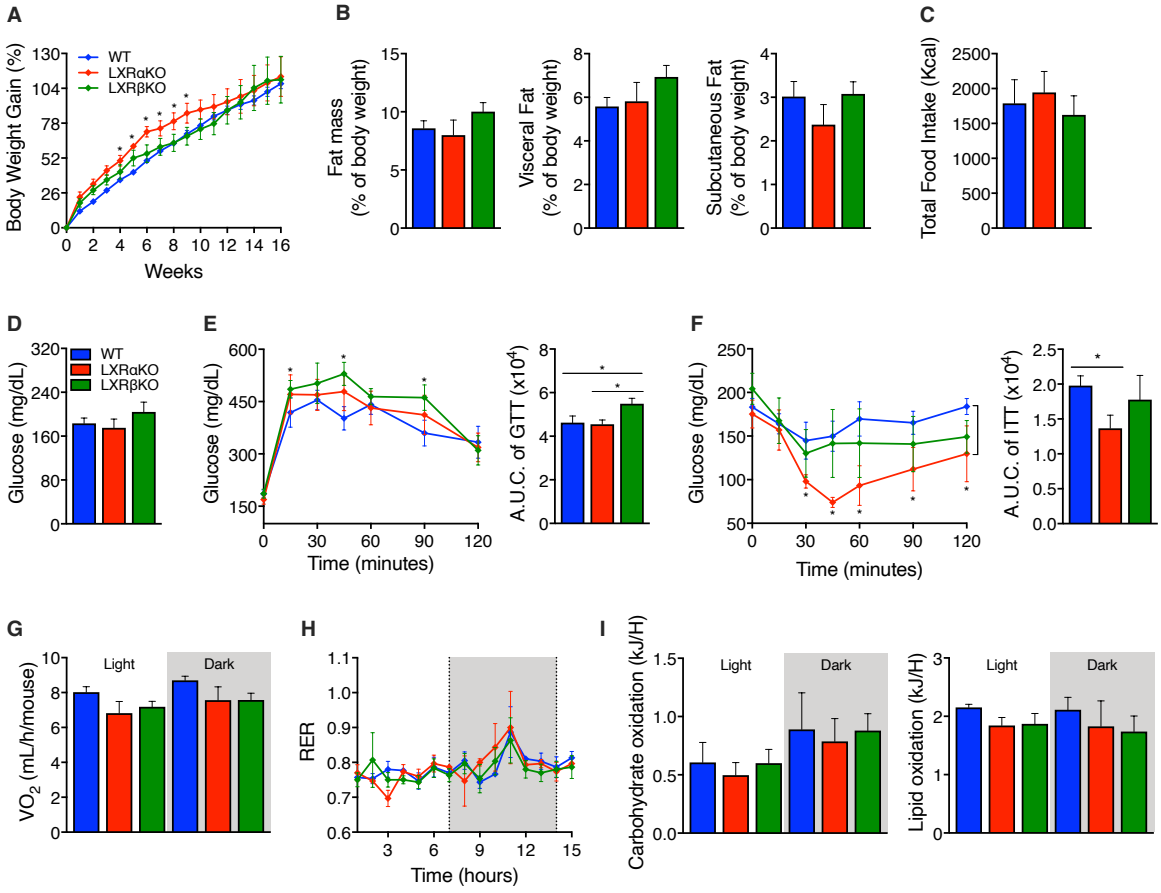

Figura 7 – *LXRα e LXRβ desempenham papéis distintos na regulação da homeostase metabólica.*
Animais WT, LXRαKO e LXRβKO foram alimentados com dieta hiperlipídica e os parâmetros metabólicos foram avaliados. **A -** Ganho de peso em animais WT, LXRαKO e LXRβKO em resposta à alimentação com dieta hiperlipídica. **B -** Determinação do acúmulo de gordura corporal no tecido adiposo visceral e subcutâneo. **C -** Avaliação do consumo alimentar nos animais em resposta a HFD. **D -** Avaliação da glicemia após 5 horas de privação alimentar. **E -** Teste de tolerância à glicose de animais WT, LXRαKO e LXRβKO alimentados com HFD. **F -** Teste de tolerância à insulina. **G -** Consumo de oxigênio de animais WT, LXRαKO e LXRβKO avaliado em gaiolas metabólicas. **H -** Determinação de RER nos animais WT e deficientes de LXRα ou LXRβ. **I -** Determinação da fonte energética utilizada por animais WT, LXRαKO e LXRβKO. Valores apresentados no gráfico correspondem a media ± SEM, sendo (*) p≤0.05, n=6 animais/grupo.

5.7. LXRα e LXRβ são essenciais para manutenção do perfil de células imunes residentes do tecido adiposo

Em resposta ao modelo de estresse metabólico induzido pela dieta hiperlipídica, a deleção de cada uma das isoformas de LXR promoveu alterações no metabolismo glicolítico (Figura 7). Tais resultados nos fizeram questionar se a deleção de uma única isoforma de LXR poderia promover alterações similares na ausência de obesidade. Para tanto, animais WT e LXRαKO ou LXRβKO foram alimentados com dieta padrão e os parâmetros metabólicos foram avaliados.

Nós observamos que a ausência de cada uma das isoformas impacta de maneira diferenciada no metabolismo dos animais, sendo encontrado que animais LXRβKO apresentam menor ganho de peso quando comparados com animais WT, ao passo que a deleção de LXRα levou ao aumento no ganho de peso (Figura 8A). Este dado é consistente com o fenótipo observado em animais obesos, onde animais LXRαKO apresentaram ganho de peso acelerado com parado com animais WT e LXRβKO (Figura 7A). Ao avaliarmos a glicemia em jejum dos animais, diferenças não foram encontradas, independente do genótipo dos animais, quando comparados a camundongos WT (Figura 8B). No entanto, frente ao estímulo com glicose exógena foi possível observar que animais LXRαKO e LXRβKO apresentam maior tolerância à glicose comparados a animais WT (Figura 8C), sem, no entanto, apresentar alterações na sensibilidade à insulina (Figura 8D), tais resultados são consistentes com dados reportados por Korach-André e colaboradores (2011), onde uma maior expressão de *Glut4* foi observada em animais deficientes de LXR (92).

Em resposta a ativação, LXRα e LXRβ levam a respostas celulares distintas (93). Assim, nós nos perguntamos se a ausência de uma isoforma específica poderia contribuir para o desenvolvimento de inflamação do tecido adiposo, na ausência de estresse metabólico. De maneira interessante, nós observamos que a deleção de LXRα não leva a alterações significativas na população de macrófagos totais residentes do tecido adiposo perigonadal (Figura 8E). No entanto, ao avaliarmos as sub-populações de macrófagos, encontramos elevada inflamação nesses animais, caracterizada pelo aumento de macrófagos M1 (Figura 8F-G), bem como pela maior expressão de citocinas pró-inflamatórias e redução de marcadores anti-inflamatórios no PgAT (Figura 8H-I). Em contrapartida, ao avaliarmos os mesmos parâmetros em animais deficientes de LXRβ uma redução global na população de ATMs foi observada (Figura 8J), a qual está associada com redução de ATMs M1 e M2 encontrada nesses animais (Figura 8K).

Assim como em outros tecidos, o balanço entre células imunes pró- e anti-inflamatórias é essencial para manutenção da homeostase tecidual (94). Nossos dados revelaram que embora animais LXRβKO massiva redução na população de macrófagos, é possível observar o desbalanço imune no tecido adiposo desses animais, caracterizado pelo aumento da razão M1/M2 (Figura 8L). Adicionalmente, similar à redução global na população de macrófagos, a avaliação da expressão de marcadores anti-inflamatórios e pró-inflamatórios

no tecido adiposo total revelou massiva redução na expressão dos marcadores *Il-1β*, *Tnf-α*, *Fizz1* e *Mgl1* (Figura 8M-N), evidenciando que embora os mecanismos de regulação desempenhado pelas isoformas de LXR sejam distintos, ambas isoformas são essenciais para o balanço imune do tecido adiposo.

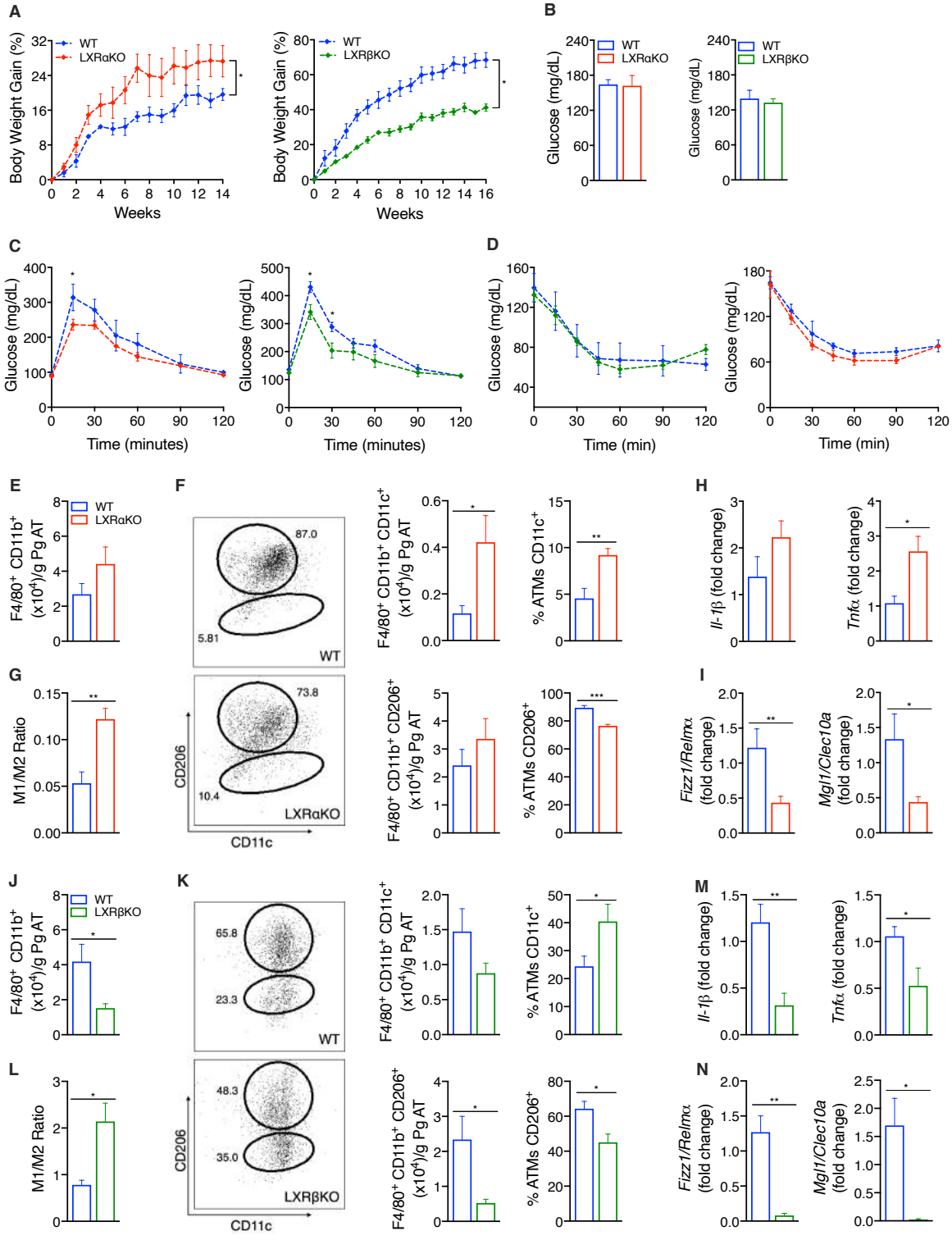

Figura 8 – *LXR é essencial para a manutenção da homeostase do tecido adiposo branco.*

Animais WT, LXRαKO e LXRβKO foram alimentados com dieta padrão e os parâmetros metabólicos foram avaliados. **A -** Ganho de peso em animais WT e LXRαKO (esquerda) ou WT e LXRβKO (direita) em resposta à alimentação com dieta controle. **B -** Avaliação da glicemia em jejum de animais WT e LXRαKO (esquerda) ou WT e LXRβKO (direita). **C -** Teste de tolerância à glicose em animais WT e LXRαKO (esquerda) ou WT e LXRβKO (direita) após 14 dias de alimentação com dieta controle. **D -** Teste de tolerância à insulina em animais WT e LXRαKO (direita) ou WT e LXRβKO (esquerda). **E -** Número absoluto de macrófagos residentes do tecido adiposo perigonadal de animais WT e LXRαKO. **F -** Percentual e número absoluto de ATMs CD206+ e CD11c+ no tecido adiposo perigonadal de animais WT e LXRαKO. **G -** Razão M1/M2 de ATMs do PgAT de animais WT e LXRαKO. **H -** Expressão gênica de marcadores pró-inflamatórios no PgAT de animais WT e LXRαKO. **I -** Expressão gênica de marcadores anti-inflamatórios no PgAT de animais WT e LXRαKO. **J -** Número absoluto de macrófagos residentes do tecido adiposo perigonadal de animais WT e LXRβKO. **K -** Percentual e número absoluto de ATMs CD206+ e CD11c+ no tecido adiposo perigonadal de animais WT e LXRβKO. **L -** Razão M1/M2 de ATMs do PgAT de animais WT e LXRβKO. **M -** Expressão gênica de marcadores pró-inflamatórios no PgAT de animais WT e LXRβKO. **N -** Expressão gênica de marcadores anti-inflamatórios no PgAT de animais WT e LXRβKO. Valores apresentados no gráfico correspondem a media ± SEM, sendo (*) $p \leq 0.05$, (**) $p \leq 0.01$, n=5 animais/grupo.

5.8. A deleção de LXRβ agrava a inflamação do tecido adiposo em camundongos obesos

A expansão do tecido adiposo em resposta à obesidade promove a quebra da homeostase tecidual, a qual é caracterizada não somente por alterações morfológicas dos adipócitos, mas também leva a alterações no fenótipo das células imunes residentes no WAT, as quais partem de um perfil regulatório/reparador para um perfil pró-inflamatório (95). Além disso, elevados níveis de colesterol promovem a ativação de células imunes (96), e, obesidade leva a alterações metabólicas em células imunes que impactam diretamente na função dessas células através de um mecanismo ainda não compreendido.

Considerando que macrófagos são as células mais abundantes do tecido adiposo de humanos e camundongos (97), nós determinamos se as principais vias metabólicas moduladas pela obesidade em macrófagos poderiam estar associadas ao metabolismo de colesterol. Para tanto, nós usamos dados do transcriptoma disponíveis na literatura (98), empregando dados do sequenciamento de RNA de Pg ATM ($F4/80^{+}CD11b^{+}$) combinando células $CD11c^{+}$ e $CD11c^{-}$ em animais magros e obesos.

Nossas análises revelaram que a via de metabolismo de colesterol é a terceira via modulada positivamente em ATMs de camundongos obesos (Figura 9A). Nós então avaliamos a expressão de genes associados ao metabolismo de colesterol e encontramos que *Nr1h3* e *Nr1h2* (LXRα e LXRβ, respectivamente), bem como genes alvo de LXR, tais como *Lpl*, *Abcg1* e *Apoe* apresentam aumento expressivo nos ATMs de animais obesos (Figura 9B), sugerindo que LXRs exercem um efeito direto em ATMs em condições de obesidade.

Nós então hipotetizamos que LXRs poderiam impactar diretamente no perfil pró-inflamatório de ATMs. Assim, a população de macrófagos residentes do tecido adiposo foi avaliada. Nossos dados revelaram uma redução da população global de ATMs em animais LXRαβKO quando comparados a animais WT (Figura 9C). Diversos grupos tem mostrado que em condições de obesidade alterações significativas são encontradas nas populações de ATMs (99). ATMs apresentam uma constelação de fenótipos (100), e, com intuito de simplificar a observação dos efeitos encontrados nós focamos no estudo de alterações bem estabelecidas, como o desbalanço imune entre macrófagos M1 (CD11c+ ou ATMs pro-inflamatórios) e M2 (CD206+ ou ATMs antiinflamatórios) (64, 101-104).

Nós observamos que a deleção de LXR promove expressiva redução nas populações de ATMs M1 e M2 (Figura 9D-E). Contudo, ao avaliarmos o balanço entre as populações de ATMs nós encontramos que animais LXRαβKO apresentam similar inflamação do tecido adiposo que animais WT obesos, observada pela similaridade na razão M1/M2 encontrada entre ambos grupos de animais (Figura 9F). Assim, embora a deficiência de LXR promova a redução na população de ATMs, em resposta a alimentação hiperlipídica as populações de macrófagos M1 e M2 são igualmente afetadas em animais WT e LXRαβKO.

Nosso próximo passo foi então investigar se a deleção de uma isoforma específica poderia estar associada com a redução nos ATMs observada em animais LXRαβKO. Nós não encontramos diferenças no número de macrófagos totais no PgAT (Figura 9G), ou nas populações M1 ou M2 de ATMs, independente do genótipo dos animais (Figura 9H-J).

Uma vez que a deleção de LXR não afetou o balanço entre ATMs M1/M2, nós decidimos avaliar se LXRs poderiam impactar diretamente sobre a função de ATMs em resposta a HFD. ATMs são células residentes em um ambiente rico em lipídeos, e, em resposta a HFD, é possível se observar a ativação de TLR4 nessas células (105), favorecendo a secreção de citocinas pró-inflamatórias que irão contribuir para o desenvolvimento de outras desordens metabólicas. Assim, nós avaliamos a expressão de citocinas pró-inflamatórias em ATMs de animais WT e deficientes de LXR. Nós observamos que ATMs de animais LXRαβKO apresentam aumentada expressão das citocinas pró-inflamatórias IL-1β, TNF-α e IL-12 (Figura 9K-O) quando comparados a animais WT. Além disso, esse efeito foi diretamente associado com a ausência de LXRβ, uma vez que animais LXRβKO apresentaram aumento significativo dessas citocinas quando comparados a animais LXRαKO

e WT alimentados com a mesma dieta (Figura 9P-T). Esses dados indicam que LXRβ é necessário para a regulação da expressão de citocinas pró-inflamatórias em ATMs, e que sua deleção contribui para o agravamento da inflamação do tecido adiposo induzida pela obesidade.

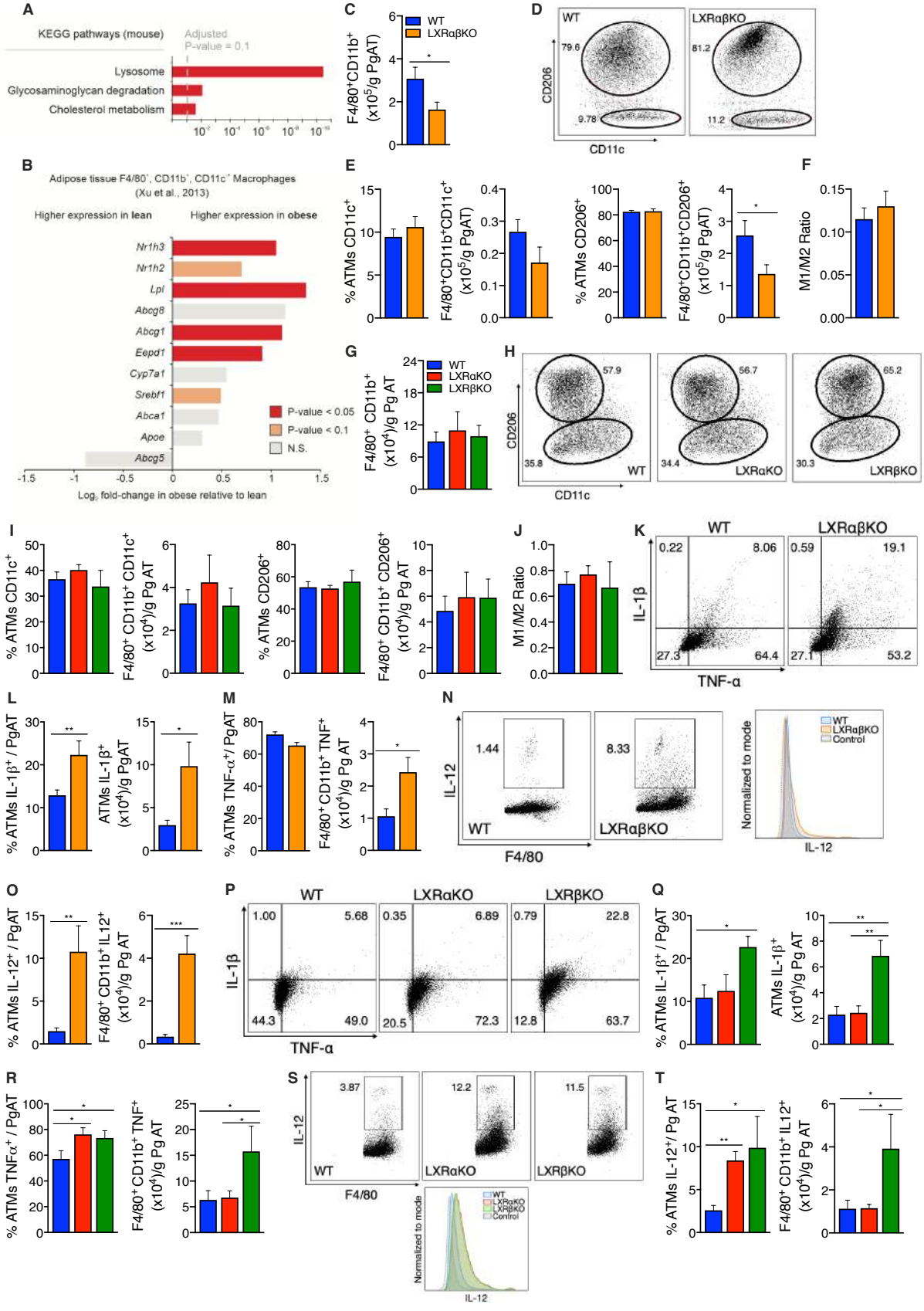

Figura 9 – *A deleção de LXRβ agrava a inflamação do tecido adiposo em camundongos obesos*
A - Análise do enriquecimento de vias metabólicas em macrófagos residentes do tecido adiposo de animais WT magros e obesos usando KEGG. **B -** Transcriptoma de ATMs (F4/80$^+$CD11b$^+$CD11c^{-+}) de animais WT magros e obesos. Valores no gráfico são representados como seguir: cinza p> 0.1; laranja p < 0.1 e vermelho p < 0.05. **C -**

T - Animais WT, LXRαKO, LXRβKO e LXRαβKO foram alimentados com dieta hiperlipídica e a inflamação do tecido adiposo foi avaliada. **C -** População de macrófagos residentes do tecido adiposo em PgAT de animais WT e LXRαβKO, n=8. **D -** Dot plots representativos da população de ATMs M1 e M2 no PgAT. **E -** Percentual e número absoluto de ATMs CD206+ e CD11c+ no tecido adiposo perigonadal. **F -** Razão M1/M2 de ATMs do PgAT de animais WT e LXRαβKO. **G -** População de macrófagos residentes do tecido adiposo em PgAT de animais WT, LXRαKO e LXRβKO, n=6. **H -** Dot plots representativos da população de ATMs M1 e M2 no PgAT. **I -** Percentual e número absoluto de ATMs CD206+ e CD11c+ no tecido adiposo perigonadal. **J -** Razão M1/M2 de ATMs do PgAT de animais WT, LXRαKO e LXRβKO. **K -** Dot plot representativo da expressão de TNF-α e IL-1β em Pg ATMs de animais WT e LXRαβKO. **L -** Representação dos números percentuais e absolutos de ATMs IL-1β+. **M -** Representação dos números percentuais e absolutos de ATMs TNF-α+. **N -** Dot plot e histograma representativos da expressão de IL-12 em Pg ATMs. **O -** Percentual e número absoluto de ATMs IL-12+. **P -** Dot plot representativo da expressão de TNF-α e IL-1β em Pg ATMs de animais WT, LXRαKO e LXRβKO. **Q -** Representação dos números percentuais e absolutos de ATMs IL-1β+. **R -** Representação dos números percentuais e absolutos de ATMs TNF-α+. **S -** Dot plot e histograma representativos da expressão de IL-12 em Pg ATMs. **T -** Percentual e número absoluto de ATMs IL-12+. Dados representam a média ± SEM, sendo (*) $p \leq 0.05$, (**) $p \leq 0.01$, (***) $p \leq 0.001$, sendo os experimentos empregando animais WT, LXRαKO e LXRβKO animais n=6, e animais WT and LXRαβKO n=7.

5.9. A deficiência de LXR em células imunes promove o acúmulo de células pró-inflamatórias no tecido adiposo

Baseado nas observações de que LXRs desempenham papel fundamental na manutenção da homeostase tecidual no PgAT, nós nos perguntamos se tais efeitos poderiam estar associados com a deleção de LXR especificamente em células imunes. Para tanto, nós realizamos o transplante de células da medula óssea de animais WT (WT→WT) ou LXRαβKO (LXRαβKO→WT) em animais WT depletados de células imunes através de irradiação gama (Figura 10A). Após confirmada a repopulação das células imunes, os animais foram alimentados com HFD ou dieta controle e os parâmetros metabólicos foram avaliados. Nossos dados revelaram que a deleção de LXR em células imunes é suficiente para impactar no ganho de peso e acúmulo de gordura corporal em animais alimentados com HFD (Figura 10 B-C), sem no entanto promover alterações no consumo alimentar (Figura 10D) ou no metabolismo de glicose (Figura 10E-G).

Para melhor investigar de que maneira a deleção de LXR em células imunes poderia contribuir para a inflamação do tecido adiposo, nós avaliamos as populações de ATMs. Nós encontramos que LXR exerce papel essencial na manutenção da homeostase imune do PgAT, uma vez que animais LXRαβKO→WT alimentados com HFD apresentaram aumentada inflamação do tecido adiposo, visto pelo aumento de ATMs totais comparados a animais WT→WT alimentados com a mesma dieta (Figura 10H).

Em adição, na ausência de obesidade, animais LXRαβKO→WT apresentaram números elevados de macrófagos M1 comparados a animais WT→WT (Figura 10I).

Consistente com nossos resultados em animais deficientes de LXR a ausência de LXR especificamente em células imunes levou ao aumento de macrófagos M1 e do infiltrado de monócitos em animais alimentados com dieta padrão, mas não em animais alimentados com HFD (Figura 10I-K).

Nosso próximo passo foi então investigar se a ausência de LXR em células imunes afetaria a função dos macrófagos residentes do PgAT. Nossos dados revelaram que ATMs isolados do PgAT de animais LXRαβKO→WT alimentados com HFD apresentam maior expressão de IL-1β (Figura 10L). Além disso, o aumento de IL-1β e IL-12 foi encontrado em animais LXRαβKO→WT alimentados com dieta controle, comparados a animais WT→WT (Figura 10L-M). Juntos, esses dados mostram que LXR desempenha um papel essencial na regulação da função de ATMs durante a obesidade.

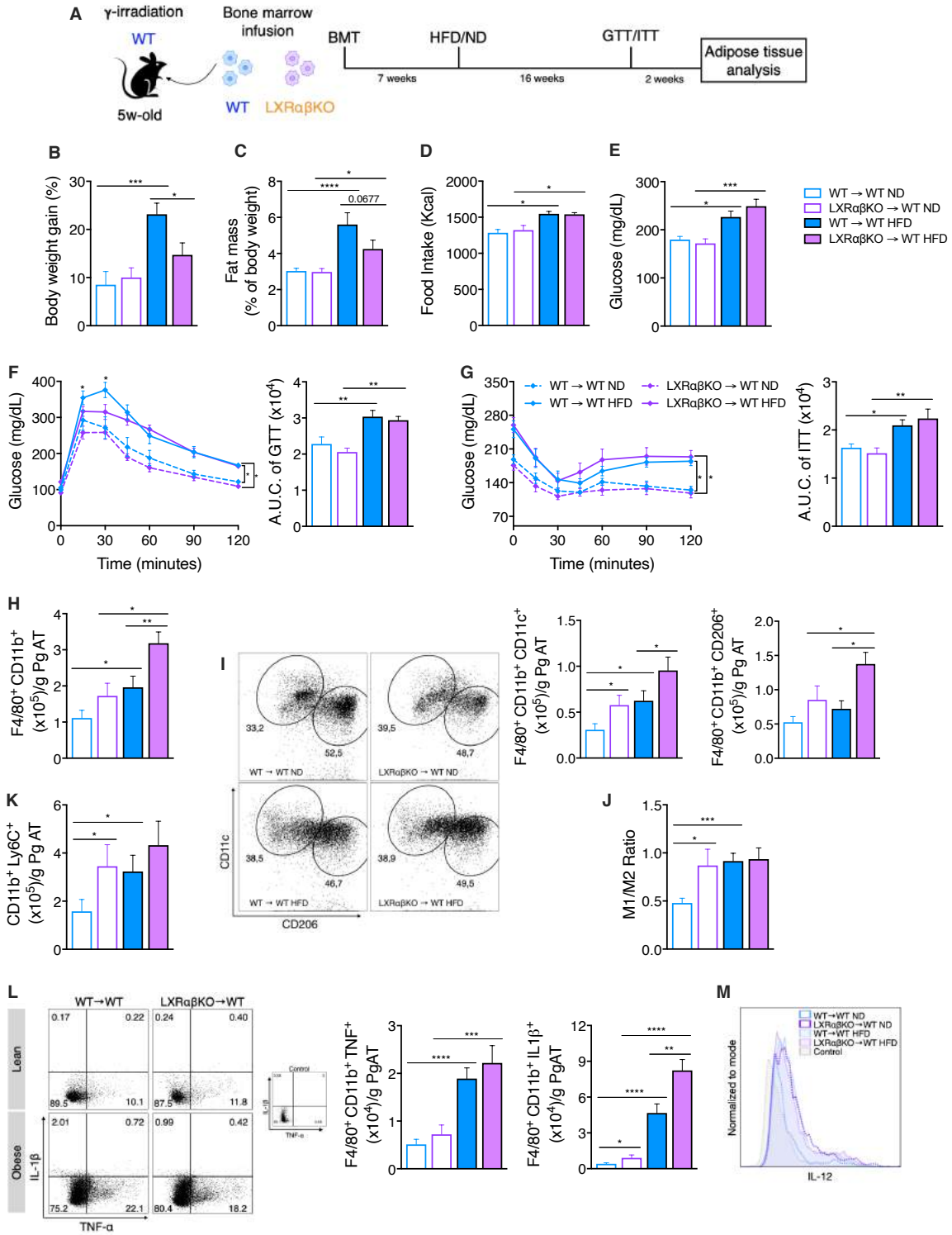

Figura 10 - *A deleção de LXR em macrófagos induz inflamação do tecido adiposo em animais magros*
A - Representação esquemática do protocolo utilizado no transplante de medula óssea (BMT) em animais alimentados com dieta padrão ou HFD. **B -** Ganho de peso corporal em resposta a BMT em animais WT→WT e LXRαβKO→WT. **C -** Massa de tecido adiposo branco em WT→WT e LXRαβKO→WT. **D -** Consumo alimentar total nos animais submetidos a BMT. **E -** Glicemia dos animais submetidos a restrição alimentar por 5 horas. **F -** Teste de tolerância à glicose. **G -** Teste de tolerância à insulina. **H -** População de macrófagos residentes do tecido adiposo em animais transplantados. **I -** Dot plots representativos e número absoluto de ATMs CD206+ e CD11c+ no tecido adiposo perigonadal. **J -** Razão M1/M2 de ATMs do PgAT de animais WT→WT e LXRαβKO→WT. **K -** Número absoluto de monócitos infiltrados no tecido adiposo perigonadal de animais transplantados. **L -** Dot plot e número absoluto de Pg ATMs TNF-α+ e IL-1β+. M - Histograma da população de ATMs IL-12+. Valores apresentados no gráfico correspondem a media ± SEM, sendo (*) p≤0.05, (**) p≤0.01, (***) p≤0.001, (****) p≤0.0001, n=10 animais/grupo.

5.10. Naringenin é um agonista de LXR em macrófagos

A isoforma LXRα tem sido diretamente associada com o aumento da síntese de ácidos graxos e a administração de agonistas de LXR não seletivos tem sido associada com o aumento dos níveis séricos de triglicerídeos (43, 88, 106, 107). Assim, a busca por novos agonistas de LXR que atuem de maneira seletiva sobre a isoforma β tem se tornado cada vez mais atrativa.

Diversos compostos tem sido mostrados capazes de atuar de maneira distinta sobre as isoformas de LXR (108), sendo pouco conhecida a atividade de tais compostos sobre LXRβ. Dentre estes compostos, o flavonóide derivado de frutas cítricas naringenin (NAR) tem sido mostrado capaz de modular a atividade de LXR, exercendo efeitos controversos em tipos celulares distintos. Baseado nisso, nós decidimos avaliar se o tratamento de macrófagos com NAR poderia atuar na regulação das respostas imunes e assim ser empregado no tratamento de doenças metabólicas em que a inflamação é um fator agravante, como a obesidade.

Para tanto, nós realizamos o tratamento de BMDMs com NAR e avaliamos sua capacidade em atuar como um agonista de LXR. Nossos resultados mostram que assim como observado com o agonista sintético GW3965, macrófagos WT tratados com NAR apresentam aumento na expressão dos genes alvo de LXR *Abca1*, *Abcg1*, *Fasn*, *Apoe* e *Lpl*, atuando, dessa forma, como um agonista de LXR em macrófagos (Figura 11A). Em adição, nós observamos que o tratamento com naringenin foi capaz de reverter a redução da expressão de *Abca1* promovida pela ativação de TLR4 em células WT (Figura 11B). Com intuito de avaliar se os efeitos observados se deviam de fato a ativação de LXR, nós realizamos o tratamento de macrófagos deficientes de LXR com NAR, nossos dados revelaram que o aumento na expressão de *Abca1* foi dependente de LXR, reforçando o papel de NAR como agonista de LXR (Figura 11C).

A ativação de LXR tem sido mostrada capaz de induzir a resposta anti-inflamatória (35, 73, 109). Além disso, dados da literatura tem reportado que o tratamento com NAR é capaz de inibir vias associadas com a resposta pró-inflamatória (110, 111). Assim, nós decidimos avaliar se o tratamento de BMDMs com NAR poderia reverter os efeitos promovidos pela ativada de TLR4 com LPS. Nossos dados revelaram que o tratamento com NAR reduziu a secreção de CCL-2, TNF-α, IL-6 e da expressão de *IL-1β* (Figura 11D), bem como promoveu o aumento da expressão do marcador anti-inflamatório *Fizz1* (Figura 11E).

Com intuito de melhor explorar os efeitos da ativação de LXR sobre a reposta de macrófagos, nós realizamos o tratamento de macrófagos polarizados para os perfis M1 (IFNγ+LPS) e M2 (IL4) com NAR. Nossos dados mostram que NAR foi capaz de promover efeitos antiinflamatórios mesmo em macrófagos já polarizados para o perfil M1, visto pela redução na expressão de *Il-12* e *Tnf-α* (Figura 11F). Ainda, nós encontramos que macrófagos M2 apresentam maior expressão de LXRα, bem como dos genes alvo de LXR *Apoe* e *Abca1* (Figura 11G), sendo ainda observado que, em resposta ao tratamento com NAR, a expressão desses genes em macrófagos não polarizados ocorre de maneira similar aos observados em macrófagos M2 (Figura 11G).

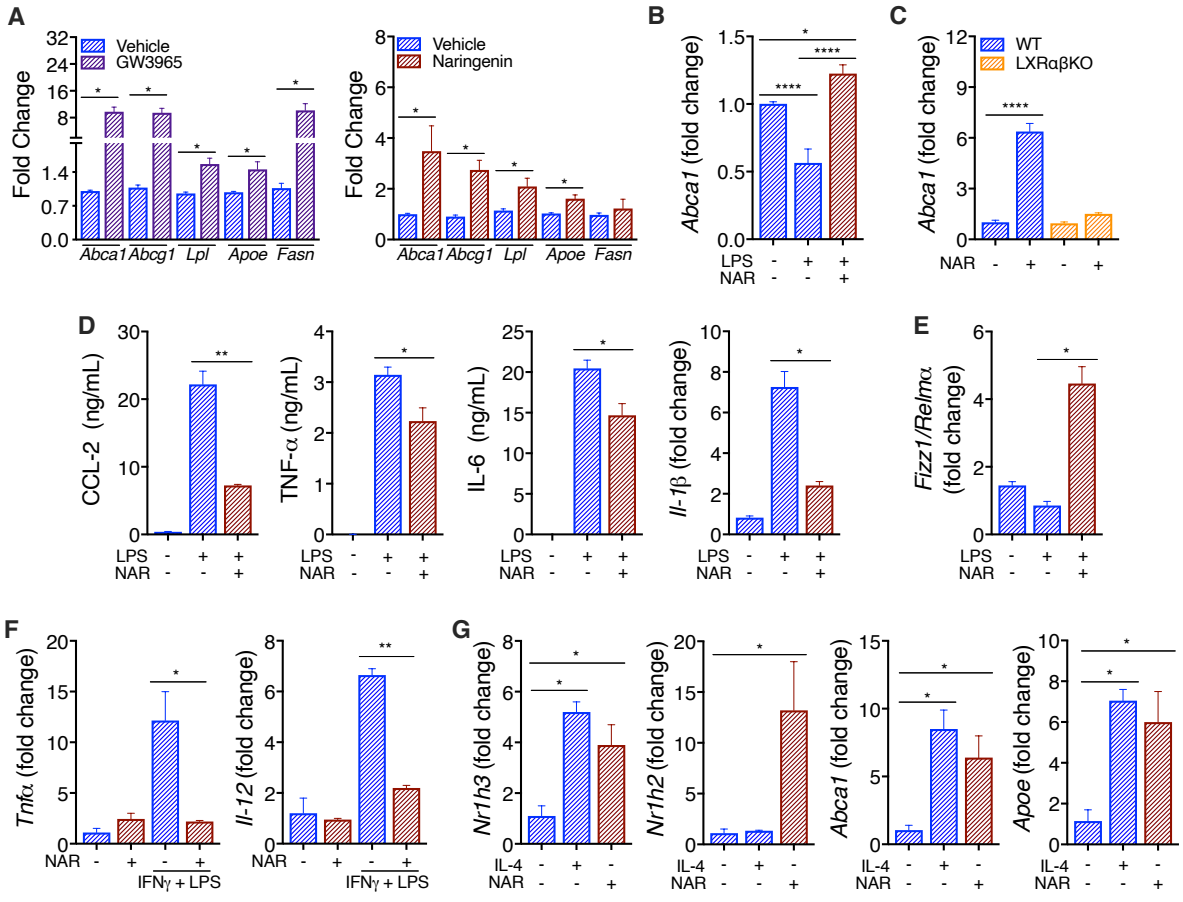

Figura 11 – *Naringenin é um agonista de LXR em macrófagos*
A - Avaliação da expressão de genes alvo de LXR em macrófagos WT tratados com GW3965 e NAR. **B -** Avaliação dos efeitos do tratamento com NAR sobre a expressão de *Abca1* em macrófagos WT ativados com LPS. **C -** Determinação da atividade de NAR como agonista de LXR em BMDMs derivadas de animais WT e LXRαβKO. **D -** Determinação do potencial anti-inflamatório da ativação de LXR induzida por NAR. **E -** Expressão de *Fizz1* em macrófagos estimulados com LPS e tratados com NAR. **F -** Expressão de *Il-12* e *Tnf-α* em macrófagos polarizados para o perfil M1 tratados com NAR. **G -** Avaliação dos genes alvo de LXR em macrófagos M2 tratados com NAR.

5.11. Naringenin aumenta a sensibilidade à insulina em animais obesos por reduzir a inflamação do tecido adiposo

Tendo em vista o potencial efeito de NAR sobre a ativação de LXR bem como seus efeitos na regulação da resposta de macrófagos, nós decidimos avaliar o impacto que o tratamento *in vivo* com NAR poderia ter sobre animais *wild type* submetidos ao modelo de obesidade induzida por dieta. Assim, animais obesos resistentes à insulina foram tratados com NAR durante 4 semanas (Figura 12A). Nossos dados mostram que o tratamento com NAR não induziu alterações no ganho de peso corporal e consumo alimentar (Figura 12B-C), bem como nos níveis séricos de triglicerídeos (Figura 12D).

Um dos grandes problemas associados a obesidade é o desenvolvimento de resistencia à insulina (84). De fato, a ativação de LXR tem sido mostrada promover efeitos benéficos em modelos de obesidade (112). Assim, nós avaliamos se o tratamento com NAR poderia impactar a resposta de animais obesos frente ao estímulo com insulina exógena. Nossos dados revelaram que a ativação de LXR com NAR promoveu maior sensibilidade à insulina em animais obesos quando comparados a animais obesos tratados com veículo (Figura 12E).

Diversos trabalhos têm mostrado uma associação direta entre inflamação do tecido adiposo e alterações na resposta à insulina (17, 19). Assim, nós decidimos avaliar como a ativação de LXR com NAR poderia afetar a população de PgATMs dos animais submetidos ao modelo de obesidade. Consistente com os dados reportados previamente, nossos resultados indicam o aumento na frequência de ATMs em animais obesos (Figura 12F).

De maneira interessante, nossos dados revelaram que o tratamento de animais obesos com NAR foi capaz de reduzir a inflamação do tecido adiposo, visto pela diminuição na população de ATMs M1 (Figura 12G-H), pelo menor infiltrado de monócitos (Figura 12I), bem como pelo número reduzido de ATMs TNF-α^+ e IL-1β^+ (Figura 12J-K). Coletivamente, nossos dados reforçam o papel terapêutico de NAR como um agonista de LXR capaz de reduzir a inflamação do tecido adiposo induzida pela obesidade, e assim, promover a melhora sensibilidade à insulina.

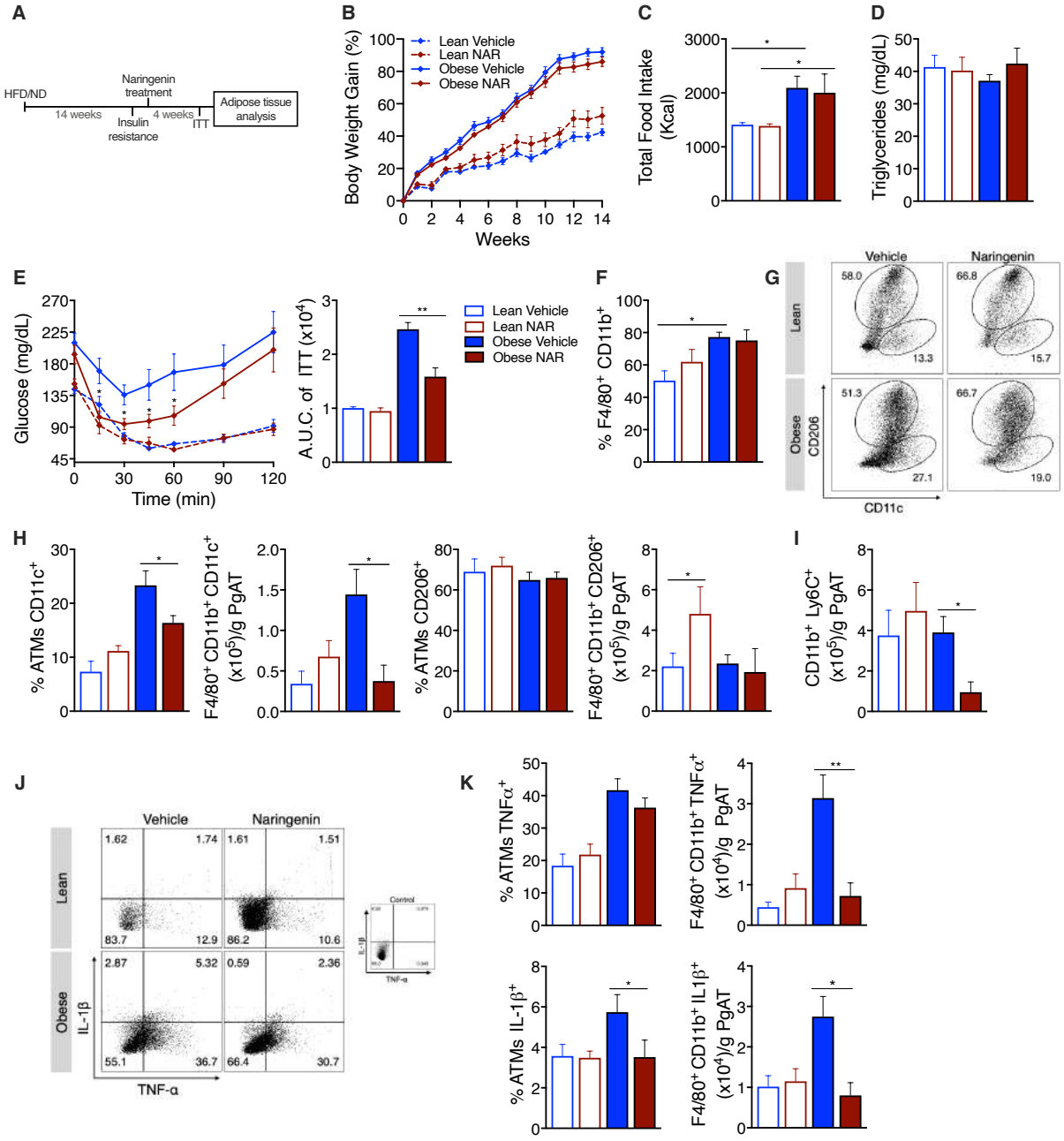

Figura 12 – *Naringenin aumenta a sensibilidade à insulina em animais obesos por reduzir a inflamação do tecido adiposo.*

A - Representação esquemática do tratamento *in vivo* com NAR empregado em animais submetidos ao modelo de obesidade ou dieta controle. **B -** Avaliação do peso corporal em animais WT alimentados com HFD ou dieta controle e tratados ou não com NAR. **C -** Consumo alimentar total. **D -** Níveis séricos de triglicerídeos. **E -** Teste de tolerância à insulina. **F -** População de macrófagos residentes do tecido adiposo em animais tratados com NAR ou veículo. **G -** Dot plots representativos de ATMs M1 e M2 no Pg AT. **H -** Percentual e número absoluto de ATMs CD206+ e CD11c+ no tecido adiposo perigonadal. **I -** Número absoluto de monócitos infiltrados no tecido adiposo perigonadal de animais tratados. **J -** Dot plot representativo das populações de Pg ATMs TNF-α+ e IL-1β+. **K -** Percentual e número absoluto de Pg ATMs TNF-α+ e IL-1β+. Valores apresentados no gráfico correspondem a media ± SEM, sendo (*) p≤0.05, (**) p≤0.01, (***) p≤0.001, (****) p≤0.0001, n=8 animais/ grupo.

5.12. Naringenin promove efeitos anti-inflamatórios por modular o metabolismo de macrófagos através da ativação de LXRβ

Diversos trabalhos tem relatado que o estímulo pró-inflamatório promove alterações metabólicas importantes em macrófagos, sendo observado um aumento da glicólise a qual é essencial para o estabelecimento da resposta efetora destas células (56-58). Assim, nós decidimos investigar como a ativação de LXR poderia modular o metabolismo de macrófagos.

Considerando as diferenças nos níveis de expressão de LXRα e LXRβ em resposta à polarização M2 (Figura 11G), nós decidimos avaliar se os efeitos antiinflamatórios observados em resposta ao tratamento com NAR poderiam estar associados com alterações no metabolismo celular bem como com a ativação de uma isoforma específica de LXR. Para tanto, macrófagos WT ou deletados de LXR foram tratados com NAR e estimulados com LPS ou polarizados para o perfil M1. Nossos resultados mostram que a ativação e polarização de macrófagos levam ao aumento na expressão de marcadores da via glicolítica, e o tratamento com NAR é capaz de reverter o aumento da expressão de *Pfkfb3* e *Ldha*, sendo esse efeito dependente de LXRβ (Figura 13A-B). Em adição, o tratamento com NAR promoveu a diminuição da atividade glicolítica em macrófagos WT estimulados com LPS (Figura 13C).

O aumento da taxa glicolítica em macrófagos estimulados tem sido associado com alterações na mitocôndria, marcadas por "quebras" no ciclo de Krebs e disfunção mitocondrial , a qual tem sido mostrada ser revertida em resposta ao estímulo anti-inflamatório (57, 113). Baseado nisso, nós investigamos se a ativação de LXR com NAR poderia levar a alterações na função mitocondrial. Assim, BMDMs foram marcadas com MitoTracker Green e MitoTracker Red, para avaliação do conteúdo mitocondrial e potencial de membrana mitocondrial respectivamente (113). Nossos resultados revelaram que o tratamento com NAR é capaz de diminuir a disfunção mitocondrial em macrófagos ativados com LPS, sendo esse efeito observado em células WT mas não em macrófagos LXRαβKO, revelando um importante envolvimento de LXRs na modulação do metabolismo de macrófagos (Figura 13D).

Nós então decidimos avaliar se NAR poderia modular a função de macrófagos através da ativação de uma isoforma específica. Consistente com a avaliação das enzimas associadas com o metabolismo glicolítico, nossos resultados mostram que o tratamento com NAR

reduziu a expressão de *Nos2* de maneira dependente de LXRβ (Figura 13E). Adicionalmente, nossos dados mostram que o aumento na expressão dos marcadores de perfil M2 *Fizz1* e *Ym1* em resposta ao tratamento com NAR ocorreu de maneira independente de uma única isoforma do receptor (Figura 13F). Juntos nossos dados sugerem que NAR é capaz de promover modulação do metabolismo celular, inibindo as respostas pró-inflamatórias por meio da ativação de LXRβ, bem como por um mecanismo adicional em que promove a indução de mediadores anti-inflamatórios de maneira independente de uma isoforma específica de LXR.

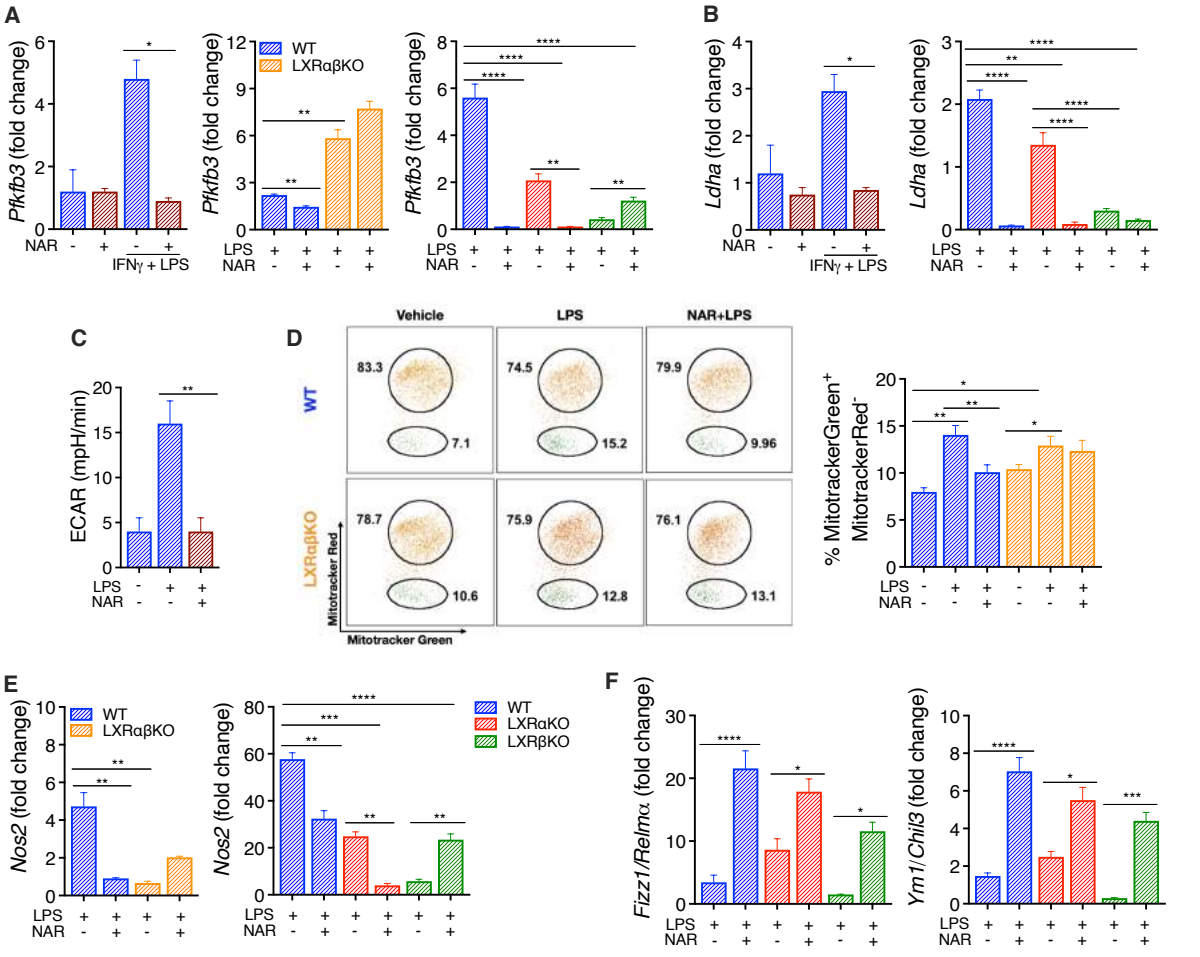

Figura 13 - *A ativação de LXR com NAR modula o metabolismo de macrófagos.*
Macrófagos derivados da medula óssea de camundongos WT, LXRαKO, LXRβKO e LXRαβKO foram pré-tratados com 0.5 μM de NAR e estimulados com 100 ng/mL LPS ou polarizados para o perfil M1 com LPS+IFNγ durante 24 horas. **A-** Avaliação da expressão de *Pfkfb3*. **B -**Avaliação da expressão de *Ldha*. **C -** Avaliação do metabolismo glicolítico de macrófagos WT tratados com NAR. **D -** Avaliação do potencial de membrana mitocondrial em resposta ao tratamento com NAR em macrófagos ativados com LPS. **E -** Determinação da expressão de *Nos2* em macrófagos WT e deficientes de LXR. **F -** Avaliação da expressão de marcadores antiinflamatórios *Fizz1* e *Ym1* em macrófagos WT ou deficientes de LXR tratados com NAR e estimulados com LPS. Dados representam a média ± SEM, sendo (*) p≤0.05, (**) p≤0.01, (***) p≤0.001, (****) p≤0.0001.

6. DISCUSSÃO

Obesidade alcançou taxas epidêmicas no mundo todo e atualmente é um problema de saúde pública. O fácil acesso a dietas hipercalóricas combinada com os avanços tecnológicos promoveram mudanças que favorecem o estilo de vida sedentário e sobrepeso. Juntamente com o sobrepeso outras doenças como desordens cardiovasculares, dislipidemias e resistencia à insulina são frequentemente observadas em indivíduos obesos (114). Assim, a busca por novos alvos terapêuticos com o potencial de tratar obesidade bem como as demais desordens associadas a essa doença tem se tornado altamente necessária.

Aqui, nós descrevemos um novo papel para LXR na regulação da homeostase do tecido adiposo. Nós mostramos que LXR é um fator chave para a manutenção do balanço imune no AT. De fato, os efeitos de LXR tem sido amplamente estudado na patogênese da aterosclerose (115-117), e esses estudos tem clarificado as ações de LXR no que se refere à modulação do metabolismo e função de macrófagos, bem como sua influência na regulação da homeostase corporal. No entanto, a maneira pela qual a ativação ou deficiência de LXR afeta a população de macrófagos residentes do tecido adiposo, especialmente em condições de obesidade permanece a ser elucidada. Além disso, poucos estudos tem focado em entender se as diferentes isoformas de LXR podem desempenhar papéis distintos na regulação do metabolismo e imunidade (91). Sendo assim, nós decidimos investigar como LXRα e LXRβ poderiam modular a função e metabolismo de macrófagos, bem como o papel de cada isoforma na regulação da homeostase corporal.

Nós encontramos que as isoformas de LXR desempenham papéis distintos *in vivo*. A deleção de LXRβ mas não de LXRα promoveu intolerância à glicose. Esses dados são consistentes com trabalhos anteriores mostrando que LXR coordena tanto o metabolismo lipídico quanto a homeostase de glicose (33, 118, 119). LXR tem sido mostrado capaz de promover a indução transcricional de Glut4, bem como induzir a produção e secreção de insulina em células β pancreáticas (118, 119), nós extrapolamos que LXRβ pode exercer um papel essencial nesse processo, no entanto, a realização de experimentos adicionais se faz necessária afim de verificar se tal função pode ser de fato atribuída a essa isoforma de LXR.

Juntamente com as alterações morfológicas que ocorrem no AT, como as alterações no tamanho e número de adipócitos e alterações no perfil de secreção de adipocinas, a obesidade induz alterações na população de células imunes residentes do tecido adiposo (48, 50, 62-64),

gerando um microambiente inflamatório marcado pela presença de macrófagos CD11c+ que secretam citocinas pró-inflamatórias bem como pelo aumentado recrutamento de monócitos para o tecido adiposo (16, 17, 65). Nossos dados mostraram que a deleção de LXR *per si* é suficiente para levar o tecido adiposo a um estado inflamatório similar ao observado em condições de obesidade, no qual o desbalanço entre macrófagos CD11c+ e CD206+ é observado. Além disso, nós encontramos que a deleção de LXRβ agrava a inflamação do tecido adiposo induzida pela obesidade. Em adição, a deleção de LXR especificamente em células imunes promoveu um quadro inflamatório no AT, o qual pode ser observado pelo aumentado número de ATMs pró-inflamatórios em animais magros e obesos.

As células imunes pró-inflamatórias possuem uma assinatura metabólica única, a qual é caracterizada pelo aumento da via glicolítica, a "quebra" do ciclo do ácido cítrico (TCA) e disfunção mitocondrial (120-123). Nós encontramos que naringenin é um agonista de LXR capaz de modular o metabolismo e função de macrófagos, promovendo a redução da taxa glicolítica, disfunção mitocondrial e consequentemente, reduzindo o perfil pró-inflamatório dessas células.

Trabalhos de outros grupos tem demonstrado que a expressão do gene alvo de LXR, *Abca1* é essencial para o transporte reverso de colesterol, e que sua ausência está diretamente ligada à patogênese da aterosclerose (117). Nossos resultados revelaram que o estímulo pró-inflamatório prejudica a expressão de *Abca1* (Figura 4F e Figura 11B), bem como promove o aumento de corpúsculos lipídicos em macrófagos (Figura 4G), levando os macrófagos a um perfil pró-inflamatório. De maneira interessante, o tratamento com NAR induziu a expressão de *Abca1* em um modo dependente de LXR (Figura 11C).

É importante destacar que diversos estudos tem sido realizados com intuito de compreender como LXR modulam a resposta imune, e como os efeitos anti-inflamatórios promovidos pela ativação de LXR poderiam ser empregadas no tratamento de doenças imuno mediadas (43, 67, 74, 75, 109, 124, 125). Contudo, foi demonstrado que os agonistas clássicos de LXR induzem a expressão de genes relacionados à síntese de ácidos graxos e, dessa forma, promovem aumento indesejado dos níveis de triglicerídeos no sangue e fígado,o qual foi associado principalmente com a ativação de LXRα (126-128).

Em nosso trabalho nós buscamos compreender como isoformas específicas desses receptores presentes em macrófagos residentes do tecido adiposo podem modular a

homeostase tecidual e resposta inflamatória. Nós descrevemos que naringenin atua como um agonista de LXRβ em macrófagos, e que tal ativação reduz a inflamação do AT, sem promover efeitos na síntese de triglicerídeos. Em adição nossos dados revelaram que a ativação de LXRβ promovida pelo tratamento com NAR induz o aumento da sensibilidade à insulina em animais obesos.

Coletivamente, nossos dados reforçam que LXRα e LXRβ exibem papéis distintos na regulação da resposta de macrófagos e homeostase de glicose. Este estudo contribui para um melhor entendimento de como as isoformas de receptores nucleares podem apresentar funções distintas e serve como o primeiro passo para o desenvolvimento de novas terapias que tenham como alvo a ativação de LXRβ e seu emprego no tratamento de doenças metabólicas associadas a inflamação.

7. CONCLUSÃO

Liver X receptors desempenham papel fundamental na regulação da homeostase corporal, e sua deleção afeta diretamente o metabolismo de glicose. Além de seu papel na regulação metabólica, LXRs são essenciais para o balanço imune de células residentes do tecido adiposo. A deleção de LXR agravou a inflamação do AT, favorecendo o estabelecimento de um perfil pró-inflamatório, marcado pelo desbalanço entre macrófagos $CD11c^+$ e $CD206^+$ em animais magros, bem como pelo agravamento de inflamação induzida pela obesidade.

Nós encontramos um novo agonista de LXR, naringenin, o qual foi capaz de promover melhora significativa no quadro de resistência à insulina induzida por obesidade, através da promoção de melhora da inflamação do tecido adiposo. Este efeito foi associado com sua capacidade em induzir o efluxo de lipídios, bem como com a menor disfunção mitocondrial e reduzida taxa glicolítica em macrófagos, o que, consequentemente levou a secreção reduzida de citocinas pró-inflamatórias em células ativadas ou polarizadas para o perfil M1 e o aumento da expressão de marcadores antiinflamatórios.

Tais efeitos apresentados pelo agonista de LXR tornam-se extremamente relevantes uma vez que em condições de obesidade um quadro inflamatório crônico é observado, sendo a secreção de citocinas pró-inflamatórias por ATMs um dos principais responsáveis pela inflamação sistêmica de baixo grau e subsequente resistência a insulina.

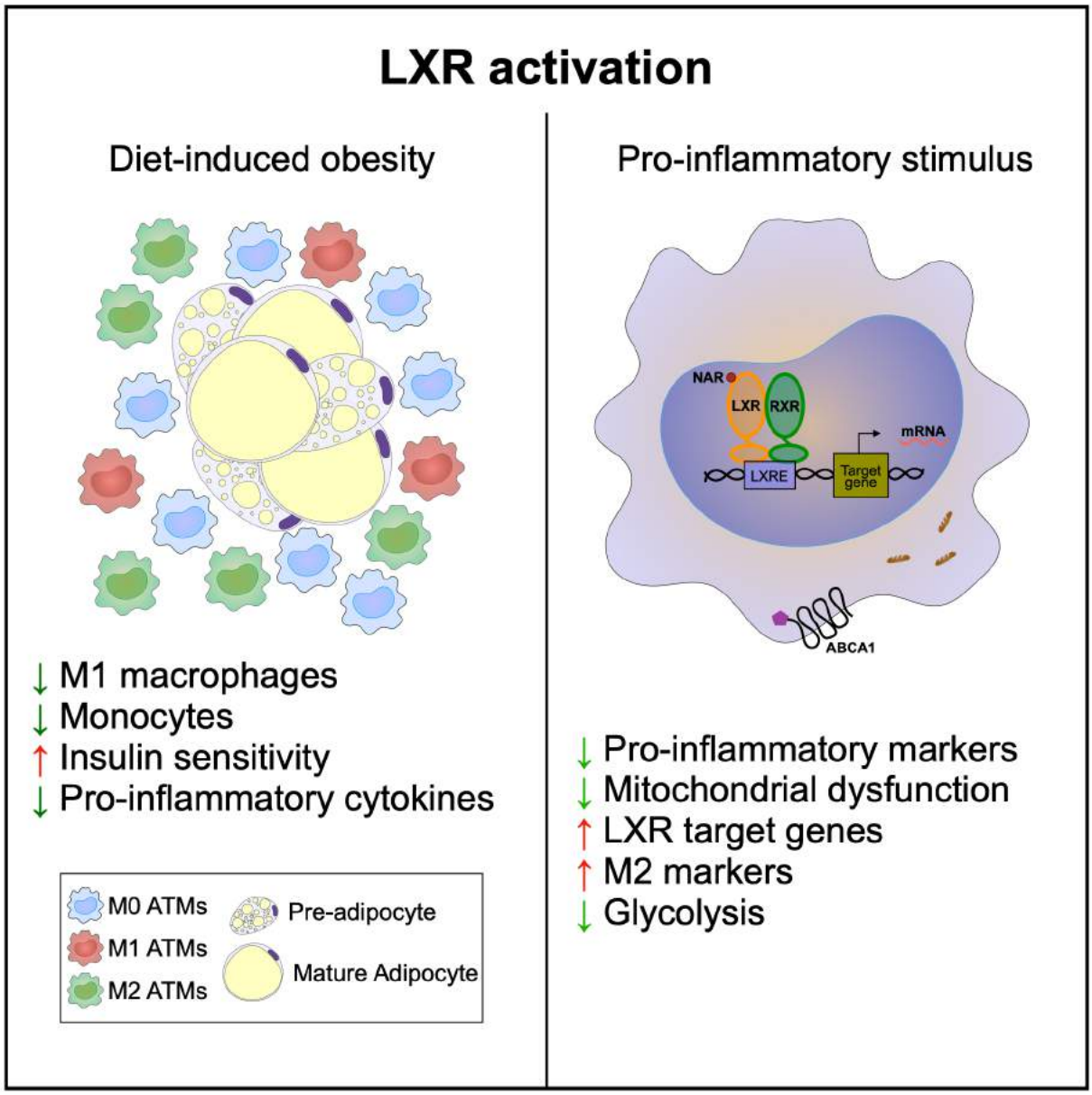

Figura 14 - *Resumo gráfico dos resultados obtidos*

Painel direito - A ativação de LXR *in vivo* promovida pelo tratamento de animais obesos com naringenin reduz a inflamação do tecido adiposo, marcada pela redução nos número de macrófagos M1, do infiltrado de monócitos, bem como pela redução da expressão de citocinas pró-inflamatórias em ATMs, resultando no aumento da sensibilidade à insulina. Painel esquerdo - *In vitro*, a ativação de LXR leva ao menor acúmulo de corpúsculos lipídicos e menor secreção de citocinas pró-inflamatórias através da modulação do metabolismo celular. NAR é capaz de reduzir a taxa glicolítica e disfunção mitocondrial em BMDMs, ao passo que promove o aumento da expressão de marcadores antiinflamatórios.

BIBLIOGRAFIA

1. N. A. Fairbridge *et al.*, Loss of CD24 in Mice Leads to Metabolic Dysfunctions and a Reduction in White Adipocyte Tissue. *PLoS One* **10**, e0141966 (2015).
2. A. Gomez-Hernandez, N. Beneit, S. Diaz-Castroverde, O. Escribano, Differential Role of Adipose Tissues in Obesity and Related Metabolic and Vascular Complications. *Int J Endocrinol* **2016**, 1216783 (2016).
3. H. The Lancet Public, Tackling obesity seriously: the time has come. *Lancet Public Health* **3**, e153 (2018).
4. P. Gonzalez-Muniesa *et al.*, Obesity. *Nat Rev Dis Primers* **3**, 17034 (2017).
5. B. P. Leitner *et al.*, Mapping of human brown adipose tissue in lean and obese young men. *Proc Natl Acad Sci U S A* **114**, 8649-8654 (2017).
6. M. E. Vazquez-Vela, N. Torres, A. R. Tovar, White adipose tissue as endocrine organ and its role in obesity. *Arch Med Res* **39**, 715-728 (2008).
7. P. Cohen, S. Kajimura, The cellular and functional complexity of thermogenic fat. *Nat Rev Mol Cell Biol* **22**, 393-409 (2021).
8. A. Chait, L. J. den Hartigh, Adipose Tissue Distribution, Inflammation and Its Metabolic Consequences, Including Diabetes and Cardiovascular Disease. *Front Cardiovasc Med* **7**, 22 (2020).
9. B. Antuna-Puente, B. Feve, S. Fellahi, J. P. Bastard, Adipokines: the missing link between insulin resistance and obesity. *Diabetes Metab* **34**, 2-11 (2008).
10. S. Galic, J. S. Oakhill, G. R. Steinberg, Adipose tissue as an endocrine organ. *Mol Cell Endocrinol* **316**, 129-139 (2010).
11. S. S. Choe, J. Y. Huh, I. J. Hwang, J. I. Kim, J. B. Kim, Adipose Tissue Remodeling: Its Role in Energy Metabolism and Metabolic Disorders. *Front Endocrinol (Lausanne)* **7**, 30 (2016).
12. E. K. Oikonomou, C. Antoniades, The role of adipose tissue in cardiovascular health and disease. *Nat Rev Cardiol* **16**, 83-99 (2019).
13. E. D. Rosen, B. M. Spiegelman, What we talk about when we talk about fat. *Cell* **156**, 20-44 (2014).
14. P. Bora, A. S. Majumdar, Adipose tissue-derived stromal vascular fraction in regenerative medicine: a brief review on biology and translation. *Stem Cell Res Ther* **8**, 145 (2017).
15. M. Longo *et al.*, Adipose Tissue Dysfunction as Determinant of Obesity-Associated Metabolic Complications. *Int J Mol Sci* **20**, (2019).
16. J. C. McNelis, J. M. Olefsky, Macrophages, immunity, and metabolic disease. *Immunity* **41**, 36-48 (2014).
17. G. S. Hotamisligil, N. S. Shargill, B. M. Spiegelman, Adipose expression of tumor necrosis factor-alpha: direct role in obesity-linked insulin resistance. *Science* **259**, 87-91 (1993).
18. G. S. Hotamisligil, Molecular mechanisms of insulin resistance and the role of the adipocyte. *Int J Obes Relat Metab Disord* **24 Suppl 4**, S23-27 (2000).
19. J. Jager, T. Gremeaux, M. Cormont, Y. Le Marchand-Brustel, J. F. Tanti, Interleukin-1beta-induced insulin resistance in adipocytes through down-regulation of insulin receptor substrate-1 expression. *Endocrinology* **148**, 241-251 (2007).

20. D. Jacobi, K. J. Stanya, C. H. Lee, Adipose tissue signaling by nuclear receptors in metabolic complications of obesity. *Adipocyte* **1**, 4-12 (2012).
21. G. A. Francis, E. Fayard, F. Picard, J. Auwerx, Nuclear receptors and the control of metabolism. *Annu Rev Physiol* **65**, 261-311 (2003).
22. V. K. Dhiman, M. J. Bolt, K. P. White, Nuclear receptors in cancer - uncovering new and evolving roles through genomic analysis. *Nat Rev Genet* **19**, 160-174 (2018).
23. G. I. Mazaira *et al.*, The Nuclear Receptor Field: A Historical Overview and Future Challenges. *Nucl Receptor Res* **5**, (2018).
24. P. Huang, V. Chandra, F. Rastinejad, Structural overview of the nuclear receptor superfamily: insights into physiology and therapeutics. *Annu Rev Physiol* **72**, 247-272 (2010).
25. R. Sever, C. K. Glass, Signaling by nuclear receptors. *Cold Spring Harb Perspect Biol* **5**, a016709 (2013).
26. N. Novac, T. Heinzel, Nuclear receptors: overview and classification. *Curr Drug Targets Inflamm Allergy* **3**, 335-346 (2004).
27. J. Sonoda, L. Pei, R. M. Evans, Nuclear receptors: decoding metabolic disease. *FEBS Lett* **582**, 2-9 (2008).
28. M. Pawlak, P. Lefebvre, B. Staels, General molecular biology and architecture of nuclear receptors. *Curr Top Med Chem* **12**, 486-504 (2012).
29. F. Rastinejad, P. Huang, V. Chandra, S. Khorasanizadeh, Understanding nuclear receptor form and function using structural biology. *J Mol Endocrinol* **51**, T1-T21 (2013).
30. V. Nurminen, S. Seuter, C. Carlberg, Primary Vitamin D Target Genes of Human Monocytes. *Front Physiol* **10**, 194 (2019).
31. V. Perissi, M. G. Rosenfeld, Controlling nuclear receptors: the circular logic of cofactor cycles. *Nat Rev Mol Cell Biol* **6**, 542-554 (2005).
32. R. M. Evans, D. J. Mangelsdorf, Nuclear Receptors, RXR, and the Big Bang. *Cell* **157**, 255-266 (2014).
33. B. A. Laffitte *et al.*, LXRs control lipid-inducible expression of the apolipoprotein E gene in macrophages and adipocytes. *Proc Natl Acad Sci U S A* **98**, 507-512 (2001).
34. S. M. Ulven, K. T. Dalen, J. A. Gustafsson, H. I. Nebb, Tissue-specific autoregulation of the LXRalpha gene facilitates induction of apoE in mouse adipose tissue. *J Lipid Res* **45**, 2052-2062 (2004).
35. A. C. Calkin, P. Tontonoz, Transcriptional integration of metabolism by the nuclear sterol-activated receptors LXR and FXR. *Nat Rev Mol Cell Biol* **13**, 213-224 (2012).
36. C. Hong, P. Tontonoz, Coordination of inflammation and metabolism by PPAR and LXR nuclear receptors. *Curr Opin Genet Dev* **18**, 461-467 (2008).
37. C. Y. Lin, J. A. Gustafsson, Targeting liver X receptors in cancer therapeutics. *Nat Rev Cancer* **15**, 216-224 (2015).
38. T. Jakobsson, E. Treuter, J. A. Gustafsson, K. R. Steffensen, Liver X receptor biology and pharmacology: new pathways, challenges and opportunities. *Trends Pharmacol Sci* **33**, 394-404 (2012).
39. P. A. Edwards, M. A. Kennedy, P. A. Mak, LXRs; oxysterol-activated nuclear receptors that regulate genes controlling lipid homeostasis. *Vascul Pharmacol* **38**, 249-256 (2002).
40. K. D. Whitney *et al.*, Liver X receptor (LXR) regulation of the LXRalpha gene in human macrophages. *J Biol Chem* **276**, 43509-43515 (2001).

41. N. Mitro *et al.*, The nuclear receptor LXR is a glucose sensor. *Nature* **445**, 219-223 (2007).
42. K. T. Dalen, S. M. Ulven, K. Bamberg, J. A. Gustafsson, H. I. Nebb, Expression of the insulin-responsive glucose transporter GLUT4 in adipocytes is dependent on liver X receptor alpha. *J Biol Chem* **278**, 48283-48291 (2003).
43. A. Ito *et al.*, LXRs link metabolism to inflammation through Abca1-dependent regulation of membrane composition and TLR signaling. *Elife* **4**, e08009 (2015).
44. L. Monteiro, J. Pereira, L. Palhinha, P. M. M. Moraes-Vieira, Leptin in the regulation of the immunometabolism of adipose tissue-macrophages. *J Leukoc Biol* **106**, 703-716 (2019).
45. D. L. Laskin, V. R. Sunil, C. R. Gardner, J. D. Laskin, Macrophages and tissue injury: agents of defense or destruction? *Annu Rev Pharmacol Toxicol* **51**, 267-288 (2011).
46. A. Shapouri-Moghaddam *et al.*, Macrophage plasticity, polarization, and function in health and disease. *J Cell Physiol* **233**, 6425-6440 (2018).
47. F. O. Martinez, S. Gordon, The M1 and M2 paradigm of macrophage activation: time for reassessment. *F1000Prime Rep* **6**, 13 (2014).
48. A. Castoldi, C. Naffah de Souza, N. O. Camara, P. M. Moraes-Vieira, The Macrophage Switch in Obesity Development. *Front Immunol* **6**, 637 (2015).
49. T. Kimura *et al.*, Polarization of M2 macrophages requires Lamtor1 that integrates cytokine and amino-acid signals. *Nat Commun* **7**, 13130 (2016).
50. J. Pereira, F. C. da Silva, P. M. M. de Moraes-Vieira, The Impact of Ghrelin in Metabolic Diseases: An Immune Perspective. *J Diabetes Res* **2017**, 4527980 (2017).
51. A. Sica, A. Mantovani, Macrophage plasticity and polarization: in vivo veritas. *J Clin Invest* **122**, 787-795 (2012).
52. S. Fujisaka *et al.*, Regulatory mechanisms for adipose tissue M1 and M2 macrophages in diet-induced obese mice. *Diabetes* **58**, 2574-2582 (2009).
53. T. Lawrence, G. Natoli, Transcriptional regulation of macrophage polarization: enabling diversity with identity. *Nat Rev Immunol* **11**, 750-761 (2011).
54. P. J. Murray, T. A. Wynn, Protective and pathogenic functions of macrophage subsets. *Nat Rev Immunol* **11**, 723-737 (2011).
55. T. Roszer, Understanding the Mysterious M2 Macrophage through Activation Markers and Effector Mechanisms. *Mediators Inflamm* **2015**, 816460 (2015).
56. F. Correa-da-Silva, J. A. S. Pereira, C. F. de Aguiar, P. M. M. de Moraes-Vieira, Mitoimmunity-when mitochondria dictates macrophage function. *Cell Biol Int* **42**, 651-655 (2018).
57. L. A. O'Neill, R. J. Kishton, J. Rathmell, A guide to immunometabolism for immunologists. *Nat Rev Immunol* **16**, 553-565 (2016).
58. B. Kelly, L. A. O'Neill, Metabolic reprogramming in macrophages and dendritic cells in innate immunity. *Cell Res* **25**, 771-784 (2015).
59. C. N. S. Breda, G. G. Davanzo, P. J. Basso, N. O. Saraiva Camara, P. M. M. Moraes-Vieira, Mitochondria as central hub of the immune system. *Redox Biol* **26**, 101255 (2019).
60. M. Gong, X. Zhuo, A. Ma, STAT6 Upregulation Promotes M2 Macrophage Polarization to Suppress Atherosclerosis. *Med Sci Monit Basic Res* **23**, 240-249 (2017).
61. C. Diskin, E. M. Palsson-McDermott, Metabolic Modulation in Macrophage Effector Function. *Front Immunol* **9**, 270 (2018).

62. A. Castrillo, P. Tontonoz, Nuclear receptors in macrophage biology: at the crossroads of lipid metabolism and inflammation. *Annu Rev Cell Dev Biol* **20**, 455-480 (2004).
63. P. M. Moraes-Vieira, E. J. Bassi, R. C. Araujo, N. O. Camara, Leptin as a link between the immune system and kidney-related diseases: leading actor or just a coadjuvant? *Obes Rev* **13**, 733-743 (2012).
64. P. M. Moraes-Vieira *et al.*, RBP4 activates antigen-presenting cells, leading to adipose tissue inflammation and systemic insulin resistance. *Cell Metab* **19**, 512-526 (2014).
65. H. Xu *et al.*, Chronic inflammation in fat plays a crucial role in the development of obesity-related insulin resistance. *J Clin Invest* **112**, 1821-1830 (2003).
66. J. Laurencikiene, M. Ryden, Liver X receptors and fat cell metabolism. *Int J Obes (Lond)* **36**, 1494-1502 (2012).
67. S. B. Joseph *et al.*, LXR-dependent gene expression is important for macrophage survival and the innate immune response. *Cell* **119**, 299-309 (2004).
68. C. Hong *et al.*, Constitutive activation of LXR in macrophages regulates metabolic and inflammatory gene expression: identification of ARL7 as a direct target. *J Lipid Res* **52**, 531-539 (2011).
69. B. Pourcet *et al.*, The nuclear receptor LXR modulates interleukin-18 levels in macrophages through multiple mechanisms. *Sci Rep* **6**, 25481 (2016).
70. J. K. Nelson *et al.*, EEPD1 Is a Novel LXR Target Gene in Macrophages Which Regulates ABCA1 Abundance and Cholesterol Efflux. *Arterioscler Thromb Vasc Biol* **37**, 423-432 (2017).
71. S. Beceiro *et al.*, Liver X Receptor Nuclear Receptors Are Transcriptional Regulators of Dendritic Cell Chemotaxis. *Mol Cell Biol* **38**, (2018).
72. I. G. Schulman, Liver X receptors link lipid metabolism and inflammation. *FEBS Lett* **591**, 2978-2991 (2017).
73. S. Ghisletti *et al.*, Cooperative NCoR/SMRT interactions establish a corepressor-based strategy for integration of inflammatory and anti-inflammatory signaling pathways. *Genes Dev* **23**, 681-693 (2009).
74. S. Ghisletti *et al.*, Parallel SUMOylation-dependent pathways mediate gene- and signal-specific transrepression by LXRs and PPARgamma. *Mol Cell* **25**, 57-70 (2007).
75. J. H. Lee *et al.*, Differential SUMOylation of LXRalpha and LXRbeta mediates transrepression of STAT1 inflammatory signaling in IFN-gamma-stimulated brain astrocytes. *Mol Cell* **35**, 806-817 (2009).
76. J. H. Lee *et al.*, Small heterodimer partner SHP mediates liver X receptor (LXR)-dependent suppression of inflammatory signaling by promoting LXR SUMOylation specifically in astrocytes. *Sci Signal* **9**, ra78 (2016).
77. E. Treuter, N. Venteclef, Transcriptional control of metabolic and inflammatory pathways by nuclear receptor SUMOylation. *Biochim Biophys Acta* **1812**, 909-918 (2011).
78. M. S. Kappus *et al.*, Activation of liver X receptor decreases atherosclerosis in Ldlr(-)/(-) mice in the absence of ATP-binding cassette transporters A1 and G1 in myeloid cells. *Arterioscler Thromb Vasc Biol* **34**, 279-284 (2014).
79. D. G. Thomas *et al.*, LXR Suppresses Inflammatory Gene Expression and Neutrophil Migration through cis-Repression and Cholesterol Efflux. *Cell Rep* **25**, 3774-3785 e3774 (2018).
80. C. Marathe *et al.*, The arginase II gene is an anti-inflammatory target of liver X receptor in macrophages. *J Biol Chem* **281**, 32197-32206 (2006).

81. B. Pourcet *et al.*, LXRalpha regulates macrophage arginase 1 through PU.1 and interferon regulatory factor 8. *Circ Res* **109**, 492-501 (2011).
82. R. H. Eckel *et al.*, Obesity and type 2 diabetes: what can be unified and what needs to be individualized? *J Clin Endocrinol Metab* **96**, 1654-1663 (2011).
83. M. T. Zanella, O. Kohlmann, Jr., A. B. Ribeiro, Treatment of obesity hypertension and diabetes syndrome. *Hypertension* **38**, 705-708 (2001).
84. R. H. Eckel, S. M. Grundy, P. Z. Zimmet, The metabolic syndrome. *Lancet* **365**, 1415-1428 (2005).
85. P. T. Bozza, K. G. Magalhaes, P. F. Weller, Leukocyte lipid bodies - Biogenesis and functions in inflammation. *Biochim Biophys Acta* **1791**, 540-551 (2009).
86. S. M. Ulven, K. T. Dalen, J. A. Gustafsson, H. I. Nebb, LXR is crucial in lipid metabolism. *Prostaglandins Leukot Essent Fatty Acids* **73**, 59-63 (2005).
87. G. Soto-Heredero, M. M. Gomez de Las Heras, E. Gabande-Rodriguez, J. Oller, M. Mittelbrunn, Glycolysis - a key player in the inflammatory response. *FEBS J* **287**, 3350-3369 (2020).
88. K. R. Steffensen, J. A. Gustafsson, Putative metabolic effects of the liver X receptor (LXR). *Diabetes* **53 Suppl 1**, S36-42 (2004).
89. A. G. N *et al.*, The nuclear receptor LXRalpha controls the functional specialization of splenic macrophages. *Nat Immunol* **14**, 831-839 (2013).
90. S. E. Kahn, R. L. Hull, K. M. Utzschneider, Mechanisms linking obesity to insulin resistance and type 2 diabetes. *Nature* **444**, 840-846 (2006).
91. A. Ramon-Vazquez *et al.*, Common and Differential Transcriptional Actions of Nuclear Receptors Liver X Receptors alpha and beta in Macrophages. *Mol Cell Biol* **39**, (2019).
92. M. Korach-Andre, A. Archer, R. P. Barros, P. Parini, J. A. Gustafsson, Both liver-X receptor (LXR) isoforms control energy expenditure by regulating brown adipose tissue activity. *Proc Natl Acad Sci U S A* **108**, 403-408 (2011).
93. S. A. Hutchinson *et al.*, Liver x receptor alpha drives chemoresistance in response to side-chain hydroxycholesterols in triple negative breast cancer. *Oncogene* **40**, 2872-2883 (2021).
94. A. D. Ruggiero, C. C. Key, K. Kavanagh, Adipose Tissue Macrophage Polarization in Healthy and Unhealthy Obesity. *Front Nutr* **8**, 625331 (2021).
95. P. Petrus *et al.*, Glutamine Links Obesity to Inflammation in Human White Adipose Tissue. *Cell Metab* **31**, 375-390 e311 (2020).
96. A. R. Tall, L. Yvan-Charvet, Cholesterol, inflammation and innate immunity. *Nat Rev Immunol* **15**, 104-116 (2015).
97. L. Russo, C. N. Lumeng, Properties and functions of adipose tissue macrophages in obesity. *Immunology* **155**, 407-417 (2018).
98. X. Xu *et al.*, Obesity activates a program of lysosomal-dependent lipid metabolism in adipose tissue macrophages independently of classic activation. *Cell Metab* **18**, 816-830 (2013).
99. A. Takei *et al.*, Myeloid HMG-CoA Reductase Determines Adipose Tissue Inflammation, Insulin Resistance, and Hepatic Steatosis in Diet-Induced Obese Mice. *Diabetes* **69**, 158-164 (2020).
100. T. Suganami, Y. Ogawa, Adipose tissue macrophages: their role in adipose tissue remodeling. *J Leukoc Biol* **88**, 33-39 (2010).

101. C. N. Lumeng, J. L. Bodzin, A. R. Saltiel, Obesity induces a phenotypic switch in adipose tissue macrophage polarization. *J Clin Invest* **117**, 175-184 (2007).
102. P. M. Moraes-Vieira *et al.*, Antigen Presentation and T-Cell Activation Are Critical for RBP4-Induced Insulin Resistance. *Diabetes* **65**, 1317-1327 (2016).
103. A. Nawaz *et al.*, CD206(+) M2-like macrophages regulate systemic glucose metabolism by inhibiting proliferation of adipocyte progenitors. *Nat Commun* **8**, 286 (2017).
104. I. Syed *et al.*, Palmitic Acid Hydroxystearic Acids Activate GPR40, Which Is Involved in Their Beneficial Effects on Glucose Homeostasis. *Cell Metab* **27**, 419-427 e414 (2018).
105. H. Shi *et al.*, TLR4 links innate immunity and fatty acid-induced insulin resistance. *J Clin Invest* **116**, 3015-3025 (2006).
106. J. J. Repa *et al.*, Regulation of mouse sterol regulatory element-binding protein-1c gene (SREBP-1c) by oxysterol receptors, LXRalpha and LXRbeta. *Genes Dev* **14**, 2819-2830 (2000).
107. S. B. Joseph, A. Castrillo, B. A. Laffitte, D. J. Mangelsdorf, P. Tontonoz, Reciprocal regulation of inflammation and lipid metabolism by liver X receptors. *Nat Med* **9**, 213-219 (2003).
108. R. Komati *et al.*, Ligands of Therapeutic Utility for the Liver X Receptors. *Molecules* **22**, (2017).
109. S. B. Joseph *et al.*, Synthetic LXR ligand inhibits the development of atherosclerosis in mice. *Proc Natl Acad Sci U S A* **99**, 7604-7609 (2002).
110. X. Liu *et al.*, The citrus flavonoid naringenin confers protection in a murine endotoxaemia model through AMPK-ATF3-dependent negative regulation of the TLR4 signalling pathway. *Sci Rep* **6**, 39735 (2016).
111. F. A. Pinho-Ribeiro *et al.*, The citrus flavonone naringenin reduces lipopolysaccharide-induced inflammatory pain and leukocyte recruitment by inhibiting NF-kappaB activation. *J Nutr Biochem* **33**, 8-14 (2016).
112. M. Gao, D. Liu, The liver X receptor agonist T0901317 protects mice from high fat diet-induced obesity and insulin resistance. *AAPS J* **15**, 258-266 (2013).
113. W. K. E. Ip, N. Hoshi, D. S. Shouval, S. Snapper, R. Medzhitov, Anti-inflammatory effect of IL-10 mediated by metabolic reprogramming of macrophages. *Science* **356**, 513-519 (2017).
114. T. M. Powell-Wiley *et al.*, Obesity and Cardiovascular Disease: A Scientific Statement From the American Heart Association. *Circulation*, CIR0000000000000973 (2021).
115. N. Levin *et al.*, Macrophage liver X receptor is required for antiatherogenic activity of LXR agonists. *Arterioscler Thromb Vasc Biol* **25**, 135-142 (2005).
116. T. Sallam *et al.*, The macrophage LBP gene is an LXR target that promotes macrophage survival and atherosclerosis. *J Lipid Res* **55**, 1120-1130 (2014).
117. T. Sallam *et al.*, Transcriptional regulation of macrophage cholesterol efflux and atherogenesis by a long noncoding RNA. *Nat Med* **24**, 304-312 (2018).
118. B. A. Laffitte *et al.*, Activation of liver X receptor improves glucose tolerance through coordinate regulation of glucose metabolism in liver and adipose tissue. *Proc Natl Acad Sci U S A* **100**, 5419-5424 (2003).
119. A. M. Efanov, S. Sewing, K. Bokvist, J. Gromada, Liver X receptor activation stimulates insulin secretion via modulation of glucose and lipid metabolism in pancreatic beta-cells. *Diabetes* **53 Suppl 3**, S75-78 (2004).

120. G. M. Tannahill *et al.*, Succinate is an inflammatory signal that induces IL-1beta through HIF-1alpha. *Nature* **496**, 238-242 (2013).
121. A. K. Jha *et al.*, Network integration of parallel metabolic and transcriptional data reveals metabolic modules that regulate macrophage polarization. *Immunity* **42**, 419-430 (2015).
122. E. L. Mills *et al.*, Succinate Dehydrogenase Supports Metabolic Repurposing of Mitochondria to Drive Inflammatory Macrophages. *Cell* **167**, 457-470 e413 (2016).
123. J. Van den Bossche *et al.*, Mitochondrial Dysfunction Prevents Repolarization of Inflammatory Macrophages. *Cell Rep* **17**, 684-696 (2016).
124. M. Pascual-Garcia *et al.*, Reciprocal negative cross-talk between liver X receptors (LXRs) and STAT1: effects on IFN-gamma-induced inflammatory responses and LXR-dependent gene expression. *J Immunol* **190**, 6520-6532 (2013).
125. J. Matalonga *et al.*, The Nuclear Receptor LXR Limits Bacterial Infection of Host Macrophages through a Mechanism that Impacts Cellular NAD Metabolism. *Cell Rep* **18**, 1241-1255 (2017).
126. J. R. Schultz *et al.*, Role of LXRs in control of lipogenesis. *Genes Dev* **14**, 2831-2838 (2000).
127. A. Grefhorst *et al.*, Stimulation of lipogenesis by pharmacological activation of the liver X receptor leads to production of large, triglyceride-rich very low density lipoprotein particles. *J Biol Chem* **277**, 34182-34190 (2002).
128. S. B. Joseph *et al.*, Direct and indirect mechanisms for regulation of fatty acid synthase gene expression by liver X receptors. *J Biol Chem* **277**, 11019-11025 (2002).

APENDICE 1

Hindawi
Journal of Diabetes Research
Volume 2017, Article ID 4527980, 15 pages
https://doi.org/10.1155/2017/4527980

Review Article

The Impact of Ghrelin in Metabolic Diseases: An Immune Perspective

Jéssica Aparecida da Silva Pereira,[1,2] Felipe Corrêa da Silva,[1] and Pedro Manoel Mendes de Moraes-Vieira[1,2]

[1]*Laboratory of Immunometabolism, Department of Genetics, Evolution and Bioagents, Institute of Biology, University of Campinas, São Paulo, SP, Brazil*
[2]*Department of Immunology, Institute of Biomedical Science, University of São Paulo, São Paulo, SP, Brazil*

Correspondence should be addressed to Pedro Manoel Mendes de Moraes-Vieira; pmvieira@unicamp.br

Received 7 May 2017; Revised 7 July 2017; Accepted 31 July 2017; Published 7 September 2017

Academic Editor: Ed Randell

Obesity and insulin resistance have reached epidemic proportions. Obesogenic conditions are associated with increased risk for the development of other comorbidities and obesity-related diseases. In metabolic disorders, there is chronic low-grade inflammation induced by the activation of immune cells, especially in metabolic relevant organs such as white adipose tissue (WAT). These immune cells are regulated by environmental and systemic cues. Ghrelin is a peptide secreted mainly by X/A-like gastric cells and acts through the growth hormone secretagogue receptor (GHS-R). This receptor is broadly expressed in the central nervous system (CNS) and in several cell types, including immune cells. Studies show that ghrelin induces an orexigenic state, and there is increasing evidence implicating an immunoregulatory role for ghrelin. Ghrelin mainly acts on the innate and adaptive immune systems to suppress inflammation and induce an anti-inflammatory profile. In this review, we discuss the immunoregulatory roles of ghrelin, the mechanisms by which ghrelin acts and potential pharmacological applications for ghrelin in the treatment of obesity-associated inflammatory diseases, such as type 2 diabetes (T2D).

1. Introduction

The incidence of obesity and insulin resistance has increased in recent years. The World Health Organization (WHO) estimates that approximately 600 million adult people are obese [1]. Obesity directly impacts the economy and the quality of life of affected patients [2, 3]. Obesity is a disease with multifactorial origins and is characterized by excessive lipid accumulation in white adipose tissue (WAT), is promoted by the imbalance between caloric intake and energy expenditure [4, 5], and has harmful consequences to the individual [6]. Obesity is a risk factor for the development of other diseases, such as type 2 diabetes (T2D), metabolic syndrome, cardiovascular diseases, atherosclerosis, and several types of cancer [6–10].

WAT is a critical organ that contributes to host metabolism. Several cell types reside in WAT that regulate WAT and systemic homeostasis, such as adipocytes and preadipocytes, fibroblasts, macrophages, T lymphocytes, and among several other immune and nonimmune cells [11–15]. During obesity, immune alterations are observed in response to WAT expansion, which lead to a low-grade chronic inflammation. This inflammatory response is induced by changes in the recruitment of new leukocytes and also by changes in the function and activation status of adipose tissue resident macrophages (ATMs) and other leukocytes [6, 16, 17]. The immune changes that occur in WAT are characterized by the reduction of anti-inflammatory cytokines, such as interleukin 10 (IL-10), and upregulation of proinflammatory cytokines, such as tumor necrosis factor-α (TNF-α). This leads to the inhibition of the insulin-signaling pathway, which results in systemic insulin resistance [17].

Disruption of adipose tissue (AT) homeostasis and the induction of chronic systemic inflammation caused by

obesity are complex processes and involve many players [16]. The disturbances within WAT microenvironment occur at the immune and metabolic levels in obesity and obesity-related conditions. Among these changes, increased levels of circulating free fatty acids (FFA) contribute to the development of insulin resistance [18]. Elevated levels of FFAs lead to the generation of new metabolites from FFA reesterification, such as diacylglycerol (DAG) [19]. DAG promotes the activation of several serine/threonine kinases, such as protein kinase C (PKC), which drastically impairs the phosphorylation of insulin receptor substrates (IRS) 1/2, thereby disrupting insulin signaling [18–20].

Another important players in the induction and control of AT inflammation are the Toll-like receptors (TLR), in particular, TLR4 [21, 22]. TLR activation leads to defective cellular function in all metabolically relevant organs, such as the liver, pancreas, and WAT [20–24]. This defect in cellular function results in immune cell activation and inflammation subsequently leading to resistance to key metabolic hormones such as insulin, leptin, and ghrelin [23–27].

Ghrelin is a peptide-hormone/cytokine widely distributed throughout the gastric mucosa made up of 28 amino acids and is mainly secreted by X/A-like enteroendocrine cells [28–31]. Ghrelin was described in 1999 as an endogenous ligand for the growth hormone secretagogue receptor (GHS-R) [32], a G-coupled receptor broadly expressed in the central nervous system (CNS) and in peripheral tissues, including nerve cells, cardiac cells, adipocytes, and immune cells [32–34].

Ghrelin has an important role in obesity and metabolic-related disorders. It is most known for its role in appetite regulation, acting directly on hypothalamic neurons responsible that were involved in feeding behavior [35]. Beyond this "classic" function, ghrelin is also an immunomodulatory hormone, providing new perspectives for its relevance in metabolic diseases [36, 37]. In obesogenic conditions, ghrelin levels are reduced with a concomitant induction of chronic low-grade inflammation [23, 38]. These data strongly suggest a role for ghrelin in obesity-related pathological conditions in establishing and maintaining "metabolic inflammation" and expand our knowledge of ghrelin beyond its role in the CNS. In this review, we will discuss the participation of ghrelin in immunomodulatory events, the impact of this regulation on metabolic disorders, and the mechanisms by which ghrelin acts.

2. Ghrelin Structure, Function, and Receptor

The GHS-R has two isoforms, GHS-R1a and GHS-R1b [39]. Only GHS-R1a triggers a signaling pathway, which is induced by the binding of ghrelin [39]. The lack of GHS-R1b isoform activity is attributed to the absence of a third intracellular loop, which prevents G protein coupling [39, 40]. There is evidence describing the interaction between ghrelin receptor and other G-coupled receptors, such as dopamine, serotonin and melanocortin receptors, and even GHS-R1b [39, 41]. These interactions lead to conformational changes in GHS-R, which impact GHS-R1a signaling [39–41].

Secreted ghrelin is found in two distinct forms in the bloodstream [42]. One is the desacyl (desoctanoyl) form (desacyl-ghrelin), which is more stable and has higher serum concentration levels compared to other ghrelin form [43–45]. Desacyl-ghrelin is suggested to be a non-GHS-R1a ligand form of ghrelin under physiological conditions [31, 43, 45]. Desacyl-ghrelin has cardioprotective effects [46–48]. However, its functional role and the receptor by which desacyl-ghrelin binds remain unknown [39, 49]. The other form of ghrelin is the acylated form (acyl-ghrelin), which undergoes a posttranslational modification on serine residue 3 [50]. This acylated form corresponds to approximately 20% of total circulating ghrelin and is responsible for the biological effects of ghrelin [51] and indicates that acylation of ghrelin is an important step for the biological activity of this peptide [51–53].

The posttranslational structural modification observed in the acylated form of ghrelin is attributed to an enzyme, discovered in 2008 by Yang and colleagues [54], which is called ghrelin-*O*-acyltransferase (GOAT). GOAT is responsible for the acylation of the preproghrelin before it is transported to the Golgi apparatus [42]. In the Golgi vesicle, proghrelin is proteolytically cleaved by the prohormone convertase 1/3 (PC 1/3) [31, 55, 56].

Acyl-ghrelin has a wide range of functions in several tissues. Acyl-ghrelin stimulates growth hormone secretion by the pituitary gland and activates the hypothalamic orexigenic axis [57]. Ghrelin serum levels are increased during caloric restriction [30]. In the hypothalamic orexigenic axis, ghrelin induces the secretion of neuropeptides, such as AgRP (agouti-related protein) and NPY (neuropeptide Y) [58], which leads to increased food consumption and reduced energy expenditure [53].

In addition to the direct effects of ghrelin on the CNS, ghrelin regulates gastrointestinal motility [59, 60], energy homeostasis [61], and the cardiovascular and reproductive systems [62]. Ghrelin also participates in the regulation of other adipokines, such as leptin, and modulates a broad number of immune functions [31, 63].

3. Ghrelin Signaling

GHS-R1a is widely distributed in different tissues [32–34], and its activation by acyl-ghrelin involves several signaling pathways [28–30]. The most studied cell type regarding the mechanisms of actions of acyl-ghrelin is hypothalamic neurons [64, 65]. In these cells, acyl-ghrelin relies on 5′ adenosine monophosphate-activated protein kinase (AMPK) [66–68]. Acyl-ghrelin AMPK-dependent signaling acts by two distinct mechanisms in hypothalamic neurons, in which intracellular calcium influx [69] and cytoplasmic nutrient sensors, such as AMPK [70] and mammalian target of rapamycin (mTOR), are the main targets triggered by the binding of acyl-ghrelin to GHS-R1a [71, 72].

AMPK activation leads to an inhibition of acetyl-CoA carboxylase (ACC) through posttranslational modifications [66]. The cellular outcome of this inhibition is increased mitochondrial metabolism due to consecutive activation of carnitine palmitoyltransferase 1 (CPT1) [73, 74]. Increased

fatty acid oxidation leads to the generation of reactive oxygen species (ROS) and consequently stimulates uncoupling protein 2 (UCP2) [75]. These events induce the expression of orexigenic neuropeptides and consequently feeding behavior [75]. AMPK activation through GHS-R1a can also be mediated by calcium calmodulin-dependent protein kinase-kinase 2 (CAMKK2) in response to elevated intracellular calcium concentrations [76–78]. There is also evidence for a dependency on Sirtuin 1 and p53 during AMPK activation through GHS-R1a signaling [79].

The cytoplasmic nutrient sensor mTOR has a key function in hypothalamic energy homeostasis [80]. Several reports indicate that the effects of acyl-ghrelin are mediated by mTOR signaling pathway activation [72, 81, 82]. Activation of this machinery is responsible for the phosphorylation of several transcriptional factors, which are key elements in the orexigenic response, such as forkhead box protein O1 (FOXO-1) and cAMP response element-binding protein (CREB) [71, 83]. These data indicate that acyl-ghrelin signaling pathway in hypothalamic neurons is dependent on the signaling machinery of nutrient sensing.

In immune cells, the mechanisms of acyl-ghrelin signaling are poorly explored. Avallone and colleagues [84] show that ghrelin signaling in macrophages is dependent on AMPK activation and peroxisome proliferator-activated receptor gamma (PPARγ) [84]. Both proteins have established anti-inflammatory roles [81–86]. Further studies are required to fully characterize acyl-ghrelin signaling in immune cells. The dependence of AMPK and PPARγ for the immunoregulatory features of acyl-ghrelin is consistent with the current understanding of ghrelin signaling events in hypothalamic neurons as well as the cellular modifications that immune cells undergo during the induction of an anti-inflammatory phenotype [85–87].

3.1. Mechanisms Independent of Nutrient Sensors. There are two physiological outcomes as resultant of ghrelin receptor activation that does not depend on the nutrient sensing machinery: (i) the activation of hypothalamic neurons that evoke feeding behavior [69] and (ii) growth hormone (GH) secretion by pituitary cells [88]. Both outcomes are a direct result of elevated calcium levels, with distinct mechanisms of action. In the first case, activation of GHS-R1a leads to a subsequent elevation of cyclic adenosine monophosphate (cAMP), mediated by the adenilate cyclase (AC)-protein kinase A (PKA) signaling pathway [89]. As a result, hypothalamic neurons involved in feeding behavior are activated [69]. In pituitary cells, activated GHS-R1a induces calcium release from endoplasmic reticulum, which results in the activation of phospholipase C (PLC)-inositol triphosphate (IP_3)-protein kinase C (PKC) pathway [39, 88].

4. Ghrelin, Obesity, and Inflammation

Tissue-secreted factors may disturb tissue homeostasis, which affects cellular and tissue metabolism and leads to systemic alterations [26]. Ghrelin and other factors regulate several aspects of metabolism and inflammation, which result in improved or worsened insulin resistance and metabolic syndrome [90–92]. Obesity-mediated metabolic disturbances increase levels of several cytokines and chemokines [91, 93]. This generates a proinflammatory status, which is a potential risk factor for the development of inflammation-induced insulin resistance [94]. One of these secreted factors is the monocyte chemotactic protein-1 (MCP-1), which is induced by the NFκB pathway to recruit monocytes [95]. Because activation of GHS-R reduces NFκB activation in endothelial cells [96], ghrelin treatment could limit immune cell activation through inhibition of NFκB activation and subsequent MCP-1 secretion. This approach may lead to the development of new therapeutic approaches to treat T2D.

Metabolic imbalance induced by obesity leads to alterations in ATM population profile [97]. The M1 ATM macrophage population expresses the cell surface marker CD11c and secretes proinflammatory cytokines, such as tumor necrosis factor-α (TNF-α), interleukin-1β (IL-1β), interleukin-6 (IL-6), and monocyte chemotactic protein-1 (MCP-1) [98]. M1 macrophages also express high levels of iNOS (inducible nitric oxide synthase) [98, 99]. M2 macrophages express cell surface markers CD206, CD301, and CD163, secrete anti-inflammatory cytokines, such as interleukin-10 (IL-10), and express high levels of arginase-1 [15, 99]. M2 ATMs are often involved in homeostasis maintenance and tissue repair [15, 100]. The increase in the number of M1 ATM population in obesity is commonly accompanied with a reduction in M2 ATM population. This imbalance, with the predominance of a proinflammatory profile, inhibits the insulin-signaling pathway [94, 101, 102]. Thus, ATM function has an important role on metabolic syndrome and T2D development, which is frequently observed during obesity [99].

In obesogenic conditions, ghrelin levels are decreased [23] and levels of proinflammatory cytokines and adipokines, such as leptin, and liver-derived proteins, such as retinol binding 4 (RBP4), are increased [5, 103, 104]. Leptin is a proinflammatory adipokine, which inhibits ghrelin secretion [105] and worsens adipose tissue inflammation [5]. These data support the hypothesis that counter regulatory functions between leptin and ghrelin are an essential step for the maintenance of homeostasis CNS (food intake and energy expenditure regulation) and in immune responses [36].

5. Immunoregulatory Functions of Ghrelin

The wide distribution of functional ghrelin receptors (GHS-R) and their expression in various immune cell populations have attracted the attention of the scientific community. Changes in ghrelin levels can directly affect immune responses and tissue homeostasis [36, 37]. Leukocytes, such as adipose tissue macrophages (ATMs), express GHS-R [106] and detect changes in energy status [107, 108]. Thus, ghrelin actions on ATMs may play a role in the maintenance of the tissue homeostasis, suggesting a link between the immune system and systemic metabolism in response to different physiological and pathological conditions such as obesity and insulin resistance [109, 110].

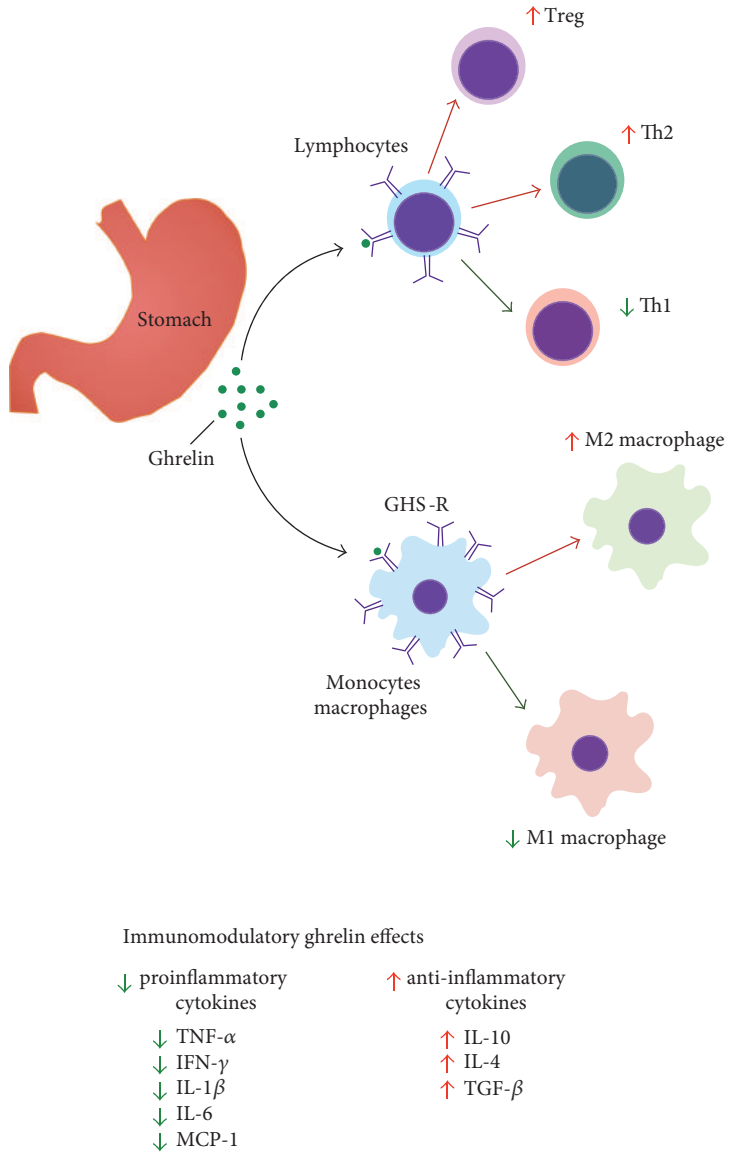

Figure 1: The immune roles of ghrelin. Ghrelin is secreted by X/A-like enteroendocrine cells. In the innate immune system, ghrelin acts on macrophages and induces an anti-inflammatory state (M2 profile) and inhibits proinflammatory macrophages (M1 profile). In the adaptive immune system, ghrelin exhibits an anti-inflammatory role. Ghrelin inhibits Th1 cells and increases the polarization of Th2 and regulatory T cells. These actions contribute to the reduced levels of proinflammatory cytokines and increased levels of anti-inflammatory cytokines.

Several studies support an immunoregulatory role for ghrelin [36, 37, 107, 111, 112]. Ghrelin acts on a diverse portfolio of leukocytes and directly alters immune cell function (Figure 1) [36, 37, 111, 112]. Dixit and colleagues [111] showed that ghrelin treatment *in vitro* inhibited the secretion of proinflammatory cytokines (IL-1β, IL-6, and TNF-α) in human monocytes, T cells, and peripheral blood mononuclear cells (PBMCs) [111]. Likewise, ghrelin treatment in human umbilical vein endothelial cells (HUVEC) reduced the secretion of IL-8 and MCP-1 and the activation of NFκB in response to TNF-α stimuli [96]. Also, rats submitted to endotoxic shock with lipopolysaccharide (LPS) and treated with ghrelin had higher rates of survival compared to controls [113]. This protective effect was mediated by ghrelin-specific GHS-R receptor binding and resulted in reduced serum levels of TNF-α, IL-6, IL-8, and MCP-1 [96, 111]. Moreover, data suggests that mitogen-activated protein kinase phosphatase-1 (MKP-1) mediates the protective effect of ghrelin against endotoxic shock [114]. MKP-1 levels are reduced in inflammatory conditions, such as norepinephrine-induced sepsis, and lead to secretion of TNF-α [114]. Jacob and colleagues [114] reported that ghrelin treatment in septic rats increased gene and protein expression of MKP-1 [114]. This restoration of MKP-1 expression may partially explain the reduction in proinflammatory cytokines in response to ghrelin treatment. These data indicate that ghrelin can limit inflammation and plays an important role in metabolic and nonmetabolic inflammatory conditions.

In vivo, ghrelin has an anti-inflammatory and antinociceptive role [13, 34, 37, 111, 115–118]. Intraperitoneal administration of ghrelin in rats submitted to pain resulted in increased levels of serum IL-10 and TGF-β and reduced pain score [118]. The anti-inflammatory action of ghrelin was also observed in a colitis model. Ghrelin treatment reduced the expression of TNF-α, INF-γ, IL-1α, IL-1β, IL-6, IL-12, IL-15, IL-17, and IL-18 and increased IL-10 levels in colonic mucosa, which improved colitis score and survival rate in mice [37].

The anti-inflammatory roles of ghrelin can be extended to other inflammatory conditions, such as rheumatoid arthritis. Administration of the ghrelin agonist growth hormone-releasing peptide-2 (GHRP-2) reduced serum IL-6 levels and improved inflammation in arthritic rats [119]. Similar observations were obtained when peritoneal macrophages were treated with GHRP-2 *in vitro* [119]. Together, this data indicates that GHS-R can be used as a novel target for the treatment of acute and chronic inflammatory diseases.

Neutrophils play a fundamental role in immune response against pathogens and are regulated by ghrelin treatment. *In vivo* studies show that ghrelin treatment reduced neutrophil count in peritoneal lavage [63]. This was not attributed to enhanced apoptosis [120]. Neutrophils treated with ghrelin had increased phagocytic capacity and enhanced bactericidal capacity [120]. On the other hand, ghrelin treatment reduced neutrophil recruitment in the airways of subjects with chronic respiratory infections, which displayed reduced IL-8 and TNF-α levels in the sputum and improved overall inflammatory status [121].

Orlova and colleagues showed that ghrelin may affect dendritic cell- (DC-) mediated antigen presentation capacity. DCs treated with ghrelin had reduced capacity to induce the secretion of IL-17 and INF-γ and enhanced capacity to induce secretion of IL-10 and TGF-β from cocultured T cells [122]. Ghrelin also modulates thymic DCs. Ghrelin administration in the thymus induced the proliferation of DCs in aged mice [123], which contributes to a more effective maturation and response of effector and regulatory (Treg) T cell differentiation [124]. Ghrelin also regulates immune cell migration and proliferation. Ghrelin treatment reduced immune cell recruitment after LPS stimulation and induced the proliferation of Treg cells [34, 125]. Together, these data indicate that ghrelin has important effects in modulating T cells, especially regulatory T cells.

The role of adaptive immunity in the CNS is a growing topic of study. One of the most established models of the role of lymphocytes in CNS homeostasis is experimental autoimmune encephalomyelitis (EAE), an animal model of multiple sclerosis [126]. This condition has a marked proinflammatory feature, mediated by T $CD4^+$ cells (Th1 and/or Th17 response) [125]. Ghrelin exerts therapeutic effects in EAE through the impairment of encephalitogenic Th1 and Th17 cells, and short-term ghrelin treatment reduces the clinical score of the disease [125]. This was associated with fewer infiltrated cells in the CNS and subsequent reduction in CNS inflammation. These effects were further improved by the induction of regulatory T cells in mice [125]. Souza-Moreira and colleagues [125] showed that ghrelin treatment suppressed M1 phenotype in microglia and reduced T cell infiltration, which was consistent with findings previously described by Theil and colleagues [125, 127]. The immunomodulatory roles of ghrelin in CNS are a result of decreased expression of proinflammatory cytokines, such as TNF-α, IL-1β, and IL-6, which indicate a noteworthy anti-inflammatory property.

6. Contrasting Roles of Ghrelin in the Immune System

There is evidence supporting the immunoregulatory role of acyl-ghrelin [107] and its beneficial effects to treat chronic inflammatory syndromes, especially acyl-ghrelin immunoprotective properties during endotoxic shock [36]. However, in sepsis, ghrelin may contribute to the higher mortality seen in septic mice [63]. This higher mortality was attributed to reduced neutrophil and natural killer cell activity, which led to increased bacterial burden [63]. Nevertheless, other authors demonstrated beneficial effects of acyl-ghrelin in the same experimental model and attributed these effects to lower inflammation in the hippocampus, observed by the reduction of TNF-α and IL-6 levels in septic brains [112].

Desacyl-ghrelin is a non-GHS-R1a ligand and was previously described as the nonactive form of ghrelin (although some authors report that desacyl-ghrelin binds to GHS-R1a when supraphysiological concentrations are induced) [34, 39, 44, 128]. Recent reports suggest that desacyl-ghrelin alters macrophage polarization *in vitro* [129]. Desacyl-ghrelin treatment decreased expression of TNF-α and CD11c and increased expression of CD206 in the mouse macrophage cell line (RAW264.7) [129]. Similar results were observed by the treatment of RAW cells with acyl-ghrelin [130]. This suggests that ghrelin treatment reduced M1 proinflammatory macrophage and increased M2 macrophage polarization [129]. These results are compatible with the observation that in humans, monocytes are the main targets for the anti-inflammatory actions of acyl-ghrelin [111]. However, the effects of acyl-ghrelin or desacyl-ghrelin treatment in bone marrow-derived macrophages or ATMs remain to be established.

Knockdown of GHS-R in mice reduced expression of TNF-α, IL-1β, IL-6, and MCP-1 in WAT of mice fed with a high-fructose corn syrup, which was associated with improved insulin sensitivity and obesity in aged mice. Also, ablation of the GHS-R promoted a shift towards a M2 profile in ATMs [106]. GHS-R ablation also limited the proinflammatory phenotype of peritoneal macrophages and ATMs, which was observed by decreased expression of proinflammatory cytokines [99].

Although a variety of studies indicates that ghrelin has an anti-inflammatory role, the controversial actions of this peptide support the need to better understand the mechanisms by which ghrelin acts on immune cells in response to different immunological challenges.

7. Ghrelin at the Neuroimmune Interface

7.1. Neuroprotective Effects of Ghrelin. In extrahypothalamic areas, acyl-ghrelin has a strong anti-inflammatory role [131–134]. Microglial cells express GHS-R, and acyl-ghrelin administration downregulates proinflammatory cytokine expression through impairment of microglial cell expansion [131–133]. The neuroprotective effects of acyl-ghrelin were extensively studied by many research groups [135–137]. In Parkinson's disease, there is a progressive neuronal degeneration of dopaminergic neurons localized in the *substantia nigra* and a concomitant increase in microglial activation. GHS-R1a is widely expressed in dopaminergic neurons in the *substantia nigra* [136, 137]. It is proposed that the neuroprotective effects of acyl-ghrelin in a Parkinson's disease context are partially due to the induction of tyrosine hydroxylase expression in dopaminergic neurons, a pivotal enzyme in dopamine biosynthesis [135]. The administration of MPTP (1-methyl-4-phenyl-1,2,3,6-tetrahydropyridine), a mitochondrial toxin, is a well-established model for Parkinson's disease studies, since there is a selective effect on dopaminergic neurons [138]. Mice treated with intraperitoneal acyl-ghrelin have lower levels of neuronal death and reduced dopamine loss [132, 133, 135]. Consistent with this phenotype, ghrelin treatment reduces proinflammatory markers, such as TNF-α and IL-1β [133]. It is proposed that the neuroprotective effects of ghrelin are also mediated through UCP2 activity [75, 135], since striatal neurons are dependent on UCP2 for optimal function [139–142].

Learning and memory retention also are influenced by acyl-ghrelin [143]. Intracerebroventricular [144] and intrahippocampal [145] acyl-ghrelin injections improve memory retention in rodents, which suggests a role for ghrelin in the molecular process of memory acquisition and/or consolidation. These results are reinforced by data published by Diano and colleagues [146], where spine density in the hippocampus is reduced in ghrelin knockout mice [146]. Data from Carlini and colleagues [144, 147] suggest that these beneficial effects are partially due to serotonergic inputs from dorsal raphe nucleus to the hippocampal circuits [147].

Several studies indicate that the brain is not a postmitotic structure in adult life [148–151]. Adult neurogenesis may be a potential therapeutic target for many neurodegenerative conditions [152–154]. The most explored structure in this context is the hippocampus [155]. There is evidence that acyl-ghrelin induces neurogenesis in brain structures related with cognition, such as the dendate gyrus of the hippocampus [156]. The classical target of ghrelin resides in the neuronal populations of the hypothalamus, and there are no reports to date describing the induction of neurogenesis by ghrelin. Therefore, neuroprotective effects of ghrelin in cognition-related structures may contribute to both the regulation of neurogenic events and the maintenance of mature resident cells [157–159].

The neuroprotective effects of ghrelin are also related to ischemic lesions, both *in vivo* and *in vitro* [160–162]. In these situations, there is insufficient blood flow into the brain. Treatment with acyl-ghrelin reduces ischemic lesions in mice by mechanisms both dependent and independent of GHS-R1a [160–162]. Here, neuroprotection is determined as reduced infarct tissue and cell death [161, 163].

7.2. Ghrelin, Stress, and Neuroinflammation. In view with the increased incidence of psychological disturbances and obesity, many groups have investigated the dynamic contribution of obesity to the development of affective disorders and how affective disorders affect obesity. Hormones that regulate energy homeostasis, such as ghrelin, may play a role in mediating psychological disturbances [164].

Serum levels of acyl- and desacyl-ghrelin, preproghrelin, and GH are increased in rodents submitted to acute and chronic stress models [164–168]. The hypothesis that increased ghrelin levels could be due to a stress response is supported by the involvement of ghrelin in neuroprotection, memory, and motivation [143]. GHS-R knockout mice have depressive behavior, which is marked by social isolation [165]. Cummings and colleagues showed that the increased ghrelin levels lead to decreased depressive behavior in rodents submitted to forced swimming test [165]. Psychological stress appears to induce inflammatory responses and is associated with compartmental alterations characterized by depressive symptoms [169]. Elevated levels of proinflammatory cytokines are found in patients with depression [170]. IL-1β and TNF-α increase serotonin uptake and metabolism, which contribute to depressive behavior. These data suggest a link between inflammatory responses and compartmental diseases [170]. GHS-R expression in the basolateral complex of the amygdala, an important region for emotional processing in rodents and humans, strongly supports the involvement of ghrelin in the modulation of emotional status and memory [171, 172]. Thus, ghrelin treatment could be an effective approach against emotional disorders due to ghrelin anti-inflammatory properties [143, 170].

Alterations in endogenous ghrelin levels and action could lead to the development of psychiatric disturbances associated to stress [172, 173]; a better understanding of how ghrelin regulates emotional behavioral disturbances is needed. These studies may contribute to the development of new targets for the treatment of diseases associated with stress and inflammation.

7.3. Ghrelin and Mediobasal Hypothalamus. The hypothalamus is a CNS structure primarily involved in global metabolic regulation [35]. There are multiple hypothalamic nuclei involved with metabolic regulation, such as the arcuate nucleus (Arc), lateral hypothalamic area (LHA), and paraventricular nucleus (PVN) [35]. The current model stipulates that Arc neuronal populations work in a binary-like system. The anorexigenic response is mediated by proopiomelanocortin (POMC) neurons, and the orexigenic response is mediated by agouti-related protein (AgRP) expressing neurons [35]. The signals induced by key metabolic hormones and nutrients are perpetuated by other neuronal populations in different hypothalamic nuclei that are synaptically connected to AgRP/POMC neurons [35]. Ghrelin exerts its orexigenic actions through AgRP neurons exclusively, since POMC neurons do not express GSH-R [174].

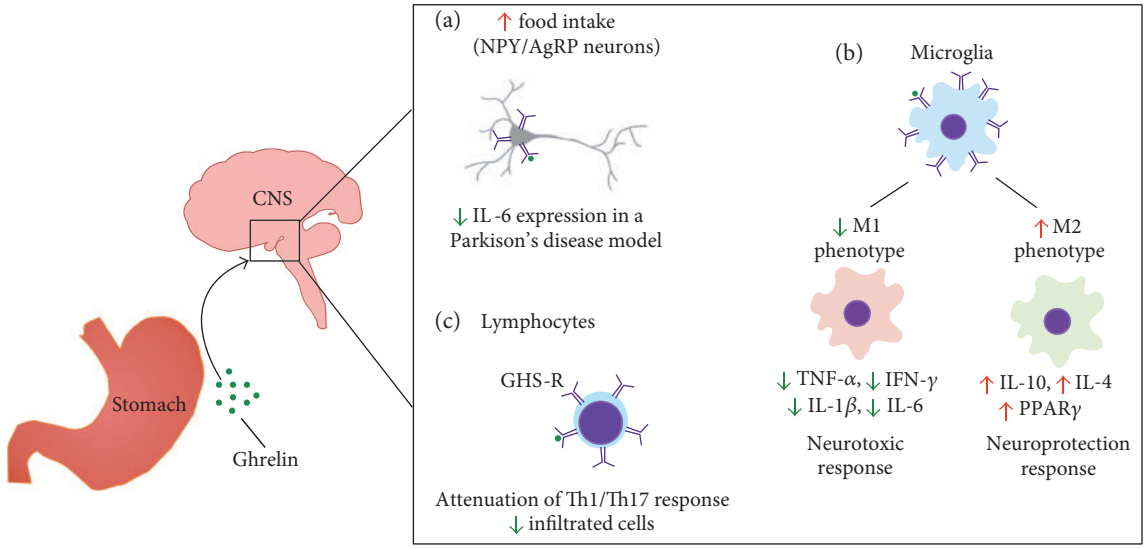

Figure 2: Ghrelin at the neuroimmune interface. Ghrelin has several functions in the CNS. (a) The classical orexigenic effect of ghrelin is mediated through activation of AgRP/NPY neurons in the mediobasal hypothalamus; it can also exert neuroprotective effects by diminishing IL-6 expression in striatal neurons in a Parkinson's disease model. (b) In microglia, ghrelin suppresses the proinflammatory phenotype and activates an anti-inflammatory program, which reinforces the neuroprotective role of ghrelin. (c) Infiltrated lymphoid cells are also decreased upon ghrelin treatment, with a marked reduction in Th1/Th17 responses.

It is known that consumption of high-fat diet (HFD) leads to activation of proinflammatory processes in the hypothalamus with marked deregulation of feeding behavior and defective energy expenditure responses [175–177]. This inflammatory process is activated in the early stages of HFD feeding, with increased cytokine expression within 24 hours after HFD intake [176]. The key cell type that coordinates inflammatory responses in CNS is the microglia [178]. Several reports in the past decade described the importance of microglial cells in the initiation and perpetuation of hypothalamic inflammation and consequently its repercussions [175–177]. Following an obesogenic stimulus, microglial cells are activated in a TLR4-dependent manner and rapidly expand, creating a proinflammatory environment. These actions are restricted to the hypothalamus in the early stages of "metabolic inflammation" [175]. A recent report demonstrated that inhibition of microglial expansion in the Arc partially restored the metabolic impairments due to an obesogenic environment [177]. Thus, microglial activation is one of the most important targets for the development of focusing on the CNS under obese conditions.

The activation of TLR4-dependent responses in resident Arc microglial cells leads to a defective ghrelin orexigenic effect in animals fed with a chow diet [179]. This data indicates that microglia can directly modulate energy homeostasis by affecting neighboring cell functions and might explain the counterintuitive phenomenon of ghrelin resistance in obesity and metabolic diseases. However, ghrelin resistance is a complex subject of study and cannot be reduced to isolated effects on microglial or neuronal cells in the hypothalamus [180]. For instance, it is not known whether ghrelin resistance is due to (i) reduced ghrelin receptor expression/translocation in the target cells, (ii) defective ghrelin transport through blood-brain barrier as observed with leptin [181], or (iii) disrupted cellular homeostasis on ghrelin responsive cells, which is a similar process that leptin responsive cells undergo in obesogenic conditions [181, 182]. It is also possible that the physiological outcome is a combination of all of these factors. Another point to be clarified is whether neurons and glial cells are both resistant to the ghrelin signal and if there is temporal concordance in the establishment of ghrelin resistance in different cell types.

7.4. Obesity and Immunity in the Central Nervous System. The participation of Th1 or Th17 cells on hypothalamic impairment in metabolic diseases has yet to be clarified. It is known that T cells can penetrate the blood-brain barrier and act locally on the brain [183]. Thus far, there is no characterization of the participation of these cell types in the induction of metabolic inflammation on the hypothalamus. It is possible that ghrelin exerts an indirect immunomodulatory effect on adaptive immunity. As briefly discussed, Arc microglial activation can lead to an increase in local TNF [176]. This signaling has multiple effects and is one modulator of adaptive immunity in the periphery, which triggers adipose tissue lipolysis and raises triglyceride levels in the blood [184]. This in turn elevates the number of B cells and T cells with a Th1-type profile [184]. Thus, in obesity and obesity-related conditions, the immunomodulatory mechanisms of ghrelin have multiple points of actions and might not be restricted to the neural tissue (Figure 2).

Long-term studies indicate that bariatric surgery promotes a significant and sustained weight loss and recovery of metabolic parameters [185]. Several works have reported alterations in ghrelin levels during the postoperative period in patients submitted to different surgical strategies, which could be a result of altered body weight and feeding behavior [165, 186–206].

Faraj and colleagues [199] reported that ghrelin levels are dynamically modulated with weight loss [199] and patients with no changes in body weight do not have altered ghrelin levels. However, the role of ghrelin in postbariatric surgery is controversial [165, 186–206]. Besides, another relevant aspect that should be considered is the different methodological approaches used for the measurement of ghrelin, which could contribute to the discrepancy in ghrelin levels reported [207, 208].

Although the exact mechanisms by which bariatric surgery leads to reduced body weight are not completely understood, alterations in nutrient influx accompanied by increased ghrelin levels could lead to reduced proinflammatory marker expression, which will result in improved metabolic inflammation and the subsequent glucose homeostasis [199, 209–212].

8. Concluding Remarks

Ghrelin is not only a gastric peptide with CNS actions but it is also an important hormone/cytokine with important pleiotropic functions. The wide distribution of GHS-R1a in different cell types, including immune cells, indicates that ghrelin acts as a potent immunomodulator with powerful anti-inflammatory roles. The anti-inflammatory effects of ghrelin are observed in immune cells of both myeloid and lymphoid lineages. In macrophages/microglia, these anti-inflammatory properties are translated into increased secretion of anti-inflammatory cytokines, elevated M2/M1 ratio, and reduced proinflammatory cytokine expression. In lymphoid cells, ghrelin signaling leads to increased Th2 and Treg cell function. Therefore, ghrelin is a secreted hormone/cytokine with important anti-inflammatory roles in metabolically relevant organs, such as WAT and the hypothalamus. Ghrelin is a promising therapeutic strategy for the treatment of chronic inflammatory conditions, such as obesity. The therapeutic function of ghrelin is currently limited by its potent orexigenic properties. The paradoxical outcomes of ghrelin used to treat metabolic diseases are the induction of appetite and the anti-inflammatory roles. Thus, more studies are required to elucidate the molecular mechanisms of ghrelin actions as well as its application as a GHS-R agonist to treat obesity and insulin resistance in individuals.

Conflicts of Interest

The authors declare that there is no conflict of interests regarding the publication of this paper.

Authors' Contributions

Jéssica Aparecida da Silva Pereira and Felipe Corrêa da Silva contributed equally to this work.

Acknowledgments

The authors acknowledge the support of the State of São Paulo Foundation for Research Support (FAPESP, no. 2015/15626-8 and no. 2017/06225-5) and CNPq. The authors also thank Dr. Jennifer Lee from Beth Israel Deaconess Medical Center and Dr. Marisa Moura Momoli for revising the manuscript.

References

[1] WHO, "Obesity and overweight 2016," http://www.who.int/mediacentre/factsheets/fs311/en/.

[2] J. Cawley, J. A. Rizzo, and K. Haas, "Occupation-specific absenteeism costs associated with obesity and morbid obesity," *Journal of Occupational and Environmental Medicine*, vol. 49, no. 12, pp. 1317–1324, 2007.

[3] D. M. Gates, P. Succop, B. J. Brehm, G. L. Gillespie, and B. D. Sommers, "Obesity and presenteeism: the impact of body mass index on workplace productivity," *Journal of Occupational and Environmental Medicine*, vol. 50, no. 1, pp. 39–45, 2008.

[4] N. A. Fairbridge, T. M. Southall, D. C. Ayre et al., "Loss of CD24 in mice leads to metabolic dysfunctions and a reduction in white adipocyte tissue," *PLoS One*, vol. 10, no. 11, article e0141966, 2015.

[5] V. Andrade-Oliveira, N. O. Camara, and P. M. Moraes-Vieira, "Adipokines as drug targets in diabetes and underlying disturbances," *Journal of Diabetes Research*, vol. 2015, Article ID 681612, 11 pages, 2015.

[6] P. M. Moraes-Vieira, E. J. Bassi, R. C. Araujo, and N. O. Câmara, "Leptin as a link between the immune system and kidney-related diseases: leading actor or just a coadjuvant?," *Obesity Reviews*, vol. 13, no. 8, pp. 733–743, 2012.

[7] M. Lafontan and M. Berlan, "Do regional differences in adipocyte biology provide new pathophysiological insights?," *Trends in Pharmacological Sciences*, vol. 24, no. 6, pp. 276–283, 2003.

[8] B. Antuna-Puente, B. Feve, S. Fellahi, and J. P. Bastard, "Adipokines: the missing link between insulin resistance and obesity," *Diabetes & Metabolism*, vol. 34, no. 1, pp. 2–11, 2008.

[9] M. Rosenbaum, M. Sy, K. Pavlovich, R. L. Leibel, and J. Hirsch, "Leptin reverses weight loss-induced changes in regional neural activity responses to visual food stimuli," *The Journal of Clinical Investigation*, vol. 118, no. 7, pp. 2583–2591, 2008.

[10] P. M. Moraes-Vieira, A. Saghatelian, and B. B. Kahn, "GLUT4 expression in adipocytes regulates de novo lipogenesis and levels of a novel class of lipids with antidiabetic and anti-inflammatory effects," *Diabetes*, vol. 65, no. 7, pp. 1808–1815, 2016.

[11] M. E. Vazquez-Vela, N. Torres, and A. R. Tovar, "White adipose tissue as endocrine organ and its role in obesity," *Archives of Medical Research*, vol. 39, no. 8, pp. 715–728, 2008.

[12] C. M. Oller do Nascimento, E. B. Ribeiro, and L. M. Oyama, "Metabolism and secretory function of white adipose tissue: effect of dietary fat," *Anais da Academia Brasileira de Ciências*, vol. 81, no. 3, pp. 453–466, 2009.

[13] S. Galic, J. S. Oakhill, and G. R. Steinberg, "Adipose tissue as an endocrine organ," *Molecular and Cellular Endocrinology*, vol. 316, no. 2, pp. 129–139, 2010.

[14] N. S. Kalupahana, N. Moustaid-Moussa, and K. J. Claycombe, "Immunity as a link between obesity and insulin resistance," *Molecular Aspects of Medicine*, vol. 33, no. 1, pp. 26–34, 2012.

[15] A. Castoldi, C. Naffah de Souza, N. O. Câmara, and P. M. Moraes-Vieira, "The macrophage switch in obesity development," *Frontiers in Immunology*, vol. 6, p. 637, 2015.

[16] S. Sun, Y. Ji, S. Kersten, and L. Qi, "Mechanisms of inflammatory responses in obese adipose tissue," *Annual Review of Nutrition*, vol. 32, pp. 261–286, 2012.

[17] J. C. McNelis and J. M. Olefsky, "Macrophages, immunity, and metabolic disease," *Immunity*, vol. 41, no. 1, pp. 36–48, 2014.

[18] G. Boden, "Obesity and free fatty acids," *Endocrinology and Metabolism Clinics of North America*, vol. 37, no. 3, pp. 635–646, 2008, viii-ix.

[19] G. Boden, "Obesity, insulin resistance and free fatty acids," *Current Opinion in Endocrinology, Diabetes, and Obesity*, vol. 18, no. 2, pp. 139–143, 2011.

[20] C. Yu, Y. Chen, G. W. Cline et al., "Mechanism by which fatty acids inhibit insulin activation of insulin receptor substrate-1 (IRS-1)-associated phosphatidylinositol 3-kinase activity in muscle," *The Journal of Biological Chemistry*, vol. 277, no. 52, pp. 50230–50236, 2002.

[21] H. Shi, M. V. Kokoeva, K. Inouye, I. Tzameli, H. Yin, and J. S. Flier, "TLR4 links innate immunity and fatty acid-induced insulin resistance," *The Journal of Clinical Investigation*, vol. 116, no. 11, pp. 3015–3025, 2006.

[22] A. C. Konner and J. C. Bruning, "Toll-like receptors: linking inflammation to metabolism," *Trends in Endocrinology and Metabolism*, vol. 22, no. 1, pp. 16–23, 2011.

[23] M. Tschop, C. Weyer, P. A. Tataranni, V. Devanarayan, E. Ravussin, and M. L. Heiman, "Circulating ghrelin levels are decreased in human obesity," *Diabetes*, vol. 50, no. 4, pp. 707–709, 2001.

[24] A. L. Mark, M. L. Correia, K. Rahmouni, and W. G. Haynes, "Selective leptin resistance: a new concept in leptin physiology with cardiovascular implications," *Journal of Hypertension*, vol. 20, no. 7, pp. 1245–1250, 2002.

[25] M. J. Song, K. H. Kim, J. M. Yoon, and J. B. Kim, "Activation of Toll-like receptor 4 is associated with insulin resistance in adipocytes," *Biochemical and Biophysical Research Communications*, vol. 346, no. 3, pp. 739–745, 2006.

[26] C. J. Andersen, K. E. Murphy, and M. L. Fernandez, "Impact of obesity and metabolic syndrome on immunity," *Advances in Nutrition*, vol. 7, no. 1, pp. 66–75, 2016.

[27] P. M. Moraes-Vieira, E. J. Bassi, R. A. Larocca et al., "Leptin deficiency modulates allograft survival by favoring a Th2 and a regulatory immune profile. [corrected]," *American Journal of Transplantation*, vol. 13, no. 1, pp. 36–44, 2013.

[28] M. L. Barreiro, F. Gaytan, J. E. Caminos et al., "Cellular location and hormonal regulation of ghrelin expression in rat testis," *Biology of Reproduction*, vol. 67, no. 6, pp. 1768–1776, 2002.

[29] S. Gnanapavan, B. Kola, S. A. Bustin et al., "The tissue distribution of the mRNA of ghrelin and subtypes of its receptor, GHS-R, in humans," *The Journal of Clinical Endocrinology and Metabolism*, vol. 87, no. 6, p. 2988, 2002.

[30] C. De Vriese and C. Delporte, "Ghrelin: a new peptide regulating growth hormone release and food intake," *The International Journal of Biochemistry & Cell Biology*, vol. 40, no. 8, pp. 1420–1424, 2008.

[31] A. Stengel and Y. Tache, "Ghrelin - a pleiotropic hormone secreted from endocrine x/a-like cells of the stomach," *Frontiers in Neuroscience*, vol. 6, p. 24, 2012.

[32] M. Kojima, H. Hosoda, Y. Date, M. Nakazato, H. Matsuo, and K. Kangawa, "Ghrelin is a growth-hormone-releasing acylated peptide from stomach," *Nature*, vol. 402, no. 6762, pp. 656–660, 1999.

[33] G. Wang, H. M. Lee, E. Englander, and G. H. Greeley Jr., "Ghrelin–not just another stomach hormone," *Regulatory Peptides*, vol. 105, no. 2, pp. 75–81, 2002.

[34] D. Baatar, K. Patel, and D. D. Taub, "The effects of ghrelin on inflammation and the immune system," *Molecular and Cellular Endocrinology*, vol. 340, no. 1, pp. 44–58, 2011.

[35] M. W. Schwartz, S. C. Woods, D. Porte Jr., R. J. Seeley, and D. G. Baskin, "Central nervous system control of food intake," *Nature*, vol. 404, no. 6778, pp. 661–671, 2000.

[36] V. D. Dixit and D. D. Taub, "Ghrelin and immunity: a young player in an old field," *Experimental Gerontology*, vol. 40, no. 11, pp. 900–910, 2005.

[37] E. Gonzalez-Rey, A. Chorny, and M. Delgado, "Therapeutic action of ghrelin in a mouse model of colitis," *Gastroenterology*, vol. 130, no. 6, pp. 1707–1720, 2006.

[38] K. Takagi, R. Legrand, A. Asakawa et al., "Anti-ghrelin immunoglobulins modulate ghrelin stability and its orexigenic effect in obese mice and humans," *Nature Communications*, vol. 4, p. 2685, 2013.

[39] C. Delporte, "Structure and physiological actions of ghrelin," *Scientifica (Cairo)*, vol. 2013, Article ID 518909, 25 pages, 2013.

[40] K. B. Chow, J. Sun, K. M. Chu, W. Tai Cheung, C. H. Cheng, and H. Wise, "The truncated ghrelin receptor polypeptide (GHS-R1b) is localized in the endoplasmic reticulum where it forms heterodimers with ghrelin receptors (GHS-R1a) to attenuate their cell surface expression," *Molecular and Cellular Endocrinology*, vol. 348, no. 1, pp. 247–254, 2012.

[41] T. D. Muller, R. Nogueiras, M. L. Andermann et al., "Ghrelin," *Molecular Metabolism*, vol. 4, no. 6, pp. 437–460, 2015.

[42] Z. B. Andrews, "Central mechanisms involved in the orexigenic actions of ghrelin," *Peptides*, vol. 32, no. 11, pp. 2248–2255, 2011.

[43] M. Korbonits, A. P. Goldstone, M. Gueorguiev, and A. B. Grossman, "Ghrelin–a hormone with multiple functions," *Frontiers in Neuroendocrinology*, vol. 25, no. 1, pp. 27–68, 2004.

[44] M. Camilleri, A. Papathanasopoulos, and S. T. Odunsi, "Actions and therapeutic pathways of ghrelin for gastrointestinal disorders," *Nature Reviews Gastroenterology & Hepatology*, vol. 6, no. 6, pp. 343–352, 2009.

[45] F. Mirzaie Bavil, G. Mohaddes, H. Ebrahimi, R. Keyhanmanesh, R. Ghiyasi, and M. R. Alipour, "Ghrelin increases lymphocytes in chronic normobaric hypoxia," *Advanced Pharmaceutical Bulletin*, vol. 4, no. 4, pp. 339–343, 2014.

[46] G. Baldanzi, N. Filigheddu, S. Cutrupi et al., "Ghrelin and des-acyl ghrelin inhibit cell death in cardiomyocytes and endothelial cells through ERK1/2 and PI 3-kinase/AKT," *The Journal of Cell Biology*, vol. 159, no. 6, pp. 1029–1037, 2002.

[47] L. Li, L. K. Zhang, Y. Z. Pang et al., "Cardioprotective effects of ghrelin and des-octanoyl ghrelin on myocardial injury induced by isoproterenol in rats," *Acta Pharmacologica Sinica*, vol. 27, no. 5, pp. 527–535, 2006.

[48] G. Togliatto, A. Trombetta, P. Dentelli et al., "Unacylated ghrelin rescues endothelial progenitor cell function in individuals with type 2 diabetes," *Diabetes*, vol. 59, no. 4, pp. 1016–1025, 2010.

[49] D. E. Cummings, "Ghrelin and the short- and long-term regulation of appetite and body weight," *Physiology & Behavior*, vol. 89, no. 1, pp. 71–84, 2006.

[50] K. Kirsz and D. A. Zieba, "Ghrelin-mediated appetite regulation in the central nervous system," *Peptides*, vol. 32, no. 11, pp. 2256–2264, 2011.

[51] T. R. Castaneda, J. Tong, R. Datta, M. Culler, and M. H. Tschöp, "Ghrelin in the regulation of body weight and metabolism," *Frontiers in Neuroendocrinology*, vol. 31, no. 1, pp. 44–60, 2010.

[52] M. Kojima, H. Hosoda, H. Matsuo, and K. Kangawa, "Ghrelin: discovery of the natural endogenous ligand for the growth hormone secretagogue receptor," *Trends in Endocrinology and Metabolism*, vol. 12, no. 3, pp. 118–122, 2001.

[53] T. Sato, Y. Nakamura, Y. Shiimura, H. Ohgusu, K. Kangawa, and M. Kojima, "Structure, regulation and function of ghrelin," *Journal of Biochemistry*, vol. 151, no. 2, pp. 119–128, 2012.

[54] J. Yang, M. S. Brown, G. Liang, N. V. Grishin, and J. L. Goldstein, "Identification of the acyltransferase that octanoylates ghrelin, an appetite-stimulating peptide hormone," *Cell*, vol. 132, no. 3, pp. 387–396, 2008.

[55] O. Al Massadi, M. H. Tschop, and J. Tong, "Ghrelin acylation and metabolic control," *Peptides*, vol. 32, no. 11, pp. 2301–2308, 2011.

[56] L. K. Chopin, I. Seim, C. M. Walpole, and A. C. Herington, "The ghrelin axis–does it have an appetite for cancer progression?," *Endocrine Reviews*, vol. 33, no. 6, pp. 849–891, 2012.

[57] M. Kojima, "The discovery of ghrelin–a personal memory," *Regulatory Peptides*, vol. 145, no. 1–3, pp. 2–6, 2008.

[58] M. Kojima and K. Kangawa, "Ghrelin: structure and function," *Physiological Reviews*, vol. 85, no. 2, pp. 495–522, 2005.

[59] Y. Masuda, T. Tanaka, N. Inomata et al., "Ghrelin stimulates gastric acid secretion and motility in rats," *Biochemical and Biophysical Research Communications*, vol. 276, no. 3, pp. 905–908, 2000.

[60] C. Dornonville de la Cour, E. Lindstrom, P. Norlén, and R. Håkanson, "Ghrelin stimulates gastric emptying but is without effect on acid secretion and gastric endocrine cells," *Regulatory Peptides*, vol. 120, no. 1–3, pp. 23–32, 2004.

[61] P. J. Delhanty and A. J. van der Lely, "Ghrelin and glucose homeostasis," *Peptides*, vol. 32, no. 11, pp. 2309–2318, 2011.

[62] H. Ueno, H. Yamaguchi, K. Kangawa, and M. Nakazato, "Ghrelin: a gastric peptide that regulates food intake and energy homeostasis," *Regulatory Peptides*, vol. 126, no. 1-2, pp. 11–19, 2005.

[63] D. Siegl, E. F. Midura, T. Annecke, P. Conzen, C. C. Caldwell, and J. Tschoep, "The effect of ghrelin upon the early immune response in lean and obese mice during sepsis," *PLoS One*, vol. 10, no. 4, article e0122211, 2015.

[64] M. Tschop, D. L. Smiley, and M. L. Heiman, "Ghrelin induces adiposity in rodents," *Nature*, vol. 407, no. 6806, pp. 908–913, 2000.

[65] M. Nakazato, N. Murakami, Y. Date et al., "A role for ghrelin in the central regulation of feeding," *Nature*, vol. 409, no. 6817, pp. 194–198, 2001.

[66] U. Andersson, K. Filipsson, C. R. Abbott et al., "AMP-activated protein kinase plays a role in the control of food intake," *The Journal of Biological Chemistry*, vol. 279, no. 13, pp. 12005–12008, 2004.

[67] D. G. Hardie, "AMPK: a key regulator of energy balance in the single cell and the whole organism," *International Journal of Obesity*, vol. 32, Supplement 4, pp. S7–S12, 2008.

[68] B. Kola, I. Farkas, M. Christ-Crain et al., "The orexigenic effect of ghrelin is mediated through central activation of the endogenous cannabinoid system," *PLoS One*, vol. 3, no. 3, article e1797, 2008.

[69] D. Kohno, H. Z. Gao, S. Muroya, S. Kikuyama, and T. Yada, "Ghrelin directly interacts with neuropeptide-Y-containing neurons in the rat arcuate nucleus: Ca2+ signaling via protein kinase A and N-type channel-dependent mechanisms and cross-talk with leptin and orexin," *Diabetes*, vol. 52, no. 4, pp. 948–956, 2003.

[70] M. Lopez, R. Lage, A. K. Saha et al., "Hypothalamic fatty acid metabolism mediates the orexigenic action of ghrelin," *Cell Metabolism*, vol. 7, no. 5, pp. 389–399, 2008.

[71] L. Martins, D. Fernandez-Mallo, M. G. Novelle et al., "Hypothalamic mTOR signaling mediates the orexigenic action of ghrelin," *PLoS One*, vol. 7, no. 10, article e46923, 2012.

[72] D. Stevanovic, V. Trajkovic, S. Müller-Lühlhoff et al., "Ghrelin-induced food intake and adiposity depend on central mTORC1/S6K1 signaling," *Molecular and Cellular Endocrinology*, vol. 381, no. 1-2, pp. 280–290, 2013.

[73] Y. Minokoshi, Y. B. Kim, O. D. Peroni et al., "Leptin stimulates fatty-acid oxidation by activating AMP-activated protein kinase," *Nature*, vol. 415, no. 6869, pp. 339–343, 2002.

[74] L. L. Anderson, S. Jeftinija, and C. G. Scanes, "Growth hormone secretion: molecular and cellular mechanisms and in vivo approaches," *Experimental Biology and Medicine (Maywood, N.J.)*, vol. 229, no. 4, pp. 291–302, 2004.

[75] Z. B. Andrews, Z. W. Liu, N. Walllingford et al., "UCP2 mediates ghrelin's action on NPY/AgRP neurons by lowering free radicals," *Nature*, vol. 454, no. 7206, pp. 846–851, 2008.

[76] K. Venkova and B. Greenwood-Van Meerveld, "Application of ghrelin to gastrointestinal diseases," *Current Opinion in Investigational Drugs*, vol. 9, no. 10, pp. 1103–1107, 2008.

[77] B. Kola and M. Korbonits, "Shedding light on the intricate puzzle of ghrelin's effects on appetite regulation," *The Journal of Endocrinology*, vol. 202, no. 2, pp. 191–198, 2009.

[78] C. T. Lim, B. Kola, and M. Korbonits, "AMPK as a mediator of hormonal signalling," *Journal of Molecular Endocrinology*, vol. 44, no. 2, pp. 87–97, 2010.

[79] C. Pemberton, P. Wimalasena, T. Yandle, S. Soule, and M. Richards, "C-terminal pro-ghrelin peptides are present in the human circulation," *Biochemical and Biophysical Research Communications*, vol. 310, no. 2, pp. 567–573, 2003.

[80] D. Cota, K. Proulx, K. A. Smith et al., "Hypothalamic mTOR signaling regulates food intake," *Science*, vol. 312, no. 5775, pp. 927–930, 2006.

[81] E. C. Villanueva, H. Munzberg, D. Cota et al., "Complex regulation of mammalian target of rapamycin complex 1 in the basomedial hypothalamus by leptin and nutritional status," *Endocrinology*, vol. 150, no. 10, pp. 4541–4551, 2009.

[82] W. Zhang, C. Zhang, D. Fritze, B. Chai, J. Li, and M. W. Mulholland, "Modulation of food intake by mTOR signalling in the dorsal motor nucleus of the vagus in male rats:

focus on ghrelin and nesfatin-1," *Experimental Physiology*, vol. 98, no. 12, pp. 1696–1704, 2013.

[83] R. Lage, M. J. Vazquez, L. Varela et al., "Ghrelin effects on neuropeptides in the rat hypothalamus depend on fatty acid metabolism actions on BSX but not on gender," *The FASEB Journal*, vol. 24, no. 8, pp. 2670–2679, 2010.

[84] R. Avallone, A. Demers, A. Rodrigue-Way et al., "A growth hormone-releasing peptide that binds scavenger receptor CD36 and ghrelin receptor up-regulates sterol transporters and cholesterol efflux in macrophages through a peroxisome proliferator-activated receptor gamma-dependent pathway," *Molecular Endocrinology*, vol. 20, no. 12, pp. 3165–3178, 2006.

[85] D. Vats, L. Mukundan, J. I. Odegaard et al., "Oxidative metabolism and PGC-1beta attenuate macrophage-mediated inflammation," *Cell Metabolism*, vol. 4, no. 1, pp. 13–24, 2006.

[86] J. Van den Bossche, J. Baardman, and M. P. de Winther, "Metabolic characterization of polarized M1 and M2 bone marrow-derived macrophages using real-time extracellular flux analysis," *Journal of Visualized Experiments*, vol. 1, no. 105, 2015.

[87] J. Van den Bossche, J. Baardman, N. A. Otto et al., "Mitochondrial dysfunction prevents repolarization of inflammatory macrophages," *Cell Reports*, vol. 17, no. 3, pp. 684–696, 2016.

[88] C. Chen, D. Wu, and I. J. Clarke, "Signal transduction systems employed by synthetic GH-releasing peptides in somatotrophs," *The Journal of Endocrinology*, vol. 148, no. 3, pp. 381–386, 1996.

[89] F. Zapata-Gonzalez, F. Rueda, J. Petriz et al., "9-cis-Retinoic acid (9cRA), a retinoid X receptor (RXR) ligand, exerts immunosuppressive effects on dendritic cells by RXR-dependent activation: inhibition of peroxisome proliferator-activated receptor gamma blocks some of the 9cRA activities, and precludes them to mature phenotype development," *Journal of Immunology*, vol. 178, no. 10, pp. 6130–6139, 2007.

[90] T. Sato, T. Ida, Y. Nakamura, Y. Shiimura, K. Kangawa, and M. Kojima, "Physiological roles of ghrelin on obesity," *Obesity Research & Clinical Practice*, vol. 8, no. 5, pp. e405–e413, 2014.

[91] F. M. Schmidt, J. Weschenfelder, C. Sander et al., "Inflammatory cytokines in general and central obesity and modulating effects of physical activity," *PLoS One*, vol. 10, no. 3, article e0121971, 2015.

[92] Y. E. Kang, J. M. Kim, K. H. Joung et al., "The roles of adipokines, proinflammatory cytokines, and adipose tissue macrophages in obesity-associated insulin resistance in modest obesity and early metabolic dysfunction," *PLoS One*, vol. 11, no. 4, article e0154003, 2016.

[93] K. Makki, P. Froguel, and I. Wolowczuk, "Adipose tissue in obesity-related inflammation and insulin resistance: cells, cytokines, and chemokines," *ISRN Inflammation*, vol. 2013, Article ID 139239, 12 pages, 2013.

[94] J. M. Olefsky and C. K. Glass, "Macrophages, inflammation, and insulin resistance," *Annual Review of Physiology*, vol. 72, pp. 219–246, 2010.

[95] S. L. Deshmane, S. Kremlev, S. Amini, and B. E. Sawaya, "Monocyte chemoattractant protein-1 (MCP-1): an overview," *Journal of Interferon & Cytokine Research*, vol. 29, no. 6, pp. 313–326, 2009.

[96] W. G. Li, D. Gavrila, X. Liu et al., "Ghrelin inhibits proinflammatory responses and nuclear factor-kappaB activation in human endothelial cells," *Circulation*, vol. 109, no. 18, pp. 2221–2226, 2004.

[97] C. N. Lumeng, J. Liu, L. Geletka et al., "Aging is associated with an increase in T cells and inflammatory macrophages in visceral adipose tissue," *Journal of Immunology*, vol. 187, no. 12, pp. 6208–6216, 2011.

[98] J. Braune, U. Weyer, C. Hobusch et al., "IL-6 regulates M2 polarization and local proliferation of adipose tissue macrophages in obesity," *Journal of Immunology*, vol. 198, no. 7, pp. 2927–2934, 2017.

[99] L. Lin, J. H. Lee, E. D. Buras et al., "Ghrelin receptor regulates adipose tissue inflammation in aging," *Aging (Albany NY)*, vol. 8, no. 1, pp. 178–191, 2016.

[100] A. Mantovani, S. K. Biswas, M. R. Galdiero, A. Sica, and M. Locati, "Macrophage plasticity and polarization in tissue repair and remodelling," *The Journal of Pathology*, vol. 229, no. 2, pp. 176–185, 2013.

[101] P. Peraldi, G. S. Hotamisligil, W. A. Buurman, M. F. White, and B. M. Spiegelman, "Tumor necrosis factor (TNF)-alpha inhibits insulin signaling through stimulation of the p55 TNF receptor and activation of sphingomyelinase," *The Journal of Biological Chemistry*, vol. 271, no. 22, pp. 13018–13022, 1996.

[102] C. de Luca and J. M. Olefsky, "Inflammation and insulin resistance," *FEBS Letters*, vol. 582, no. 1, pp. 97–105, 2008.

[103] P. M. Moraes-Vieira, M. M. Yore, P. M. Dwyer, I. Syed, P. Aryal, and B. B. Kahn, "RBP4 activates antigen-presenting cells, leading to adipose tissue inflammation and systemic insulin resistance," *Cell Metabolism*, vol. 19, no. 3, pp. 512–526, 2014.

[104] P. M. Moraes-Vieira, A. Castoldi, P. Aryal, K. Wellenstein, O. D. Peroni, and B. B. Kahn, "Antigen presentation and T-cell activation are critical for RBP4-induced insulin resistance," *Diabetes*, vol. 65, no. 5, pp. 1317–1327, 2016.

[105] S. P. Kalra, N. Ueno, and P. S. Kalra, "Stimulation of appetite by ghrelin is regulated by leptin restraint: peripheral and central sites of action," *The Journal of Nutrition*, vol. 135, no. 5, pp. 1331–1335, 2005.

[106] X. Ma, L. Lin, J. Yue et al., "Ghrelin receptor regulates HFCS-induced adipose inflammation and insulin resistance," *Nutrition & Diabetes*, vol. 3, article e99, 2013.

[107] D. D. Taub, "Novel connections between the neuroendocrine and immune systems: the ghrelin immunoregulatory network," *Vitamins and Hormones*, vol. 77, pp. 325–346, 2008.

[108] C. Camell and C. W. Smith, "Dietary oleic acid increases M2 macrophages in the mesenteric adipose tissue," *PLoS One*, vol. 8, no. 9, article e75147, 2013.

[109] F. Ginhoux and S. Jung, "Monocytes and macrophages: developmental pathways and tissue homeostasis," *Nature Reviews Immunology*, vol. 14, no. 6, pp. 392–404, 2014.

[110] S. S. Choe, J. Y. Huh, I. J. Hwang, J. I. Kim, and J. B. Kim, "Adipose tissue remodeling: its role in energy metabolism and metabolic disorders," *Frontiers in Endocrinology (Lausanne)*, vol. 7, p. 30, 2016.

[111] V. D. Dixit, E. M. Schaffer, R. S. Pyle et al., "Ghrelin inhibits leptin- and activation-induced proinflammatory cytokine expression by human monocytes and T cells," *The Journal of Clinical Investigation*, vol. 114, no. 1, pp. 57–66, 2004.

[112] H. Wei, X. Cao, Q. Zeng et al., "Ghrelin inhibits proinflammatory responses and prevents cognitive impairment in septic rats," *Critical Care Medicine*, vol. 43, no. 5, pp. e143–e150, 2015.

[113] L. Chang, J. Zhao, J. Yang, Z. Zhang, J. Du, and C. Tang, "Therapeutic effects of ghrelin on endotoxic shock in rats," *European Journal of Pharmacology*, vol. 473, no. 2-3, pp. 171–176, 2003.

[114] A. Jacob, D. Rajan, B. Pathickal et al., "The inhibitory effect of ghrelin on sepsis-induced inflammation is mediated by the MAPK phosphatase-1," *International Journal of Molecular Medicine*, vol. 25, no. 1, pp. 159–164, 2010.

[115] S. Miyake and T. Yamamura, "Ghrelin: friend or foe for neuroinflammation," *Discovery Medicine*, vol. 8, no. 41, pp. 64–67, 2009.

[116] M. Ersahin, H. Z. Toklu, C. Erzik et al., "The anti-inflammatory and neuroprotective effects of ghrelin in subarachnoid hemorrhage-induced oxidative brain damage in rats," *Journal of Neurotrauma*, vol. 27, no. 6, pp. 1143–1155, 2010.

[117] C. Liu, J. Huang, H. Li et al., "Ghrelin accelerates wound healing through GHS-R1a-mediated MAPK-NF-kappaB/GR signaling pathways in combined radiation and burn injury in rats," *Scientific Reports*, vol. 6, article 27499, 2016.

[118] F. Azizzadeh, J. Mahmoodi, S. Sadigh-Eteghad, F. Farajdokht, and G. Mohaddes, "Ghrelin exerts analgesic effects through modulation of IL-10 and TGF-beta levels in a rat model of inflammatory pain," *Iranian Biomedical Journal*, vol. 21, no. 2, pp. 114–119, 2017.

[119] M. Granado, T. Priego, A. I. Martín, M. A. Villanúa, and A. López-Calderón, "Anti-inflammatory effect of the ghrelin agonist growth hormone-releasing peptide-2 (GHRP-2) in arthritic rats," *American Journal of Physiology, Endocrinology and Metabolism*, vol. 288, no. 3, pp. E486–E492, 2005.

[120] B. Li, M. Zeng, H. Zheng et al., "Effects of ghrelin on the apoptosis of human neutrophils in vitro," *International Journal of Molecular Medicine*, vol. 38, no. 3, pp. 794–802, 2016.

[121] T. Kodama, J. Ashitani, N. Matsumoto, K. Kangawa, and M. Nakazato, "Ghrelin treatment suppresses neutrophil-dominant inflammation in airways of patients with chronic respiratory infection," *Pulmonary Pharmacology & Therapeutics*, vol. 21, no. 5, pp. 774–779, 2008.

[122] E. G. Orlova, S. V. Shirshev, and O. A. Loginova, "Leptin and ghrelin regulate dendritic cell maturation and dendritic cell induction of regulatory T-cells," *Doklady Biological Sciences*, vol. 462, pp. 171–174, 2015.

[123] V. D. Dixit, H. Yang, Y. Sun et al., "Ghrelin promotes thymopoiesis during aging," *The Journal of Clinical Investigation*, vol. 117, no. 10, pp. 2778–2790, 2007.

[124] J. Oh and J. S. Shin, "The role of dendritic cells in central tolerance," *Immune Network*, vol. 15, no. 3, pp. 111–120, 2015.

[125] L. Souza-Moreira, V. Delgado-Maroto, M. Morell, F. O'Valle, R. G. Del Moral, and E. Gonzalez-Rey, "Therapeutic effect of ghrelin in experimental autoimmune encephalomyelitis by inhibiting antigen-specific Th1/Th17 responses and inducing regulatory T cells," *Brain, Behavior, and Immunity*, vol. 30, pp. 54–60, 2013.

[126] S. D. Miller and W. J. Karpus, "Experimental autoimmune encephalomyelitis in the mouse," *Current Protocols in Immunology*, vol. 1, 2007, Chapter 15:Unit 15 1.

[127] M. M. Theil, S. Miyake, M. Mizuno et al., "Suppression of experimental autoimmune encephalomyelitis by ghrelin," *Journal of Immunology*, vol. 183, no. 4, pp. 2859–2866, 2009.

[128] L. L. Anderson, S. Jeftinija, C. G. Scanes et al., "Physiology of ghrelin and related peptides," *Domestic Animal Endocrinology*, vol. 29, no. 1, pp. 111–144, 2005.

[129] C. C. Au, M. M. Docanto, H. Zahid et al., "Des-acyl ghrelin inhibits the capacity of macrophages to stimulate the expression of aromatase in breast adipose stromal cells," *The Journal of Steroid Biochemistry and Molecular Biology*, vol. 170, pp. 49–53, 2017.

[130] T. Waseem, M. Duxbury, H. Ito, S. W. Ashley, and M. K. Robinson, "Exogenous ghrelin modulates release of pro-inflammatory and anti-inflammatory cytokines in LPS-stimulated macrophages through distinct signaling pathways," *Surgery*, vol. 143, no. 3, pp. 334–342, 2008.

[131] M. E. Bamberger, M. E. Harris, D. R. McDonald, J. Husemann, and G. E. Landreth, "A cell surface receptor complex for fibrillar beta-amyloid mediates microglial activation," *The Journal of Neuroscience*, vol. 23, no. 7, pp. 2665–2674, 2003.

[132] H. Jiang, L. J. Li, J. Wang, and J. X. Xie, "Ghrelin antagonizes MPTP-induced neurotoxicity to the dopaminergic neurons in mouse substantia nigra," *Experimental Neurology*, vol. 212, no. 2, pp. 532–537, 2008.

[133] M. Moon, H. G. Kim, L. Hwang et al., "Neuroprotective effect of ghrelin in the 1-methyl-4-phenyl-1,2,3,6-tetrahydropyridine mouse model of Parkinson's disease by blocking microglial activation," *Neurotoxicity Research*, vol. 15, no. 4, pp. 332–347, 2009.

[134] E. Lim, S. Lee, E. Li, Y. Kim, and S. Park, "Ghrelin protects spinal cord motoneurons against chronic glutamate-induced excitotoxicity via ERK1/2 and phosphatidylinositol-3-kinase/Akt/glycogen synthase kinase-3beta pathways," *Experimental Neurology*, vol. 230, no. 1, pp. 114–122, 2011.

[135] Z. B. Andrews, D. Erion, R. Beiler et al., "Ghrelin promotes and protects nigrostriatal dopamine function via a UCP2-dependent mitochondrial mechanism," *The Journal of Neuroscience*, vol. 29, no. 45, pp. 14057–14065, 2009.

[136] X. M. Guan, H. Yu, O. C. Palyha et al., "Distribution of mRNA encoding the growth hormone secretagogue receptor in brain and peripheral tissues," *Brain Research. Molecular Brain Research*, vol. 48, no. 1, pp. 23–29, 1997.

[137] J. M. Zigman, J. E. Jones, C. E. Lee, C. B. Saper, and J. K. Elmquist, "Expression of ghrelin receptor mRNA in the rat and the mouse brain," *The Journal of Comparative Neurology*, vol. 494, no. 3, pp. 528–548, 2006.

[138] V. Jackson-Lewis and S. Przedborski, "Protocol for the MPTP mouse model of Parkinson's disease," *Nature Protocols*, vol. 2, no. 1, pp. 141–151, 2007.

[139] Z. B. Andrews, S. Diano, and T. L. Horvath, "Mitochondrial uncoupling proteins in the CNS: in support of function and survival," *Nature Reviews Neuroscience*, vol. 6, no. 11, pp. 829–840, 2005.

[140] Z. B. Andrews, B. Horvath, C. J. Barnstable et al., "Uncoupling protein-2 is critical for nigral dopamine cell survival in a mouse model of Parkinson's disease," *The Journal of Neuroscience*, vol. 25, no. 1, pp. 184–191, 2005.

[141] B. Conti, S. Sugama, J. Lucero et al., "Uncoupling protein 2 protects dopaminergic neurons from acute 1,2,3,6-methyl-

phenyl-tetrahydropyridine toxicity," *Journal of Neurochemistry*, vol. 93, no. 2, pp. 493–501, 2005.

[142] Z. B. Andrews, A. Rivera, J. D. Elsworth et al., "Uncoupling protein-2 promotes nigrostriatal dopamine neuronal function," *The European Journal of Neuroscience*, vol. 24, no. 1, pp. 32–36, 2006.

[143] H. Omrani, M. R. Alipour, F. Farajdokht, H. Ebrahimi, M. Mesgari Abbasi, and G. Mohaddes, "Effects of chronic ghrelin treatment on hypoxia-induced brain oxidative stress and inflammation in a rat normobaric chronic hypoxia model," *High Altitude Medicine & Biology*, vol. 18, no. 2, pp. 145–151, 2017.

[144] V. P. Carlini, M. E. Monzon, M. M. Varas et al., "Ghrelin increases anxiety-like behavior and memory retention in rats," *Biochemical and Biophysical Research Communications*, vol. 299, no. 5, pp. 739–743, 2002.

[145] V. P. Carlini, M. Ghersi, H. B. Schiöth, and S. R. de Barioglio, "Ghrelin and memory: differential effects on acquisition and retrieval," *Peptides*, vol. 31, no. 6, pp. 1190–1193, 2010.

[146] S. Diano, S. A. Farr, S. C. Benoit et al., "Ghrelin controls hippocampal spine synapse density and memory performance," *Nature Neuroscience*, vol. 9, no. 3, pp. 381–388, 2006.

[147] V. P. Carlini, R. C. Gaydou, H. B. Schiöth, and S. R. de Barioglio, "Selective serotonin reuptake inhibitor (fluoxetine) decreases the effects of ghrelin on memory retention and food intake," *Regulatory Peptides*, vol. 140, no. 1-2, pp. 65–73, 2007.

[148] J. Altman and G. D. Das, "Autoradiographic and histological evidence of postnatal hippocampal neurogenesis in rats," *The Journal of Comparative Neurology*, vol. 124, no. 3, pp. 319–335, 1965.

[149] J. A. Paton and F. N. Nottebohm, "Neurons generated in the adult brain are recruited into functional circuits," *Science*, vol. 225, no. 4666, pp. 1046–1048, 1984.

[150] G. L. Ming and H. Song, "Adult neurogenesis in the mammalian brain: significant answers and significant questions," *Neuron*, vol. 70, no. 4, pp. 687–702, 2011.

[151] D. A. Lee and S. Blackshaw, "Functional implications of hypothalamic neurogenesis in the adult mammalian brain," *International Journal of Developmental Neuroscience*, vol. 30, no. 8, pp. 615–621, 2012.

[152] R. A. Marr, R. M. Thomas, and D. A. Peterson, "Insights into neurogenesis and aging: potential therapy for degenerative disease?," *Future Neurology*, vol. 5, no. 4, pp. 527–541, 2010.

[153] H. Jun, S. Mohammed Qasim Hussaini, M. J. Rigby, and M. H. Jang, "Functional role of adult hippocampal neurogenesis as a therapeutic strategy for mental disorders," *Neural Plasticity*, vol. 2012, Article ID 854285, 20 pages, 2012.

[154] K. S. Radad, R. Moldzio, M. Al-Shraim, B. Kranner, C. Krewenka, and W. D. Rausch, "Recent advances on the role of neurogenesis in the adult brain: therapeutic potential in Parkinson's and Alzheimer's diseases," *CNS & Neurological Disorders Drug Targets*, vol. 16, 2017.

[155] A. Sahay, K. N. Scobie, A. S. Hill et al., "Increasing adult hippocampal neurogenesis is sufficient to improve pattern separation," *Nature*, vol. 472, no. 7344, pp. 466–470, 2011.

[156] M. Moon, S. Kim, L. Hwang, and S. Park, "Ghrelin regulates hippocampal neurogenesis in adult mice," *Endocrine Journal*, vol. 56, no. 3, pp. 525–531, 2009.

[157] W. Zhang, T. R. Lin, Y. Hu et al., "Ghrelin stimulates neurogenesis in the dorsal motor nucleus of the vagus," *The Journal of Physiology*, vol. 559, Part 3, pp. 729–737, 2004.

[158] I. Johansson, S. Destefanis, N. D. Aberg et al., "Proliferative and protective effects of growth hormone secretagogues on adult rat hippocampal progenitor cells," *Endocrinology*, vol. 149, no. 5, pp. 2191–2199, 2008.

[159] S. Wildman and A. Hewison, "Rediscovering a history of nursing management: from nightingale to the modern matron," *International Journal of Nursing Studies*, vol. 46, no. 12, pp. 1650–1661, 2009.

[160] H. Chung, E. Kim, D. H. Lee et al., "Ghrelin inhibits apoptosis in hypothalamic neuronal cells during oxygen-glucose deprivation," *Endocrinology*, vol. 148, no. 1, pp. 148–159, 2007.

[161] Y. Miao, Q. Xia, Z. Hou, Y. Zheng, H. Pan, and S. Zhu, "Ghrelin protects cortical neuron against focal ischemia/reperfusion in rats," *Biochemical and Biophysical Research Communications*, vol. 359, no. 3, pp. 795–800, 2007.

[162] Y. Liu, L. Chen, X. Xu, E. Vicaut, and R. Sercombe, "Both ischemic preconditioning and ghrelin administration protect hippocampus from ischemia/reperfusion and upregulate uncoupling protein-2," *BMC Physiology*, vol. 9, p. 17, 2009.

[163] Y. Liu, P. S. Wang, D. Xie, K. Liu, and L. Chen, "Ghrelin reduces injury of hippocampal neurons in a rat model of cerebral ischemia/reperfusion," *The Chinese Journal of Physiology*, vol. 49, no. 5, pp. 244–250, 2006.

[164] J. C. Chuang and J. M. Zigman, "Ghrelin's roles in stress, mood, and anxiety regulation," *International Journal of Peptide*, vol. 2010, Article ID 460549, 5 pages, 2010.

[165] D. E. Cummings, D. S. Weigle, R. S. Frayo et al., "Plasma ghrelin levels after diet-induced weight loss or gastric bypass surgery," *The New England Journal of Medicine*, vol. 346, no. 21, pp. 1623–1630, 2002.

[166] E. Kristenssson, M. Sundqvist, M. Astin et al., "Acute psychological stress raises plasma ghrelin in the rat," *Regulatory Peptides*, vol. 134, no. 2-3, pp. 114–117, 2006.

[167] M. Lutter, I. Sakata, S. Osborne-Lawrence et al., "The orexigenic hormone ghrelin defends against depressive symptoms of chronic stress," *Nature Neuroscience*, vol. 11, no. 7, pp. 752-753, 2008.

[168] M. Ochi, K. Tominaga, F. Tanaka et al., "Effect of chronic stress on gastric emptying and plasma ghrelin levels in rats," *Life Sciences*, vol. 82, no. 15-16, pp. 862–868, 2008.

[169] G. M. Slavich and M. R. Irwin, "From stress to inflammation and major depressive disorder: a social signal transduction theory of depression," *Psychological Bulletin*, vol. 140, no. 3, pp. 774–815, 2014.

[170] R. Dantzer, J. C. O'Connor, G. G. Freund, R. W. Johnson, and K. W. Kelley, "From inflammation to sickness and depression: when the immune system subjugates the brain," *Nature Reviews Neuroscience*, vol. 9, no. 1, pp. 46–56, 2008.

[171] M. Alvarez-Crespo, K. P. Skibicka, I. Farkas et al., "The amygdala as a neurobiological target for ghrelin in rats: neuroanatomical, electrophysiological and behavioral evidence," *PLoS One*, vol. 7, no. 10, article e46321, 2012.

[172] R. M. Meyer, A. Burgos-Robles, E. Liu, S. S. Correia, and K. A. Goosens, "A ghrelin-growth hormone axis drives stress-induced vulnerability to enhanced fear," *Molecular Psychiatry*, vol. 19, no. 12, pp. 1284–1294, 2014.

[173] S. J. Spencer, T. L. Emmerzaal, T. Kozicz, and Z. B. Andrews, "Ghrelin's role in the hypothalamic-pituitary-adrenal axis

stress response: implications for mood disorders," *Biological Psychiatry*, vol. 78, no. 1, pp. 19–27, 2015.

[174] M. G. Willesen, P. Kristensen, and J. Rømer, "Co-localization of growth hormone secretagogue receptor and NPY mRNA in the arcuate nucleus of the rat," *Neuroendocrinology*, vol. 70, no. 5, pp. 306–316, 1999.

[175] M. Milanski, G. Degasperi, A. Coope et al., "Saturated fatty acids produce an inflammatory response predominantly through the activation of TLR4 signaling in hypothalamus: implications for the pathogenesis of obesity," *The Journal of Neuroscience*, vol. 29, no. 2, pp. 359–370, 2009.

[176] J. P. Thaler, C. X. Yi, E. A. Schur et al., "Obesity is associated with hypothalamic injury in rodents and humans," *The Journal of Clinical Investigation*, vol. 122, no. 1, pp. 153–162, 2012.

[177] C. Andre, O. Guzman-Quevedo, C. Rey et al., "Inhibiting microglia expansion prevents diet-induced hypothalamic and peripheral inflammation," *Diabetes*, vol. 66, no. 4, pp. 908–919, 2017.

[178] S. Kalin, F. L. Heppner, I. Bechmann, M. Prinz, M. H. Tschöp, and C. X. Yi, "Hypothalamic innate immune reaction in obesity," *Nature Reviews Endocrinology*, vol. 11, no. 6, pp. 339–351, 2015.

[179] W. L. Reis, C. X. Yi, Y. Gao, M. H. Tschöp, and J. E. Stern, "Brain innate immunity regulates hypothalamic arcuate neuronal activity and feeding behavior," *Endocrinology*, vol. 156, no. 4, pp. 1303–1315, 2015.

[180] H. Cui, M. Lopez, and K. Rahmouni, "The cellular and molecular bases of leptin and ghrelin resistance in obesity," *Nature Reviews Endocrinology*, vol. 13, no. 6, pp. 338–351, 2017.

[181] K. El-Haschimi, D. D. Pierroz, S. M. Hileman, C. Bjørbaek, and J. S. Flier, "Two defects contribute to hypothalamic leptin resistance in mice with diet-induced obesity," *The Journal of Clinical Investigation*, vol. 105, no. 12, pp. 1827–1832, 2000.

[182] K. W. Williams, T. Liu, X. Kong et al., "Xbp1s in Pomc neurons connects ER stress with energy balance and glucose homeostasis," *Cell Metabolism*, vol. 20, no. 3, pp. 471–482, 2014.

[183] R. M. Ransohoff, P. Kivisakk, and G. Kidd, "Three or more routes for leukocyte migration into the central nervous system," *Nature Reviews Immunology*, vol. 3, no. 7, pp. 569–581, 2003.

[184] M. S. Kim, J. Yan, W. Wu, G. Zhang, Y. Zhang, and D. Cai, "Rapid linkage of innate immunological signals to adaptive immunity by the brain-fat axis," *Nature Immunology*, vol. 16, no. 5, pp. 525–533, 2015.

[185] S. H. Chang, C. R. Stoll, J. Song, J. E. Varela, C. J. Eagon, and G. A. Colditz, "The effectiveness and risks of bariatric surgery: an updated systematic review and meta-analysis, 2003-2012," *JAMA Surgery*, vol. 149, no. 3, pp. 275–287, 2014.

[186] B. Geloneze, M. A. Tambascia, V. F. Pilla, S. R. Geloneze, E. M. Repetto, and J. C. Pareja, "Ghrelin: a gut-brain hormone: effect of gastric bypass surgery," *Obesity Surgery*, vol. 13, no. 1, pp. 17–22, 2003.

[187] F. Leonetti, G. Silecchia, G. Iacobellis et al., "Different plasma ghrelin levels after laparoscopic gastric bypass and adjustable gastric banding in morbid obese subjects," *The Journal of Clinical Endocrinology and Metabolism*, vol. 88, no. 9, pp. 4227–4231, 2003.

[188] E. Lin, N. Gletsu, K. Fugate et al., "The effects of gastric surgery on systemic ghrelin levels in the morbidly obese," *Archives of Surgery*, vol. 139, no. 7, pp. 780–784, 2004.

[189] R. Morinigo, R. Casamitjana, V. Moizé et al., "Short-term effects of gastric bypass surgery on circulating ghrelin levels," *Obesity Research*, vol. 12, no. 7, pp. 1108–1116, 2004.

[190] M. T. Garcia-Unzueta, R. Fernandez-Santiago, A. Domínguez-Díez, L. Vazquez-Salví, J. C. Fernández-Escalante, and J. A. Amado, "Fasting plasma ghrelin levels increase progressively after biliopancreatic diversion: one-year follow-up," *Obesity Surgery*, vol. 15, no. 2, pp. 187–190, 2005.

[191] F. B. Langer, M. A. Reza Hoda, A. Bohdjalian et al., "Sleeve gastrectomy and gastric banding: effects on plasma ghrelin levels," *Obesity Surgery*, vol. 15, no. 7, pp. 1024–1029, 2005.

[192] J. L. Chan, E. C. Mun, V. Stoyneva, C. S. Mantzoros, and A. B. Goldfine, "Peptide YY levels are elevated after gastric bypass surgery," *Obesity (Silver Spring)*, vol. 14, no. 2, pp. 194–198, 2006.

[193] E. V. Kotidis, G. Koliakos, T. S. Papavramidis, and S. T. Papavramidis, "The effect of biliopancreatic diversion with pylorus-preserving sleeve gastrectomy and duodenal switch on fasting serum ghrelin, leptin and adiponectin levels: is there a hormonal contribution to the weight-reducing effect of this procedure?," *Obesity Surgery*, vol. 16, no. 5, pp. 554–559, 2006.

[194] S. N. Karamanakos, K. Vagenas, F. Kalfarentzos, and T. K. Alexandrides, "Weight loss, appetite suppression, and changes in fasting and postprandial ghrelin and peptide-YY levels after Roux-en-Y gastric bypass and sleeve gastrectomy: a prospective, double blind study," *Annals of Surgery*, vol. 247, no. 3, pp. 401–407, 2008.

[195] E. Ram, T. Vishne, D. Diker et al., "Impact of gastric banding on plasma ghrelin, growth hormone, cortisol, DHEA and DHEA-S levels," *Obesity Surgery*, vol. 15, no. 8, pp. 1118–1123, 2005.

[196] B. Uzzan, J. M. Catheline, C. Lagorce et al., "Expression of ghrelin in fundus is increased after gastric banding in morbidly obese patients," *Obesity Surgery*, vol. 17, no. 9, pp. 1159–1164, 2007.

[197] J. M. Liou, J. T. Lin, W. J. Lee et al., "The serial changes of ghrelin and leptin levels and their relations to weight loss after laparoscopic minigastric bypass surgery," *Obesity Surgery*, vol. 18, no. 1, pp. 84–89, 2008.

[198] B. Olivan, J. Teixeira, M. Bose et al., "Effect of weight loss by diet or gastric bypass surgery on peptide YY3-36 levels," *Annals of Surgery*, vol. 249, no. 6, pp. 948–953, 2009.

[199] M. Faraj, P. J. Havel, S. Phélis, D. Blank, A. D. Sniderman, and K. Cianflone, "Plasma acylation-stimulating protein, adiponectin, leptin, and ghrelin before and after weight loss induced by gastric bypass surgery in morbidly obese subjects," *The Journal of Clinical Endocrinology and Metabolism*, vol. 88, no. 4, pp. 1594–1602, 2003.

[200] C. Holdstock, B. E. Engstrom, M. Ohrvall, L. Lind, M. Sundbom, and F. A. Karlsson, "Ghrelin and adipose tissue regulatory peptides: effect of gastric bypass surgery in obese humans," *The Journal of Clinical Endocrinology and Metabolism*, vol. 88, no. 7, pp. 3177–3183, 2003.

[201] G. Fruhbeck, F. Rotellar, J. L. Hernández-Lizoain et al., "Fasting plasma ghrelin concentrations 6 months after gastric bypass are not determined by weight loss or changes in insulinemia," *Obesity Surgery*, vol. 14, no. 9, pp. 1208–1215, 2004.

[202] K. Schindler, G. Prager, T. Ballaban et al., "Impact of laparoscopic adjustable gastric banding on plasma ghrelin, eating behaviour and body weight," *European Journal of Clinical Investigation*, vol. 34, no. 8, pp. 549–554, 2004.

[203] R. Stoeckli, R. Chanda, I. Langer, and U. Keller, "Changes of body weight and plasma ghrelin levels after gastric banding and gastric bypass," *Obesity Research*, vol. 12, no. 2, pp. 346–350, 2004.

[204] M. Sundbom, C. Holdstock, B. E. Engström, and F. A. Karlsson, "Early changes in ghrelin following Roux-en-Y gastric bypass: influence of vagal nerve functionality?," *Obesity Surgery*, vol. 17, no. 3, pp. 304–310, 2007.

[205] B. A. Whitson, D. B. Leslie, T. A. Kellogg et al., "Entero-endocrine changes after gastric bypass in diabetic and nondiabetic patients: a preliminary study," *The Journal of Surgical Research*, vol. 141, no. 1, pp. 31–39, 2007.

[206] X. Chang, H. Yan, H. Bian et al., "Serum retinol binding protein 4 is associated with visceral fat in human with nonalcoholic fatty liver disease without known diabetes: a cross-sectional study," *Lipids in Health and Disease*, vol. 14, p. 28, 2015.

[207] H. Hosoda, K. Doi, N. Nagaya et al., "Optimum collection and storage conditions for ghrelin measurements: octanoyl modification of ghrelin is rapidly hydrolyzed to desacyl ghrelin in blood samples," *Clinical Chemistry*, vol. 50, no. 6, pp. 1077–1080, 2004.

[208] H. Hosoda and K. Kangawa, "Standard sample collections for blood ghrelin measurements," *Methods in Enzymology*, vol. 514, pp. 113–126, 2012.

[209] C. Compher and K. O. Badellino, "Obesity and inflammation: lessons from bariatric surgery," *JPEN Journal of Parenteral and Enteral Nutrition*, vol. 32, no. 6, pp. 645–647, 2008.

[210] B. D. Netto, S. C. Bettini, A. P. Clemente et al., "Roux-en-Y gastric bypass decreases pro-inflammatory and thrombotic biomarkers in individuals with extreme obesity," *Obesity Surgery*, vol. 25, no. 6, pp. 1010–1018, 2015.

[211] V. G. Sams, C. Blackledge, N. Wijayatunga et al., "Effect of bariatric surgery on systemic and adipose tissue inflammation," *Surgical Endoscopy*, vol. 30, no. 8, pp. 3499–3504, 2016.

[212] U. B. Pajvani, M. E. Trujillo, T. P. Combs et al., "Fat apoptosis through targeted activation of caspase 8: a new mouse model of inducible and reversible lipoatrophy," *Nature Medicine*, vol. 11, no. 7, pp. 797–803, 2005.

APENDICE 2

Cell Biology International ISSN 1065-6995
doi: 10.1002/cbin.10921

MINI-REVIEW

Mitoimmunity—when mitochondria dictates macrophage function

Felipe Corrêa-da-Silva[1], Jéssica A. S. Pereira[1,2], Cristhiane F. de Aguiar[1] and Pedro M. M. de Moraes-Vieira[1,2]*

1 Laboratory of Immunometabolism, Department of Genetics, Evolution, Microbiology and Immunology, Institute of Biology, University of Campinas, São Paulo, Brazil
2 Department of Immunology, Institute of Biomedical Science, University of São Paulo, São Paulo, Brazil

Abstract

In the past decade, several reports have appointed the importance of mitochondria in the immune response. Our understanding of mitochondria evolved from a simple supplier of energy into a platform necessary for immunorregulation. Proinflammatory responses are associated with enhanced glycolytic activity and breakdown of the TCA cycle. Mitochondrial reactive species of oxygen (mROS) are key regulators of classically activated macrophages, with substantial impact in the anti-microbicidal activity and pro-inflammatory cytokine secretion of macrophages. The inflammasome activation in macrophages is dependent on mROS production and mitochondrial regulation and mitochondrial dynamics and functionality direct impact inflammatory responses. Alternative activated macrophage metabolism relies on fatty acid oxidation, and the mechanism responsible for this phenotype is not fully elucidated. Thus, cellular metabolism and mitochondria function is a key immunoregulatory feature of macrophage biology. In this review, we will provide insights into recently reported evidences of mitochondria-related metabolic nodes, which are important for macrophage physiology.

Keywords: inflammation; macrophage; metabolism; mitochondria

Introduction

Mitochondria are organelles present in a broad spectrum of eukaryotes and have the primary function of providing energy for cellular processes. Mitochondria appeared from the engulfment of proteobacterium by a eukaryotic progenitor (Lane and Martin, 2010). Mitochondria are morphologically composed of two functionally distinct membranes—the permeable/outer and impermeable/inner membrane (Sazanov, 2015). The energetic pathways in mitochondria are complex processes, which use electrochemistry energy from electrons to produce the energy carrier molecule adenosine triphosphate (ATP). These processes happen in the mitochondrial matrix and involve the protein complex called Electron Transport Chain (ETC). The global coordination of energy through mitochondria is highly dynamic and mostly dependent on the nutritional status (Cantó et al., 2010; Hardie, 2011; Mihaylova and Shaw, 2011). Mitochondrial biogenesis and function is directly regulated by the availability of mitochondria-related molecules, such as ATP and nicotinamide adenosine nucleotide (NADH) (Cantó et al., 2010; Hardie, 2011; Mihaylova and Shaw, 2011).

Recently, several reports demonstrated the importance of mitochondria in immunity (Bae et al., 2012; Van den Bossche et al., 2012, 2016 Tannahill et al., 2013; Palsson-McDermott et al., 2015; Millet et al., 2016; Nemeth et al., 2016). Immune cells, such as macrophages, once activated mount an immune response that involves the production of cytokines, lipids, reactive species of oxygen (ROS), and cellular rearrangements (O'Neill, 2015). To appropriately respond, immune cells are extremely dependent on mitochondrial function, putting this organelle as the central platform for immune regulation (Mills et al., 2017). Mitochondria-derived factors are able to regulate inflammatory events, such as the activation of innate immunity receptors and the subsequent cytokine and ROS production (Pastorino and Hoek, 2008; Zhang et al., 2010; Horner et al., 2011; Nakahira et al., 2011; Shimada et al., 2012; Moon et al., 2015, Weinberg et al., 2015; West et al., 2015, Wolf et al., 2016).

*Corresponding author: e-mail: pmvieira@unicamp.br
Felipe Corrêa-da-Silva, Jéssica Aparecida da Silva Pereira, and Pedro Manoel Mendes de Moraes-Vieira contributed equally to this work.

Metabolic regulation of macrophage polarization

Macrophages spans a spectrum of phenotypes and the optimal constellation of markers to define pro- and anti-inflammatory macrophages is still evolving. Nevertheless, in a simplified manner, macrophages can assume two distinct profiles, called M1 or M2, which are dependent on the stimuli employed during its activation (Castoldi et al., 2015; Weinberg et al., 2015). M1 or classically activated macrophages respond to bacterial lipopolysaccharide (LPS) and Th1-type of cytokines, such as IFN-γ (Arango Duque and Descoteaux, 2014; Moraes-Vieira et al., 2014; Castoldi et al., 2015, Pereira, 2017). M1 macrophages are involved in immune responses against pathogens and are characterized by the secretion of pro-inflammatory cytokines, such as TNF-α, IL-6, and IL-1β (Arango Duque and Descoteaux, 2014; Moraes-Vieira et al., 2014; Pereira, 2017). In contrast, M2 or alternatively activated macrophages participate in tissue repair and homeostasis, orchestrating the tissue immune responses (Colegio et al., 2014). The polarization of M2 macrophages is induced by Th2-type of cytokines, such as IL-4, IL-5, and IL-13, and these macrophages produce preferentially anti-inflammatory cytokines, such as IL-10 (Colegio et al., 2014).

The cascade of events that follows activation of macrophages leads to a metabolic profile switch, which will directly impact macrophages function (Mills et al., 2017). Depending on microenvironment cues, there is a marked preference for glycolytic over oxidative metabolism, even in the presence of oxygen. This phenomenon is called "Warburg effect," which is commonly found in proinflammatory and classically activated M1 macrophages (Weinberg et al., 2015). The switch from oxidative metabolism into aerobic glycolysis is an important factor for macrophage polarization. Moreover, an accurate regulation of mitochondrial function during this process is a critical step for macrophage-induced cytokine secretion and for the successful elimination of pathogens (Weinberg et al., 2015).

In general terms, pro-inflammatory cells exhibit a more glycolytic profile whereas anti-inflammatory cells rely mostly on oxidative metabolism (Bae et al., 2012; Van den Bossche et al., 2012, 2016; Tannahill et al., 2013; Palsson-McDermott et al., 2015; Millet et al., 2016; Nemeth et al., 2016). The disruption of mitochondrial metabolism and glycolysis enhancement in proinflammatory macrophages promotes the synthesis of metabolites which are necessary for the immune response and generates nicotinamide adenine dinucleotide phosphate (NADPH), which supports ROS production and fatty acid synthesis (O'Neill, 2015). Also, in classically activated macrophages there are structural modifications in the ECT, which allow mitochondrial ROS (mROS) generation (Garaude et al., 2016, Mills et al., 2016).

The alternative polarization of macrophages, known as the anti-inflammatory or repairing phenotype, is characterized by a distinct mitochondrial-dependent metabolic profile (Vats et al., 2006a; Huang et al., 2014, 2016; Namgaladze and Brune, 2014; Van den Bossche et al., 2015). In mitochondria, macromolecules are oxidized for energy generation. For example, in the cytoplasm, glucose is converted into pyruvate, which is oxidized inside the mitochondria through several reactions of the TCA (Ernster and Schatz, 1981). Furthermore, M2 macrophages also require oxidative metabolism, particularly fatty acid oxidation (Vats et al., 2006b; Huang et al., 2014, 2016; Namgaladze and Brune, 2014; Van den Bossche et al., 2015).

Inflammasomes at the immunometabolic interface

Inflammasomes are molecular complexes formed upon response to a variety of physiologic and pathogenic stimuli. Inflammasomes are key nodes in innate immunity with direct impact on pathogen and dysfunctional/dead cells clearance (Guo et al., 2015). The final outcome of inflammasome activation is the secretion of IL-1β and IL-18, two important proinflammatory cytokines (Guo et al., 2015). The two best-characterized inflammasomes are the NLRP3 and NLRC4 and their activation is highly dependent on mitochondrial function and alterations in the mitochondrial system directly affect the inflammasome activity (West et al., 2011a; Tannahill et al., 2013; Weinberg et al., 2015; Mills et al., 2016).

A report published by Tannahill et al. (2013) showed that LPS-activated macrophages have increased levels of succinate, which directly stabilize hypoxia inducible factor-1α (HIF-1α), resulting in the subsequent release of IL-1β. Supporting this data, Mills and colleagues showed that increased oxidation of succinate in mitochondria, via succinate dehydrogenase (SDH), combined with elevated mitochondrial membrane potential leaded to mROS production (Tannahill et al., 2013). The same group demonstrated that increased levels of succinate are responsible for HIF-1α stabilization and the subsequent IL-1β secretion (Weinberg et al., 2015). This succinate/Hif-1α axis is dependent on the activity of the enzyme prolyl hydroxylase (PHD) (Tannahill et al., 2013; Mills et al., 2016). Bone marrow derived macrophages (BMDMs) treated with α-ketoglutarate, a PHD substrate, leaded to the inhibition of the succinate accumulation. This inhibition reduced expression and secretion of IL-1β in a HIF-1α-dependent manner (Tannahill et al., 2013). Lampropoulou et al. (2016) also explored the Hif-1α/IL-1β axis and found that itaconate, an anti-bacterial component able to inhibit the isocitrate lyase in bacteria and found in abundance in the mitochondria of activated macrophages, inhibits SDH activity. This inhibition results in an anti-inflammatory profile (Lampropoulou et al., 2016; Meiser et al., 2016). The levels of itaconate modify mitochondrial respiratory fluctuations in LPS-activated macrophages

(Lampropoulou et al., 2016), which direct impacts pro-inflammatory cytokine production.

The activation of extracellular Toll-like receptors (TLR1, TLR2, and TLR4) induces mROS production in a mechanism that is dependent on the translocation of tumor necrosis factor receptor-associated 6 (TRAF6) into the outer membrane of mitochondria (West et al., 2011a). There, TRAF6 interacts with evolutionary conserved signaling intermediate in Toll pathways (ECSIT) (Kopp et al., 1999; West et al., 2011a). TRAF6 promotes ECSIT ubquitination, which is required for induction of mROS production and the subsequent enhancement of macrophage anti-bactericidal activity (West et al., 2011a). These authors also demonstrated that these events are exclusive of extracellular TLRs (West et al., 2011b). MROS are not involved with antiviral responses, which are mediated by intracellular pattern recognition receptors (West et al., 2011b).

It is clear that the regulation of IL-1β secretion mediated by the inflammasome is dependent on mitochondrial function (Zhou et al., 2011; Iyer et al., 2013; Wynosky-Dolfi et al., 2014; Park et al., 2015; Zhong et al., 2016; Traba et al., 2017). Zhou et al. (2011) demonstrated that mROS activates the NLRP3 inflammasome machinery. Once activated, the NLRP3 inflammasome components co-localize with mitochondrial clusters (Zhou et al., 2011). This indicates that the NLRP3 inflammasome machinery is able to sense mitochondrial signals (Zhou et al., 2011). Mitochondria is essential for inflammasome regulation (Wynosky-Dolfi et al., 2014). For instance, aberrant mitochondrial dynamics leads to increased secretion of IL-1β by macrophages (Park et al., 2015).

Zhong et al. (2016) also explored the regulatory loop between key transcriptional effectors involved in immune cell activation with the NLRP3 inflammasome machinery. The NFκB is a classical proinflammatory transcriptional factor engaged with the expression of proinflammatory cytokines, chemokines, and several other components of the innate immunity (Zhong et al., 2016). The activation of inflammasome induces mitochondrial damage/dysfunction (Weinberg et al., 2015). The NFκB signaling adaptor p62 recognizes damaged mitochondria, and induces mitochondria autophagic clearance (Zhong et al., 2016). Ablation of p62 in macrophages induces excessive secretion of IL-1β and accumulation of damaged mitochondria (Zhong et al., 2016). Thus, NFκB signaling components are able to restrain excessive inflammation through inhibition of mitochondrial damage, which limits the NLRP3 inflammasome activation. Other groups also studied the importance of damaged mitochondria clearance in immune cells. The process of removing damaged or excessive mitochondria is called mitophagy, and is a type of selective autophagy critical for maintaining cellular homeostasis and mitochondrial population (Ding and Yin, 2012). Defects in mitophagy are associated with accumulation of damaged mitochondria and mROS, which leads to pathophysiologic conditions. Kim et al. (2016) demonstrated that stress-inducible protein (SESN2) plays a role in promoting mitophagy in macrophages in response to NLRP3 inflammasome activation. Sesn2-deficient mice have defects in mitophagy that leads to hyperactivation of NLRP3 and increased mortality in animal models of sepsis (Kim et al., 2016). Recently, Eddie Ip and colleagues demonstrated a role for IL-10 in mitophagy. They showed that the absence of IL-10 results in the accumulatiom of damaged mitochondria inmacrophages. This results in dysregulated activation of the NLRP3 inflammasome and the subsequent increased secretion of IL-1β, which contributes to the aggravation of colitis (Ip et al., 2017). Furthermore, Esteban-Martínez et al. (2017) also described a role for mitophagy in regulating the glycolytic shift associated with M1 macrophages polarization.

Concluding remarks

Mitochondria are essential regulators of innate immunity. During inflammation there are several alterations in the microenvironment and cellular processes, which are sensed by the mitochondria. Understanding the dynamic relationship between mitochondria and immune cell physiology is essential to better comprehend the pathways involved in inflammation initiation and resolution. We still know little about the role of mitochondria during immune responses. We must better comprehend how this organelle modifies the outcome of immune cell activation or inhibition. Understanding the importance of mitochondria in the regulation of immune responses may lead to the discovery of unknown metabolic pathways, which may lead to the development of new treatments for inflammatory diseases.

Acknowledgments

The authors acknowledge the support of the State of São Paulo Foundation for Research Support (FAPESP, no. 2015/15626-8, no. 2017/06225-5,no. 2017/12848-5, no. 2017/00079-7), National Council for Scientific and Technological Development (CNPq) and FAEPEX. This manuscript is part of the series Mitochondria and energy metabolism, which refers to the proceedings of the X MitoMeeting, organized by Anibal E Vercesi, Helena Oliveira, and Leonardo R Silveira, held in Guapé MG, Brazil, April 27th–30th 2017.

References

Arango Duque G, Descoteaux A (2014) Macrophage cytokines: involvement in immunity and infectious diseases. Front Immunol 5: 491.

Bae S, Kim H, Lee N, Won C, Kim HR, Hwang YI, Song YW, Kang JS, Lee WJ (2012) Alpha-enolase expressed on the surfaces of

monocytes and macrophages induces robust synovial inflammation in rheumatoid arthritis. J Immunol 189: 365–72.

Cantó C, Jiang LQ, Deshmukh AS, Mataki C, Coste A, Lagouge M, Zierath JR, Auwerx J (2010) Interdependence of AMPK and SIRT1 for metabolic adaptation to fasting and exercise in skeletal muscle. Cell Metab 11: 213–19.

Castoldi A, Naffah de Souza C, Camara NO, Moraes-Vieira PM (2015) The macrophage switch in obesity development. Front Immunol 6: 637.

Colegio OR, Chu NQ, Szabo AL, Chu T, Rhebergen AM, Jairam V, Cyrus N, Brokowski CE, Eisenbarth SC, Phillips GM, Cline GW, Phillips AJ, Medzhitov R (2014) Functional polarization of tumour-associated macrophages by tumour-derived lactic acid. Nature 513: 559–63.

Ding WX, Yin XM (2012) Mitophagy: mechanisms, pathophysiological roles, and analysis. Biol Chem 393: 547–64.

Ernster L, Schatz G (1981) Mitochondria: a historical review. J Cell Biol 91(3 Pt 2): 227s–55s.

Esteban-Martínez L, Sierra-Filardi E, McGreal RS, Salazar-Roa M, Mariño G, Seco E, Durand S, Enot D, Graña O, Malumbres M, Cvekl A, Cuervo AM, Kroemer G, Boya P (2017) Programmed mitophagy is essential for the glycolytic switch during cell differentiation. EMBO J 36: 1688–706.

Garaude J, Acin-Perez R, Martinez-Cano S, Enamorado M, Ugolini M, Nistal-Villan E, Hervás-Stubbs S, Pelegrín P, Sander LE, Enríquez JA, Sancho D (2016) Mitochondrial respiratory-chain adaptations in macrophages contribute to antibacterial host defense. Nat Immunol 17: 1037–45.

Guo H, Callaway JB, Ting JP (2015) Inflammasomes: mechanism of action, role in disease, and therapeutics. Nat Med 21: 677–87.

Hardie DG (2011) Sensing of energy and nutrients by AMP-activated protein kinase. Am J Clin Nutr 93: 891S–96S.

Horner SM, Liu HM, Park HS, Briley J, Gale M, Jr. (2011) Mitochondrial-associated endoplasmic reticulum membranes (MAM) form innate immune synapses and are targeted by hepatitis C virus. Proc Natl Acad Sci USA 108: 14590–5.

Huang SC, Everts B, Ivanova Y, O'Sullivan D, Nascimento M, Smith AM, Beatty W, Love-Gregory L, Lam WY, O'Neill CM, Yan C, Du H, Abumrad NA, Urban JF Jr, Artyomov MN, Pearce EL, Pearce EJ (2014) Cell-intrinsic lysosomal lipolysis is essential for alternative activation of macrophages. Nat Immunol 15: 846–55.

Huang SC, Smith AM, Everts B, Colonna M, Pearce EL, Schilling JD, Pearce E (2016) Metabolic reprogramming mediated by the mTORC2-IRF4 signaling axis is essential for macrophage alternative activation. Immunity 45: 817–30.

Ip WKE, Hoshi N, Shouval DS, Snapper S, Medzhitov R (2017) Anti-inflammatory effect of IL-10 mediated by metabolic reprogramming of macrophages. Science 356: 513–19.

Iyer SS, He Q, Janczy JR, Elliott EI, Zhong Z, Olivier AK, Sadler JJ, Knepper-Adrian V, Han R, Qiao L, Eisenbarth SC, Nauseef WM, Cassel SL, Sutterwala FS (2013) Mitochondrial cardiolipin is required for Nlrp3 inflammasome activation. Immunity 39: 311–23.

Kim MJ, Bae SH, Ryu JC, Kwon Y, Oh JH, Kwon J, Moon JS, Kim K, Miyawaki A, Lee MG, Shin J, Kim YS, Kim CH, Ryter SW, Choi AM, Rhee SG, Ryu JH, Yoon JH (2016) SESN2/sestrin2 suppresses sepsis by inducing mitophagy and inhibiting NLRP3 activation in macrophages. Autophagy 12: 1272–91.

Kopp E, Medzhitov R, Carothers J, Xiao C, Douglas I, Janeway CA, Ghosh S (1999) ECSIT is an evolutionarily conserved intermediate in the Toll/IL-1 signal transduction pathway. Genes Dev 13: 2059–71.

Lampropoulou V, Sergushichev A, Bambouskova M, Nair S, Vincent EE, Loginicheva E, Cervantes-Barragan L, Ma X, Huang SC, Griss T, Weinheimer CJ, Khader S, Randolph GJ, Pearce EJ, Jones RG, Diwan A, Diamond MS, Artyomov MN (2016) Itaconate links inhibition of succinate dehydrogenase with macrophage metabolic remodeling and regulation of inflammation. Cell Metab 24: 158–66.

Lane N, Martin W (2010) The energetics of genome complexity. Nature 467: 929–34.

Meiser J, Kramer L, Sapcariu SC, Battello N, Ghelfi J, D'Herouel AF, Skupin A, Hiller K (2016) Pro-inflammatory macrophages sustain pyruvate oxidation through pyruvate dehydrogenase for the synthesis of itaconate and to enable cytokine expression. J Biol Chem 291: 3932–46.

Millet P, Vachharajani V, McPhail L, Yoza B, McCall CE (2016) GAPDH binding to TNF-alpha mRNA contributes to posttranscriptional repression in monocytes: a novel mechanism of communication between inflammation and metabolism. J Immunol 196: 2541–51.

Mills E, Kelly B, O'Neill L (2017) Mitochondria are the powerhouses of immunity. Nat Immunol 18(5): 488–98.

Mills EL, Kelly B, Logan A, Costa ASH, Varma M, Bryant CE, Tourlomousis P, Däbritz JHM, Gottlieb E, Latorre I, Corr SC, McManus G, Ryan D, Jacobs HT, Szibor M, Xavier RJ, Braun T, Frezza C, Murphy MP, O'Neill LA (2016) Succinate dehydrogenase supports metabolic repurposing of mitochondria to drive inflammatory macrophages. Cell 167: 457–70. e13.

Moon JS, Hisata S, Park MA, DeNicola GM, Ryter SW, Nakahira K, Choi AMK (2015) MTORC1-induced HK1-Dependent glycolysis regulates NLRP3 inflammasome activation. Cell Rep 12: 102–15.

Moraes-Vieira PM, Yore MM, Dwyer PM, Syed I, Aryal P, Kahn BB (2014) RBP4 activates antigen-presenting cells, leading to adipose tissue inflammation and systemic insulin resistance. Cell Metab 19(3): 512–26.

Nakahira K, Haspel JA, Rathinam VA, Lee SJ, Dolinay T, Lam HC, Englert JA, Rabinovitch M, Cernadas M, Kim HP, Fitzgerald KA, Ryter SW, Choi AM (2011) Autophagy proteins regulate innate immune responses by inhibiting the release of mitochondrial DNA mediated by the NALP3 inflammasome. Nat Immunol 12: 222–30.

Namgaladze D, Brune B (2014) Fatty acid oxidation is dispensable for human macrophage IL-4-induced polarization. Biochim Biophys Acta 1841: 1329–35.

Nemeth B, Doczi J, Csete D, Kacso G, Ravasz D, Adams D, Kiss G, Nagy AM, Horvath G, Tretter L, Mócsai A, Csépányi-Kömi R, Iordanov I, Adam-Vizi V, Chinopoulos C (2016) Abolition of mitochondrial substrate-level phosphorylation by itaconic acid

produced by LPS-induced Irg1 expression in cells of murine macrophage lineage. FASEB J 30: 286–300.

O'Neill LA (2015) A broken krebs cycle in macrophages. Immunity 42: 393–4.

Palsson-McDermott EM, Curtis AM, Goel G, Lauterbach MA, Sheedy FJ, Gleeson LE, van den Bosch MW, Quinn SR, Domingo-Fernandez R, Johnston DG, Jiang JK, Israelsen WJ, Keane J, Thomas C, Clish C, Vander Heiden M, Xavier RJ, O'Neill LA (2015) Pyruvate kinase M2 regulates Hif-1alpha activity and IL-1beta induction and is a critical determinant of the warburg effect in LPS-activated macrophages. Cell Metab 21: 65–80.

Park S, Won JH, Hwang I, Hong S, Lee HK, Yu JW (2015) Defective mitochondrial fission augments NLRP3 inflammasome activation. Sci Rep 5: 15489.

Pastorino JG, Hoek JB (2008) Regulation of hexokinase binding to VDAC. J Bioenerg Biomembr 40: 171–82.

Pereira JS, da Silva FC, Mendes-Vieira PMM (2017) The impact of ghrelin in metabolic diseases: an immune perspective. J Diabetes Res. https://doi.org/10.1155/2017/4527980

Sazanov LA (2015) A giant molecular proton pump: structure and mechanism of respiratory complex I. Nat Rev Mol Cell Biol 16: 375–88.

Shimada K, Crother TR, Karlin J, Dagvadorj J, Chiba N, Chen S, Ramanujan VK, Wolf AJ, Vergnes L, Ojcius DM, Rentsendorj A, Vargas M, Guerrero C, Wang Y, Fitzgerald KA, Underhill DM, Town T, Arditi M (2012) Oxidized mitochondrial DNA activates the NLRP3 inflammasome during apoptosis. Immunity 36: 401–14.

Tannahill GM, Curtis AM, Adamik J, Palsson-McDermott EM, McGettrick AF, Goel G, Frezza C, Bernard NJ, Kelly B, Foley NH, Zheng L, Gardet A, Tong Z, Jany SS, Corr SC, Haneklaus M, Caffrey BE, Pierce K, Walmsley S, Beasley FC, Cummins E, Nizet V, Whyte M, Taylor CT, Lin H, Masters SL, Gottlieb E, Kelly VP, Clish C, Auron PE, Xavier RJ, O'Neill LA (2013) Succinate is an inflammatory signal that induces IL-1beta through HIF-1alpha. Nature 496: 238–42.

Traba J, Geiger SS, Kwarteng-Siaw M, Han K, Ra OH, Siegel RM, Gius D, Sack MN (2017) Prolonged fasting suppresses mitochondrial NLRP3 inflammasome assembly and activation via SIRT3-mediated activation of superoxide dismutase 2. J Biol Chem 292: 12153–64.

Van den Bossche J, Baardman J, de Winther MP (2015) Metabolic characterization of polarized M1 and M2 bone marrow-derived macrophages using real-time extracellular flux analysis. J Vis Exp. https://doi.org/10.3791/53424

Van den Bossche J, Baardman J, Otto NA, van der Velden S, Neele AE, van den Berg SM, Luque-Martin R, Chen HJ, Boshuizen MC, Ahmed M, Hoeksema MA, de Vos AF, de Winther MP (2016) Mitochondrial dysfunction prevents repolarization of inflammatory macrophages. Cell Rep 17: 684–96.

Van den Bossche J, Lamers WH, Koehler ES, Geuns JM, Alhonen L, Uimari A, Pirnes-Karhu S, Van Overmeire E, Morias Y, Brys L, Vereecke L, De Baetselier P, Van Ginderachter JA (2012) Pivotal Advance: Arginase-1-independent polyamine production stimulates the expression of IL-4-induced alternatively activated macrophage markers while inhibiting LPS-induced expression of inflammatory genes. J Leukoc Biol 91: 685–99.

Vats D, Mukundan L, Odegaard JI, Zhang L, Smith KL, Morel CR, Wagner RA, Greaves DR, Murray PJ, Chawla A (2006a) Oxidative metabolism and PGC-1beta attenuate macrophage-mediated inflammation. Cell Metab 4: 13–24.

Vats D, Mukundan L, Odegaard JI, Zhang L, Smith KL, Morel CR, Wagner RA, Greaves DR, Murray PJ, Chawla A (2006b) Oxidative metabolism and PGC-1beta attenuate macrophage-mediated inflammation. Cell Metab 4: 13–24.

Weinberg SE, Sena LA, Chandel NS (2015) Mitochondria in the regulation of innate and adaptive immunity. Immunity 42: 406–17.

West AP, Brodsky IE, Rahner C, Woo DK, Erdjument-Bromage H, Tempst P, Walsh MC, Choi Y, Shadel GS, Ghosh S (2011a) TLR signalling augments macrophage bactericidal activity through mitochondrial ROS. Nature 472: 476–80.

West AP, Shadel GS, Ghosh S (2011b) Mitochondria in innate immune responses. Nat Rev Immunol 11: 389–402.

West AP, Khoury-Hanold W, Staron M, Tal MC, Pineda CM, Lang SM, Bestwick M, Duguay BA, Raimundo N, MacDuff DA, Kaech SM, Smiley JR, Means RE, Iwasaki A, Shadel GS (2015) Mitochondrial DNA stress primes the antiviral innate immune response. Nature 520: 553–7.

Wolf AJ, Reyes CN, Liang W, Becker C, Shimada K, Wheeler ML, Cho HC, Popescu NI, Coggeshall KM, Arditi M, Underhill DM (2016) Hexokinase is an innate immune receptor for the detection of bacterial peptidoglycan. Cell 166: 624–36.

Wynosky-Dolfi MA, Snyder AG, Philip NH, Doonan PJ, Poffenberger MC, Avizonis D, Zwack EE, Riblett AM, Hu B, Strowig T, Flavell RA, Jones RG, Freedman BD, Brodsky IE (2014) Oxidative metabolism enables Salmonella evasion of the NLRP3 inflammasome. J Exp Med 211: 653–68.

Zhang Q, Raoof M, Chen Y, Sumi Y, Sursal T, Junger W, Brohi K, Itagaki K, Hauser CJ(2010) Circulating mitochondrial DAMPs cause inflammatory responses to injury. Nature 464: 104–7.

Zhong Z, Umemura A, Sanchez-Lopez E, Liang S, Shalapour S, Wong J, He F, Boassa D, Perkins G, Ali SR, McGeough MD, Ellisman MH, Seki E, Gustafsson AB, Hoffman HM, Diaz-Meco MT, Moscat J, Karin M (2016) NF-kappaB restricts inflammasome activation via elimination of damaged mitochondria. Cell 164: 896–910.

Zhou R, Yazdi AS, Menu P, Tschopp J (2011) A role for mitochondria in NLRP3 inflammasome activation. Nature 469: 221–5.

Received 16 October 2017; accepted 17 December 2017.
Final version published online 22 January 2018.

APENDICE 3

DOI: 10.1002/JLB.MR1218-478R

JLB JOURNAL OF LEUKOCYTE BIOLOGY

REVIEW

Leptin in the regulation of the immunometabolism of adipose tissue-macrophages

Lauar Monteiro[1] | Jéssica Aparecida da Silva Pereira[1,2] | Lohanna Palhinha[3] | Pedro Manoel M. Moraes-Vieira[1,2]

[1]Laboratory of Immunometabolism, Department of Genetics, Evolution, Microbiology and Immunology, Institute of Biology, University of Campinas, Sao Paulo, Brazil

[2]Department of Immunology, Institute of Biomedical Sciences, University of Sao Paulo, Sao Paulo, Brazil

[3]Laboratory of Immunopharmacology, Oswaldo Cruz Institute, Oswaldo Cruz Foundation (FIOCRUZ), Rio de Janeiro, Rio de Janeiro, Brazil

Correspondence
Prof. Pedro Manoel M Moraes-Vieira, Laboratory of Immunometabolism, Department of Genetics, Evolution, Microbiology and Immunology, Institute of Biology, University of Campinas, Rua Monteiro Lobato 255, Bloco H, Campinas, SP, 13083-862, Brazil.
Email: pmvieira@unicamp.br

Abstract

Obesity is a pandemic disease affecting around 15% of the global population. Obesity is a major risk factor for other conditions, such as type 2 diabetes and cardiovascular diseases. The adipose tissue is the main secretor of leptin, an adipokine responsible for the regulation of food intake and energy expenditure. Obese individuals become hyperleptinemic due to increased adipogenesis. Leptin acts through the leptin receptor and induces several immunometabolic changes in different cell types, including adipocytes and Mϕs. Adipose tissue resident Mϕs (ATMs) are the largest leukocyte population in the adipose tissue and these ATMs are in constant contact with the excessive leptin levels secreted in obese conditions. Leptin activates both the JAK2-STAT3 and the PI3K-AKT-mTOR pathways. The activation of these pathways leads to intracellular metabolic changes, with increased glucose uptake, upregulation of glycolytic enzymes, and disruption of mitochondrial function, as well as immunologic alterations, such as increased phagocytic activity and proinflammatory cytokines secretion. Here, we discuss the immunometabolic effects of leptin in Mϕs and how hyperleptinemia can contribute to the low-grade systemic inflammation in obesity.

KEYWORDS
obesity, inflammation, leptin, immunometabolism

1 | INTRODUCTION

Obesity is a chronic disease characterized by excessive lipid accumulation in the white adipose tissue (WAT) in response to the imbalance between food intake and energy expenditure.[1] Currently, obesity is one of the most prevalent diseases in the world. The World Health Organization estimates that about 650 million adults are obese, showing body mass index (BMI) equal or over 30, which is frequently accompanied by other health disturbances, such as type 2 diabetes (T2D), cardiovascular diseases, and metabolic syndrome, and thus, impaired quality of life and life expectancy.[2–6]

The white adipose tissue is extremely important for nutrient storage, which confers to WAT an important role in the maintenance of energetic homeostasis.[7–10] Since WAT is constituted by a variety of immune and non-immune cells, the alterations in the visceral WAT promoted by obesity are characterized by increased lipid accumulation in white adipocytes and by the infiltration of pro-inflammatory immune cells in this tissue, which leads to the development of chronic low grade inflammation.[11]

Several works have reported that these alterations in visceral WAT are an important risk factor to the development of obesity-related disorders, such as T2D and insulin resistance.[3,4,10,12,13] The

Abbreviations: ACAT-1, Acetyl-CoA acetyltransferase; AgRP, agouti protein; AMPK, 5′ AMP-activated protein kinase; ARG-1, arginase-1; ATM, adipose tissue resident Mϕ; BMI, body mass index; CD, cluster of differentiation; CPT-1, carnitine palmitoyltransferase-1; Db, Diabetes (gene); DC, dendritic cell; DIO, diet-induced obese; DTH, delayed-type hypersensitivity; EIC, experimentally induced colitis; FAO, fatty acid oxidation; FFA, free fatty acid; FIP, fibro-inflammatory progenitors; GLUT1, glucose transporter 1; HFD, high fat diet; HIF-1α, Hypoxia-inducible factor 1-alpha; ILC, innate lymphoid cell; iNKT, invariant natural killer cell; IRF4, interferon regulatory factor 4; IRS, insulin receptor substrate; JKN, JunN-terminal kinase; KC, Kupffer cell; LDH, lactate dehydrogenase; Lep-R, Leptin receptor; Mgl, Mϕ galactose-type lectin; mTOR, mammalian target of rapamycin; mTORC, mTOR complex; NPY, neuropeptide Y; Ob, Obese (gene); Ob-R, leptin receptor; PFKFB3, 6-phosphofructo-2-kinase/fructose-2,6-biphosphatase 3; PGC-1β, PPARgamma-coactivator-1beta; PKM2, pyruvate kinase M2; POMC, proopiomelanocortin; PPARγ, peroxisome proliferator-activated receptor γ; PTP1B, phosphotyrosine phosphatase 1B; rAAV, recombinant adeno-associated virus; ROS, reactive oxygen species; SAT, subcutaneous adipose tissue; SIRT1, Sirtuin 1; SOCS3, cytokine signaling suppressor 3; SQ-WAT, subcutaneous adipose tissue; T2D, type 2 diabetes; UCP1, uncoupling protein 1; VAT, visceral adipose tissue; WAT, white adipose tissue.

Received: 4 January 2019 | Revised: 19 March 2019 | Accepted: 26 April 2019

increased susceptibility to develop such disorders has a direct association with immune imbalance, which is marked by the excess of pro-inflammatory cytokines and reduction of anti-inflammatory cytokines promoted by the alterations in the polarization status of adipose tissue resident Mϕs (ATMs).[11,14,15]

Besides the role of WAT for nutrient storage, this organ has an important participation in the regulation of a variety of metabolic processes.[9] WAT secretes several hormones/cytokines, which are named adipokines.[16] Adipokines can be differentially secreted in different portions of the adipose tissue.[17] Also, adipokines are involved in the adipocyte maturation, systemic nutritional communication, and metabolic regulation of a variety of cellular types.[2,9,17] In addition, some adipokines, such as leptin, are increased during obesity, which support their involvement in obesity-associated cardiovascular disease, insulin resistance, and immune imbalance.[2,9,17] This indicates that adipokines can be a link between the metabolism and the immune system.[2,8,9,13]

2 | LEPTIN AND LEPTIN RECEPTOR—A BRIEF HISTORY

The discovery of leptin is dated in the year of 1950, when the first observation of the recessive genetic alterations that happened in C57BL/6 animals, and led the animals to the development of morbid obesity was registered.[18] The gene located in chromosome 6, in which the mutation was observed, was named *Obese* (*ob*) due to the morbid obesity phenotype generated in response to its mutation. Accordingly, the animals in which this gene is mutated were given the nomenclature ob/ob.[18]

The cloning of the *ob* gene enabled the identification of a highly conserved protein with 167 amino acids in human and mice, which is secreted according to the amount of adipose tissue mass, and is present in high levels in the bloodstream of obese individuals and is absent in ob/ob animals.[19–22] The administration of this protein was reported to promote the reduction of food intake and weight gain in ob/ob mice and diet-induced obese animals (DIO), which was a key step in the development of several new studies aimed at understanding the mechanisms involved in regulating metabolism and the pathogenesis of obesity.[21,23,24]

Leptin, from greek *leptós*, which means thin, is a 16 kDa monomeric nonglycosylated protein secreted as a product of the *ob* gene.[21] Leptin is mainly secreted by WAT, and this adipokine belongs to the superfamily of cytokines due its elevated similarity with others cytokines, such as IL-6, IL-12, and G-CSF.[25,26] The elucidation of leptin crystal structure enabled the characterization of leptin as a pleiotropic protein, which can act as a link between immune responses and the neuroendocrine system.[20,25,27,28]

The identification of leptin receptor is dated about 20 years after the first report of leptin.[29] Similar as the leptin discovery, the leptin receptor was identified through studies involving animals with a spontaneous genetic mutation in the *Diabetes* (*db*) gene, which is located in chromosome 4.[29,30] The mutation in *db* gene generated a phenotype characterized by hyperphagia, obesity, hyperglycemia, and hyperinsulinemia, and the animals in which this mutation was first observed were termed db/db.[31,32] The phenotypic similarity between the genetic mutation of *ob* and *db* gene took the scientific community interest to the necessity of more studies with db/db and ob/ob mice. In this way, parabiosis studies performed by Coleman[31] were a major breakthrough to leptin functional studies.[31,33] Coleman observed that one factor, later named leptin, was absent in ob/ob mice.[31] Also, the inability to respond to this factor could be the reason for the metabolic disturbances observed in db/db mice.[20]

Few years later, Bray and York[30] showed that hypothalamic damage leads to excessive food intake and weight gain alterations, which results in obesity. These studies were determinant for the hypothesis that leptin could act in the hypothalamus and thus, promote a signaling mechanism to induce the sensation of satiety.[22,23,30,34] However, the description of the leptin receptor, named Ob-R or Lep-R, happened just in 1995, after cloning and identification of a class I receptor that belongs to the superfamily of the gp130 cytokine receptors, which are widely distributed in a variety of cellular types, and are responsible for leptin actions.[29,35–37] Since then, several works were conducted to elucidate how leptin modulates the function of a variety of cells, its mechanism of secretion and its involvement in the regulation of immune responses.[19,21–24,38]

3 | LEPTIN RECEPTORS AND SIGNALING

Leptin receptors are widely distributed in a variety of cell types, and have a key role in the regulation of central and peripheral actions of leptin.[29,35–37,39] There are 6 isoforms of leptin receptor (Ob-R), which have high homology between humans and rodents.[29,33,40] These receptors are encoded by the *lepr* gene (humans) and *db* gene (mice), situated in the chromosome 4, and every isoform shows high affinity for leptin.[41,42]

The leptin receptor isoforms are distinguished by the letters a-f, which are classified in long (Ob-Rb), short (Ob-Ra, Ob-Rc, Ob-Rd, Ob-Rf), or secreted (Ob-Re) forms.[41,42] In general, leptin receptors have an extracellular invariable domain, with 816 aas, and a variant intracellular domain, except the isoform Ob-Re, which does not have a transmembrane domain (Fig. 1).[33,43,44]

The multiple isoforms of the leptin receptor are generated in response to an alternative splicing, which results in the generation of proteins that have intracellular domains with different sequences and lengths,[45–48] ranging from 34 aas (short isoform) to 303 aas in its long isoform.[33] The intracellular domain of Ob-R receptors presents a conserved portion (box1), constituted by 6-17 aas, which have a key role in the association and activation of the tyrosine kinase JAK2, and another facultative domain (box2), which has 49-60 aas and is required for maximum activation of JAK2.[43,49]

The most well-characterized isoform of leptin receptor is the long form, Ob-Rb, which is present in the most varied cell types, such as Mϕs, β-pancreatic cells, endothelial cells, among others.[25,39] It is mostly found in the hypothalamus,[44] in areas responsible for the

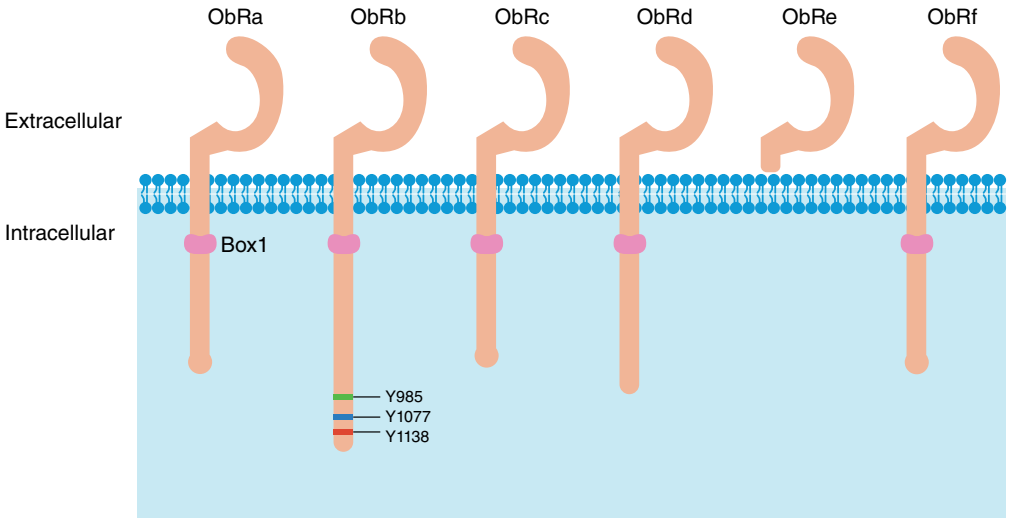

FIGURE 1 **Leptin receptor isoforms and signaling.** There are 6 isoforms of leptin receptor (Ob-R) and they are classified as long (Ob-Rb), short (Ob-Ra, Ob-Rc,Ob-Rd, Ob-Rf), and secreted (Ob-Re). Leptin receptors have an extracellular invariable domain, containing 816 amino acids, and intracellular domains that differ in sequences and lengths. The intracellular domain contains a conserved portion (box1), with a key role in the activation of JAK2, and a facultative domain (box2), required for maximum activation of JAK2. The long isoform (Ob-Rb) is present in several cell types, including Mϕs. Ob-Rb presents 3 conserved tyrosines in their elongated intracellular domain required for activation of JAK2-STAT3 pathway. The short isoforms lack the sequences necessary for signal transduction and are involved in the transport and degradation of leptin in different tissues. The secreted isoform (Ob-Re) acts as a soluble transporter of leptin and promotes the association of leptin with hypothalamic Ob-Rb receptors

control of appetite and body weight.[25,37] Ob-Rb receptor is the only isoform that has an elongated intracellular domain with the required sequences for signal transduction. This isoform has 3 conserved tyrosines in its intracellular domain that allow the binding of molecules responsible for the activation of different signaling pathways, being the only isoform capable of promoting the activation of the JAK STAT3 cellular signaling pathway.[43,47,49,50] Several studies have demonstrated that one of the main forms of leptin activity occurs through the activation of the pathway JAK2-STAT3, which has been pointed out as one of the main mechanisms by which leptin promotes satiety and control of energy expenditure.[27,35,36,51,52]

In response to the association of leptin, the Ob-Rb receptor undergoes a process of dimerization and conformational change, which induces the catalytic activity of the protein JAK2, and thus, leading to the phosphorylation of 3 tyrosine residues located in the Ob-Rb receptor, which promotes the activation of different signaling proteins.[53–55] The Tyr1138 tyrosine phosphorylation promotes the activation of STAT3, which after being phosphorylated by JAK2 dimerizes and translocates to the nucleus, where it induces the expression of anorexigenic peptides such as proopiomelanocortin (POMC), and the suppression of orexigenic peptides such as the neuropeptide Y (NPY) and agouti protein (AgRP). In addition, leptin binding to its receptor also regulates the expression of the cytokine signaling suppressor 3 (SOCS3), which is responsible for STAT3 inhibition, and the subsequent disruption of leptin-induced actions.[27,35,51,53,54,56–58]

Other signaling pathways independent of STAT3 are regulated by leptin in different cell types.[27,54,59–61] Different groups reported the induction of pathways such as ERK, PI3K/Akt/mTOR, p38 MAPK, and AMPK/SIRT1 in response to leptin binding to Ob-Rb receptors.[25,27,35,59,62] Some reports show that the activation of JAK2 promotes the phosphorylation of the insulin receptor substrate (IRS), which induces the activation of PI3K and consequently of protein kinase B, also known as Akt, thus promoting the modulation of anorexigenic/orexigenic peptide levels.[63] STAT3-independent mechanisms are also observed in relation to the control of JAK2 activation and termination of leptin signaling, in which phosphotyrosine phosphatase 1B (PTP1B), a protein present on the surface of the endoplasmic reticulum, is responsible for promoting dephosphorylation of JAK receptor after internalization of the Ob-Rb receptor.[25,64,65] The effects of leptin in the CNS have been extensively studied and described in other works.[66–68] We will not extend the discussion on this topic, since this is not the main focus of this review.

4 | EFFECTS OF PERIPHERAL AND CENTRAL LEPTIN IN IMMUNE RESPONSE

Central leptin resistance affects hypothalamic nuclei and leads to a disruption in the regulation of food intake.[69] The white adipose tissue also develops leptin resistance, marked by a decrease in STAT3 activation in diet-induced obese mice, that leads to reduced ObRb expression.[70,71] However, efficient leptin signaling still happens in other tissues under obesogenic conditions.[69] Previous work from Enriori et al. showed that sympathetic outflow stimulated by leptin in brown adipocytes continues to work despite the central leptin resistance caused by obesity.[72]

Elevation of leptin concentrations in the cerebrospinal fluid and specific brain sites is responsible for leptin effects on food intake.[73]

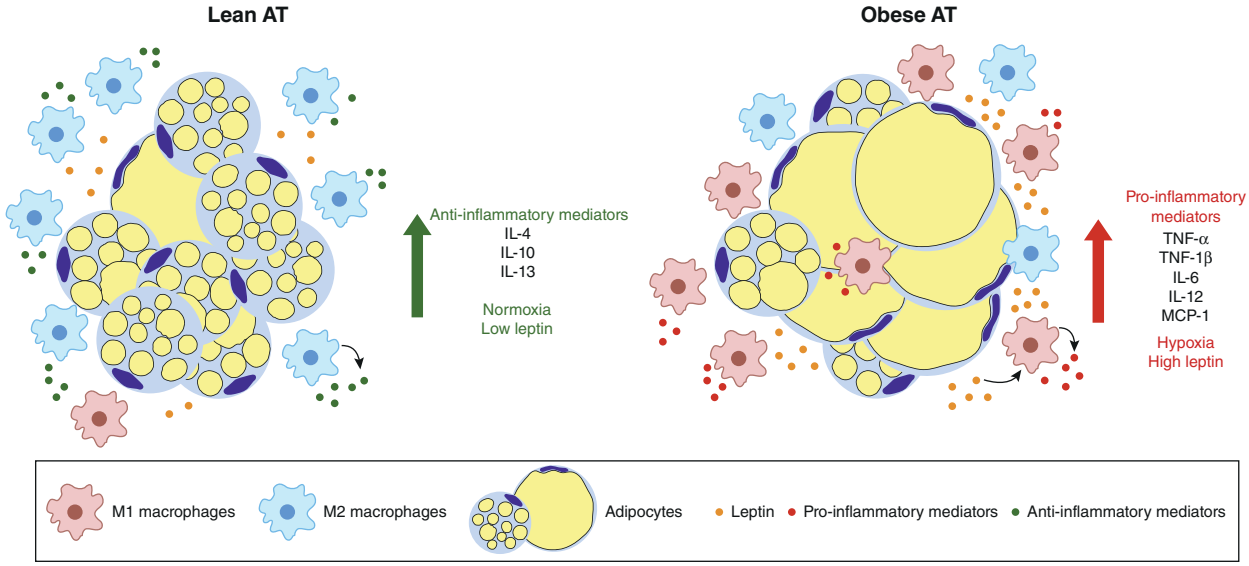

FIGURE 2 **Leptin role in adipose tissue immunoregulation.** Under physiological conditions, ATMs present anti-inflammatory characteristics, with secretion of IL-10, IL- 4, and IL-13. Obesity leads to exacerbated adipocyte size and number, which results in increased leptin secretion that is accompanied by the inflammatory phenotype observed in obesity. Leptin induces the up-regulation of MCP-1 in the adipose tissue, consequently increasing the number of infiltrating proinflammatory blood monocyte-derived Mϕs. Obese adipose tissue, with excessive leptin levels becomes hypoxic. Leptin also induces the expression of HIF-1α in ATMs, favoring the production of proinflammatory mediators. Elevated leptin concentrations in obese adipose tissue promotes a shift in Mϕ immunometabolic profile, leading to higher secretion of proinflammatory cytokines, such as TNF-α, IL-6, IL-12, and IL-1β

Yet, when administered by intravenous injection, leptin is not able to reduce food intake, due to the limitations of leptin transport once it comes across the blood-brain barrier.[73]

Inflammatory signals, such as LPS, stimulate leptin expression and release from the adipose tissue.[74,75] Peripheral administration of leptin reverts the enhanced thymocyte apoptosis in ob/ob mice and increases Th1 pattern of cytokine release, leading to a susceptibility to autoimmune diseases.[27,76,77] Early works have shown that peripheral injection of recombinant leptin improves T cell-mediated immune responses after fasting. Whereas central leptin treatment—using a recombinant adeno- associated virus (rAAV) system to deliver leptin gene directly into rat brain—reduced circulating leptin levels and body fat, as well as T cell-mediated delayed-type hypersensitivity (DTH) response. This was an indicative that leptin has a direct effect on immune cells that does not require adipose tissue signaling.[78,79]

5 | LEPTIN AND THE ADIPOSE TISSUE

Leptin discovery was an important breakthrough regarding the function of adipose tissue, now defined as an indispensable immunoendocrine organ.[80–82] Although the levels of leptin are correlated to the fat mass, its fluctuations accompany the energy status of the organism in a long-term fashion, increasing with energy surplus and decreasing during low energy periods such as fasting or cold exposure.[83,84] It is known that the different depots of white adipose tissue have different biology and functions, with increments in the visceral adipose tissue (VAT) being strongly linked to adipocyte dysfunction, insulin resistance, and metabolic syndrome.[85,86] On the other hand, subcutaneous adipose tissue (SAT, or also known as SQ WAT) is recognized for its greater capacity to store lipids and its contribution to proper glucose homeostasis.[87] SAT buffers the excess fat, which otherwise would be toxic if in the circulation and accumulated ectopically or in VAT.[88] Consistently, insulin resistance is associated with lower levels of circulating leptin and reduced adipogenic capacity in the SAT of obese individuals, compared to insulin sensitive subjects.[89] Among adipose tissue depots, SAT is also the main source of leptin in humans[86,90] and it is tempting to speculate whether the role of leptin in this fat depot is beneficial or detrimental. In addition, the concentration of leptin in the adipose tissue microenvironment may be even higher than its serum levels, but this question remains to be addressed. Nevertheless, leptin autocrine and paracrine actions in adipocytes remain so far unexplored, although many studies have demonstrated the impact of leptin central signaling in the regulation of adipocyte physiology.[91,92]

A few studies aimed to determine the local effects of leptin in adipose tissues and adipocytes.[93–95] For example, treatment of epididymal WAT explants from rats with leptin for 1–2 h resulted in increased lipolysis.[93,95] However, in these cases, it is difficult to assume a direct effect of leptin on adipocytes because, as aforementioned, WAT is composed of a variety of cell types with Mϕs making up for up to 50% of the total cell number in adipose tissue during obesity.[96,97] Besides, it is known that leptin activates immune cells and induces the production of TNF-α,[98] a known lipolytic factor,[99–102] which favors a proinflammatory and prolipolytic milieu in the WAT (Fig. 2).[98–102] Importantly, TNF-α together with other adipokines and cytokines from resident and

recruited immune cells compose the adipose tissue microenvironment, which can modulate adipogenesis and proliferation of adipocyte precursor cells.[103] In another study, adipocytes were isolated from rat subcutaneous, epididymal, and perirenal adipose tissue and then stimulated with leptin for 2 h.[94] The authors concluded that leptin induced lipolysis in cells from these 3 fat depots by measuring the levels of secreted glycerol, a metabolite from the breakdown of stored triacylglycerol.[94] They also inferred that the optimal dose, with the strongest stimulation of lipolysis, was 10^{-6} M (16,000 ng/mL) of leptin, which corresponds to more than 300 times the plasma levels of leptin in obese humans.[90] On the other hand, a recent study performed by Yue and colleagues showed that ObR specific deletion in the bone marrow stromal cells induced osteogenic differentiation at the expense of adipogenesis in the bone marrow of mice.[104] Also, they showed that the deletion reduced the total number of adipocytes and increased bone volume in high fat diet-fed mice, compared to DIO wild-type animals. These results suggest that leptin directly signals in stromal cells, being essential for their commitment with the adipocyte fate and for their proper differentiation.[104] Although this work increased our comprehension on the local effects of leptin in adipocytes and in precursor cell fate, many studies are still necessary to puzzle out the mechanisms of action of leptin and its roles in the direct modulation of adipogenesis and/or lipolysis. We cannot exclude the possibility that leptin may induce adipogenesis on precursor cells and lipolysis on mature adipocytes, but new studies are still necessary to unravel the resulting effect of physiological leptin concentrations on cells at different stages of adipocyte differentiation.

Although the above-mentioned evidences for a local proadipogenic effect of leptin in precursor cells and adipocytes, leptin signaling in nervous cells is known to induce energy expenditure through the modulation of glucose homeostasis and lipid metabolism.[91] For instance, Zeng and colleagues showed that adipocytes are surrounded by sympathetic fibers, creating what they called "neuro-adipose junctions," which directly induce adipocyte lipolysis via peripheral neuronal stimulation.[92] Thus, leptin seems to have different actions in adipocytes depending on the type of signaling (local or neuronal). It is tempting to speculate that, during obesity, with the development of leptin central resistance, the peripheral effects of leptin on inflammatory and precursor cells may prevail. Nevertheless, how exactly these 2 signaling branches (lipolysis and lipogenesis/adipogenesis) are in harmony is definitely a question worthy of enlightenment.

Regarding brown adipose tissue, leptin increases the expression of uncoupling protein 1 (UCP1), one of the key proteins that mediate non-shivering thermogenesis.[105] Although leptin-deficient mice have lower body temperature and are hypothermic under low temperatures, the induction of thermogenesis by leptin is still controversial as the role of leptin in thermoregulation is linked to reductions in thermal conductance.[106] This places leptin as an essential factor for heat conservation, rather than heat generation (thermogenesis) itself.[106] Even though brown adipose tissue metabolism is a very interesting and wide issue, it is well discussed elsewhere[91,107] and is not in the scope of this review.

In summary, leptin signals in adipocytes, precursor cells, as well as in immune cells toward a complex equilibrium of metabolic and inflammatory pathways yet to be fully comprehended. In the growing WAT, leptin signaling together with other adipokines and cytokines, induces the recruitment and activation of immune cells, contributing to a proinflammatory milieu and the consequent release of free fatty acids that exacerbate obesity-related adipose tissue inflammation, in which Mϕs play a major role.[108]

6 | RESIDENT MϕS

Mϕs were first described by Elie Metchnikoff in 1892 as a phagocytic system.[109] Later, in 1968, van Furth and Cohn described several populations of Mϕs originated from blood monocytes.[110] A study using blood monocytes-depleted mice showed that Mϕs were able to maintain local proliferation in various tissues.[111] This discovery was corroborated by many other studies later in the 20th century showing the presence of tissue resident Mϕs.[112–116] These Mϕs had a distinct origin during embryonic development and were not derived from the bone marrow. Unlike blood monocytes that migrate to the tissue, resident Mϕs are originated in the yolk sac and fetal liver and maintain the homeostasis of the tissue.[117] This was an important breakthrough, considering all the different functions of tissue resident Mϕs in health and disease that we know of today. Kupffer cells (KCs) in the liver, microglia in the brain and osteoclasts in the bone are examples of resident Mϕs with major roles in tissue immune surveillance.[117]

7 | Mϕ POLARIZATION

Mϕs are important mediators of the innate immunity, with significant roles at keeping tissue homeostasis and fighting pathogens. Mϕs produce numerous types of cytokines, which mediate pro- or anti-inflammatory responses upon specific stimuli.[118] Mϕs are very plastic cells and can undergo polarization toward distinct profiles.[119–123] There is a large variation of Mϕ phenotypes, but for didactic reasons we use a well-accepted model with the populations that are best described.[124–128] There are 2 populations of Mϕs that were extensively studied and are well characterized. The classically activated Mϕs, or M1, which are induced by TLR4 activation and IFN-γ.[129] M1 Mϕs have a proinflammatory pattern, with high phagocytic activity and intense production of bactericidal mediators, due to large expression of nitric oxide synthase (iNOS) and reactive oxygen species (ROS) generation.[15,129] The alternatively activated Mϕs, or M2, are induced by interleukin 4 (IL-4) and mediate responses against helminths. M2 Mϕs also participate in the resolution phase of inflammation and tissue repair, express high levels of arginase-1 (ARG-1) and secrete the anti-inflammatory cytokine IL-10.[129,130] The M1\M2 characterization was proposed by Mills and collaborators in view of the adopted model for T helper lymphocytes. Once activated by IL-12, T helper 1 (Th1) cells produce large amounts of IFN-γ. Whereas Th2 cells, which are induced by IL-4, secrete Th2 types of cytokines, such as

IL-4 and IL-13. The balance between M1/M2 responses is crucial for systemic homeostasis.[118,131]

8 | Mϕ METABOLISM—AN OVERVIEW

M1 and M2 Mϕs execute different functions with distinctive immunologic profiles. In addition, M1 and M2 Mϕs are also distinctive metabolically. In the last decade, a large number of studies showed that Mϕs when activated shift their metabolism from oxidative phosphorylation to aerobic glycolysis.[127,129,132] This change in intracellular metabolism also happens in tumor cells.[133] This phenomenon is called the Warburg Effect.[134] It was first described in the 1920s during cancer studies.[134] The Warburg Effect consists on a shift to glycolysis by tumor cells, even when oxygen is available for ATP generation. This is an important feature of tumor cells metabolism, because relying on glycolysis means fast ATP production (even though the final ATP count of glycolysis is much lower than oxidative metabolism in the mitochondria, the reaction occurs up to 100 times faster).[135] Cancer cells proliferate at abnormally high rates and the increased glucose uptake fuels the glycolytic flux providing carbon sources for anabolic processes necessary for the biosynthesis of molecules and cell proliferation.[133,136] The changes in intracellular metabolism, with enhanced glucose uptake are accompanied by mitochondrial remodeling, with accumulation of dysfunctional mitochondria, which have diminished respiratory capacity.[136,137]

Immune cells undergo similar metabolic changes upon activation and engage on what is called aerobic glycolysis. Activated and pro-inflammatory lymphocytes, dendritic cells, and Mϕs perform aerobic glycolysis instead of oxidative respiration and accumulate dysfunctional, nonrespiratory mitochondria even during normoxia.[127,128,138–142] Metabolic reprogramming is a critical process, which directly influences Mϕ function. Mϕs need to promote fast responses that require intense protein and lipid synthesis to support the production of antibacterial and inflammatory mediators, such as proinflammatory cytokines, NO, and ROS.[127,143] Enhanced glycolysis has become one of the signatures of the pro-inflammatory activity by Mϕs.[127] Increased levels of glucose transporter 1 (GLUT1), as well as determinant enzymes in the glycolytic flux—such as 6-phosphofructo-2-kinase/fructose-2,6-biphosphatase 3 (PFKFB3), pyruvate kinase M2 (PKM2), and lactate dehydrogenase (LDH)—are associated with higher rates of proinflammatory cytokine expression.[127,144] The importance of glycolysis on Mϕ inflammatory function was determined by different studies that showed elevated cytokine expression and phagocytic activity by glycolytic Mϕs.[145,146]

The proinflammatory profile has been extensively associated with the metabolic shift to glycolysis and accumulation of dysfunctional mitochondria.[138,140,147] These are characteristics observed in lipopolysaccharide (LPS)-activated Mϕs, and also in polarized M1 Mϕs. TLR4 activation by LPS activates the hypoxia-inducible factor-1α (HIF-1α), a transcription factor induced by hypoxic conditions, responsible for the induction of glycolysis and the expression of IL-1β in Mϕs.[148] This all means that when Mϕs leave the quiescent state, they undergo intense metabolic reprogramming to feed their new immunologic demands.

Unlike the proinflammatory Mϕs, M2 Mϕs present higher oxygen consumption rates, with the absence of dysfunctional mitochondria.[149] M2 Mϕs have enhanced activity of PPARγ-coactivator-1β (PGC-1β) and signal transducer and activator of transcription 6 (STAT6), 2 important transcription factors, which are induced by IL-4 and greatly inhibit the production of proinflammatory cytokines.[150] Another important feature of M2 Mϕs is the increased expression of IL-10, a known anti-inflammatory cytokine. IL-10 contributes to Mϕ metabolic modulation, by inhibiting the mammalian target of rapamycin (mTOR).[140] mTOR is a key intracellular metabolic sensor, with almost antagonizing roles from AMP-activated protein kinase (AMPK).[141] AMPK is an inhibitor of mTOR and can activate mitophagy, which is essential for the maintenance of respiratory mitochondria for oxidative metabolism.[151–153] The complex 1 of mTOR (mTORC1) increases glycolysis and dysfunctional mitochondria in different cell types.[153,154] On the other hand, the complex 2 of mTOR (mTORC2) is essential for M2 activity in IL-4-stimulated Mϕs. Parallel induction of STAT6 by IL-4 receptor and mTORC2 leads to IRF4 expression and M2 response.[124] The role of mTORC1 and mTORC2 in Mϕ immunometabolism is not yet fully understood, but the activation of either complex seems to induce opposite responses in Mϕs.

Until very recently, fatty acid oxidation (FAO) was thought to be an essential step for M2 polarization. However, a growing number of studies showed that, even though FAO and the expression of peroxisome proliferator-activated receptor γ (PPARγ)—a nuclear receptor that controls the expression of lipid metabolism-related genes—are increased in M2 Mϕs, FAO is not required for M2 polarization.[155,156] In fact, IL-4 stimulated Mϕs boost glucose utilization and that is an essential step for M2 polarization.[124] Increased FAO, however, is not an essential step for M2 polarization. Mϕs treated with low concentrations (≥10 μM) of etomoxir, an inhibitor of carnitine palmitoyltransferase-1 (CPT-1)—a mitochondrial enzyme necessary for FAO, did not show reduced M2 polarization.[155] This concentration is enough to block CPT-1 activity.[155] Earlier studies utilized a high dose of 200 μM of etomoxir, which disturbs intracellular coenzyme A (CoA) homeostasis and inhibits M2 polarization.[155,156] Mϕs can present different metabolic profiles depending on where they are located and which roles they are supposed to engage.[111,147] The patterns of metabolic behavior in resident Mϕs result in distinct immune profiles, which are important to attend specific tissue necessities.

9 | ADIPOSE TISSUE RESIDENT MϕS IN OBESITY

The larger leukocyte population in the adipose tissue are the ATMs and the number of ATMs increases with adiposity, going from ~15% in lean mice up to ~50% in obese mice.[97,157] The majority of the Mϕs in lean adipose tissue are characteristically M2-like, which

means they express classic M2 markers, such as the surface markers CD206, CD301, CD163, and other genes that promote anti-inflammatory protein transcription, including ARG-1 and IL-10.[15] These M2-like Mϕs are responsible for tissue maintenance and present anti-inflammatory aspects.[14,15,158,159]

In obese individuals, there is an unbalance in the proportion of M2-/M1-like ATMs. This switch in ATM phenotype is caused by the infiltration of pro-inflammatory Mϕs, which disrupts adipose tissue homeostasis and leads to inflammation and insulin resistance (Fig. 2).[14] Besides that obese adipose tissue creates a hypoxic environment, which forces the resident Mϕs to adapt and change their core metabolism.[160] Other obesity-associated factors, such as adipogenesis and insulin induce the up-regulation of HIF-1α mRNA and protein levels, which promote tissue inflammatory response.[161–164] In the same way, deletion of HIF-1α in Mϕs protects mice from HFD-induced inflammation, by reducing the formation of hypoxic "crown-like" structures and inducing the expression of angiogenic factors that are necessary for adipose tissue physiological remodeling.[165]

Adipocytes express monocyte chemoattractant protein-1 (MCP-1, also known as CCL2), which has high affinity with CCR2.[166,167] This is the mechanism by which CCR2 circulating monocytes are recruited to the adipose tissue and differentiate into proinflammatory Mϕs.[166,167] In obesity, MCP-1 levels are elevated in the adipose tissue.[168] When overexpressed in the adipose tissue, MCP-1 leads to exacerbated Mϕ recruitment and insulin resistance.[169,170] On the other hand, CCR2 deficiency in mice protects against diet induced insulin resistance.[168] This does not mean that the number of M2-like ATMs is reduced in obesity. Obese adipose tissue present increased total cell number—including Mϕs, and the number of M2-like Mϕs remains the highest. However, the proportion in the M1/M2 rate is altered, with an increase in the percentage of M1-like proinflammatory Mϕs.[159]

CD11c is an integrin that is expressed in DCs, Mϕs, and even B cells.[171,172] In cases of obesity, proinflammatory CD11c$^+$ Mϕs accumulate in the adipose tissue, forming "crown-like" structures around necrotic adipocytes.[173,174] CD11c$^+$ ATMs show increased proinflammatory features, including decreased IL-10 expression and high proinflammatory cytokines production (IL-6, TNF, IL-1β) and iNOS expression. The M2-like ATMs are identified as F4/80$^+$CD206$^+$CD11c$^-$.[14,159,171] Although human ATMs are of an anti-inflammatory phenotype, they are able to induce several proinflammatory mediators, being characterized as F4/80$^+$CD206$^+$CD11c$^+$. This means that the M2-likeMϕs conserve their main function in the tissue, while also being able to secrete proinflammatory cytokines and chemokines.[175,176] This sort of M2 Mϕ with proinflammatory roles has been recently studied in different contexts also in mice.[126] Another important aspect of CD11c$^+$ Mϕs is the fact that they can impair glucose uptake by adipocytes and are a major contributor to insulin resistance.[174]

Aside from Mϕs, T cells in fat depots help maintain tissue homeostasis. Obesogenic conditions increase the number and frequency of proinflammatory Mϕs and effector T cells, including both CD4 Th cells and CD8 cytotoxic T cells.[177–179] In contrast, immune cells with regulatory profiles and cells associated with type 2 immune responses, such as type 2 innate lymphoid cells (ILC2), invariant natural killer cells (iNKT) and regulatory T cells are reduced in obese individuals.[180–182] Metabolic disorders and adipose tissue inflammation are associated with this disruption in adipose tissue homeostasis, which strongly relies on type 2 immune cells regulation and repair.[182] Leptin supresses regulatory T cell differentiation and is a key regulator of T effector cells differentiation, such as Th17. Leptin is necessary for HIF-1α expression, which is important for the up-regulation of glycolytic metabolism in effector T cells.[183]

WAT inflammation is associated with activation of immune cells, the presence of enlarged, unhealthy adipocytes and the accumulation of collagen fibers in the tissue. A recent study identified a new inflammatory subpopulation of cells in the adipose tissue of mice.[184] A combined technique of single-cell RNA-sequencing and FACS isolation was utilized to identify the so called fibro-inflammatory progenitors (FIPs) cells residing around the blood vessels in the visceral adipose tissue of mice.[184,185] FIPs can activate immune cells in WAT and contribute to WAT remodeling and fibrosis.[184]

10 | LEPTIN AND Mϕ IMMUNOREGULATION

The role of leptin as in inductor of Mϕ proinflammatory immune response has been reviewed in different works.[186,187] The functional isoform of Ob-Rb is not expressed only in the hypothalamus, but also in several cell types of innate and adaptive immunity.[25,186–191] In the immune system, leptin activates proinflammatory cells, promoting Th1 types of response, and mediating the production of the other proinflammatory cytokines, such as TNF-α, IL-12, or IL-6.[187,192,193] Conversely, leptin receptor is also up-regulated by proinflammatory signals.[194] Leptin is also an important mediator of autoimmune conditions.[193] Matarese and colleagues showed that ob/ob mice are protected from experimental autoimmune encephalomyelitis, an animal model of multiple sclerosis.[77] Another study by Siegmund and collaborators described how ob/ob mice are resistant to acute and chronic intestinal inflammation induced by dextran sodium sulphate and to colitis induced by trinitrobenzene sulphonic acid (experimentally induced colitis, EIC). They showed that CD8$^+$ intraepithelial lymphocytes had reduced capacity of IFN-γ production and were also significantly reduced in number.[195] There are several studies linking leptin to lymphocyte-dependent responses. Leptin deficiency results in enhanced Th2 responses and allograft survival and impairs Th17 differentiation.[78,196,197] However, the role of leptin in innate immunity has not been as extensively investigated.

The activation of the long isoform of the human leptin receptor in PBMCs can lead to the activation of 2 signaling pathways, PI3K and mitogen-activated protein kinase (MAPK).[188] This is also true in Mϕs, since leptin treatment resulted in enhanced TNF-α production accompanied by a dose-dependent increase of MAPK activity in LPS-stimulated Kupffer cells.[190] MAPKs are a family of proinflammatory proteins that can be activated by LPS and induce the release of inflammatory mediators by Mϕs.[198] Besides cytokine production,

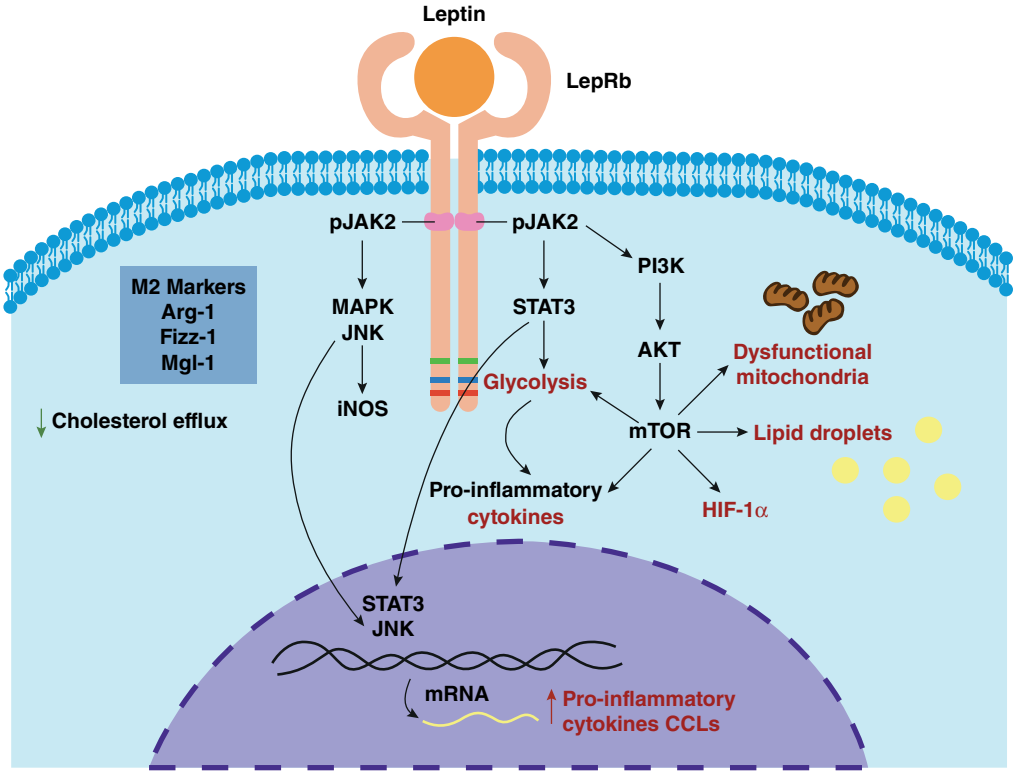

FIGURE 3 **Mechanisms of leptin-induced immunometabolic changes in Mϕs.** Leptin signalizes through LepRb, the functional isoform of the leptin receptors, which is expressed by Mϕs. The phenotype presented by Mϕs upon leptin treatment resembles a proinflammatory M2 Mϕ. Leptin leads to upregulation of typical M2 markers, such as ARG-1, FIZZ-1, and MGL-1, while also activating proinflammatory MAPKs. Activation of JNK by leptin results in up-regulation of iNOS and proinflammatory cytokines. JAK2-STAT3activation that occurs after leptin treatment leads to the migration of phosphorylated STAT3 to the nucleus, where it promotes the expression of CCLs. STAT3 also increases the expression of enzymes that regulate glycolytic flux. Leptin also activates the PI3K-AKT-mTOR pathway, thereby increasing glycolysis, HIF-1α expression, and consequently, proinflammatory cytokine expression. mTOR activation by leptin leads to lipid droplets formation and reduced cholesterol efflux in Mϕs. mTOR also contributes to the accumulation of dysfunctional mitochondria in Mϕs, by inhibiting mitophagy and disrupting homeostatic mitochondrial remodelling

leptin also up-regulates phagocytic function in Mϕs.[199] In human Mϕs, leptin enhances CCLs expression, via activation of the canonical JAK2-STAT3 pathway and potentiates LPS response (Fig. 3).[200,201]

Obesity leads to exacerbated leptin release by the adipose tissue. In obese mice, saturated free fatty acids (FFAs) produce a proinflammatory Mϕ phenotype that is mechanistically distinct from M1 or M2 activation.[202,203] During differentiation of monocytes into Mϕs, Ob-Rb is up-regulated and maintained after differentiation, providing stronger responses to leptin by Mϕs.[204] Leptin up-regulates Acetyl-CoA acetyltransferase (ACAT-1) expression via PI3K-JAK2 signaling in human Mϕs.[204] ACAT-1 is a mitochondrial protein that induces cholesteryl ester formation from cholesterol. Thus, leptin accelerates cholesteryl ester accumulation within the cell, thereby suppressing cholesterol efflux.[204] Besides, leptin can activate the mTOR pathway via PI3K signaling in Mϕs (Fig. 3).[60] A study by Maya-Monteiro and colleagues showed that leptin induces the activation of mTORC1, leading to the formation of lipid droplets. The newly formed lipid bodies were sites of 5-lipoxygenase localization and correlated with an enhanced capacity of leukotriene B4 production, inducing an inflammatory phenotype.[59]

mTOR activation by leptin in Mϕs is a clear indicative of metabolic modulation, since mTOR is not only involved in lipid metabolism, but can also induce glycolysis and mitochondrial remodeling.[60,153] The effects of leptin in the metabolism of Mϕs still not known. However, metabolic modulation by leptin has been recently described in tilapia (*Oreochromis mossambicus*) pituitary.[205] A study demonstrated through transcriptome analysis that leptin regulates PFKFB3, a critical stimulator of phosphofructokinase (PFK), the rate limiting enzyme for glycolysis, and the glycolytic enzyme GAPDH. Both PFK activity and mRNA expression are correlated with lactate production, the final product of the glycolytic pathway. They also showed that leptin up-regulates HIF-1α mRNA levels. Besides that, constitutive STAT3 activation leads to higher rates of glycolysis. In addition, inhibition of STAT3 resulted in the suppression of these responses, indicating that leptin stimulates glycolysis through a STAT3-dependent mechanism.[205] The metabolic phenotype observed after leptin treatment resembles the metabolic switch by which Mϕs undergo upon activation. The microenvironment in obese adipose tissue retains higher levels of leptin secreted by adipocytes. Adipose tissue resident Mϕs are exposed to the excessive contact of with leptin in the obese adipose tissue. This could be an

important step to take in the study of Mϕ metabolic reprogramming and obesity-induced inflammation.

11 | LEPTIN IN ADIPOSE TISSUE Mϕ IMMUNOMETABOLIC MODULATION

Exacerbated TNF-α concentration is a trait observed in several obesity-associated conditions, such as T2D, cardiovascular diseases, and inflammation.[3,14,31,159,206] This is closely related to obesity morbidity and mortality.[6,207] Excessive cytokine secretion during these cases rely on altered Mϕ activity in the adipose tissue.[97,208] ATMs are in constant contact with secreted leptin in the adipose tissue environment and can be directly affected when leptin levels are unbalanced. The immunoregulatory effects of leptin were first noticed during studies in rodents with genetic abnormalities in leptin or leptin receptor that became obese at a young age, now known as ob/ob and db/db.[209–212] Mϕs from mice with impaired leptin signaling have deficient phagocytic activity and proinflammatory cytokine production and treatment with exogenous leptin ameliorates Mϕ function in ob/ob animals.[213] Leptin treatment in ob/ob female mice also improved insulin resistance while inducing M2 markers expression (Fig. 3) (ARG-1, Fizz-1, Mgl1/2).[214] Human Mϕs respond similarly to leptin treatment.[175] CD14 human Mϕs were isolated and treated with leptin or polarized in culture toward an M1 phenotype (with IFN-γ) or an M2 phenotype (with IL-4). When treated with leptin in culture, Mϕs also up-regulated the expression of typical M2 markers, while being able to secrete high levels of TNF-α, IL-6, IL-1β, IL-1ra, IL-10, MCP-1, and MIP-1α, which are characteristic for M1 cells.[175] This suggests that leptin is a strong contributor to the distinct phenotype observed in ATMs. The production of these inflammatory factors is under the transcriptional control of JNK—a key inflammatory protein in the MAPK family, and NF-κB. Both JNK and NF-κB are significantly up-regulated in the adipose tissue.[97,215] Both inductors of the inflammatory response differ in their upstream signaling components. However, previous studies showed that leptin induces the activation of MAPKs as one of its inflammatory mechanisms.[11,188,190] Both JNK and NF-κB pathways are induced by mediators that have been implicated in the occurrence of insulin resistance, such as FFAs, proinflammatory cytokines, oxidative stress, and endoplasmic reticulum stress.[216] Leptin signaling in ATMs leads to the activation of pathways linked to the pathogenesis of different metabolic regulated diseases.

Human leptin stimulates Mϕ proliferation in a dose-dependent manner, meaning hyperleptinemic conditions can induce ATM proliferation. Leptin also activates circulating monocytes and induces the secretion of TNF-α and IL-6 and the expression of activation surface markers, such as CD25, HLA-DR, CD38, CD71, CD11b, and CD11c.[217] Besides that, leptin induces the expression of adhesion molecules in the endothelial cells of the stromal vascular compartment, which can increase Mϕ infiltration to the adipose tissue.[208,218] The enhanced levels of leptin secreted in the obese adipose tissue is, in part, responsible for the unbalanced accumulation and activation of Mϕs in the adipose tissue. These Mϕs have a distinct phenotype, being characteristically M2-like with high proinflammatory features, which are accompanied by a switch in cell core metabolism.

12 | CONCLUDING REMARKS

During obesity, leptin levels are significantly increased and lead to a disruption in physiological function.[219] Mϕ metabolic reprogramming has been the target of studies from different perspectives. The metabolic switch to glycolysis is a marker of proinflammatory signaling, which is marked by up-regulation of glycolytic enzymes, such as GLUT1, PFKFB3, PKM2, and LDH. Other changes include accumulation of dysfunctional mitochondria with reduced respiratory capacity and induction of metabolic regulators, such as mTOR and HIF-1α. ATMs are phenotypically close to M2 Mϕs and maintain adipose tissue homeostasis. Both adipocytes and ATMs can be modulated by excessive leptin concentrations, resulting in proinflammatory responses. Leptin can activate different intracellular pathways, derived from STAT3 or PI3K activation. Both signals can induce metabolic and functional changes in Mϕs. Leptin promotes proinflammatory cytokines release and lipid body formation, as well as activate factors related to glycolytic switch. Obesity is a multifactorial disease, which complicates the induction of a drug with specific targets to ameliorate obesity-related low-grade chronic inflammation. Leptin signaling is a key factor to be considered as a therapeutic target, due to its many roles in Mϕ modulation. In this review, we regarded the importance of leptin in obese conditions by exploring different works focused on immunologic and metabolic approaches.

AUTHORSHIP

L.M., J.A.S.P., and L.P. wrote the manuscript and made figures. P.M.M.M.-V. edited and revised the manuscript.

ACKNOWLEDGMENTS

The authors thank the São Paulo Research Foundation - FAPESP (grant numbers 2015/15626-8, 2016/23328-0, and 2017/00079-7), the Brazilian National Council for Scientific and Technological Development - CNPq (141553/2017-0), and Coordination of Superior Level Staff Improvement - CAPES for the funding and support.

DISCLOSURE

The authors declare no conflict of interest.

REFERENCES

1. Fairbridge NA, Southall TM, Ayre DC, et al. Loss of CD24 in mice leads to metabolic dysfunctions and a reduction in white adipocyte tissue. *PLoS One*. 2015;10:e0141966.
2. Antuna-Puente B, Feve B, Fellahi S, Bastard JP. Adipokines: the missing link between insulin resistance and obesity. *Diabetes Metab*. 2008;34:2-11.

3. Eckel RH, Kahn SE, Ferrannini E, et al. Obesity and type 2 diabetes: what can be unified and what needs to be individualized? *J Clin Endocrinol Metab*. 2011;96:1654-1663.
4. Lafontan M, Berlan M. Do regional differences in adipocyte biology provide new pathophysiological insights? *Trends Pharmacol Sci*. 2003;24:276-283.
5. Rosenbaum M, Sy M, Pavlovich K, Leibel RL, Hirsch J. Leptin reverses weight loss-induced changes in regional neural activity responses to visual food stimuli. *J Clin Invest*. 2008;118:2583-2591.
6. The Lancet Public Health. Tackling obesity seriously: the time has come. *Lancet Public Health*. 2018; 3(4):e153. https://doi.org/10.1016/S2468-2667(18)30053-7
7. Galic S, Oakhill JS, Steinberg GR. Adipose tissue as an endocrine organ. *Mol Cell Endocrinol*. 2010;316:129-139.
8. Kalupahana NS, Moustaid-Moussa N, Claycombe KJ. Immunity as a link between obesity and insulin resistance. *Mol Aspects Med*. 2012;33:26-34.
9. Oller do Nascimento CM, Ribeiro EB, Oyama LM. Metabolism and secretory function of white adipose tissue: effect of dietary fat. *An Acad Bras Cienc*. 2009;81:453-466.
10. Vazquez-Vela ME, Torres N, Tovar AR. White adipose tissue as endocrine organ and its role in obesity. *Arch Med Res*. 2008;39:715-728.
11. McNelis JC, Olefsky JM. Macrophages, immunity, and metabolic disease. *Immunity* 2014;41:36-48.
12. Hassan M, Latif N, Yacoub M. Adipose tissue: friend or foe? *Nat Rev Cardiol*. 2012;9:689-702.
13. Maury E, Brichard SM. Adipokine dysregulation, adipose tissue inflammation and metabolic syndrome. *Mol Cell Endocrinol*. 2010;314:1-16.
14. Castoldi A, Naffah de Souza C, Camara NO, Moraes-Vieira PM. The macrophage switch in obesity development. *Front Immunol*. 2015;6:637.
15. Pereira J, da Silva FC, de Moraes-Vieira PMM. The impact of ghrelin in metabolic diseases: an immune perspective. *J Diabetes Res*. 2017;2017:4527980.
16. Andrade-Oliveira V, Camara NO, Moraes-Vieira PM. Adipokines as drug targets in diabetes and underlying disturbances. *J Diabetes Res*. 2015;2015:681612.
17. Harwood HJ Jr. The adipocyte as an endocrine organ in the regulation of metabolic homeostasis. *Neuropharmacology*. 2012;63:57-75.
18. Ingalls AM, Dickie MM, Snell GD. Obese, a new mutation in the house mouse. *J Hered*. 1950;41:317-318.
19. Barinaga M. "Obese" protein slims mice. *Science*. 1995;269:475-476.
20. Friedman JM, Halaas JL. Leptin and the regulation of body weight in mammals. *Nature*. 1998;395:763-770.
21. Halaas JL, Gajiwala KS, Maffei M, et al. Weight-reducing effects of the plasma protein encoded by the obese gene. *Science*. 1995;269:543-546.
22. Zhang Y, Proenca R, Maffei M, Barone M, Leopold L, Friedman JM. Positional cloning of the mouse obese gene and its human homologue. *Nature*. 1994;372:425-432.
23. Campfield LA, Smith FJ, Guisez Y, Devos R, Burn P. Recombinant mouse OB protein: evidence for a peripheral signal linking adiposity and central neural networks. *Science*. 1995;269:546-549.
24. Pelleymounter MA, Cullen MJ, Baker MB, et al. Effects of the obese gene product on body weight regulation in ob/ob mice. *Science*. 1995;269:540-543.
25. La Cava A, Matarese G. The weight of leptin in immunity. *Nat Rev Immunol*. 2004;4:371-379.
26. Zhang F, Basinski MB, Beals JM, et al. Crystal structure of the obese protein leptin-E100. *Nature* 1997;387:206-209.
27. Bernotiene E, Palmer G, Gabay C. The role of leptin in innate and adaptive immune responses. *Arthritis Res Ther*. 2006;217.
28. Friedman JM. Leptin, leptin receptors, and the control of body weight. *Nutr Rev*. 1998;56:s38-46; discussion s54-75.
29. Tartaglia LA, Dembski M, Weng X, et al. Identification and expression cloning of a leptin receptor, OB-R. *Cell* 1995;83:1263-1271.
30. Bray GA, York DA. Hypothalamic and genetic obesity in experimental animals: an autonomic and endocrine hypothesis. *Physiol Rev* 1979;59:719-809.
31. Coleman DL. Effects of parabiosis of obese with diabetes and normal mice. *Diabetologia* 1973;9:294-298.
32. Halaas JL, Friedman JM. Leptin and its receptor. *J Endocrinol* 1997;155:215-216.
33. Tartaglia LA. The leptin receptor. *J Biol Chem* 1997;272:6093-6096.
34. Maffei M, Fei H, Lee GH, et al. Increased expression in adipocytes of ob RNA in mice with lesions of the hypothalamus and with mutations at the db locus. *Proc Natl Acad Sci USA*. 1995a;92:6957-6960.
35. Folch J, Patraca I, Martinez N, et al. The role of leptin in the sporadic form of Alzheimer's disease. Interactions with the adipokines amylin, ghrelin and the pituitary hormone prolactin. *Life Sci*. 2015;140:19-28.
36. Fruhbeck G, Salvador J. Relation between leptin and the regulation of glucose metabolism. *Diabetologia* 2000;43:3-12.
37. Li Z, Ceccarini G, Eisenstein M, Tan K, Friedman JM. Phenotypic effects of an induced mutation of the ObRa isoform of the leptin receptor. *Mol Metab*. 2013;2:364-375.
38. Maffei M, Halaas J, Ravussin E, et al. Leptin levels in human and rodent: measurement of plasma leptin and ob RNA in obese and weight-reduced subjects. *Nat Med* 1995b;1:1155-1161.
39. Zhang F, Chen Y, Heiman M, Dimarchi R. Leptin: structure, function and biology. *Vitam Horm* 2005;71:345-372.
40. Chen H, Charlat O, Tartaglia LA, et al. Evidence that the diabetes gene encodes the leptin receptor: identification of a mutation in the leptin receptor gene in db/db mice. *Cell* 1996;84:491-495.
41. Paracchini V, Pedotti P, Taioli E. Genetics of leptin and obesity: a HuGE review. *Am J Epidemiol* 2005;162:101-114.
42. Peelman F, Zabeau L, Moharana K, Savvides SN, Tavernier J. 20 years of leptin: insights into signaling assemblies of the leptin receptor. *J Endocrinol* 2014;223:T9-23.
43. Ahima RS, Osei SY. Leptin signaling. *Physiol Behav*. 2004;81:223-241.
44. Lee GH, Proenca R, Montez JM, et al. Abnormal splicing of the leptin receptor in diabetic mice. *Nature* 1996;379:632-635.
45. Dam J, Jockers R. Hunting for the functions of short leptin receptor isoforms★. *Mol. Metab*. 2013;327-328.
46. Lam QL, Lu L. Role of leptin in immunity. *Cell Mol Immunol* 2007;4:1-13.
47. Paz-Filho G, Mastronardi C, Franco CB, Wang KB, Wong ML, Licinio J. Leptin: molecular mechanisms, systemic pro-inflammatory effects, and clinical implications. *Arq Bras Endocrinol Metabol* 2012;56:597-607.
48. Thon M, Hosoi T, Ozawa K. Possible integrative actions of leptin and insulin signaling in the hypothalamus targeting energy homeostasis. *Front Endocrinol* 2016;7:138
49. Ceddia RB. Direct metabolic regulation in skeletal muscle and fat tissue by leptin: implications for glucose and fatty acids homeostasis. *Int J Obes* 2005;9:1175-1183.
50. Schaab M, Kratzsch J. The soluble leptin receptor. *Best Pract Res Clin Endocrinol Metab*. 2015;29:661-670.
51. Ahima RS. Revisiting leptin's role in obesity and weight loss. *J Clin Invest* 2008;118:2380-2383.
52. Li MD. Leptin and beyond: an odyssey to the central control of body weight. *Yale J Biol Med* 2011;84:1-7.
53. Morton GJ, Schwartz MW. Leptin and the central nervous system control of glucose metabolism. *Physiol Rev* 2011;91:389-411.
54. Sahu A. Intracellular leptin-signaling pathways in hypothalamic neurons: the emerging role of phosphatidylinositol-3 kinase-phosphodiesterase-3B-cAMP pathway. *Neuroendocrinology*. 2011;201-210.

55. Scotece M, Mobasheri A. Leptin in osteoarthritis: Focus on articular cartilage and chondrocytes. *Life Sci* 2015;140:75-78.
56. Crujeiras AB, Carreira MC, Cabia B, Andrade S, Amil M, Casanueva FF. Leptin resistance in obesity: an epigenetic landscape. *Life Sci* 2015;140:57-63.
57. Morton GJ, Cummings DE, Baskin DG, Barsh GS, Schwartz MW. Central nervous system control of food intake and body weight. *Nature* 2006;443:289-295.
58. Schwartz MW, Woods SC, Porte D Jr, Seeley RJ, Baskin DG. Central nervous system control of food intake. *Nature* 2000;404:661-671.
59. Maya-Monteiro CM, Almeida PE, D'Avila H, et al. Leptin induces macrophage lipid body formation by a phosphatidylinositol 3-kinase- and mammalian target of rapamycin-dependent mechanism. *J Biol Chem* 2008;283:2203-2210.
60. Maya-Monteiro CM, Bozza PT. Leptin and mTOR: partners in metabolism and inflammation. *Cell Cycle* 2008;7:1713-1717.
61. Naylor C, Petri WA Jr. Leptin regulation of immune responses. *Trends Mol Med* 2016;22:88-98.
62. Minokoshi Y, Kim YB, Peroni OD, et al. Leptin stimulates fatty-acid oxidation by activating AMP-activated protein kinase. *Nature* 2002;415:339-343.
63. Amitani M, Asakawa A, Amitani H, Inui A. The role of leptin in the control of insulin-glucose axis. *Front Neurosci* 2013;7:51:
64. Matarese G, Carrieri PB, Montella S, De Rosa V, La Cava A. Leptin as a metabolic link to multiple sclerosis. *Nat Rev Neurol* 2010;6:455-461.
65. Zabolotny JM, Bence-Hanulec KK, Stricker-Krongrad A, et al. PTP1B regulates leptin signal transduction in vivo. *Dev Cell* 2002;2:489-495.
66. Buchanan C, Mahesh V, Zamorano P, Brann D. Central nervous system effects of leptin. *Trends Endocrinol Metab* 1998;9:146-150.
67. Flak JN, Myers MG Jr. Minireview: CNS mechanisms of leptin action. *Mol Endocrinol* 2016;30:3-12.
68. Li XM, Yan HJ, Guo YS, Wang D. The role of leptin in central nervous system diseases. *Neuroreport* 2016;27:350-355.
69. Harris RB. Direct and indirect effects of leptin on adipocyte metabolism. *Biochim Biophys Acta* 2014;1842:414-423.
70. Wang MY, Orci L, Ravazzola M, Unger RH. Fat storage in adipocytes requires inactivation of leptin's paracrine activity: implications for treatment of human obesity. *Proc Natl Acad Sci USA*. 2005;102:18011-18016.
71. Wang Z, Zhou YT, Kakuma T, et al. Leptin resistance of adipocytes in obesity: role of suppressors of cytokine signaling. *Biochem Biophys Res Commun* 2000;277:20-26.
72. Enriori PJ, Sinnayah P, Simonds SE, Garcia Rudaz C, Cowley MA. Leptin action in the dorsomedial hypothalamus increases sympathetic tone to brown adipose tissue in spite of systemic leptin resistance. *J Neurosci*. 2011;31:12189-12197.
73. Ramsey JJ, Kemnitz JW, Colman RJ, Cunningham D, Swick AG. Different central and peripheral responses to leptin in rhesus monkeys: brain transport may be limited. *J Clin Endocrinol Metab* 1998;83:3230-3235.
74. Grunfeld C, Zhao C, Fuller J, et al. Endotoxin and cytokines induce expression of leptin, the ob gene product, in hamsters. *J Clin Invest* 1996;97:2152-2157.
75. Landman RE, Puder JJ, Xiao E, Freda PU, Ferin M, Wardlaw SL. Endotoxin stimulates leptin in the human and nonhuman primate. *J Clin Endocrinol Metab* 2003;88:1285-1291.
76. Howard JK, Lord GM, Matarese G, et al. Leptin protects mice from starvation-induced lymphoid atrophy and increases thymic cellularity in ob/ob mice. *J Clin Invest* 1999;104:1051-1059.
77. Matarese G, Di Giacomo A, Sanna V, et al. Requirement for leptin in the induction and progression of autoimmune encephalomyelitis. *J Immunol* 2001;166:5909-5916.
78. Moraes-Vieira PM, Bassi EJ, Larocca RA, et al. Leptin deficiency modulates allograft survival by favoring a Th2 and a regulatory immune profile. [corrected]. *Am J Transplant*. 2013;13:36-44.
79. Zhang Y, Wilsey JT, Frase CD, et al. Peripheral but not central leptin prevents the immunosuppression associated with hypoleptinemia in rats. *J Endocrinol*. 2002;174:455-461.
80. Grant RW, Dixit VD. Adipose tissue as an immunological organ. *Obesity*. 2015;23:512-518.
81. Kershaw EE, Flier JS. Adipose tissue as an endocrine organ. *J Clin Endocrinol Metab* 2004;89:2548-2556.
82. Stolarczyk E. Adipose tissue inflammation in obesity: a metabolic or immune response? *Curr Opin Pharmacol*. 2017;37:35-40.
83. Boden G, Chen X, Mozzoli M, Ryan I. Effect of fasting on serum leptin in normal human subjects. *J Clin Endocrinol Metab*. 1996;81:3419-3423.
84. Hardie LJ, Rayner DV, Holmes S, Trayhurn P. Circulating leptin levels are modulated by fasting, cold exposure and insulin administration in lean but not Zucker (fa/fa) rats as measured by ELISA. *Biochem Biophys Res Commun* 1996;223:660-665.
85. Tu AW, Humphries KH, Lear SA. Longitudinal changes in visceral and subcutaneous adipose tissue and metabolic syndrome: results from the Multicultural Community Health Assessment Trial (M-CHAT). *Diabetes Metab Syndr*. 2017;11(Suppl 2):S957-S961.
86. Wajchenberg BL, Giannella-Neto D, da Silva ME, Santos RF. Depot-specific hormonal characteristics of subcutaneous and visceral adipose tissue and their relation to the metabolic syndrome. *Horm Metab Res*. 2002;34:616-621.
87. Booth AD, Magnuson AM, Fouts J, et al. Subcutaneous adipose tissue accumulation protects systemic glucose tolerance and muscle metabolism. *Adipocyte* 2018;7:261-272.
88. Vegiopoulos A, Rohm M, Herzig S. Adipose tissue: between the extremes. *EMBO J* 2017;36:1999-2017.
89. Almuraikhy S, Kafienah W, Bashah M, et al. Interleukin-6 induces impairment in human subcutaneous adipogenesis in obesity- associated insulin resistance. *Diabetologia* 2016;59:2406-2416.
90. Van Harmelen V, Reynisdottir S, Eriksson P, et al. Leptin secretion from subcutaneous and visceral adipose tissue in women. *Diabetes* 1998;47:913-917.
91. Varela L, Horvath TL. Leptin and insulin pathways in POMC and AgRP neurons that modulate energy balance and glucose homeostasis. *EMBO Rep* 2012;13:1079-1086.
92. Zeng W, Pirzgalska RM, Pereira MM, et al. Sympathetic neuro-adipose connections mediate leptin-driven lipolysis. *Cell* 2015;163:84-94.
93. Jaubert AM, Penot G, Niang F, Durant S, Forest C. Rapid nitration of adipocyte phosphoenolpyruvate carboxykinase by leptin reduces glyceroneogenesis and induces fatty acid release. *PLoS One* 2012;7:e40650.
94. Rodriguez VM, Macarulla MT, Echevarria E, Portillo MP. Lipolysis induced by leptin in rat adipose tissue from different anatomical locations. *Eur J Nutr* 2003;42:149-153.
95. Siegrist-Kaiser CA, Pauli V, Juge-Aubry CE, et al. Direct effects of leptin on brown and white adipose tissue. *J Clin Invest* 1997;100:2858-2864.
96. Li C, Xu MM, Wang K, Adler AJ, Vella AT, Zhou B. Macrophage polarization and meta-inflammation. *Transl Res*.. 2018;191:29-44.
97. Weisberg SP, McCann D, Desai M, Rosenbaum M, Leibel RL, Ferrante AW Jr. Obesity is associated with macrophage accumulation in adipose tissue. *J Clin Invest* 2003;112:1796-1808.
98. Souza-Almeida G, D'Avila H, Almeida PE, et al. Leptin mediates in vivo neutrophil migration: involvement of tumor necrosis factor-alpha and CXCL1. *Front Immunol* 2018;9:111.

99. Jin D, Sun J, Huang J, He Y, Yu A, Yu X, Yang Z. TNF-alpha reduces g0s2 expression and stimulates lipolysis through PPAR-gamma inhibition in 3T3-L1adipocytes. *Cytokine* 2014;69:196-205.
100. Luo L, Liu M. Adipose tissue in control of metabolism. *J Endocrinol* 2016;231:R77-R99.
101. Souza SC, de Vargas LM, Yamamoto MT, et al. Overexpression of perilipin A and B blocks the ability of tumor necrosis factor alpha to increase lipolysis in 3T3-L1 adipocytes. *J Biol Chem* 1998;273: 24665-24669.
102. Tesz GJ, Guilherme A, Guntur KV, et al. Tumor necrosis factor alpha (TNFalpha) stimulates Map4k4 expression through TNFalpha receptor 1 signaling to c-Jun and activating transcription factor 2. *J Biol Chem* 2007;282:19302-19312.
103. Jeffery E, Wing A, Holtrup B, et al. The adipose tissue microenvironment regulates depot-specific adipogenesis in obesity. *Cell Metab.* 2016;24:142-150.
104. Yue R, Zhou BO, Shimada IS, Zhao Z, Morrison SJ. Leptin receptor promotes adipogenesis and reduces osteogenesis by regulating mesenchymal stromal cells in adult bone marrow. *Cell Stem cell* 2016;18:782-796.
105. Chu X, Nishimura K, Jisaka M, Nagaya T, Shono F, Yokota K. Up-regulation of adipogenesis in adipocytes expressing stably cyclooxygenase-2 in the antisense direction. *Prostaglandins Other Lipid Mediat.* 2010;91:1-9.
106. Kaiyala KJ, Ogimoto K, Nelson JT, Muta K, Morton GJ. Physiological role for leptin in the control of thermal conductance. *Mol Metab.* 2016;5:892-902.
107. Marlatt KL, Ravussin E. Brown Adipose tissue: an update on recent findings. *Curr Obesity Rep* 2017;6:389-396.
108. Boura-Halfon S, Pecht T, Jung S, Rudich A. Obesity and dysregulated central and peripheral macrophage-neuron cross-talk. *Eur J Immunol.* 2018.
109. Metchnikoff, E. *Leçons sur la pathologie comparée de l'inflammation: faites à l'Institut Pasteur en avril et mai 1891*. G. Masson, 1892.
110. van Furth R, Cohn ZA. The origin and kinetics of mononuclear phagocytes. *J Exp Med* 1968;128:415-435.
111. Sawyer RT, Strausbauch PH, Volkman A. Resident macrophage proliferation in mice depleted of blood monocytes by strontium-89. *Lab Invest* 1982;46:165-170.
112. Czernielewski JM, Demarchez M. Further evidence for the self-reproducing capacity of Langerhans cells in human skin. *J Invest Dermatol* 1987;88:17-20.
113. Epelman S, Lavine KJ, Randolph GJ. Origin and functions of tissue macrophages. *Immunity* 2014;41:21-35.
114. Naito M, Umeda S, Yamamoto T, et al. Development, differentiation, and phenotypic heterogeneity of murine tissue macrophages. *J Leukoc Biol* 1996;59:133-138.
115. Parwaresch MR, Wacker HH. Origin and kinetics of resident tissue macrophages. Parabiosis studies with radiolabelled leucocytes. *Cell Tissue Kinet* 1984;17:25-39.
116. Volkman A, Chang NC, Strausbauch PH, Morahan PS. Differential effects of chronic monocyte depletion on macrophage populations. *Lab Invest* 1983;49:291-298.
117. Davies LC, Jenkins SJ, Allen JE, Taylor PR. Tissue-resident macrophages. *Nat Immunol* 2013;14:986-995.
118. Abbas KA. *Cellular and Molecular Immunology*. 9th ed. Amsterdam, the Netherlands: Elsevier 2018.
119. Ginhoux F, Guilliams M. Tissue-resident macrophage ontogeny and homeostasis. *Immunity* 2016;44:439-449.
120. Guilliams M, Ginhoux F, Jakubzick C, et al. Dendritic cells, monocytes and macrophages: a unified nomenclature based on ontogeny. *Nat Rev Immunol.* 2014;14:571-578.
121. Mass E, Ballesteros I, Farlik M, et al. Specification of tissue-resident macrophages during organogenesis. *Science* 2016;353: aaf4238
122. McGovern N, Schlitzer A, Gunawan M, et al. Population of monocyte-derived macrophages. *Immunity* 2015;42:391.
123. Penny HL, Sieow JL, Adriani G, et al. Warburg metabolism in tumor-conditioned macrophages promotes metastasis in human pancreatic ductal adenocarcinoma. *Oncoimmunology* 2016;5: e1191731.
124. Huang SC, Smith AM, Everts B, et al. Metabolic reprogramming mediated by the mTORC2-IRF4 signaling axis is essential for macrophage alternative activation. *Immunity* 2016;45:817-830.
125. Jha AK, Huang SC, Sergushichev A, et al. Network integration of parallel metabolic and transcriptional data reveals metabolic modules that regulate macrophage polarization. *Immunity* 2015;42: 419-430.
126. Moraes-Vieira PM, Yore MM, Dwyer PM, Syed I, Aryal P, Kahn BB. RBP4 activates antigen-presenting cells, leading to adipose tissue inflammation and systemic insulin resistance. *Cell Metab* 2014b;19:512-526.
127. O'Neill LA, Kishton RJ, Rathmell J. A guide to immunometabolism for immunologists. *Nature reviews. Immunology* 2016;16: 553-565.
128. Pearce EL, Pearce EJ. Metabolic pathways in immune cell activation and quiescence. *Immunity* 2013;38:633-643.
129. Galván-Peña S, O'Neill LAJ. Metabolic reprograming in macrophage polarization. *Front Immunol* 2014;5:420
130. Odegaard JI, Chawla A. Alternative macrophage activation and metabolism. *Annu Rev Pathol* 2011;6:275-297.
131. Mills CD, Kincaid K, Alt JM, Heilman MJ, Hill AM. M-1/M-2 macrophages and the Th1/Th2 paradigm. *J Immunol* 2000;164: 6166-6173.
132. Diskin C, Palsson-McDermott EM. Metabolic modulation in macrophage effector function. *Front Immunol* 2018;9:270.
133. Vander Heiden MG, Cantley LC, Thompson CB. Understanding the Warburg effect: the metabolic requirements of cell proliferation. *Science* 2009;324:1029-1033.
134. Warburg O. The metabolism of carcinoma cells. *Cancer Res.* 1925;9. https://doi.org/10.1158/jcr.1925.148
135. Shestov AA, Liu X, Ser Z, et al. Quantitative determinants of aerobic glycolysis identify flux through the enzyme GAPDH as a limiting step. *ELife* 2014;3. https://doi.org/10.7554/eLife.03342
136. Liberti MV, Locasale JW. The Warburg effect: how does it benefit cancer cells? *Trends Biochem Sci* 2016;41:211-218.
137. Warburg O. On the origin of cancer cells. *Science* 1956;123:309-314.
138. Buck MD, O'Sullivan D, Klein Geltink RI, et al. Mitochondrial dynamics controls T cell fate through metabolic programming. *Cell* 2016;166:63-76.
139. Chang CH, Curtis JD, Maggi LB, et al. Posttranscriptional control of T cell effector function by aerobic glycolysis. *Cell* 2013;153: 1239-1251.
140. Ip WKE, Hoshi N, Shouval DS, Snapper S, Medzhitov R. Anti-inflammatory effect of IL-10 mediated by metabolic reprogramming of macrophages. *Science* 2017;356:513-519.
141. Krawczyk CM, Holowka T, Sun J, et al. Toll-like receptor-induced changes in glycolytic metabolism regulate dendritic cell activation. *Blood* 2010;115:4742-4749.
142. Laemmli UK. Cleavage of structural proteins during the assembly of the head of bacteriophage T4. *Nature* 1970;227:680-685.
143. Rodriguez-Prados JC, Traves PG, Cuenca J, et al. Substrate fate in activated macrophages: a comparison between innate, classic, and alternative activation. *J Immunol* 2010;185:605-614.
144. Freemerman AJ, Johnson AR, Sacks GN, et al. Metabolic reprogramming of macrophages: glucose transporter 1 (GLUT1)-mediated glucose metabolism drives a proinflammatory phenotype. *J Biol Chem* 2014;289:7884-7896.
145. Michl J, Ohlbaum DJ, Silverstein SC. 2-Deoxyglucose selectively inhibits Fc and complement receptor-mediated phagocytosis in

mouse peritoneal macrophages II. Dissociation of the inhibitory effects of 2-deoxyglucose on phagocytosis and ATP generation. *J Exp Med* 1976;144:1484-1493.
146. Pavlou S, Wang L, Xu H, Chen M. Higher phagocytic activity of thioglycollate- elicited peritoneal macrophages is related to metabolic status of the cells. *J Inflam.* 2017;14:4.
147. Zhao G, Cao K, Xu C, et al. Crosstalk between mitochondrial fission and oxidative stress in paraquat- induced apoptosis in mouse alveolar type II cells. *Int J Biol Sci.* 2017;13:888-900.
148. Tannahill GM, Curtis AM, Adamik J, et al. Succinate is an inflammatory signal that induces IL-1beta through HIF-1alpha. *Nature* 2013;496:238-242.
149. Van den Bossche J, O'Neill LA, Menon D. Macrophage immunometabolism: where are we (going)? *Trends Immunol* 2017;38: 395-406.
150. Vats D, Mukundan L, Odegaard JI, et al. Oxidative metabolism and PGC-1beta attenuate macrophage-mediated inflammation. *Cell Metab.* 2006;4:13-24.
151. Kim J, Kundu M, Viollet B, Guan K-L. AMPK and mTOR regulate autophagy through direct phosphorylation of Ulk1. *Nat Cell Biol* 2011;13:132.
152. Nath N, Khan M, Rattan R, et al. Loss of AMPK exacerbates experimental autoimmune encephalomyelitis disease severity. *Biochem Biophys Res Commun* 2009;386:16-20.
153. Powell JD, Pollizzi KN, Heikamp EB, Horton MR. Regulation of immune responses by mTOR. *Annu Rev Immunol* 2012;30:39-68.
154. Laplante M, Sabatini DM. mTOR signaling in growth control and disease. *Cell* 2012;149:274-293.
155. Divakaruni AS, Hsieh WY, Minarrieta L, et al. Etomoxir inhibits macrophage polarization by disrupting CoA homeostasis. *Cell Metab* 2018;28:490-503.e497.
156. Van den Bossche J, van der Windt GJW. Fatty Acid oxidation in macrophages and T cells: time for reassessment? *Cell Metab* 2018;28:538-540.
157. Cho KW, Morris DL, Lumeng CN. Flow cytometry analyses of adipose tissue macrophages. *Methods Enzymol* 2014;537:297-314.
158. Boutens L, Stienstra R. Adipose tissue macrophages: going off track during obesity. *Diabetologia.* 2016;59:879-894.
159. Lumeng CN, Bodzin JL, Saltiel AR. Obesity induces a phenotypic switch in adipose tissue macrophage polarization. *J Clin Invest* 2007;117:175-184.
160. Trayhurn P, Wang B, Wood IS. Hypoxia in adipose tissue: a basis for the dysregulation of tissue function in obesity? *Br J Nutr* 2008;100:227-235.
161. Fujisaka S, Usui I, Ikutani M, et al. Adipose tissue hypoxia induces inflammatory M1 polarity of macrophages in an HIF-1alpha-dependent and HIF- 1alpha-independent manner in obese mice. *Diabetologia* 2013;56:1403-1412.
162. He Q, Gao Z, Yin J, Zhang J, Yun Z, Ye J. Regulation of HIF-1{alpha}activity in adipose tissue by obesity-associated factors: adipogenesis, insulin, and hypoxia. *Am J Physiol Endocrinol Metab* 2011;300:E877-E885.
163. Kim SY, Choi YJ, Joung SM, Lee BH, Jung YS, Lee JY. Hypoxic stress up-regulates the expression of Toll-like receptor 4 in macrophages via hypoxia-inducible factor. *Immunology* 2010;129: 516-524.
164. Kim SY, Jeong E, Joung SM, Lee JY. PI3K/Akt contributes to increased expression of Toll-like receptor 4 in macrophages exposed to hypoxic stress. *Biochem Biophys Res Commun* 2012;419:466-471.
165. Takikawa A, Mahmood A, Nawaz A, et al. HIF-1alpha in myeloid cells promotes adipose tissue remodeling toward insulin resistance. *Diabetes* 2016;65:3649-3659.
166. Serbina NV, Pamer EG. Monocyte emigration from bone marrow during bacterial infection requires signals mediated by chemokine receptor CCR2. *Nat Immunol* 2006;7:311-317.
167. Tacke F, Randolph GJ. Migratory fate and differentiation of blood monocyte subsets. *Immunobiology* 2006;211:609-618.
168. Weisberg SP, Hunter D, Huber R, et al. CCR2 modulates inflammatory and metabolic effects of high-fat feeding. *J Clin Invest* 2006;116:115-124.
169. Amano SU, Cohen JL, Vangala P, et al. Local proliferation of macrophages contributes to obesity-associated adipose tissue inflammation. *Cell Metab* 2014;19:162-171.
170. Kamei N, Tobe K, Suzuki R, et al. Overexpression of monocyte chemoattractant protein-1 in adipose tissues causes macrophage recruitment and insulin resistance. *J Biol Chem* 2006;281:26602-26614.
171. Nguyen MT, Favelyukis S, Nguyen AK, et al. A subpopulation of macrophages infiltrates hypertrophic adipose tissue and is activated by free fatty acids via Toll-like receptors 2 and 4 and JNK-dependent pathways. *J Biol Chem* 2007;282:35279-35292.
172. Rubtsov AV, Rubtsova K, Kappler JW, Jacobelli J, Friedman RS, Marrack P. CD11c-expressing B cells are located at the T cell B cell border in spleen and are potent antigen presenting cells. *J Immunol* 2015;195:71-79.
173. Cinti S, Mitchell G, Barbatelli G, et al. Adipocyte death defines macrophage localization and function in adipose tissue of obese mice and humans. *J Lipid Res* 2005;46:2347-2355.
174. Wentworth JM, Naselli G, Brown WA, et al. Pro-inflammatory CD11c+CD206+ adipose tissue macrophages are associated with insulin resistance in human obesity. *Diabetes* 2010;59:1648-1656.
175. Acedo SC, Gambero S, Cunha FG, Lorand-Metze I, Gambero A. Participation of leptin in the determination of the macrophage phenotype: an additional role in adipocyte and macrophage crosstalk. *In Vitro Cell Dev Biol Anim.* 2013;49:473-478.
176. Zeyda M, Farmer D, Todoric J, et al. Human adipose tissue macrophages are of an anti-inflammatory phenotype but capable of excessive pro-inflammatory mediator production. *Int J. Obes.* 2007;31:1420-1428.
177. Kaminski DA, Randall TD. Adaptive immunity and adipose tissue biology. *Trends Immunol* 2010;31:384-390.
178. Khan IM, Dai Perrard XY, Perrard JL, et al. Attenuated adipose tissue and skeletal muscle inflammation in obese mice with combined CD4+ and CD8+ T cell deficiency. *Atherosclerosis* 2014;233:419-428.
179. Schipper HS, Prakken B, Kalkhoven E, Boes M. Adipose tissue-residentimmune cells: key players in immunometabolism. *Trends Endocrinol Metab* 2012;23:407-415.
180. Feuerer M, Herrero L, Cipolletta D, et al. Lean, but not obese, fat is enriched for a unique population of regulatory T cells that affect metabolic parameters. *Nat Med* 2009;15:930-939.
181. Molofsky AB, Nussbaum JC, Liang HE, et al. Innate lymphoid type 2 cells sustain visceral adipose tissue eosinophils and alternatively activated macrophages. *J Exp Med* 2013;210:535-549.
182. Wang Q, Wu H. T cells in adipose tissue: critical players in immunometabolism. *Front Immunol.* 2018;9:2509.
183. Gerriets VA, Danzaki K, Kishton RJ, et al. Leptin directly promotes T-cell glycolytic metabolism to drive effector T-cell differentiation in a mouse model of autoimmunity. *Eur J Immunol.* 2016;46: 1970-1983.
184. Hepler C, Shan B, Zhang Q, et al. Identification of functionally distinct fibro-inflammatory and adipogenic stromal subpopulations in visceral adipose tissue of adult mice. *eLife* 2018;7:
185. See P, Lum J, Chen J, Ginhoux F. A Single-Cell Sequencing Guide for Immunologists. *Front Immunol* 2018;9:2425.
186. Lafrance V, Inoue W, Kan B, Luheshi GN. Leptin modulates cell morphology and cytokine release in microglia. *Brain Behav Immun* 2010;24:358-365.
187. Lee SM, Choi HJ, Oh CH, Oh JW, Han JS. Leptin increases TNF-alphaexpression and production through phospholipase D1 in Raw 264.7 cells. *PLoS One* 2014;9:e102373.

188. Martin-Romero C, Sanchez-Margalet V. Human leptin activates PI3K and MAPK pathways in human peripheral blood mononuclear cells: possible role of Sam68. *Cell Immunol* 2001;212:83-91.
189. Matarese G, Moschos S, Mantzoros CS. Leptin in immunology. *J Immunol*. 2005;174:3137-3142.
190. Shen J, Sakaida I, Uchida K, Terai S, Okita K. Leptin enhances TNF-alphaproduction via p38 and JNK MAPK in LPS-stimulated Kupffer cells. *Life Sci*. 2005;77:1502-1515.
191. Zarkesh-Esfahani H, Pockley G, Metcalfe RA, et al. High-dose leptin activates human leukocytes via receptor expression on monocytes. *J Immunol*. 2001;167:4593-4599.
192. Procaccini C, Jirillo E, Matarese G. Leptin as an immunomodulator. *Mol Aspects Med*. 2012;33:35-45.
193. Procaccini C, Pucino V, Mantzoros CS, Matarese G. Leptin in autoimmune diseases. *Metabolism*. 2015;64:92-104.
194. Sanchez-Margalet V, Martin-Romero C, Santos-Alvarez J, Goberna R, Najib S, Gonzalez-Yanes C. Role of leptin as an immunomodulator of blood mononuclear cells: mechanisms of action. *Clin Exp Immunol*. 2003;133:11-19.
195. Siegmund B, Lehr HA, Fantuzzi G. Leptin: a pivotal mediator of intestinal inflammation in mice. *Gastroenterology* 2002;122:2011-2025.
196. Moraes-Vieira PM, Larocca RA, Bassi EJ, et al. Leptin deficiency impairs maturation of dendritic cells and enhances induction of regulatory T and Th17 cells. *Eur J Immunol* 2014a;44:794-806.
197. Reis BS, Lee K, Fanok MH, et al. Leptin receptor signaling in T cells is required for Th17 differentiation. *J Immunol*. 2015;194:5253-5260.
198. Rao KM. MAP kinase activation in macrophages. *J Leukoc Biol*. 2002;69:3-10.
199. Mancuso P, Gottschalk A, Phare SM, Peters-Golden M, Lukacs NW, Huffnagle GB. Leptin-deficient mice exhibit impaired host defense in Gram-negative pneumonia. *J Immunol*. 2002;168:4018-4024.
200. Fernández-Riejos P, Najib S, Santos-Alvarez J, et al. Role of Leptin in the Activation of Immune Cells. *Mediators Inflamm*. 2010;2010:568343.
201. Kiguchi N, Maeda T, Kobayashi Y, Fukazawa Y, Kishioka S. Leptin enhances CC-chemokine ligand expression in cultured murine macrophage. *Biochem Biophys Res Commun*. 2009;384:311-315.
202. Coats BR, Schoenfelt KQ, Barbosa-Lorenzi VC, et al. Metabolically activated adipose tissue macrophages perform detrimental and beneficial functions during diet-induced obesity. *Cell Rep*. 2017;20:3149-3161.
203. Kratz M, Coats BR, Hisert KB et al. Metabolic dysfunction drives a mechanistically distinct proinflammatory phenotype in adipose tissue macrophages. *Cell Metab*. 2014;20:614-625.
204. Hongo S, Watanabe T, Arita S, et al. Leptin modulates ACAT1 expression and cholesterol efflux from human macrophages. *Am J Physiol Endocrinol Metab*. 2009;297:E474-E482.
205. Douros JD, Baltzegar DA, Reading BJ, et al. Leptin stimulates cellular glycolysis through a STAT3 dependent mechanism in tilapia. *Front Endocrinol*. 2018;9:465.
206. Lord GM. Leptin as a proinflammatory cytokine. *Contrib Nephrol*. 2006;151:151-164.
207. Moura EC, Claro RM. Estimates of obesity trends in Brazil, 2006-2009. *Int J Public Health*. 2012;57:127-133.
208. Wellen KE, Hotamisligil GS. Obesity-induced inflammatory changes in adipose tissue. *J Clin Invest*. 2003;112:1785-1788.
209. Coleman DL. A historical perspective on leptin. *Nat Med*. 2010;16:1097-1099.
210. Considine RV, Sinha MK, Heiman ML, et al. Serum immunoreactive-leptin concentrations in normal-weight and obese humans. *N Engl J Med*. 1996;334:292-295.
211. de la Brousse FC, Shan B, Chen JL. Identification of the promoter of the mouse obese gene. *Proc Natl Acad Sci USA*. 1996;93:4096-4101.
212. Harris RB, Zhou J, Redmann SM Jr, et al. A leptin dose-response study in obese (ob/ob) and lean (+/?) mice. *Endocrinology* 1998;139:8-19.
213. Loffreda S, Yang SQ, Lin HZ, et al. Leptin regulates proinflammatory immune responses. *FASEB J*. 1998;12:57-65.
214. Hoffmann A, Kralisch S, Duhring S, et al. Effects of leptin on macrophages in vivo. *Atherosclerosis*. 2014;235:e194.
215. Xu H, Barnes GT, Yang Q, et al. Chronic inflammation in fat plays a crucial role in the development of obesity-related insulin resistance. *J Clin Invest*. 2003;112:1821-1830.
216. Solinas G, Karin M. JNK1 and IKKbeta: molecular links between obesity and metabolic dysfunction. *FASEB J*. 2010;24:2596-2611.
217. Santos-Alvarez J, Goberna R, Sanchez-Margalet V. Human leptin stimulates proliferation and activation of human circulating monocytes. *Cell Immunol* 1999;194:6-11.
218. Bai Y, Sun Q. Macrophage recruitment in obese adipose tissue. *Obes Rev*. 2015;16:127-136.
219. Moraes-Vieira PM, Bassi EJ, Araujo RC, Câmara NO. Leptin as a link between the immune system and kidney-related diseases: leading actor or just a coadjuvant? *Obes Rev*. 2012; 8:733-743

How to cite this article: Monteiro L, Pereira JAdS, Palhinha L, Moraes-Vieira PMM. Leptin in the regulation of the immunometabolism of adipose tissue-macrophages. *J Leukoc Biol*. 2019;1-14. https://doi.org/10.1002/JLB.MR1218-478R

APENDICE 4

PNAS
www.pnas.org

Main Manuscript for

Activation of liver X receptor β reduces adipose tissue inflammation and improves insulin sensitivity during obesity

Jessica A.S. Pereira[1,2], Gerson Profeta de Souza[3†], João V. Virgilio-da-Silva[1,2†], Juliana S. Prodonoff[1†], Gisele de Castro[1,2], Leonardo F. Pimentel[1], Felippe Mousovich-Neto[3], Gustavo G. Davanzo[1], Cristhiane F. Aguiar[1], Cristiane N. S. Breda[2,4], Marcia G. Guereschi[5], Ronaldo C. Araújo[6], Helder Nakaya[7], Marcelo A. Mori[3,9,10], Diorge P. Souza[8], Niels O. S. Câmara[2,4], Alexandre S. Basso[5], Pedro M. Moraes-Vieira[1,2,9,10*]

1 - Laboratory of Immunometabolism, Department of Genetics, Evolution, Microbiology and Immunology, Institute of Biology - University of Campinas.

2 – Graduate program in Immunology, Institute of Biomedical Sciences - University of Sao Paulo.

3- Laboratory of Ageing Biology, Department of Biochemistry and tissue biology, Institute of Biology - University of Campinas.

4 - Laboratory of Transplant Immunobiology, Institute of Biomedical Sciences - University of Sao Paulo.

5 - Laboratory of Neuroimmunology, Department of Microbiology, Immunology and Parasitology, Paulista Medical School, Federal University of Sao Paulo, Sao Paulo, Brazil.

6 - Laboratory of Exercise Genetics and Metabolism, Department of Biophysics Federal University of Sao Paulo, Sao Paulo, Brazil.

7 - Department of Clinical and Toxicological Analyses, School of Pharmaceutical Sciences, University of Sao Paulo (USP), Sao Paulo, Brazil.

8 - Division of Cell Biology, MRC, Laboratory of Molecular Biology, Cambridge, United Kingdom

9 - Experimental Medicine Research Cluster (EMRC), University of Campinas.

10 - Obesity and comorbidities research center (OCRC), University of Campinas, Brazil.

† - Contributed Equally to this work

* Pedro M Moraes-Vieira, Laboratory of Immunometabolism, Department of Genetics, Evolution, Microbiology and Immunology, Institute of Biology, University of Campinas, Rua Monteiro Lobato 255, BLH, 1st floor, Cidade Universitária Zeferino Vaz, Campinas, SP, 13083-862, Phone: +55 19 3521-6121

Email: pmvieira@unicamp.br

Author Contributions: JASP designed and performed experiments, analyzed data, wrote the manuscript and made the figures. GPS, JVV, JSP, ACC, GC, LFP, FMN, GGD, CFA, CNS, MG performed experiments. HN performed the bioinformatic analysis. RCA, MASM, ASB, NOSC provided equipment, reagents and expertise. PMMMV coordinated the project, designed experiments, wrote and edited the manuscript.

Competing Interest Statement: The authors declare no conflict of interests regarding the publication of this paper

Classification: Major: Biological Sciences. Minor classification: Immunology and Inflammation

Keywords: Liver X receptors; Adipose tissue inflammation; Obesity; Insulin resistance.

This PDF file includes:

Main Text

Figures 1 to 4

Abstract

Liver X receptors (LXR) regulates cholesterol homeostasis and immune response. Cholesterol levels are commonly increased in obesity and contribute for pro-inflammatory responses. The role of LXR in obesity-induced adipose tissue (AT) inflammation, macrophage phenotype and glucose homeostasis remain to be elucidated. Here, we show that LXR deletion boosts AT inflammation in an LXRβ-dependent manner. LXR deficiency in immune cells aggravates obesity-induced AT inflammation by increasing CD11c+ and IL-1β+ AT macrophage (ATM) numbers. Finally, we identified naringenin (NAR) as an LXR agonist in macrophages. NAR treatment reduced pro-inflammatory cytokines expression in activated macrophages. Obese mice treated with NAR displayed increased insulin sensitivity and reduced AT inflammation. Together, we show a distinct role for each LXR isoform in the regulation of AT inflammation and glucose homeostasis. LXRβ expression in immune cells is necessary for AT pro/anti-inflammatory balance. LXRβ has the potential to become a therapeutic target to treat AT inflammation and insulin resistance.

Significance Statement

Obesity has reached epidemic rates and contributes for the development of many other disorders, as cardiovascular disease and diabetes. A shift in the resident adipose tissue macrophage population toward a pro-inflammatory profile is frequently found in obese people. However, how obesity affects nuclear receptors and AT macrophages function is still unknown. Here we show that ATMs from obese animals have enriched cholesterol pathway, and LXR deletion boost the lipid accumulation in macrophages, while increase the adipose tissue inflammation in a LXRβ-dependent manner, while LXRβ activation increase insulin sensitivity by reducing adipose tissue inflammation.

Main Text

Introduction

Liver X receptors (LXR) are transcriptional factors that act as cholesterol sensors and regulate the efflux, degradation and transport of cholesterol, through the expression of ATP binding cassette (ABC) transporters, apolipoproteins and other genes related to the reverse cholesterol transport (1-3). LXR activation occurs in response to endogenous ligands, such as oxysterols (4-6), or synthetic molecules, such as T0901317 and GW3965 (7, 8). LXR also play a role in glucose homeostasis and carbohydrate metabolism by regulating the expression of glucose transporter 4 (GLUT4) and controlling insulin secretion and hepatic glucose metabolism (5, 9-12). LXR have two isoforms, LXRα and LXRβ, which have high homology but distinct expression patterns (3, 13). LXRα expression is restricted to visceral organs and immune cells, such as macrophages (14, 15)(16), while LXRβ is ubiquitously expressed (3).

Obesity is marked by chronic low-grade inflammation (17, 18). Obese people commonly display increased cholesterol and glucose levels, which can affect LXR expression and activation (19). Furthermore, obesity-induced AT inflammation contributes to impaired insulin sensitivity, which is a major risk factor for the development of type 2 diabetes (20). Several immune cell types participate in the regulation of AT inflammation and insulin sensitivity (21). In lean mice and humans, macrophages maintain AT homeostasis (22). Obesity induces the accumulation of inflammatory macrophages and other pro-inflammatory immune cells, leading to AT inflammation and the subsequent insulin resistance (23).

Adipose tissue macrophages (ATM) span a constellation of phenotypes and obesity triggers phenotypic changes in ATM populations (24). Simplistically, ATM phenotypes are usually divided in a tissue maintenance/anti-inflammatory phenotype and a pro-inflammatory phenotype (20, 25-28). Alternatively activated ATM numbers are higher in lean AT and these macrophages express CD206 (mannose receptor), macrophage galactose-type lectin (MGL), transforming growth factor-β (TGF-β), IL-10, among others, and thus, contribute to AT homeostasis and repair (29-31). Classically activated ATM express CD11c (integrin alpha X) and pro-inflammatory cytokines and chemokines, such as TNF-α, IL-1β, IL-6 and CCL-2 and iNOS (26, 32-38). Obesity induces an imbalance between $CD206^{+}$ and $CD11c^{+}$ macrophages, which contribute to the development of insulin resistance, type 2 diabetes and atherosclerosis in obese subjects (39).

Several studies have attributed an anti-inflammatory role for LXR (40-42). Agonists of LXR inhibit the activation of NFκB, as well the expression of pro-inflammatory genes in macrophages (3, 43, 44). However, the role of each LXR isoform in macrophages and in the regulation of ATM metabolism and function during obesity remains unclear. Here, we show that the deletion of any LXR isoform results in immune imbalance in AT of lean animals. In response to high fat diet (HFD), only LXRβ deficiency aggravates obesity-induced AT inflammation. LXRα and β-deficient animals display increased numbers of IL-1β$^+$ ATM in the perigonadal AT (PgAT). Moreover, the deletion of both LXR isoforms specifically in immune cells is sufficient to alter AT immune phenotype, observed by increased monocyte infiltration and CD11c$^+$ ATM numbers in lean animals, and increased expression of pro-inflammatory cytokines in both lean and obese animals. Finally, we found that the citrus-derived flavonoid naringenin acts as a novel LXRβ agonist in macrophages. Naringenin treatment reduces the expression of pro-inflammatory markers by reducing LPS-induced glycolysis and mitochondrial dysfunction in macrophages. In vivo, naringenin-induced LXRβ activation in obese mice reduces the number of AT pro-inflammatory macrophages, mitigating insulin resistance.

Results

LXR deficiency affects body weight gain and insulin sensitivity in HFD-fed mice

Obesity is caused by the imbalance between energy intake and energy expenditure, which promotes the expansion of white adipose depots and increases circulating fatty acids and cholesterol levels (45). In turn, increased cholesterol levels may directly lead to LXR activation (4). Aiming to determine the effects of LXR during obesity, we analyzed the systemic metabolic effects of LXRα and β deletion (LXRαβKO) in mice fed a high fat diet (HFD) for 12 weeks. LXR deficiency inhibited HFD-induced weight gain and AT expansion (Fig. 1A and Fig. S1A) with no changes on cumulative food intake (Fig. 1B and Fig. S1B). Next, we determined the role of LXR in the regulation of glucose homeostasis under obesogenic conditions. HFD-fed LXRαβKO mice had no alterations in fasting blood glucose levels (Fig. 1C), but displayed increased insulin sensitivity and glucose intolerance when compared to HFD-fed wild-type (WT) controls (Fig. 1D-E and Fig. S1C). We next investigated if the reduced weight gain in HFD-fed LXRαβKO was associated with changes in energy expenditure. HFD-fed LXRαβKO mice displayed reduced oxygen consumption compared to WT animals in the same diet (Fig. 1F). In addition, the energy expenditure was reduced in LXRαβKO (Fig. S1D), with no changes in mice activity (Fig. S1E). We then explored whether LXRαβKO could affect fuel source for energy generation. LXRαβKO used glucose as the preferential fuel for energy production, while HFD-fed WT animals primarily used lipids (Fig. 1G-H). These data indicate that LXR are important regulators of energy balance and contribute to the maintenance of whole-body glucose homeostasis.

LXRα deletion is sufficient to improve insulin sensitivity in obese mice

LXR isoforms has been showed to induce distinct cellular response upon activation (46). However, whether LXRα and LXRβ may promote distinct effects over the whole-body metabolism is still unknown. We fed WT, LXRαKO and LXRβKO mice with HFD and evaluated the effects of individual deletion of the LXR isoforms on HFD-induced weight gain and systemic glucose homeostasis. LXRαKO and LXRβKO mice gained similar weight as WT controls (Fig. 1I). Also, neither LXRα nor LXRβ deletion promoted changes in food intake, fat mass and fasting glycemia (Fig. 1J-K and Fig. S1F). LXRαKO mice displayed increased insulin sensitivity under obesogenic conditions compared to WT controls and LXRβKO mice (Fig. 1L). LXRβKO presented impaired glucose tolerance compared to WT controls and LXRαKO mice (Fig. 1M). In order to verify whether LXRα or LXRβ deletion could affect energy expenditure and energy source under obesogenic conditions, indirect calorimetry analysis was performed. Both LXRαKO and LXRβKO mice had similar oxygen consumption and energy expenditure as WT controls (Fig. 1N and Fig. S1G). Also, both LXRαKO and LXRβKO mice displayed similar preference for lipids as fuel for energy production, similar to WT mice (Fig. 1O). Together, our data show that, albeit there is a high overlap between the transcriptional function of LXRα and LXRβ (13, 47), each LXR isoform displays a distinct role in the regulation of systemic glucose homeostasis.

LXR is necessary for ATM inflammatory balance in lean white adipose tissue

Obesity disturbs AT homeostasis, which includes not only the alteration in adipocyte size and morphology, but also comprises the switch from a reparatory into a pro-inflammatory profile in a variety of immune cells (18). Increased cholesterol levels activate pro-inflammatory pathways in immune cells (48). Also, obesity promotes metabolic adaptations in immune cells, such as ATM, directly affecting their function through a still not completely understood mechanism. Because macrophages are the most abundant immune cell population in AT of obese mice and humans (49), we first determined if the main metabolic pathways modulated by the disruption of AT homeostasis are related to cholesterol metabolism. We evaluated RNA-sequencing data from Pg ATM ($F4/80^+CD11b^+$) combining $CD11c^+$ and $CD11c^-$ cells in both lean and obese animals. We observed that among the most modulated pathways during obesity, such as the lysosome pathway, as previously described (50), cholesterol metabolism is upregulated in ATM from obese mice (Fig. 2A). Next, we analyzed the expression of genes related to cholesterol metabolism and found a marked increase in the expression of *Nr1h3* and *Nr1h2* (LXRα and LXRβ, respectively), and of LXR-target genes *Lpl*, *Abcg1* and *Apoe* (Fig. 2B). These data suggest that LXR may have a direct effect on ATM phenotype and function during obesity.

We hypothesized that LXR may directly impact ATM pro-inflammatory profile. We observed that the lack of both LXR isoforms in HFD-fed mice reduced the total number of ATM and the number of $CD11c^+$ and $CD206^+$ ATMs in PgAT in comparison to WT mice fed with the same diet (Fig. 2C and Fig. S2A). Despite the reduction in the total macrophage population, LXRαβKO mice displayed a similar CD11c/CD206 ratio when compared to WT HFD-fed mice (Fig. 2C). Thus, LXR deficiency leads to a global reduction in macrophage population, affecting in a similar manner both $CD11c^+$ and $CD206^+$ ATM populations.

Despite the changes in ATM density in LXRαβKO mice, we found that individual deletion of LXR isoforms did not affect the total number of perigonadal ATM compared to WT mice when subjected to HFD (Fig. 2D and Fig. S2B). We also evaluated ATM populations in chow-fed LXR single knockout mice and observed that chow-fed LXRαKO mice have increased number of ATM in PgAT, with increased numbers of $CD11c^+$ ATM (Fig. S2C-E). In addition, the lack of LXRβ promoted a generalized reduction of ATM numbers, marked by a massive reduction in the numbers of $CD206^+$ ATM (Fig. S2F-H). Together, this data suggests that LXRα and LXRβ are important for preserve ATM numbers and have an overlapping function in the maintenance of $CD11c^+$ and $CD206^+$ ATM populations upon HFD, with distinct roles in $CD11c^+$ and $CD206^+$ ATMs when mice are fed a chow diet.

LXRβ deletion aggravates obesity-induced AT inflammation

Since the concomitant deletion of LXRα and LXRβ did not change the CD11c/CD206 ratio in HFD-fed mice, we decided to investigate whether LXR may direct impact macrophage function, since ATMs numbers were reduced in both LXRα and LXRβ knockout animals. Because ATM reside in a lipid rich environment and lipid droplets are associated with a pro-inflammatory phenotype (22, 51), we evaluated the systemic effects of LXR deletion by analyzing the presence of lipid droplets in macrophages residing outside AT. LXRαβKO macrophages isolated from the peritoneal cavity displayed elevated lipid droplet levels (Fig. 2E). Given that LXR deficient macrophages are loaded with lipid droplets, macrophages from WT, LXRαβKO, LXRαKO and LXRβKO mice were challenged with the TLR4 agonist LPS to evaluate their inflammatory fitness. Deletion of both LXR isoforms in macrophages resulted in increased LPS-induced IL-12 and TNF-α secretion (Fig. 2F). LXRβ and not LXRα mediated this enhanced effect on the secretion of IL-12 and TNF-α induced by LPS (Fig. 2F). Thus, LXRβ is required for macrophage inflammatory fitness and its absence potentiates macrophage pro-inflammatory profile.

Given that HFD consumption is associated with TLR4 activation in AT (52) and the role of LXR in the control of lipid homeostasis and regulation of immune responses (40), we next investigated whether the increased secretion of pro-inflammatory cytokines observed in LXR deficient macrophages could be extrapolated to ATM under metabolic stress induced by HFD. We observed that ATM from both HFD-fed LXRαβKO and LXRβKO mice have increased expression of IL-12, TNF-α and IL-1β compared with ATMs from WT mice fed with the same diet (Fig. 2G and Fig. S3). These data indicate that LXRβ is necessary to limit the secretion of pro-inflammatory cytokines by macrophages and that the deletion of LXRβ results in increased AT inflammation, which contributes to inflammation-induced insulin resistance and enhanced glucose intolerance (Fig. 1L-M).

Expression of LXR in immune cells is necessary for fatty acid synthesis and body weight gain in HFD-fed animals

Because we observed that LXR deficiency affects macrophage inflammatory fitness, we next hypothesized that the observed phenotype in whole body LXR deficient mice could be, at least in part, due to the lack of LXR specifically in immune cells, such as macrophages. Bone marrow cells from WT (WT→WT) or LXRαβKO (LXRαβKO→WT) animals were transferred into sublethally irradiated C57BL/6J WT recipient mice (Fig. 3A). These mice were then fed with HFD for 16 weeks. We observed that the lack of LXR in immune cells resulted in reduced HFD-induced weight gain (Fig. 3B) and reduced fat mass (Fig. 3C). No changes in food intake were observed between WT→WT and LXRαβKO→WT animals (Fig. 3D). LXRαβKO→WT animals had no changes in fasting blood glucose levels and glucose tolerance (Fig. 3E-F).

LXR deficiency in immune cells increases the accumulation of pro-inflammatory ATMs in HFD-fed mice

To investigate whether LXR deficiency in macrophages is involved in the increased AT inflammation observed in LXR deficient mice (Fig. 2), we evaluated ATM populations in PgAT of bone marrow transplanted animals (Fig. 3G-J). We observed that LXR have an essential role in the maintenance of AT immune homeostasis, since LXRαβKO→WT mice had increased AT inflammation, observed by increased number of ATMs in LXRαβKO→WT HFD-fed mice compared to WT→WT HFD-fed mice (Fig. 3G). Also, LXRαβKO→WT chow-fed mice had increased numbers of $CD11c^+$ ATMs compared to WT→WT chow-fed mice (Fig. 3G). The lack of LXR in immune cells increased the percentage of $CD11c^+$ in chow-fed mice, but not in HFD-fed mice (Fig. 3H). ATM isolated from PgAT of HFD-fed LXRαβKO→WT mice had increased expression of IL-1β and TNF-α (Fig. 3I and Extended Data Fig. 4A). Also, LXRαβKO→WT chow-fed mice displayed enhanced IL-1β and IL-12 expression in ATM of HFD-fed mice (Fig. 3I and Extended Data Fig. 4B). The increased monocyte infiltration in the PgAT on chow-fed mice (Fig. 3J) indicate that LXR deficiency in immune cells imprints an immune imbalance that is exacerbated once mice is challenged with HFD. Together, these data indicate that LXR deficiency in immune cells increases obesity-induced AT inflammation through the enhancement of ATMs pro-inflammatory profile.

Naringenin is an LXR agonist in macrophages and improves obesity-induced insulin resistance

LXRα has been directly associated with increased fatty acid synthesis and administration of non-selective LXR agonists has been reported to increase blood triglyceride levels (41, 53-55). Thus, because of the detrimental effects of LXRα activation on lipid metabolism, the search for new selective LXRβ agonists has emerged as an attractive therapeutic target. Several compounds have been shown to modulate LXR, and, in some cases, display opposite effects in each LXR isoform (56). Among them, the citrus-derived flavonoid compound naringenin (NAR) has been shown to modulate LXR activity through controversial effects on LXRα (57, 58). For example, NAR treatment reduces fatty acid synthesis, alleviates atherosclerotic lesions (59) and promotes anti-inflammatory effects in mice (60, 61). The effects of NAR on LXRβ are poorly understood. Thus, we decided to investigate whether NAR could act as a modulator of LXR in macrophages and be used as a potential therapeutic approach to treat HFD-induced insulin resistance. Macrophages were treated with NAR and the expression of LXR target genes evaluated. We observed that similar to the widely used synthetic LXR agonist, GW3965, NAR-treated WT macrophages had increased expression of the LXR target genes *Abca1*, *Abcg1*, *Apoe* and *Lpl*, but not of the fatty acid synthesis-related gene *Fasn* (Fig. 4A), indicating that NAR acts as an LXR agonist in macrophages. NAR had no effect on LXRαβKO macrophages (Fig. S4C), which demonstrate that in macrophages NAR mediated effects are dependent on LXR expression. The absence of changes in *Fasn* expression raise the question if NAR could be binding preferentially in LXRβ in macrophages. Thus, a molecular docking analysis of NAR on LXRβ was carried out to probe the LXRβ-NAR interaction (Fig. S4D-E). The binding site of the lowest energy solution (-9.4 kcal/mol; Fig. S4F) superposes relatively well to the interaction region of all 25 ligands (full and partial agonists and antagonists) which structures have been experimentally solved in complex with the LXRβ LBD. Thus, this indicates that the ligand binding domain of LXRβ can mediate the interaction with naringenin.

We next evaluated if NAR treatment modulates macrophage function. NAR treatment prior to LPS-induced macrophage activation resulted in reduced secretion of CCL2, IL-6 and TNF-α, and reduced expression of *Il-1β* (Fig. 4B). NAR treatment also increased the expression of the alternatively activated macrophage-related marker *Fizz1* (Fig. 4B), reinforcing the anti-inflammatory potential of NAR. TLR4 activation has been shown to impair cholesterol efflux in macrophages due to the inhibition of LXRs transcriptional activity (40). Also, the expression of *Abca1* has been proposed to play a critical role in the anti-inflammatory activity of LXRs (55). Consistent with these reports, we found that LPS-stimulated macrophages have reduced expression of *Abca1*, which was reversed by NAR treatment (Fig. 4B). Together, these data show that NAR is a potential LXRβ agonist with important anti-inflammatory properties.

Naringenin improves insulin sensitivity and adipose tissue inflammation in obese mice

We next evaluated the in vivo effects of LXR activation with NAR in obesity and the subsequent effect on AT inflammation and insulin resistance. LXR activation was shown to have beneficial effects in obese and diabetic models (8). However, the clinical usage of LXR synthetic agonists are still a challenge because of elevated lipid accumulation and triglycerides levels (62). We observed that obese and insulin resistant mice treated with NAR for 4 weeks did not affect body weight, food intake and circulating levels of triglycerides (Fig. 4C-D). This indicate that NAR does not possess the harmful effects of other LXRs agonists on increasing the levels of triglycerides. Also, NAR-treated obese mice displayed improved insulin sensitivity compared to obese vehicle-treated group (Fig. 4E). Next, we investigated if the increased insulin sensitivity observed in NAR-treated animals could be associated with reduced AT inflammation. Obese mice displayed increased percentage and number of Pg ATMs (Fig. 4F). Treatment with NAR did not affect the total number of Pg ATM (Fig. 4F), but reduced the number of $CD11c^+$ ATM and monocyte in Pg AT of HFD-fed mice and increased the number of $CD206^+$ ATM in PgAT of chow-fed mice (Fig. 4F and Fig. S4G). Also, obese mice treated with NAR displayed reduced numbers of $TNF\text{-}\alpha^+$ and $IL\text{-}1\beta^+$ ATMs in PgAT (Fig. 4F and Fig. S4H). Collectively, these data reinforce the therapeutic potential of NAR as an LXR agonist to decrease obesity-induced AT inflammation and ameliorate obesity-induced insulin resistance.

Naringenin modulates the metabolism and function of macrophages through a LXRβ-dependent mechanism

Because we found that naringenin possess both *in vitro* and *in vivo* anti-inflammatory effects, we decided to further investigate if the mechanism through which NAR affects macrophages phenotype. LPS and IFN-γ polarized macrophages displayed increased expression of pro-inflammatory markers, and increased expression of the glycolytic enzymes *Ldha* and *Pfkfb3*, which were all reduced upon NAR treatment (Fig. 4G). In addition, NAR treatment of non-polarized macrophages induced equivalent expression of *Nr1h3*, *Apoe* and *Abca1* to those found in IL-4-polarized macrophages (Fig. 4H). Moreover, NAR treatment also increased the expression of *Nr1h2* (LXRβ) in IL-4-polarized macrophages (Fig. 4H). NAR treatment also reduced the expression of *Pfkfb3, Ldha* and *Nos2* in LPS-activated macrophages in a LXRβ-dependent manner (Fig. 4I). Because NAR reduced the expression of glycolytic enzymes in both LPS and IFN-γ polarized- and LPS-activated macrophages (Fig. 4G-I), and that LPS activation induces the metabolic adaptation of macrophages marked by increased glycolysis and mitochondrial dysfunction (63-68), we hypothesized that the mechanism by which NAR modulates macrophage function may involve the metabolic adaptation of these cells. NAR treatment prior to LPS activation reduced LPS-induced glycolysis (Fig. 4J). Moreover, NAR treatment decreased the LPS-induced mitochondrial dysfunction in macrophages, indicating that NAR acts thorough LXRβ to modulate macrophage metabolism and inflammatory fitness (Fig. 4J). Collectively, these data indicate that NAR-induced LXRβ activation limits macrophage activation, reduces glycolytic metabolism, and restores mitochondrial function.

Discussion

Obesity has reached epidemic rates worldwide and is a serious public health problem. Easy access to hyper caloric diets combined with technologic advances has promoted changes that favor a sedentary lifestyle and overweight. In combination with overweight, cardiovascular disorders, dyslipidemia and insulin resistance are frequently observed in obese subjects (69).

Thus, the search for new therapeutic targets to treat obesity-associated disorders has become increasingly necessary.

Here, we describe a new role for LXR in the regulation of adipose tissue homeostasis. We show that LXR is a key factor for the maintenance of the immune balance in AT. Indeed, LXR effects has been extensively studied in the pathogenesis of atherosclerosis (70-72), and these studies have shed the light for LXR actions on macrophage metabolism and their influence in the whole body homeostasis. However, is poorly understood how LXR deficiency/activation may affect resident adipose tissue macrophages, specially during obesity. Moreover, few studies have focused in understand the roles of the distinct LXR isoforms (47). We decided to investigate how LXRα and LXRβ could modulate the whole body metabolism and macrophage response. We found that LXR isoforms display differential roles in vivo. Deletion of LXRβ and not of LXRα promotes glucose intolerance. These data are consistent with previous works showing that LXR coordinates both lipid and glucose homeostasis (1, 10, 73). LXR has been showed to promote the transcriptional induction of Glut4 (10), we extrapolate that LXRβ may exert an essential role in this process, however, further analysis must be performed in order to verify such function for this LXR isoform.

Together with the changes in adipocyte size and adipokine secretion, obesity triggers changes in the AT resident immune population (26, 32, 33, 36, 38), generating an inflammatory microenvironment marked by the presence of CD11c+ macrophages secreting pro-inflammatory cytokines and enhanced monocyte infiltration (35, 74, 75). Our data showed that the absence of LXR *per si* is sufficient to lead the adipose tissue for an obesity-like inflamed status, in which the imbalance between CD11c+ and CD206+ macrophages is observed. Moreover we found that LXRβ deletion aggravates HFD-induced AT inflammation and LXR deletion specifically in immune cells leads to AT inflammation, observed by increased pro-inflammatory ATM accumulation.

Pro-inflammatory cells presents a unique metabolic signature, which is caracterized by increased glycolytic pathway activity, the disruption of tricarboxylic acid (TCA) cycle and mitochondrial dysfunction (63, 76-78). We found that naringenin is an LXR agonist which modulates macrophage metabolism and function by reducing glycolysis, mitochondrial dysfunction and the subsequent pro-inflammatory phenotype.

Other groups has demonstrate that the expression of the LXR target gene *Abca1* is essential for macrophage reverse cholesterol transport, and its absence is causally linked to the pathogenesis of atherosclerosis (72). Our findings reveal that the pro-inflammatory stimulus impairs *Abca1* expression (Fig. 4B) and increase lipid droplet accumulation in macrophages (data not shown), driving the macrophages to a pro-inflammatory profile, and NAR induces *Abca1* in an LXR dependent manner.

A variety of studies aimed to understand how LXR modulates the immune system and how the anti-inflammatory effects promoted by the LXR activation could be used to treat immune-mediated diseases (42, 43, 55, 79-82). However, classical LXR agonists has been showed to induce the expression of genes related to fatty acid synthesis, and thus, promoting increased levels of triglycerides in the blood and liver (83, 84), specially by the activation of LXRα. Finally, we described that naringenin is a LXRβ agonist in macrophages, and naringenin-induced LXRβ activation improves obesity-induced insulin resistance and reduces AT inflammation, with no effects on triglycerides synthesis. However, we cannot exclude the fact that LXR acts in several other cell types, such as hepatocytes, adipocytes, neurons, beta cells, among others, to regulate whole body homeostasis, which could only be promptly evaluated in future works with access to LXR-floxed mice. Our work focuses on understanding how specific isoforms of liver X receptors from adipose tissue macrophages can modulate adipose tissue inflammation and insulin sensitivity. Collectively, our data reinforce that LXRα and LXRβ display distinct roles in the regulation of macrophage response and whole-body glucose homeostasis. This study contributes for a better understand on how nuclear receptors isoforms may display distinct functions and serves as the first step for the development of new therapies targeting LXRβ in the treatment of immune-mediated metabolic diseases.

Materials and Methods

A detailed methods employed in this paper is available in SI appendix, and include the following topics:

Animal studies and metabolic analysis

- Ethics and genetic background
- Diet-induced obesity
- In vivo naringenin treatment
- Glucose and Insulin Tolerance Test
- Triglycerides
- Evaluation of energy metabolism
- Evaluation of adipose tissue inflammation
- Bone marrow transplant

In vitro macrophage analysis

- Cell culture
- Cytokine secretion evaluation
- Lipid droplet staining
- RNA extraction and cDNA synthesis
- Gene expression analysis by RT-qPCR
- Macrophage metabolism assay
- Mitochondrial potential evaluation

Analysis from RNA sequencing data.
Docking
Statistical analysis

Acknowledgments
This work was supported by the São Paulo Research Foundation - FAPESP (grant numbers 2015/15626-8, 2017/00079-7, 19/25973-8, 19/19435-3 and 2019/04780-7), the Brazilian National Council for Scientific and Technological Development - CNPq (141553/2017-0), and Coordination of Superior Level Staff Improvement - CAPES for the funding and support.

References

1. B. A. Laffitte *et al.*, LXRs control lipid-inducible expression of the apolipoprotein E gene in macrophages and adipocytes. *Proc Natl Acad Sci U S A* **98**, 507-512 (2001).
2. S. M. Ulven, K. T. Dalen, J. A. Gustafsson, H. I. Nebb, Tissue-specific autoregulation of the LXRalpha gene facilitates induction of apoE in mouse adipose tissue. *J Lipid Res* **45**, 2052-2062 (2004).
3. A. C. Calkin, P. Tontonoz, Transcriptional integration of metabolism by the nuclear sterol-activated receptors LXR and FXR. *Nat Rev Mol Cell Biol* **13**, 213-224 (2012).
4. D. J. Peet, B. A. Janowski, D. J. Mangelsdorf, The LXRs: a new class of oxysterol receptors. *Curr Opin Genet Dev* **8**, 571-575 (1998).
5. N. Mitro *et al.*, The nuclear receptor LXR is a glucose sensor. *Nature* **445**, 219-223 (2007).
6. I. G. Schulman, Liver X receptors link lipid metabolism and inflammation. *FEBS Lett* **591**, 2978-2991 (2017).
7. C. K. Glass, S. Ogawa, Combinatorial roles of nuclear receptors in inflammation and immunity. *Nat Rev Immunol* **6**, 44-55 (2006).
8. M. Gao, D. Liu, The liver X receptor agonist T0901317 protects mice from high fat diet-induced obesity and insulin resistance. *AAPS J* **15**, 258-266 (2013).
9. K. T. Dalen, S. M. Ulven, K. Bamberg, J. A. Gustafsson, H. I. Nebb, Expression of the insulin-responsive glucose transporter GLUT4 in adipocytes is dependent on liver X receptor alpha. *J Biol Chem* **278**, 48283-48291 (2003).
10. B. A. Laffitte *et al.*, Activation of liver X receptor improves glucose tolerance through coordinate regulation of glucose metabolism in liver and adipose tissue. *Proc Natl Acad Sci U S A* **100**, 5419-5424 (2003).
11. G. Chen, G. Liang, J. Ou, J. L. Goldstein, M. S. Brown, Central role for liver X receptor in insulin-mediated activation of Srebp-1c transcription and stimulation of fatty acid synthesis in liver. *Proc Natl Acad Sci U S A* **101**, 11245-11250 (2004).

12. A. M. Efanov, S. Sewing, K. Bokvist, J. Gromada, Liver X Receptor Activation Stimulates Insulin Secretion via Modulation of Glucose and Lipid Metabolism in Pancreatic Beta-Cells. *Diabetes* **53**, S75-S78 (2004).
13. P. A. Edwards, M. A. Kennedy, P. A. Mak, LXRs; oxysterol-activated nuclear receptors that regulate genes controlling lipid homeostasis. *Vascul Pharmacol* **38**, 249-256 (2002).
14. D. J. Peet *et al.*, Cholesterol and bile acid metabolism are impaired in mice lacking the nuclear oxysterol receptor LXR alpha. *Cell* **93**, 693-704 (1998).
15. B. Wang, P. Tontonoz, Liver X receptors in lipid signalling and membrane homeostasis. *Nat Rev Endocrinol* **14**, 452-463 (2018).
16. K. D. Whitney *et al.*, Liver X receptor (LXR) regulation of the LXRalpha gene in human macrophages. *J Biol Chem* **276**, 43509-43515 (2001).
17. C. Y. Han *et al.*, Adipocyte-Derived Versican and Macrophage-Derived Biglycan Control Adipose Tissue Inflammation in Obesity. *Cell Rep* **31**, 107818 (2020).
18. P. Petrus *et al.*, Glutamine Links Obesity to Inflammation in Human White Adipose Tissue. *Cell Metab* **31**, 375-390 e311 (2020).
19. J. Laurencikiene, M. Ryden, Liver X receptors and fat cell metabolism. *Int J Obes (Lond)* **36**, 1494-1502 (2012).
20. P. M. Moraes-Vieira *et al.*, Antigen Presentation and T-Cell Activation Are Critical for RBP4-Induced Insulin Resistance. *Diabetes* **65**, 1317-1327 (2016).
21. J. M. Fernandez-Real, J. C. Pickup, Innate immunity, insulin resistance and type 2 diabetes. *Trends Endocrinol Metab* **19**, 10-16 (2008).
22. S. Daemen, J. D. Schilling, The Interplay Between Tissue Niche and Macrophage Cellular Metabolism in Obesity. *Front Immunol* **10**, 3133 (2019).
23. A. Takei *et al.*, Myeloid HMG-CoA Reductase Determines Adipose Tissue Inflammation, Insulin Resistance, and Hepatic Steatosis in Diet-Induced Obese Mice. *Diabetes* **69**, 158-164 (2020).
24. T. Suganami, Y. Ogawa, Adipose tissue macrophages: their role in adipose tissue remodeling. *J Leukoc Biol* **88**, 33-39 (2010).
25. C. N. Lumeng, J. L. Bodzin, A. R. Saltiel, Obesity induces a phenotypic switch in adipose tissue macrophage polarization. *J Clin Invest* **117**, 175-184 (2007).
26. P. M. Moraes-Vieira *et al.*, RBP4 activates antigen-presenting cells, leading to adipose tissue inflammation and systemic insulin resistance. *Cell Metab* **19**, 512-526 (2014).
27. A. Nawaz *et al.*, CD206(+) M2-like macrophages regulate systemic glucose metabolism by inhibiting proliferation of adipocyte progenitors. *Nat Commun* **8**, 286 (2017).
28. I. Syed *et al.*, Palmitic Acid Hydroxystearic Acids Activate GPR40, Which Is Involved in Their Beneficial Effects on Glucose Homeostasis. *Cell Metab* **27**, 419-427 e414 (2018).
29. G. Raes *et al.*, Arginase-1 and Ym1 are markers for murine, but not human, alternatively activated myeloid cells. *J Immunol* **174**, 6561; author reply 6561-6562 (2005).
30. V. Bourlier *et al.*, Remodeling phenotype of human subcutaneous adipose tissue macrophages. *Circulation* **117**, 806-815 (2008).
31. D. L. Morris, K. Singer, C. N. Lumeng, Adipose tissue macrophages: phenotypic plasticity and diversity in lean and obese states. *Curr Opin Clin Nutr Metab Care* **14**, 341-346 (2011).
32. A. Castrillo, P. Tontonoz, Nuclear receptors in macrophage biology: at the crossroads of lipid metabolism and inflammation. *Annu Rev Cell Dev Biol* **20**, 455-480 (2004).
33. P. M. Moraes-Vieira, E. J. Bassi, R. C. Araujo, N. O. Camara, Leptin as a link between the immune system and kidney-related diseases: leading actor or just a coadjuvant? *Obes Rev* **13**, 733-743 (2012).
34. F. O. Martinez, S. Gordon, The M1 and M2 paradigm of macrophage activation: time for reassessment. *F1000Prime Rep* **6**, 13 (2014).
35. J. C. McNelis, J. M. Olefsky, Macrophages, immunity, and metabolic disease. *Immunity* **41**, 36-48 (2014).
36. A. Castoldi, C. Naffah de Souza, N. O. Camara, P. M. Moraes-Vieira, The Macrophage Switch in Obesity Development. *Front Immunol* **6**, 637 (2015).

37. T. Kimura *et al.*, Polarization of M2 macrophages requires Lamtor1 that integrates cytokine and amino-acid signals. *Nat Commun* **7**, 13130 (2016).
38. J. Pereira, F. C. da Silva, P. M. M. de Moraes-Vieira, The Impact of Ghrelin in Metabolic Diseases: An Immune Perspective. *J Diabetes Res* **2017**, 4527980 (2017).
39. V. Serbulea *et al.*, Macrophage phenotype and bioenergetics are controlled by oxidized phospholipids identified in lean and obese adipose tissue. *Proc Natl Acad Sci U S A* **115**, E6254-E6263 (2018).
40. A. Castrillo *et al.*, Crosstalk between LXR and toll-like receptor signaling mediates bacterial and viral antagonism of cholesterol metabolism. *Mol Cell* **12**, 805-816 (2003).
41. S. B. Joseph, A. Castrillo, B. A. Laffitte, D. J. Mangelsdorf, P. Tontonoz, Reciprocal regulation of inflammation and lipid metabolism by liver X receptors. *Nat Med* **9**, 213-219 (2003).
42. S. B. Joseph *et al.*, LXR-dependent gene expression is important for macrophage survival and the innate immune response. *Cell* **119**, 299-309 (2004).
43. S. B. Joseph *et al.*, Synthetic LXR ligand inhibits the development of atherosclerosis in mice. *Proc Natl Acad Sci U S A* **99**, 7604-7609 (2002).
44. S. Ghisletti *et al.*, Cooperative NCoR/SMRT interactions establish a corepressor-based strategy for integration of inflammatory and anti-inflammatory signaling pathways. *Genes Dev* **23**, 681-693 (2009).
45. B. M. Spiegelman, J. S. Flier, Obesity and the regulation of energy balance. *Cell* **104**, 531-543 (2001).
46. S. A. Hutchinson *et al.*, Liver x receptor alpha drives chemoresistance in response to side-chain hydroxycholesterols in triple negative breast cancer. *Oncogene* **40**, 2872-2883 (2021).
47. A. Ramon-Vazquez *et al.*, Common and Differential Transcriptional Actions of Nuclear Receptors Liver X Receptors alpha and beta in Macrophages. *Mol Cell Biol* **39** (2019).
48. A. R. Tall, L. Yvan-Charvet, Cholesterol, inflammation and innate immunity. *Nat Rev Immunol* **15**, 104-116 (2015).
49. L. Russo, C. N. Lumeng, Properties and functions of adipose tissue macrophages in obesity. *Immunology* **155**, 407-417 (2018).
50. X. Xu *et al.*, Obesity activates a program of lysosomal-dependent lipid metabolism in adipose tissue macrophages independently of classic activation. *Cell Metab* **18**, 816-830 (2013).
51. P. T. Bozza, K. G. Magalhaes, P. F. Weller, Leukocyte lipid bodies - Biogenesis and functions in inflammation. *Biochim Biophys Acta* **1791**, 540-551 (2009).
52. H. Shi *et al.*, TLR4 links innate immunity and fatty acid-induced insulin resistance. *J Clin Invest* **116**, 3015-3025 (2006).
53. J. J. Repa *et al.*, Regulation of mouse sterol regulatory element-binding protein-1c gene (SREBP-1c) by oxysterol receptors, LXRalpha and LXRbeta. *Genes Dev* **14**, 2819-2830 (2000).
54. K. R. Steffensen, J. A. Gustafsson, Putative metabolic effects of the liver X receptor (LXR). *Diabetes* **53 Suppl 1**, S36-42 (2004).
55. A. Ito *et al.*, LXRs link metabolism to inflammation through Abca1-dependent regulation of membrane composition and TLR signaling. *Elife* **4**, e08009 (2015).
56. R. Komati *et al.*, Ligands of Therapeutic Utility for the Liver X Receptors. *Molecules* **22** (2017).
57. J. Goldwasser *et al.*, Transcriptional regulation of human and rat hepatic lipid metabolism by the grapefruit flavonoid naringenin: role of PPARalpha, PPARgamma and LXRalpha. *PLoS One* **5**, e12399 (2010).
58. J. Saenz *et al.*, Grapefruit Flavonoid Naringenin Regulates the Expression of LXRalpha in THP-1 Macrophages by Modulating AMP-Activated Protein Kinase. *Mol Pharm* **15**, 1735-1745 (2018).
59. J. M. Assini *et al.*, Naringenin prevents cholesterol-induced systemic inflammation, metabolic dysregulation, and atherosclerosis in Ldlr(-)/(-) mice. *J Lipid Res* **54**, 711-724 (2013).
60. X. Liu *et al.*, The citrus flavonoid naringenin confers protection in a murine endotoxaemia model through AMPK-ATF3-dependent negative regulation of the TLR4 signalling pathway. *Sci Rep* **6**, 39735 (2016).

61. F. A. Pinho-Ribeiro *et al.*, The citrus flavonone naringenin reduces lipopolysaccharide-induced inflammatory pain and leukocyte recruitment by inhibiting NF-kappaB activation. *J Nutr Biochem* **33**, 8-14 (2016).
62. B. L. Heckmann *et al.*, Liver X receptor alpha mediates hepatic triglyceride accumulation through upregulation of G0/G1 Switch Gene 2 expression. *JCI Insight* **2**, e88735 (2017).
63. A. K. Jha *et al.*, Network integration of parallel metabolic and transcriptional data reveals metabolic modules that regulate macrophage polarization. *Immunity* **42**, 419-430 (2015).
64. B. Kelly, L. A. O'Neill, Metabolic reprogramming in macrophages and dendritic cells in innate immunity. *Cell Res* **25**, 771-784 (2015).
65. L. A. O'Neill, A broken krebs cycle in macrophages. *Immunity* **42**, 393-394 (2015).
66. W. K. E. Ip, N. Hoshi, D. S. Shouval, S. Snapper, R. Medzhitov, Anti-inflammatory effect of IL-10 mediated by metabolic reprogramming of macrophages. *Science* **356**, 513-519 (2017).
67. F. Correa-da-Silva, J. A. S. Pereira, C. F. de Aguiar, P. M. M. de Moraes-Vieira, Mitoimmunity-when mitochondria dictates macrophage function. *Cell Biol Int* **42**, 651-655 (2018).
68. F. Correa da Silva *et al.*, Ghrelin effects on mitochondrial fitness modulates macrophage function. *Free Radic Biol Med* **145**, 61-66 (2019).
69. T. M. Powell-Wiley *et al.*, Obesity and Cardiovascular Disease: A Scientific Statement From the American Heart Association. *Circulation* 10.1161/CIR.0000000000000973, CIR0000000000000973 (2021).
70. N. Levin *et al.*, Macrophage liver X receptor is required for antiatherogenic activity of LXR agonists. *Arterioscler Thromb Vasc Biol* **25**, 135-142 (2005).
71. T. Sallam *et al.*, The macrophage LBP gene is an LXR target that promotes macrophage survival and atherosclerosis. *J Lipid Res* **55**, 1120-1130 (2014).
72. T. Sallam *et al.*, Transcriptional regulation of macrophage cholesterol efflux and atherogenesis by a long noncoding RNA. *Nat Med* **24**, 304-312 (2018).
73. A. M. Efanov, S. Sewing, K. Bokvist, J. Gromada, Liver X receptor activation stimulates insulin secretion via modulation of glucose and lipid metabolism in pancreatic beta-cells. *Diabetes* **53 Suppl 3**, S75-78 (2004).
74. G. S. Hotamisligil, N. S. Shargill, B. M. Spiegelman, Adipose expression of tumor necrosis factor-alpha: direct role in obesity-linked insulin resistance. *Science* **259**, 87-91 (1993).
75. H. Xu *et al.*, Chronic inflammation in fat plays a crucial role in the development of obesity-related insulin resistance. *J Clin Invest* **112**, 1821-1830 (2003).
76. G. M. Tannahill *et al.*, Succinate is an inflammatory signal that induces IL-1beta through HIF-1alpha. *Nature* **496**, 238-242 (2013).
77. E. L. Mills *et al.*, Succinate Dehydrogenase Supports Metabolic Repurposing of Mitochondria to Drive Inflammatory Macrophages. *Cell* **167**, 457-470 e413 (2016).
78. J. Van den Bossche *et al.*, Mitochondrial Dysfunction Prevents Repolarization of Inflammatory Macrophages. *Cell Rep* **17**, 684-696 (2016).
79. S. Ghisletti *et al.*, Parallel SUMOylation-dependent pathways mediate gene- and signal-specific transrepression by LXRs and PPARgamma. *Mol Cell* **25**, 57-70 (2007).
80. J. H. Lee *et al.*, Differential SUMOylation of LXRalpha and LXRbeta mediates transrepression of STAT1 inflammatory signaling in IFN-gamma-stimulated brain astrocytes. *Mol Cell* **35**, 806-817 (2009).
81. M. Pascual-Garcia *et al.*, Reciprocal negative cross-talk between liver X receptors (LXRs) and STAT1: effects on IFN-gamma-induced inflammatory responses and LXR-dependent gene expression. *J Immunol* **190**, 6520-6532 (2013).
82. J. Matalonga *et al.*, The Nuclear Receptor LXR Limits Bacterial Infection of Host Macrophages through a Mechanism that Impacts Cellular NAD Metabolism. *Cell Rep* **18**, 1241-1255 (2017).
83. J. R. Schultz *et al.*, Role of LXRs in control of lipogenesis. *Genes Dev* **14**, 2831-2838 (2000).
84. S. B. Joseph *et al.*, Direct and indirect mechanisms for regulation of fatty acid synthase gene expression by liver X receptors. *J Biol Chem* **277**, 11019-11025 (2002).

Figures and Tables

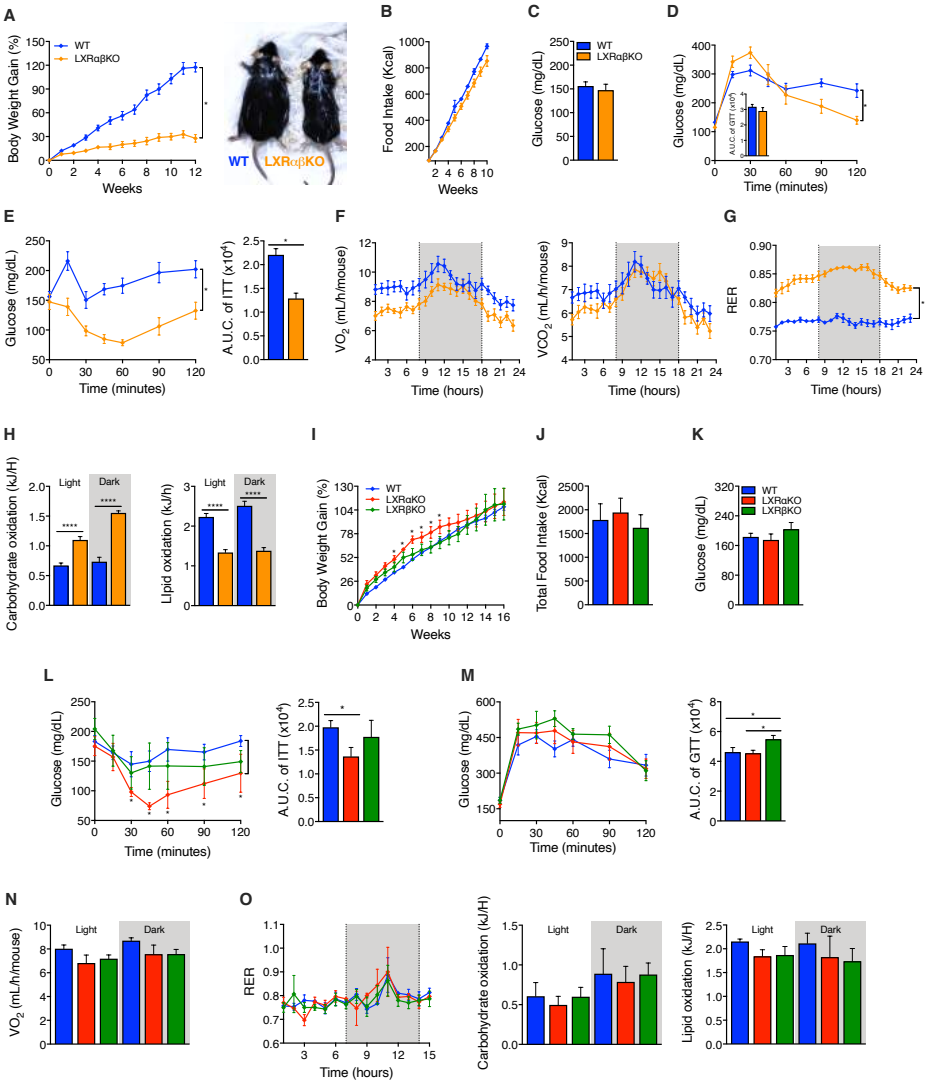

Fig. 1. LXRα and LXRβ display distinct role in the metabolic homeostasis. (A) Body weight gain and representative image of WT and LXRαβKO HFD-fed mice (n= 7 mice/group). **(B)** Food intake in HFD fed animals (n= 7 mice/group). **(C)** Blood glucose levels after 5 hours of fasting (n= 7 mice/group). **(D)** Glucose Tolerance Test (GTT) and area under curve (AUC) (n= 7 mice/group). **(E)** Insulin Tolerance Test (ITT) and area under curve (AUC) (n= 7 mice/group). **(F)** Wild type and LXRαβKO mice were housed under 12 h light-dark cycles, and metabolic cages were used to monitor oxygen consumption rate (VO2) and carbon dioxide consumption rate (VCO2) (n= 7 mice/group). **(G)** The respiratory exchange ratio (RER) was calculated by the ratio between VCO2 and VO2 (n= 7 mice/group). **(H)** Carbohydrate and fat oxidation in WT and LXRαβKO mice was calculated using VO2 and VCO2 values (n= 7 mice/group). **(I)** Body weight gain in WT, LXRαKO and LXRβKO mice HFD-fed mice (n = 6 mice/group). **(J)** Total food intake in WT, LXRαKO and LXRβKO mice HFD-fed mice (n = 6 mice/group). **(K)** Blood glucose levels in WT, LXRαKO and LXRβKO HFD-fed mice after 5 hours of fasting (n = 6 mice/group). **(L)** ITT and AUC of HFD WT, LXRαKO and LXRβKO mice (n = 6 mice/group). **(M)** Glucose Tolerance Test (GTT) in WT, LXRαKO and LXRβKO HFD-fed mice (n = 6 mice/group). **(N)** O_2 consumption (VO_2) in WT, LXRαKO and LXRβKO HFD-fed mice, evaluated in metabolic cage (n = 6 mice/group). **(O)** Evaluation of RER, carbohydrate oxidation and lipid oxidation in WT, LXRαKO and LXRβKO HFD-fed mice, evaluated in metabolic cage (n = 6 mice/group). Values in the graph represents mean ± SEM. (A-J) t test, *p<0.05, **p<0.01, and ***p<0.001. (K-O) One-way ANOVA, *post-hoc* Bonferroni test, *p<0.05.

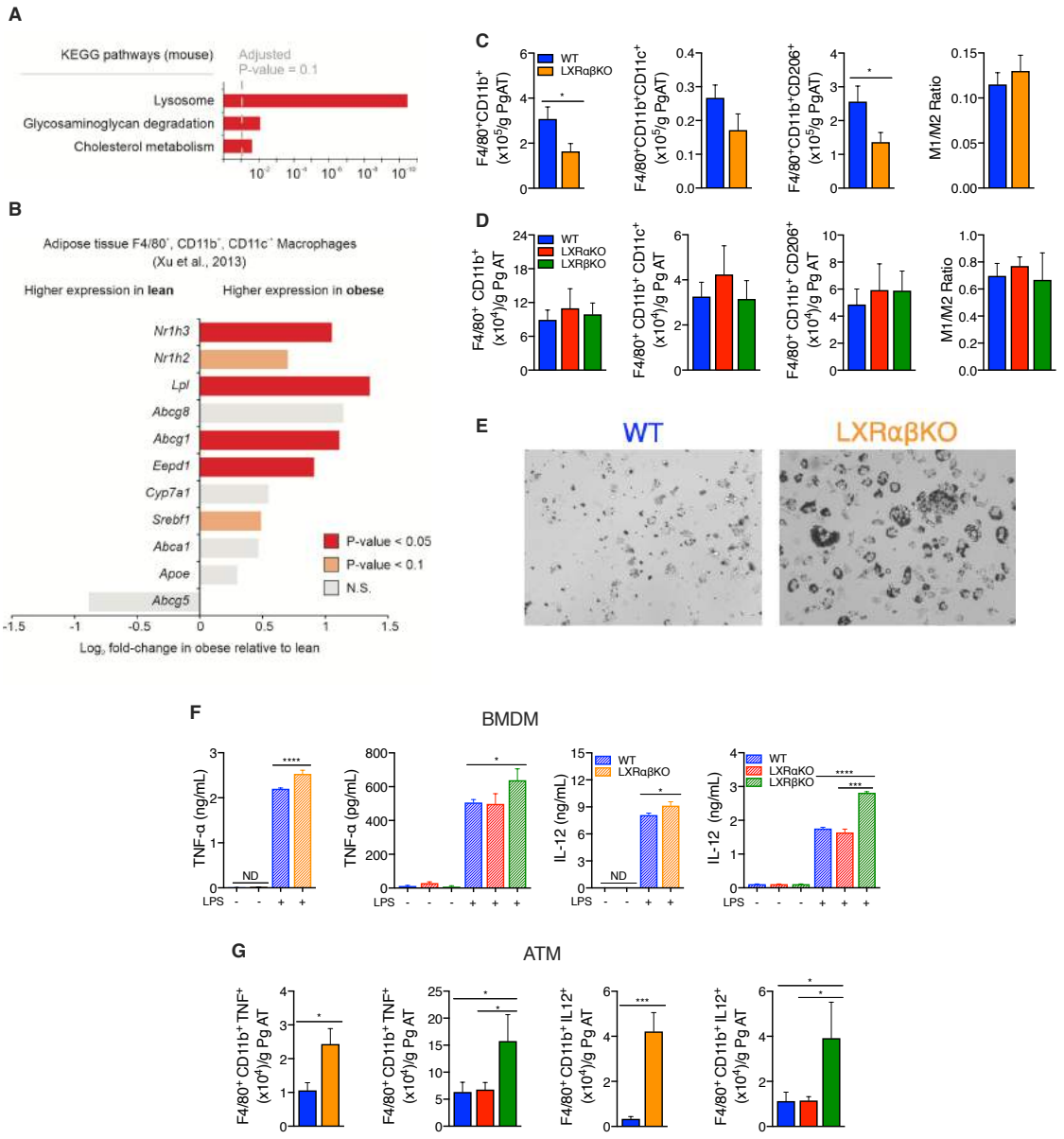

Fig. 2. The lack of LXR impairs the immune balance in PgAT. (A) KEGG pathway enrichment analysis in adipose tissue macrophages from lean and obese WT mice. **(B)** Transcriptomic profile of ATM ($F4/80^+CD11b^+CD11c^{-+}$) in lean and obese WT animals. Values in the graph are represented as the following: grey p> 0.1; orange p< 0.1 and red p< 0.05. **(C)** Adipose tissue macrophage population of WT and LXRαβKO in PgAT of HFD-fed animals (n=7 mice/group). **(D)** Macrophage population in PgAT of HFD WT, LXRαKO and LXRβKO animals (n=6 mice/group). **(E)** Lipid droplet evaluation in WT and LXRαβKO peritoneal macrophages stained with oil red O. **(F)** Evaluation of IL-12 and TNF-α secretion in WT and LXR deficient BMDMs after 24 hours of LPS stimuli. **(G)** IL-12 and TNF-α expression in ATM from WT, LXRαKO and LXRβKO HFD-fed mice (n=6 mice/group) and WT and LXRαβKO HFD-fed mice (n=7 mice/group). Values in the graph represents mean ± SEM. *p<0.05, **p<0.01, and ***p<0.001.

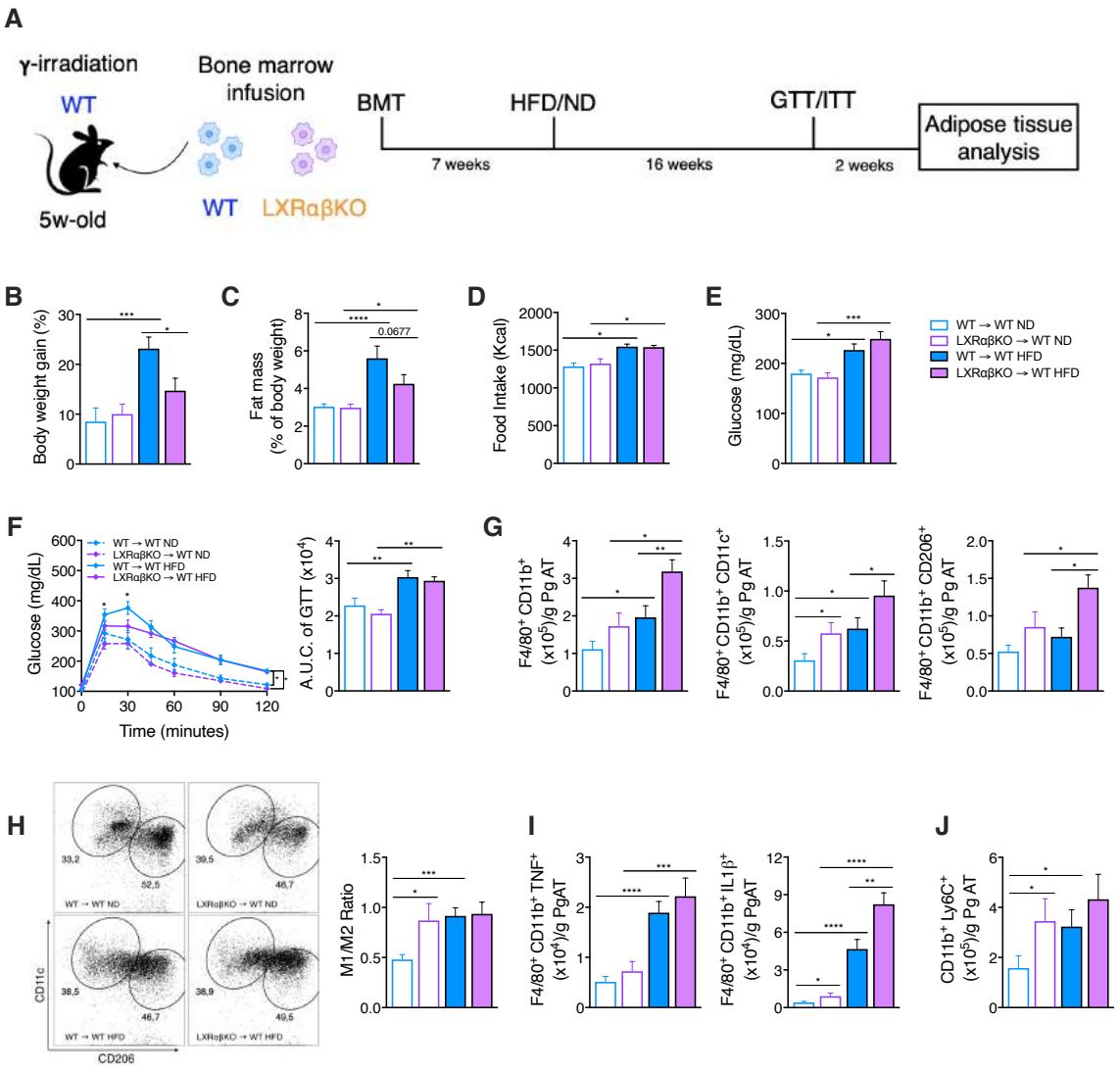

Fig. 3. LXR deletion in macrophages induces adipose tissue inflammation in lean animals. **(A)** Illustration showing the bone marrow transplantation (BMT) protocol in chow- and HFD-fed mice. **(B)** Body weight gain in response to BMT in WT→WT and LXRαβKO→WT chow- and HFD-fed mice (n=10 mice/group). **(C)** White adipose tissue mass in WT→WT and LXRαβKO→WT chow- and HFD-fed mice (n=10 mice/group). **(D)** Total food intake in BMT chow- and HFD-fed mice (n=10 mice/group). **(E)** Fasting blood glucose levels in WT→WT and LXRαβKO→WT chow- and HFD-fed mice (n=10 mice/group). **(F)** Glucose tolerance test (n=10 mice/group). **(G)** Adipose tissue macrophage populations in PgAT of BMT animals (n=10 mice/group). **(H)** Immune balance between M1 and M2 ATM (n=10 mice/group). **(I)** TNF-α and IL-1β expression in ATM from BMT mice (n=10 mice/group). **(J)** Monocyte infiltration in PgAT of WT→WT and LXRαβKO→WT chow- and HFD-fed mice (n=10 mice/group). Values in the graph represents mean ± SEM. p*≤0.05, p***≤0.005, p***≤0.0005, p****≤0.0001.

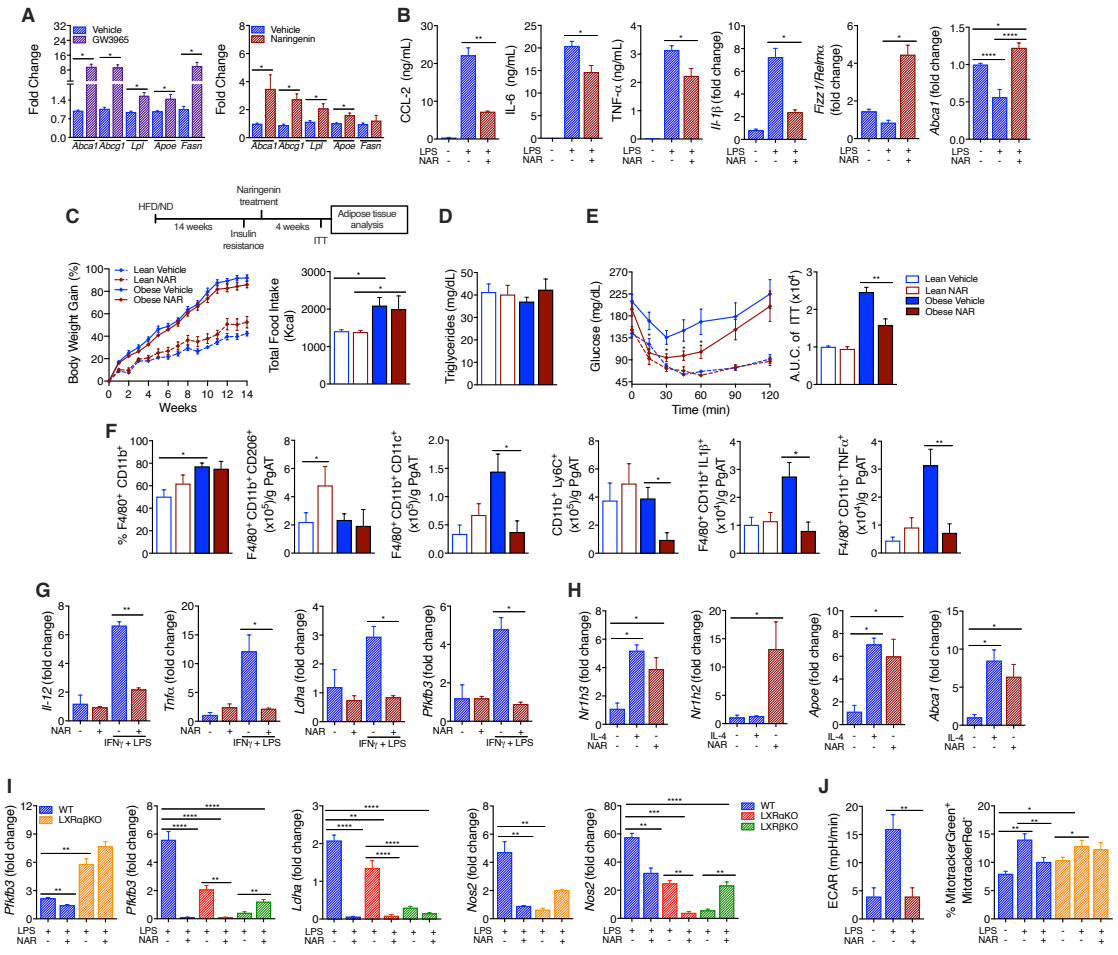

Fig. 4. LXRβ activation improves insulin sensitivity by reduce adipose tissue inflammation in obese animals. (A) LXR target genes expression in WT macrophages treated with GW3965 or Naringenin (NAR). **(B)** Evaluation of NAR treatment over the response of LPS-activated macrophages. **(C)** Illustration showing in vivo LXR activation protocol (upper), Body weight gain and food intake. **(D)** Blood triglycerides levels were determined by colorimetric assay after 5 hours of fasting. **(E)** Insulin tolerance test in control and NAR-treated animals. **(F)** Evaluation of PgAT inflammation in response to LXR activation. **(G)** Effects of LXR activation in macrophages polarized with LPS+IFNγ. **(H)** LXR and LXR target genes expression in IL-4-stimulated macrophages. **(I)** Pro-inflammatory markers expression in LPS-activated WT and LXR deficient macrophages. **(J)** Glycolytic metabolism measured by Seahorse and mitochondrial dysfunction evaluation by flow cytometry in WT and LXR deficient macrophages in response to NAR treatment. Values in the graph of in vivo experiments represents mean of 8 animals/group ± SEM. In vitro experiments graphs are the representative for three independent experiments. p*≤0.05, p***≤0.005, p***≤0.0005, p****≤0.0001.

APENDICE 5

ARTICLES
https://doi.org/10.1038/s41591-021-01390-x

nature medicine

Check for updates

Self-tunable engineered yeast probiotics for the treatment of inflammatory bowel disease

Benjamin M. Scott[1,2,3,9,11], Cristina Gutiérrez-Vázquez[4,11], Liliana M. Sanmarco[4], Jessica A. da Silva Pereira[4], Zhaorong Li[4], Agustín Plasencia[4], Patrick Hewson[4], Laura M. Cox[4], Madelynn O'Brien[4], Steven K. Chen[1], Pedro M. Moraes-Vieira[5], Belinda S. W. Chang[1,6,7], Sergio G. Peisajovich[1,7,10] and Francisco J. Quintana[4,8]✉

Inflammatory bowel disease (IBD) is a complex chronic inflammatory disorder of the gastrointestinal tract. Extracellular adenosine triphosphate (eATP) produced by the commensal microbiota and host cells activates purinergic signaling, promoting intestinal inflammation and pathology. Based on the role of eATP in intestinal inflammation, we developed yeast-based engineered probiotics that express a human P2Y2 purinergic receptor with up to a 1,000-fold increase in eATP sensitivity. We linked the activation of this engineered P2Y2 receptor to the secretion of the ATP-degrading enzyme apyrase, thus creating engineered yeast probiotics capable of sensing a pro-inflammatory molecule and generating a proportional self-regulated response aimed at its neutralization. These self-tunable yeast probiotics suppressed intestinal inflammation in mouse models of IBD, reducing intestinal fibrosis and dysbiosis with an efficacy similar to or higher than that of standard-of-care therapies usually associated with notable adverse events. By combining directed evolution and synthetic gene circuits, we developed a unique self-modulatory platform for the treatment of IBD and potentially other inflammation-driven pathologies.

IBD is a complex chronic inflammatory disorder of the gastrointestinal tract that includes Crohn's disease and ulcerative colitis[1]. Most available IBD therapies suppress the immune system systemically, increasing the risk of infections and some types of cancer while not benefiting all patients[2]. Hence, there is an unmet clinical need for localized and tunable IBD therapies.

The microbiome controls important immune functions in health and also in the context of multiple diseases including IBD[3–5]. The role of the microbiome in disease pathogenesis and anti-inflammatory effects of certain commensal microorganisms support the use of probiotic-based therapies for IBD[6]. Unmanipulated probiotics, however, use built-in anti-inflammatory mechanisms, which have been evolutionarily selected to optimize host–commensal interactions in the healthy gut but not in the context of pathologic inflammation[7].

Recent advances in synthetic biology enabled engineering of probiotics to deliver therapeutic proteins in response to disease-associated signals[8–10]. One such signal relevant to IBD is eATP, which is released by activated immune cells and commensal bacteria. eATP signals via purinergic receptors to boost pro-inflammatory cytokine production and effector T cell activation, suppress regulatory T cell (T_{reg}) responses and promote enteric neuron apoptosis, among other biological responses thought to contribute to IBD pathology[11–14]. eATP signaling is limited by the membrane-bound ectonucleoside triphosphate diphosphohydrolase 1 (ENTPD1 or CD39), which hydrolyzes eATP into AMP; CD73 then metabolizes AMP into immunosuppressive adenosine. CD39 limits eATP-driven pro-inflammatory responses, while it boosts differentiation, stability and function of T_{reg} cells[14–16]. Purinergic signaling is therefore a candidate therapeutic target for IBD, with the caveat that, although adenosine has acute anti-inflammatory effects, persistent activation of adenosine signaling can cause fibrosis, which is further exacerbated by cytokines[17,18]. Thus, therapeutic targeting of purinergic signaling requires a regulated approach to intervene when and where needed, responsive to pro-inflammatory concentrations of eATP but self-limited to minimize the side effects associated with persistent adenosine signaling.

Saccharomyces yeast species have long been known for their use in foods, and certain species are considered safe probiotics[19]. *Saccharomyces cerevisiae* has a well-defined signal transduction pathway, the mating pathway, that can be functionally linked to human G protein-coupled receptors (GPCRs), enabling controlled expression of proteins in response to stimuli relevant to human physiology[20,21]. We combined directed evolution and synthetic biology approaches to develop *S. cerevisiae* probiotics, which, in response to eATP detected via an engineered human P2Y2 GPCR, secrete the CD39-like eATP-degrading enzyme apyrase. These self-tunable engineered probiotic yeasts suppress experimental intestinal inflammation in mice and could provide a new therapeutic platform for IBD and other inflammatory disorders.

Results

Directed evolution of the human P2Y2 receptor. The P2Y2 receptor is a GPCR that senses eATP and also extracellular uridine triphosphate (eUTP)[17] and has previously been functionally expressed

[1]Department of Cell and Systems Biology, University of Toronto, Toronto, Ontario, Canada. [2]Biosystems and Biomaterials Division, National Institute of Standards and Technology, Gaithersburg, MD, USA. [3]Department of Chemistry and Biochemistry, University of Maryland, College Park, MD, USA. [4]Ann Romney Center for Neurologic Diseases, Brigham and Women's Hospital, Harvard Medical School, Boston, MA, USA. [5]Department of Genetics, Evolution, Microbiology and Immunology, Institute of Biology; Experimental Medicine Research Cluster (EMRC), and Obesity and Comorbidities Research Center (OCRC), University of Campinas, Campinas, Brazil. [6]Department of Ecology and Evolutionary Biology, University of Toronto, Toronto, Ontario, Canada. [7]Centre for the Analysis of Genome Evolution and Function, University of Toronto, Toronto, Ontario, Canada. [8]Broad Institute of MIT and Harvard, Cambridge, MA, USA. [9]Present address: Concordia University, Montreal, Quebec, Canada. [10]Present address: Illumina Inc., San Diego, CA, USA. [11]These authors contributed equally: Benjamin M. Scott, Cristina Gutiérrez-Vázquez. ✉e-mail: fquintana@rics.bwh.harvard.edu

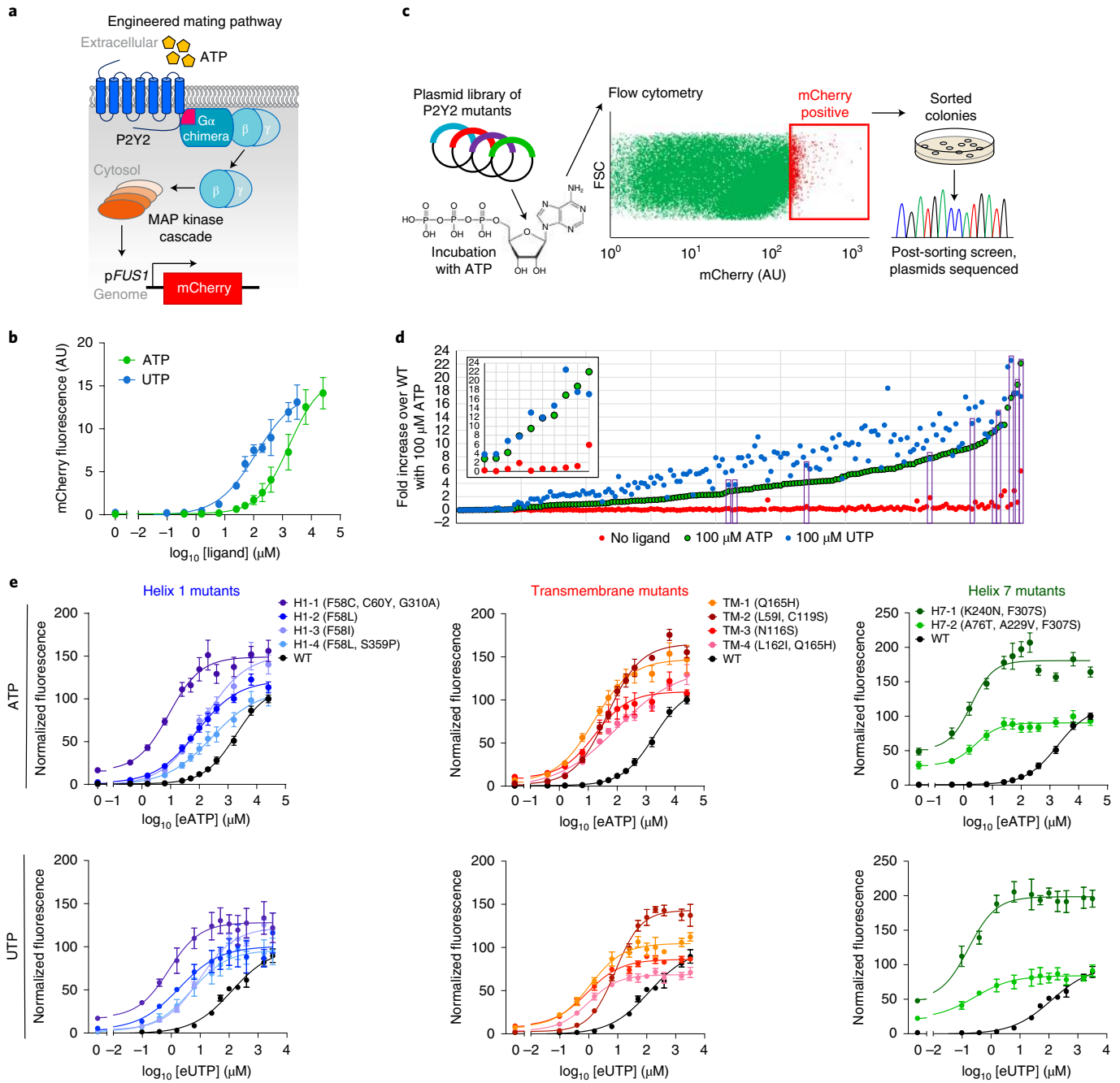

Fig. 1 | Directed evolution of the human P2Y2 receptor. a, Schematic of engineered human P2Y2 receptor activation functionally coupled to the expression of a fluorescent reporter protein, mCherry, using the mating-responsive promoter p*FUS1*. Modifications to the mating pathway included knockout of genes encoding the negative regulator Sst2 and Far1, which halts cell growth in the WT mating pathway. The chimeric Gα protein (Gpa1–$G\alpha_{i3}$) contains the five C-terminal amino acids of mammalian $G\alpha_{i3}$. MAP, mitogen-activated protein. **b**, Cells expressing the human WT P2Y2 receptor were treated with UTP or ATP, and mCherry fluorescence was quantified by flow cytometry. $n = 6$ colonies for ATP, $n = 3$ colonies for UTP. Data points represent the mean, and error bars represent s.e.m. AU, arbitrary units; [ligand], ligand concentration. **c**, A plasmid library of mutants for the human P2Y2 receptor generated by error-prone PCR was transformed into the Gpa1-$G\alpha_{i3}$ mCherry reporter strain. Cells were treated with 100 μM ATP, and flow cytometry was used to select for highly activating mutants (top 1% of mCherry fluorescence). Individual yeast colonies were then screened to confirm the desired phenotype and sequenced. FSC, forward scatter. **d**, Randomly selected yeast colonies were incubated with the indicated ligand for 6 h, and mCherry fluorescence was quantified. Data represent fold increase over the response from WT human P2Y2 receptor activated with 100 μM ATP. Ten yeast colonies were selected for detailed characterization (purple boxes); their responses to 100 μM ATP and 100 μM UTP are shown in the inset. **e**, Many mutations in the human P2Y2 receptor increased the sensitivity and maximum response to eATP and eUTP. mCherry fluorescence is represented as a percentage of the maximum WT response to eATP. Mutants are grouped based on the location of mutant residues. $n = 6$ colonies for the response to eATP and $n = 3$ colonies for the response to eUTP. Data points represent the mean, and error bars represent s.e.m.

in yeast[20]. Both eUTP and eATP are released from mammalian cells, but, due to lower intracellular concentrations of UTP, released eUTP concentrations are only 10–30% those of eATP[22]. Importantly, eATP, but not eUTP, activates P2X7 receptor signaling[17], which is associated with intestinal pathology[13,23]. We first engineered the human P2Y2 receptor to increase its sensitivity to eATP when

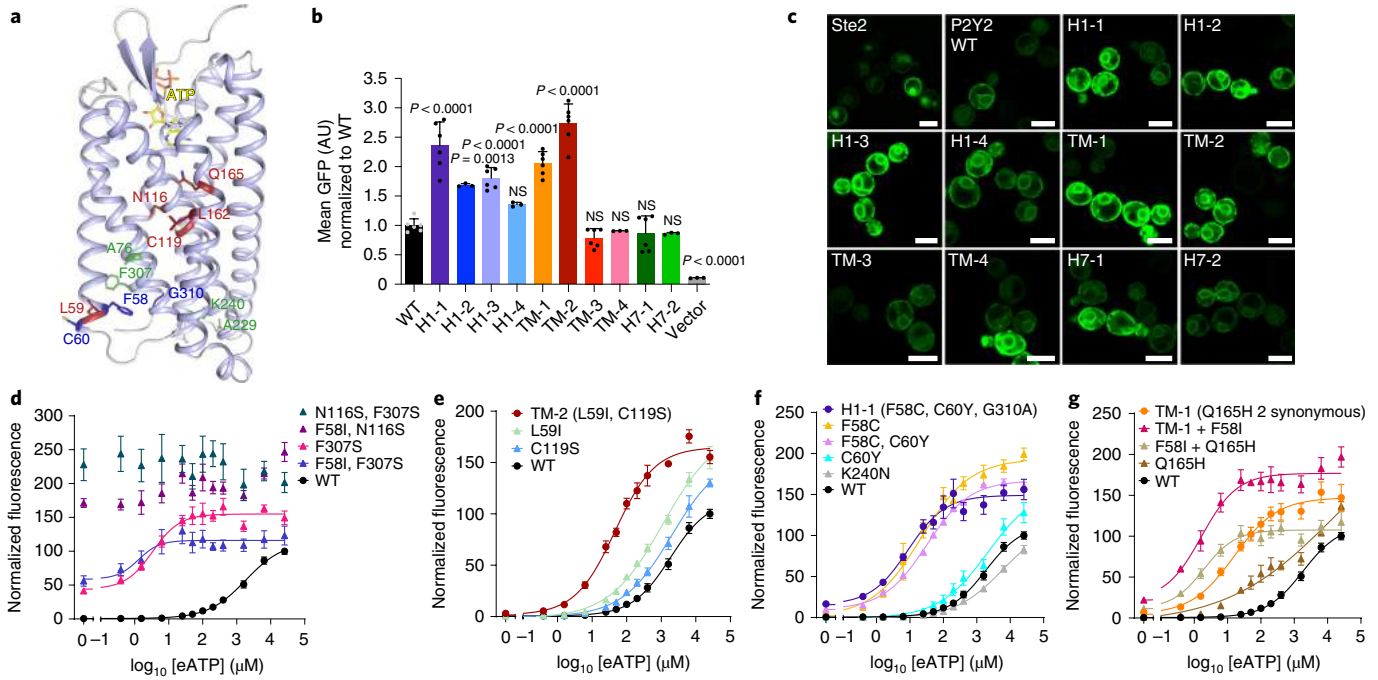

Fig. 2 | Characterization of human P2Y2 receptor mutants. a, Human P2Y2 receptor structure with residues mutated following directed evolution highlighted. The top ten mutant P2Y2 receptors with enhanced ATP sensitivity were grouped based on the location of key mutant residues: helix 1 (blue), helix 7 (green) and the transmembrane region (red). **b**, Expression of C-terminal GFP-tagged human P2Y2 receptor mutants in yeast was quantified by flow cytometry. Mean GFP values were normalized to that of WT P2Y2-GFP. $n = 3$ colonies for H1-2, H1-4, TM-4, H7-2 and vector and $n = 6$ for the rest; error bars represent s.d. One-way ANOVA, Dunnett's post hoc test; NS, not significant; *P* values are indicated versus WT P2Y2-GFP. **c**, GFP-tagged endogenous yeast Ste2 GPCR and human P2Y2 receptor mutants were examined by confocal microscopy. Scale bars, 5 μm; images are representative of two independent experiments. **d**–**g**, eATP sensitivity of mutant mCherry fluorescence is represented as a percentage of the maximum WT response to eATP. Data points represent the mean. **d**, The combination of the N116S substitution with either F58I or F307S resulted in fully constitutively active human P2Y2 receptor. The F307S substitution alone conferred constitutive activity, improved sensitivity and improved maximum response to eATP. $n = 6$ colonies per group. **e**, Non-additive effects contributed to increased activity of the human P2Y2 receptor TM-2 mutants. The L59I and C119S substitutions alone conferred a moderate increase in sensitivity to eATP. The combined effect was less than the one detected in the TM-2 mutant, indicating a non-additive change. $n = 6$ colonies per group. **f**, By analyzing each mutation in the H1-1 mutant separately, F58C was identified as the primary substitution influencing activity. The K240N substitution from the H7-1 mutant did not increase eATP sensitivity. $n = 6$ colonies for H1-1 and WT, $n = 3$ otherwise. **g**, The TM-1 mutant harbored synonymous mutations, in addition to the Q165H substitution. The synonymous mutations contributed to increased eATP sensitivity, including when they were combined with the F58I substitution. $n = 6$ colonies for H1-1 and WT, $n = 3$ otherwise. Error bars represent s.e.m.

expressed in yeast. To establish a platform amenable to directed evolution, we coupled the human P2Y2 receptor to the yeast mating pathway via a chimeric yeast Gpa1–human $G\alpha_{i3}$ protein and monitored pathway activation using a fluorescent mCherry reporter controlled by the mating-responsive *FUS1* promoter (p*FUS1*) (Fig. 1a, Supplementary Table 1 and Extended Data Fig. 1a–c) (Reporter yeast strains in the Methods). The Gpa1–$G\alpha_{i3}$ p*FUS1*-mCherry strain transformed with a plasmid constitutively expressing human P2Y2 showed a dose-dependent response to its agonists eATP and eUTP, with log half-maximum effective concentrations ($logEC_{50}$) of 3.27 and 2.09 μM, respectively (Fig. 1b) (Flow cytometry evaluation of response to ATP and UTP in the Methods).

Physiological eATP levels associated with inflammation have been detected in the 100 μM to high mM range[24]. However, yeast expressing wild-type (WT) P2Y2 showed a weak response to 100 μM eATP, as determined by flow cytometry analysis of mCherry expression (Fig. 1b). Thus, we applied directed evolution to generate yeast-expressed human P2Y2 receptor mutant proteins that show increased sensitivity to eATP. To achieve this goal, we generated a plasmid library of human P2Y2 receptor mutants using error-prone PCR (Supplementary Table 2) and then isolated yeast by flow cytometry expressing the highest (top 1%) levels of p*FUS1*-driven mCherry fluorescence after treatment with 100 μM eATP (Fig. 1c) (Directed evolution of human P2Y2 receptor in the Methods).

We performed multiple iterative rounds of flow cytometry-based selection to isolate mutants displaying the desired increase in eATP sensitivity (Extended Data Fig. 2). Finally, in a post-sorting screening step, we further assessed the function of the engineered human P2Y2 receptor mutants (Fig. 1d). For most of the analyzed colonies, an increased response to eATP was concomitant with an increased response to eUTP.

We focused on human P2Y2 receptor mutants that showed an enhanced response to eATP and a high eATP/eUTP response ratio concomitant with no constitutive expression of mCherry. Plasmid sequencing revealed a diverse range of P2Y2 genotypes (gene symbol *P2RY2*), with up to three nonsynonymous mutations in the gene encoding the receptor (Supplementary Table 3). Eight of the 19 human P2Y2 mutants harbored a mutation at site F58[1.57], and we also observed mutations at nearby residues L59[1.58] and C60[1.59] and at Q165[4.57] and F307[7.54].

We selected ten P2Y2 mutants for detailed characterization; each mutant was named using a unique identifier based on the location of the mutated residue(s) (Supplementary Table 4). In dose–response studies, the engineered P2Y2 receptors were more sensitive to both eATP and eUTP (Fig. 1e). When compared to the WT human P2Y2 receptor, the selected mutants showed a 10–1,000-fold decrease in the EC_{50} for eATP and up to a 1.8-fold increase in the maximum mating pathway response. This increased sensitivity was also observed

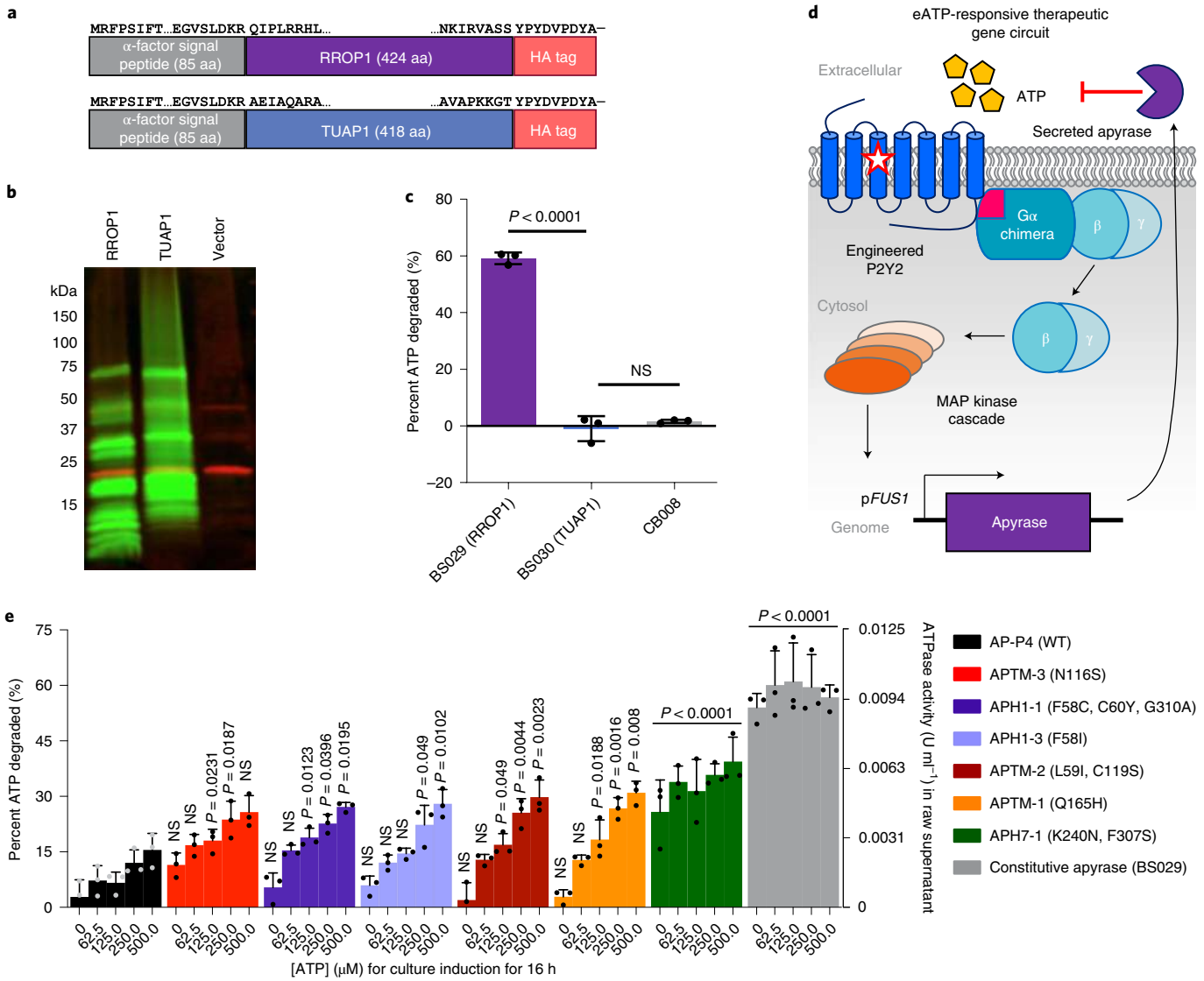

Fig. 3 | eATP-responsive secretion of ATPase by engineered yeast. a, Modified apyrase peptide sequences used as therapeutic response elements. Natural signal peptides were replaced with the yeast α-factor signal peptide to facilitate secretion, and an HA tag was added to the C terminus. aa, amino acids. **b**, Cell lysates from yeast strains constitutively expressing potato apyrase (RROP1) or wheat apyrase (TUAP1) or not expressing any apyrase (vector). Green bands correspond to the HA tag on apyrase; red bands indicate the cytoplasmic protein Pgk1 loading control. Image is representative of two independent experiments. **c**, Culture supernatant from strains constitutively secreting potato apyrase (RROP1) or wheat apyrase (TUAP1) were incubated for 30 min with ATP at 50 μM, and residual ATP levels were quantified; the yeast parent strain that does not express apyrase was used as a negative control (CB008). $n = 3$ samples per group. One-way ANOVA, Tukey's post hoc test. **d**, Schematic of engineered human P2Y2 receptor activation functionally coupled to the expression of RROP1 apyrase using the mating-responsive promoter p*FUS1*. Upon activation of the receptor by eATP, apyrase is expressed and secreted by the yeast. Secreted apyrase dephosphorylates eATP, in turn shutting off the gene circuit. **e**, Engineered yeast strains harboring a P2Y2–RROP1 gene circuit were incubated for 16 h with the indicated concentration of ATP. ATPase activity was quantified by incubating culture supernatant with 50 μM ATP for 30 min and then measuring residual ATP levels. ATPase unit = 1 μmol ATP to ADP per min. $n = 3$ samples per group. Two-way ANOVA, Dunnett's post hoc test, versus the WT response at the same ATP concentration. *P* values are indicated. Error bars represent s.d.

in response to eUTP stimulation, except for strains harboring the Q165H[4.57] substitution (TM-1, TM-4), in which the maximum mating pathway response was 1.4-fold to twofold higher for eATP than that for eUTP. Thus, the application of directed evolution resulted in the generation of human P2Y2 receptor mutants with increased responsiveness to eATP.

P2Y2 receptor mutants with increased sensitivity to eATP. Key residues that participate in the binding of nucleotides and the activation of human P2Y2 receptor have been identified[25], but mutations detected in the selected P2Y2 receptor mutants did not involve these residues. Instead, the mutations that we identified involved residues peripheral to the ligand-binding pocket or residues located on the intracellular-facing side of the receptor (Fig. 2a).

To determine the molecular mechanisms responsible for the increased sensitivity of the selected P2Y2 receptor mutants, we analyzed their expression levels using receptor mutants tagged with C-terminal GFP. Expression in yeast was increased when F58[1.57] was mutated to a smaller hydrophobic residue ('H1' mutants) and also in transmembrane (TM)-1 and TM-2 mutants (Fig. 2b,c and Supplementary Table 3). However, these mutations did not involve residues homologous to previously described mutations that

improve human GPCR expression in yeast[26]. Thus, our findings identify unique residues that influence human P2Y2 expression.

We detected increased responsiveness and signaling in the absence of agonist (constitutive activity) in P2Y2 mutants harboring the N116S$^{3.35}$ and F307S$^{7.54}$ substitutions (TM-3, H7-1 and H7-2 mutants) (Fig. 1e). Interestingly, these mutants showed expression levels similar to those of the WT P2Y2 receptor. The N116S$^{3.35}$ substitution likely disrupts a conserved hydrogen-bonding network with D79$^{2.50}$ and N298$^{7.45}$, and the lack of these stabilizing interhelical interactions leads to increased signaling in the absence of agonist[27]. Based on known interactions of similar residues in other GPCRs, we predict that the F307S$^{7.54}$ substitution facilitates rotation of Y$^{7.53}$ into the active conformation, resulting in constitutive activity and increased eATP sensitivity[28].

To further investigate mechanisms responsible for the differential activity of P2Y2 receptor mutants, we evaluated the effects of mutations alone or in combination. Certain substitutions (C60Y, K240N, G310A) did not cooperate to further increase P2Y2 receptor responsiveness to eATP, while others had deleterious effects (A76T and A229V, L162I, S359P) or exhibited positive epistasis when combined (N116S with F58I or F307S, L59I and C119S) (Fig. 2d–f). Synonymous mutations in the TM-1 mutant sequence increased P2Y2 receptor sensitivity toward eATP, which could be further increased by incorporating the F58I substitution (Fig. 2g). In the human P2Y2 receptor homology model docked with ATP, Q165$^{4.57}$ is oriented toward the adenine ring of ATP. These findings suggest that the Q165H substitution favors receptor interactions with ATP that result in increased downstream signaling. These effects of the Q165H substitution are further amplified by increased expression of the human P2Y2 receptor driven by F58I or synonymous substitutions. In summary, none of the tested combinations of mutations were superior to the original set of ten selected human P2Y2 receptor mutants, which provided a range of improved sensitivity to physiological concentrations of eATP associated with inflammation.

eATP-driven ATPase activity in engineered yeasts. We next incorporated a therapeutic response element in the yeast synthetic gene circuit responsive to eATP. We focused on apyrases, which hydrolyze pro-inflammatory eATP and participate in its conversion into immunosuppressive adenosine[14]. We selected the apyrase encoded by *RROP1* in potato (*Solanum tuberosum*), which has potent ATPase activity and reduces inflammation in a mouse model of IBD when delivered intraperitoneally[23], and apyrase from wheat *Triticum urartu* (referred to as TUAP1 here), based on its sequence homology to RROP1 in apyrase regions and reported high levels of activity[29] (Extended Data Fig. 3a). To enable secretion by yeast, we replaced the endogenous apyrase N-terminal signal peptide with the MFα1 signal peptide and added a C-terminal hemagglutinin (HA) tag to monitor expression (Fig. 3a).

We detected multiple protein bands when apyrase was expressed by yeast, suggesting that it may be partially degraded (Fig. 3b). However, commercially available potato apyrase has bands at 15 and 25 kDa, and apyrases expressed in yeast are glycosylated, resulting in multiple protein bands[30]. Culture supernatants from yeasts expressing RROP1 (BS029) or TUAP1 (BS030) showed ATPase activity equivalent to ~280 pM or <62.5 pM, respectively, of commercial apyrase per µl raw supernatant (Fig. 3c and Extended Data Fig. 3b,c) (Quantification of secreted ATPase activity in the Methods). Thus, we chose RROP1 as a therapeutic response element for subsequent studies.

We then co-introduced sensing (P2Y2) and responding (RROP1) elements into the genome of the same yeast strains using a CRISPR–Cas9-based approach. We selected six human P2Y2 receptor mutants for integration into the yeast genome based on their low EC_{50}, high dynamic range and high maximum activation. We also removed the hygromycin (Hyg)B selection marker from the yeast genome to ensure that the final strain would not contain an antibiotic resistance gene while retaining uracil auxotrophy, an important consideration for biocontainment and safety of an engineered microbe.

eATP induced ATPase enzymatic activity in a dose-dependent manner in culture supernatants from yeast strains containing the P2Y2–RROP1 gene circuit (Fig. 3d,e) (Induction of apyrase secretion with ATP in the Methods). Moreover, ATPase activity was higher in yeast strains expressing engineered P2Y2 receptors than that in the one expressing the WT receptor. For example, at 125 µM ATP, we detected a 2.2- to 4.7-fold increase in ATPase activity in yeast strains harboring engineered P2Y2 receptors, while a 1.7- to 2.5-fold increase was detected at the maximum eATP concentration (Supplementary Table 5).

We estimated the theoretical maximum activity of secreted ATPase with a yeast strain constitutively overexpressing RROP1 (strain BS029, 'constitutive apyrase' or conAP). After culturing yeast with 500 µM ATP, strains harboring engineered P2Y2 receptor mutant proteins showed 45–69% of the ATPase activity of conAP, while WT P2Y2 showed only 27%. Collectively, these findings show that, through the combination of directed evolution and gene-circuit engineering, we generated yeast strains that secrete functional ATPase in response to physiological levels of eATP.

eATP-responsive yeast ameliorate intestinal inflammation. We then evaluated the anti-inflammatory activity of the APTM-3 engineered yeast strain that expresses apyrase in an eATP-dependent manner

Fig. 4 | eATP-responsive engineered yeasts ameliorate chemically induced colitis. a, ATP levels and mCherry$^+$ yeasts in the fecal content of each portion of the gut from TNBS-treated mice 2 h after administration of eATP-inducible indCherry KG (left) or conCherry KG (constitutive mCherry) (right). $n=5$ mice for conCherry KG and $n=4$ mice for indCherry KG. **b**, Changes in body weight following TNBS rectal administration. $n=10$ mice for ethanol, $n=8$ mice for conAP and $n=9$ otherwise. **c**, Colon length of mice from experimental groups in **b**. $n=3$ mice for ethanol and Ctrl and $n=4$ mice for conAP and indAP. **d**, H&E staining at 200× (top) and 400× (bottom) magnifications. One representative colon section per group is shown. Open arrowheads, immune cell infiltrates in the mucosa with structure disruption. Black arrows, immune cells infiltration at the submucosa. Black brackets, edematous submucosa. Scale bars, 100 µm. Data are representative of three independent experiments. **e**, Histomorphology disease scores of mice from groups as in **b** (Histological evaluation in the Methods). $n=3$ mice for Ctrl, $n=4$ mice for conAP and $n=5$ otherwise. **f**, Changes in body weight following TNBS rectal administration. $n=4$ mice for ethanol, $n=5$ otherwise. **g**, Colon length in mice shown in **f**. $n=4$ mice for ethanol and indAP yeasts, $n=7$ for isotype control antibody and anti-α4β7 antibody and $n=6$ for anti-TNF antibody. **h**, RNA-seq analysis of colon samples from mice of groups in **b**. Heatmap of differentially expressed genes. **i**, FOXP3$^+$ T_{reg} cells in mesenteric lymph nodes of groups in **b**. $n=3$ samples. **j**, Quantitative (q)PCR for *Foxp3*, *Ifng* and *Il17* mRNA expression in the colon of groups in **b**. $n=9$–17 samples (Source data). **k**, Changes in body weight during DSS-induced colitis in mice treated as in **b**. $n=5$ mice for ethanol, $n=10$ mice for conAP and $n=13$ otherwise. **l**, NanoString gene-expression analysis in the colon from the groups in **k**. Heatmap of differentially expressed genes. Data are representative of two independent experiments with three pooled mice per group. **m**, qPCR for *Nos2*, *Ccl2* and *Il1b* expression in the colon from the groups in **k**. $n=5$–9 samples (Source data). Data are representative of three independent experiments. *P* values are indicated. Two-way ANOVA, Tukey's post hoc test for **b**,**f**,**k**. One-way ANOVA, Tukey's or Sidak's post hoc tests for selected multiple comparisons for **c**,**e**,**g**,**i**,**j**. Bars represent the mean, and error bars represent s.e.m.

('inducible apyrase' strain or indAP). We selected this yeast strain because it secretes low levels of apyrase when unstimulated, yet its ATPase activity was greater than or similar to ATPase activity detected in other engineered P2Y2–RROP1 strains (Fig. 3e). In addition, its increased sensitivity to eATP can be directly connected to a single substitution in P2Y2 with a known mechanism of action (N116S[3.35]).

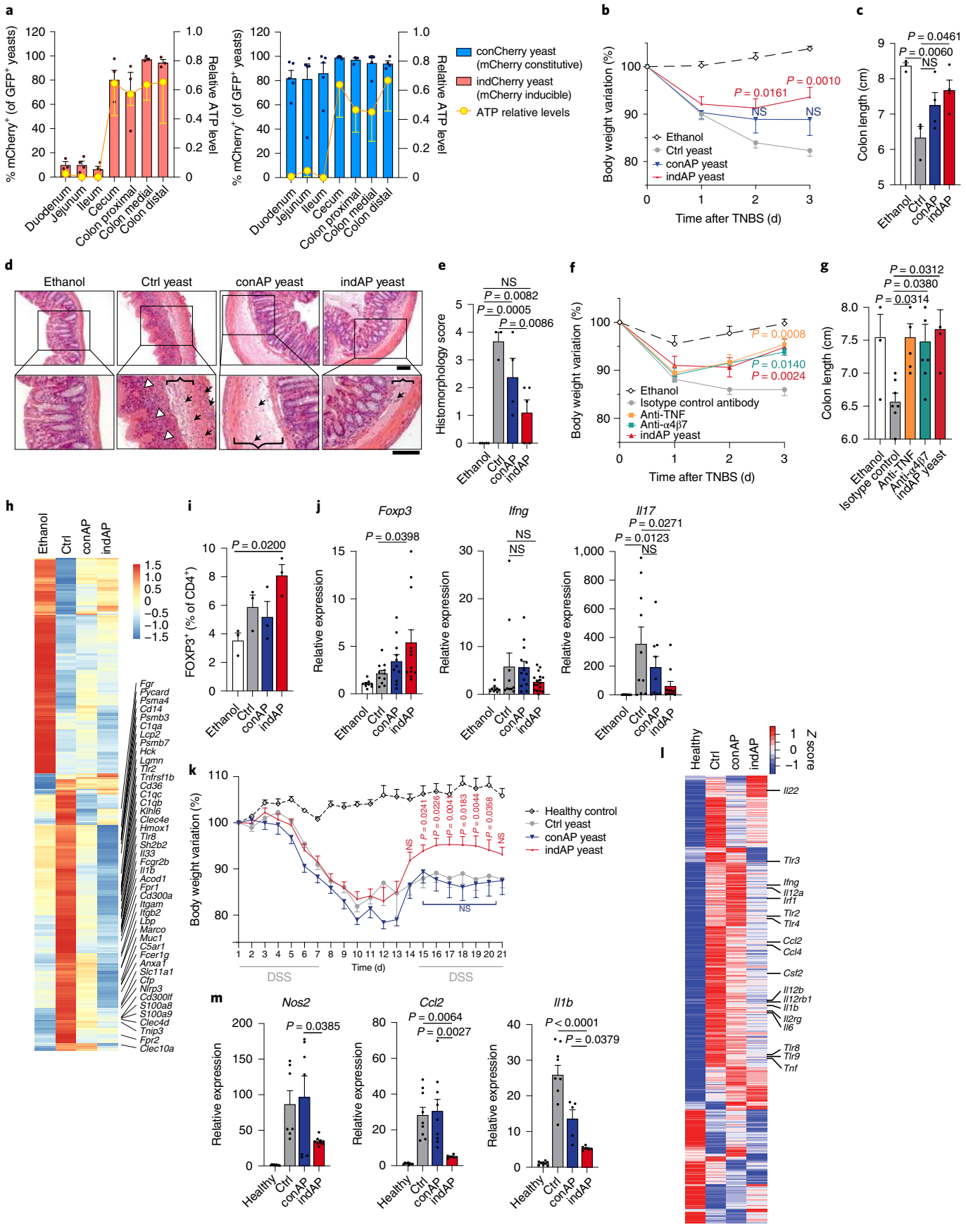

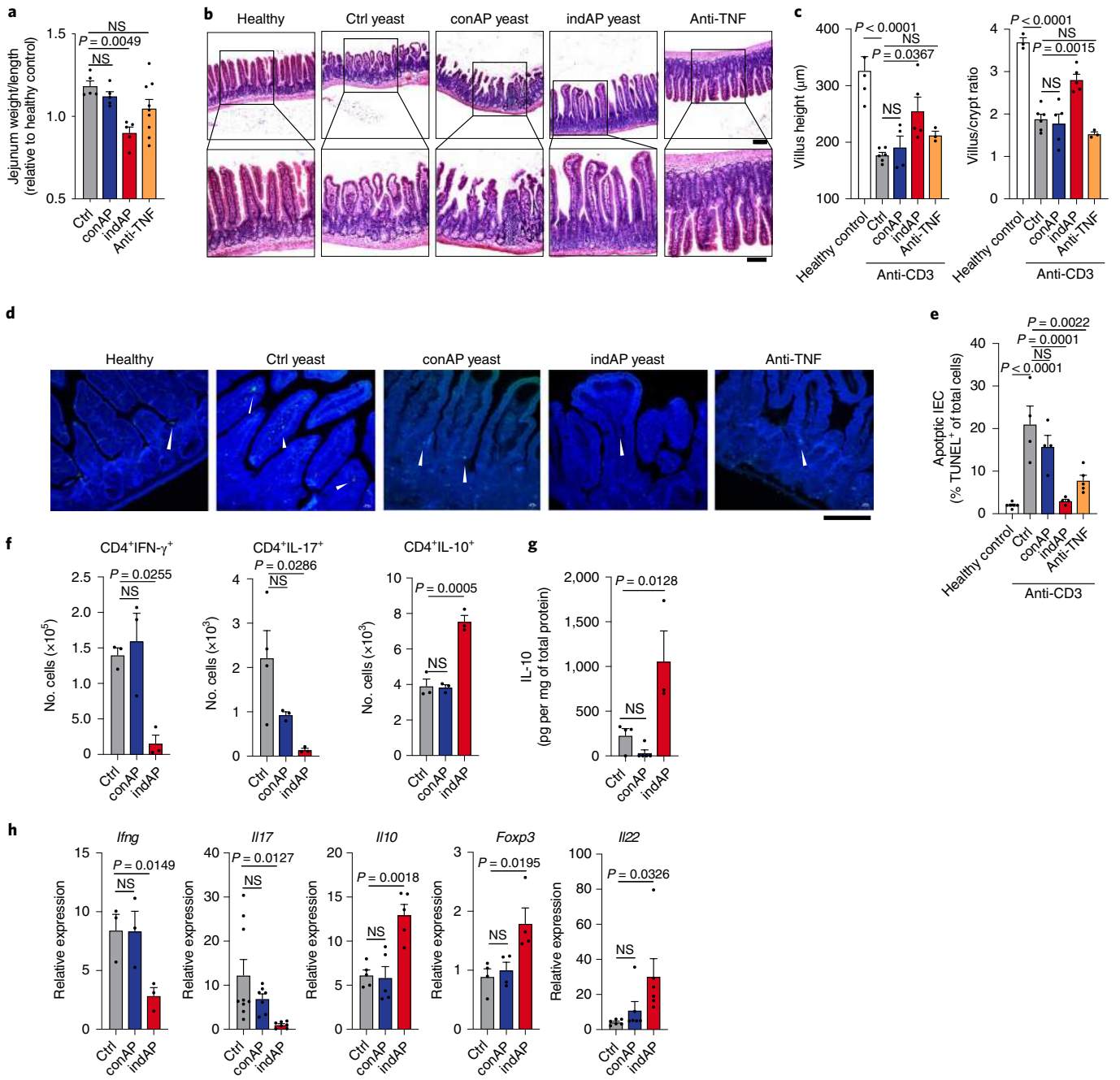

Fig. 5 | eATP-responsive engineered yeasts ameliorate anti-CD3 antibody-induced enteritis. a, Jejunal weight/length ratio measured 3 h after anti-CD3 monoclonal antibody administration. $n = 9$ mice for the anti-TNF antibody and $n = 5$ otherwise. **b**, H&E staining at 100× (top) and 200× (bottom) total magnifications. A representative jejunum section of each group 24 h after injection with the anti-CD3 antibody is shown. Scale bars, 100 μm. **c**, Villus height and ratio of villus height/crypt depth were measured from H&E staining images. $n = 6$ mice for Ctrl, $n = 3$ mice for anti-TNF antibody and $n = 4$ otherwise. **d**, Terminal uridine nick-end labeling (TUNEL) analysis of jejunal tissue 24 h after injection. Scale bar, 100 μm; 400× total magnification. **e**, Average number of TUNEL$^+$ cells per field. Ten fields per mouse were quantified. One-way ANOVA followed by Tukey's post hoc test. $n = 6$ mice for healthy control, $n = 5$ mice for anti-TNF antibody and $n = 4$ otherwise. IEC, intestinal epithelial cells. **f**–**h**, Intestinal T cells in the jejunum analyzed 24 h after injection with the anti-CD3 antibody. **f**, Jejunal infiltrating IFN-γ$^+$, IL-17$^+$ and IL-10$^+$ CD4$^+$ T cells analyzed by flow cytometry. $n = 3$ mice. **g**, IL-10 in the jejunum quantified by ELISA. $n = 4$ mice for Ctrl, $n = 5$ mice for conAP and $n = 3$ mice for indAP. **h**, qPCR for *Ifng*, *Il17*, *Il10*, *Foxp3* and *Il22* expression in the jejunum. $n = 3$ mice per group for *Ifng*, $n = 7$ for *Il17*, $n = 5$ for *Il10*, $n = 4$ for *Foxp3* and $n = 6$ for *Il22*. All presented data are representative of two independent experiments. *P* values are indicated. Bars represent the mean, and error bars represent s.e.m. One-way ANOVA followed by Tukey's post hoc test for **a**,**c**,**e**–**h**.

We first evaluated the viability of the engineered yeasts in the murine digestive tract. To address this point, we incorporated an antibiotic resistance cassette with a constitutive GFP reporter ('KG' strains) into the CB008 parent strain (from now on named 'Ctrl'), conAP and indAP engineered yeast strains to generate G418-resistant strains, levels of which can be easily quantified in fecal cultures (Yeast culture from mouse feces in the Methods). We detected viable antibiotic-resistant yeasts in feces at 6 h, but not at

24 or 48 h, after oral administration of Ctrl KG, conAP KG or indAP KG yeasts, suggesting that these probiotics are viable in the gut but do not colonize it (Extended Data Fig. 4a).

Increased local eATP levels are associated with intestinal inflammation[11,13,24] (Extended Data Fig. 4b). Thus, to analyze the activation of P2Y2 signaling in engineered yeasts during experimental colitis, we used a strain in which the activation of mutant TM-3 P2Y2 induces mCherry expression (indCherry KG) or a constitutively mCherry-expressing control strain (conCherry KG) (Fig. 1b). Both strains constitutively express GFP, allowing for easy detection in the gut content (Extended Data Fig. 4c). Following oral administration, we detected mCherry expression in indCherry KG engineered yeasts in the cecum and colon, concomitant with increased local eATP levels in trinitrobenzenesulfonic acid (TNBS)-treated mice (Fig. 4a). mCherry expression was not induced in the indCherry KG strain administered to naive mice, in which eATP levels were not locally increased (Extended Data Fig. 4d). Conversely, mCherry expression was detected throughout the gastrointestinal tract of mice that received the conCherry KG strain, regardless of eATP levels (Fig. 4a). Moreover, when we compared mCherry expression under the control of WT or mutant TM-3 P2Y2 in vivo, we detected higher mCherry expression levels in yeasts expressing the mutant TM-3 P2Y2 (indCherry KG versus WTCherry KG strains), highlighting the importance of increased P2Y2 sensitivity for the detection of eATP levels associated with intestinal inflammation (Extended Data Fig. 4e). In sum, these data indicate that the engineered yeast are viable in the digestive tract and that the TM-3 P2Y2 mutant responds in vivo to eATP levels associated with intestinal inflammation.

We then evaluated the therapeutic value of the engineered yeasts administered orally in a model of TNBS-induced colitis (see TNBS-induced mouse colitis model in the Methods for more details). We administered daily the indAP yeast strain, in which apyrase is induced following activation of mutant TM-3 P2Y2 by eATP. As controls, we used the parent strain Ctrl and the conAP strain, which constitutively express apyrase. indAP administration ameliorated TNBS-induced colitis, as indicated by evaluation of weight loss, colon shortening and histological analysis of intestinal pathology (Fig. 4b-e). Of note, the beneficial effects of indAP yeasts in TNBS-induced colitis were comparable to those achieved by the administration of anti-tumor necrosis factor (TNF) or anti-α4β7 integrin blocking antibodies, similar to those used to treat patients with IBD (Fig. 4f,g). Due to their systemic and unspecific nature, these treatments present substantial side effects, which could potentially be overcome with the engineered yeast strains presented in this study[31–33].

We detected decreased expression of pro-inflammatory genes in colon samples from mice treated with apyrase-producing yeast strains conAP and indAP; these effects were more pronounced in the indAP group (Fig. 4h). Indeed, treatment with the indAP strain, but not with conAP, led to increased numbers of forkhead box (FOX) $P3^+$ T_{reg} cells in mesenteric lymph nodes and reduced the expression of pro-inflammatory cytokines interferon (IFN)-γ and interleukin (IL)-17, associated with intestinal inflammation[34,35] (Fig. 4i,j).

To further evaluate the therapeutic potential of engineered apyrase-expressing yeasts, we used the dextran sulfate sodium (DSS)-induced model of colitis (refer to DSS-induced mouse colitis model in the Methods for details). Treatment with indAP, but not with conAP, interfered with the weight loss associated with DSS-induced colitis (Fig. 4k). Moreover, transcriptional analysis of colon samples revealed that indAP treatment resulted in decreased expression of genes associated with IBD and intestinal inflammation[34–36] (Fig. 4l,m). Pretreatment with indAP for 3 d before the start of DSS administration did not result in significant disease amelioration (Extended Data Fig. 4f), suggesting that indAP predominantly arrests inflammation and T cell-driven pathology taking place at late stages of the disease model[37].

Finally, we tested indAP in the mouse model of enteritis induced by administration of an anti-CD3 T cell-activating monoclonal antibody[38,39] (Anti-CD3 antibody-induced enteritis in the Methods). This model is characterized by T cell-driven inflammation in the small intestine and fluid accumulation in the jejunal lumen 3 h after anti-CD3 antibody administration, a phenomenon known as enteropooling[38,39]. The administration of indAP, but not that of conAP, significantly reduced enteropooling (Fig. 5a). indAP administration also decreased jejunal mucosal pathology, as indicated by decreased villous disruption and intestinal epithelial cell apoptosis (Fig. 5b–e). Moreover, indAP administration led to a decrease in jejunum-infiltrating T helper T_H1 and T_H17 cells, concomitant with increased numbers of IL-10-producing $CD4^+$ T cells (Fig. 5f). In agreement with these findings, indAP administration was associated with increased IL-10 levels in jejunum samples (Fig. 5g,h). Of note, TNF blockade decreased apoptosis as previously described[40] (Fig. 5d,e) but did not significantly ameliorate other parameters associated with anti-CD3 antibody-induced pathology (Fig. 5a,c). In sum, these findings demonstrate that eATP-responsive yeasts harboring a synthetic P2Y2–RROP1 gene circuit ameliorate intestinal inflammation.

eATP-responsive yeasts limit colitis-associated fibrosis and dysbiosis. Although yeast strains constitutively expressing high levels of apyrase have anti-inflammatory effects, they may also promote additional pathogenic responses. Indeed, we detected fibrotic lesions in the colon of mice undergoing TNBS-induced colitis treated with the Ctrl strain and also with constitutive apyrase-expressing conAP yeast strains. However, we detected a significant reduction in fibrosis in mice treated with the eATP-inducible indAP engineered yeast strain (Fig. 6a,b). These findings suggest that controlled modulation of purinergic signaling is needed to manage intestinal inflammation and avoid unwanted deleterious side effects.

Fig. 6 | eATP-responsive engineered yeast probiotics limit fibrosis and dysbiosis. a, Masson's trichrome staining for fibrosis on sections from mice with TNBS-induced colitis or ethanol-treated controls at 200× (top) and 400× (bottom) magnifications. A representative colon section of each group is shown. Fibrotic regions are stained in blue and highlighted with yellow arrows. Scale bars, 100 μm. Data are representative of two independent experiments. **b**, Histology fibrosis scores of mice from groups from **a**. $n=5$ samples for ethanol, $n=7$ samples for Ctrl, $n=8$ samples for conAP and $n=9$ samples for indAP. One-way ANOVA followed by Tukey's post hoc test. **c**–**h**, High-throughput gene-sequencing analysis of the V4 region of the microbial 16S rRNA gene in fecal samples from mice with TNBS-induced colitis or ethanol-treated controls. **c**, α-diversity of the fecal microbiome. Shannon's index, which measures evenness and richness of the ecosystem, was calculated at a sequencing depth of 4,000 reads per sample. $n=4$ samples for indAP and $n=3$ otherwise. Kruskal–Wallis nonparametric ANOVA test. **d**,**e**, β-diversity. **d**, Principal-coordinate analysis (PCoA) based on unweighted UniFrac metrics. **e**, Pairwise unweighted UniFrac distances to the ethanol control group. PERMANOVA analysis ($n=10$ permutations for ethanol, $n=15$ permutations for Ctrl, $n=20$ permutations for conAP and indAP). **f**, Relative abundance of bacteria classified at a family-level taxonomy. **g**, Relative abundance of the *Lachnospiraceae* family and one of its genera, *Roseburia*. $n=3$ samples for ethanol and Ctrl and $n=4$ samples for conAP and indAP. Kruskal–Wallis nonparametric ANOVA test. **h**, Linear discriminant analysis effect size, $P<0.05$ for the indAP versus Ctrl comparison. Each cladogram represents all taxa detected at >0.1%, shown at the kingdom through the genus phylogenetic level. A yellow circle depicts taxa present but not enriched. Red circles are enriched in indAP, and green circles are enriched in Ctrl. *P* values are indicated. Bars represent the mean, and error bars represent s.e.m.

Probiotics engineered to act in an inducible and localized manner are likely to minimize disturbances of the gut microbiome. To investigate whether constitutive versus inducible apyrase production by engineered yeast strains differ in their effects on the gut microbiome, we performed 16S rRNA sequencing of fecal samples from healthy mice or mice with TNBS-induced colitis treated with

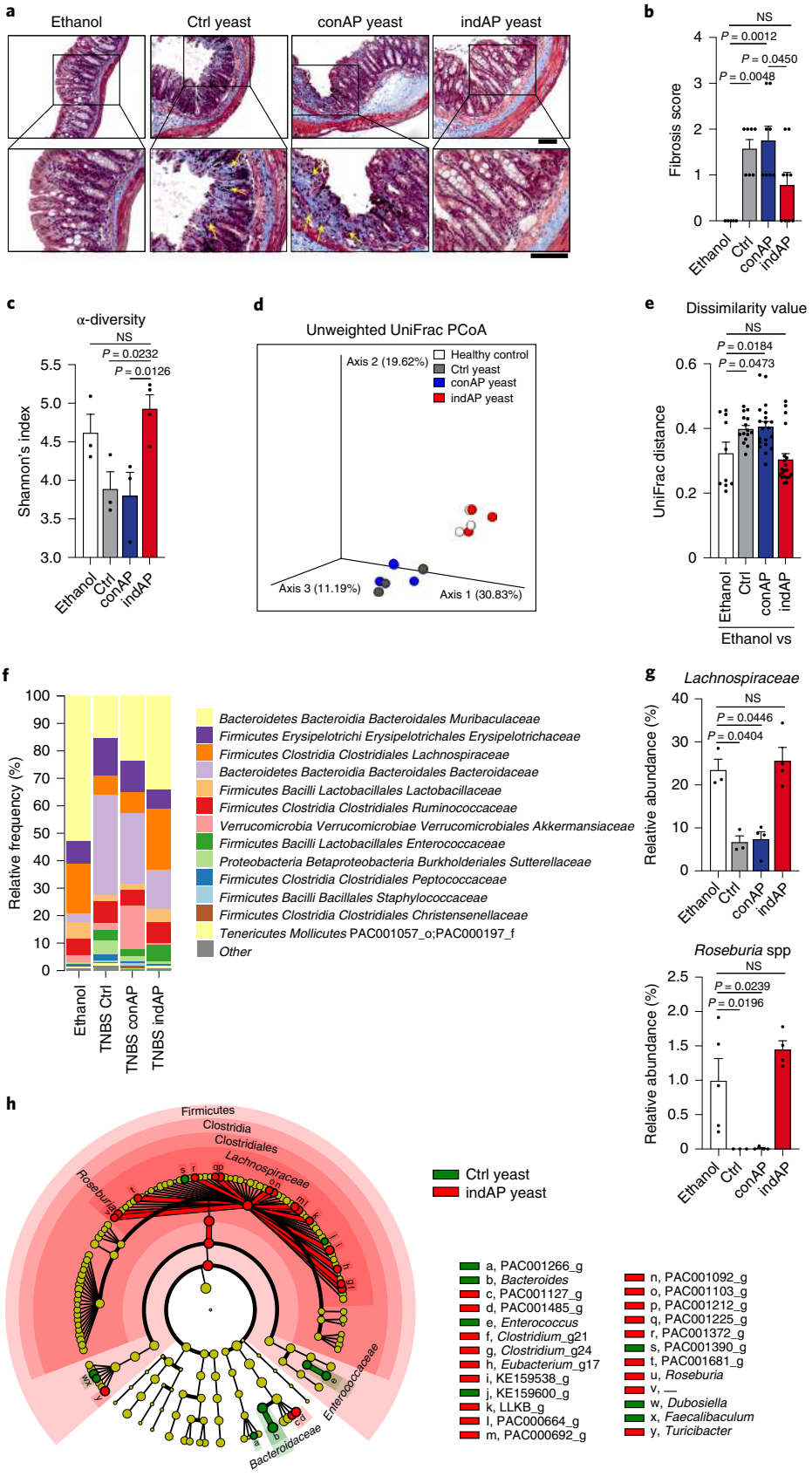

engineered yeasts (refer to Microbiome (16S) sequencing and analysis in the Methods for extended details). In agreement with previous reports[41], induction of colitis with TNBS reduced microbiome diversity within each sample, as indicated by analysis of the Shannon entropy index of α-diversity (Fig. 6c). A similar reduction in microbiome diversity was detected after treatment with the conAP yeast strain. However, treatment with the indAP engineered yeast strain expressing inducible apyrase resulted in microbiome diversity levels similar to those detected in naive mice (Fig. 6c).

We then analyzed β-diversity, which measures differences in microbiome composition between samples (Fig. 6d,e), revealing significant differences between the control group and TNBS-treated mice treated with either Ctrl or constitutive apyrase conAP yeast strains. Strikingly, β-diversity analysis revealed that TNBS-treated mice treated with the indAP engineered strain harbored a microbiome similar to that of mice in which colitis had not been induced, suggesting that the engineered yeast strain in which apyrase expression is induced by eATP re-establishes a healthy microbiome (Fig. 6d,e).

Finally, we analyzed the taxonomic composition of the microbiome in the different treatment groups. Several taxa of commensal bacteria were shown to be decreased in IBD and ameliorate intestinal inflammation[3,5]. For example, *Clostridium* cluster XIVa, associated with induction of T_{reg} cells, is consistently depleted in people with IBD and acute colitis[42]. We found that the *Lachnospiraceae* family, included in *Clostridium* cluster XIVa, was significantly reduced in TNBS-treated mice treated with Ctrl and conAP yeast strains but not in TNBS-treated mice treated with the indAP strain (Fig. 6f–h). Moreover, within the *Lachnospiraceae* family, the *Roseburia* genus was decreased in mice treated with Ctrl and conAP yeast strains but not in indAP-treated TNBS-treated mice. Of note, *Roseburia* spp. were shown to promote T_{reg} development through a butyrate-dependent mechanism[43]. In sum, these findings suggest that inducible production of apyrase by the indAP engineered yeast strain enables anti-inflammatory effects of eATP depletion and adenosine production, without unwanted side effects associated with fibrosis and microbiome dysregulation.

Discussion

The modulation of the eATP–adenosine balance is an attractive strategy to treat inflammation. However, clinical application of this approach requires inducible systems to minimize unwanted side effects such as immunosuppression and fibrosis[14,16,18]. Here we report the development of engineered yeasts that, in response to the metabolite eATP produced in the inflamed gut, secrete apyrase, which depletes pro-inflammatory eATP and promotes the generation of immunosuppressive adenosine. This approach suppresses intestinal inflammation, while reducing fibrosis and promoting the recovery of a healthy microbiome, minimizing the dysbiosis associated with the pathology of IBD and other human disorders[4,5].

The engineered yeasts that we developed harbor a self-tunable P2Y2–RROP1 gene circuit responsive to pro-inflammatory eATP in a time- and location-specific manner. By engineering the human P2Y2 GPCR, we were able to tune the anti-inflammatory response to physiological eATP levels. Multiple mechanisms contribute to the increase in eATP sensitivity, including increased expression and stabilization of the active receptor conformation. The wide range of solutions selected in response to the challenge imposed by our directed evolution strategy highlights the intrinsic plasticity of GPCR signaling networks. The therapeutic yeast platform described herein could be further optimized by making it responsive to multiple stimuli in the inflamed microenvironment using logic gates[44] and also by incorporating multiple anti-inflammatory mechanisms, such as secreting cytokines and blocking antibodies, which may otherwise cause undesired side effects when administered systemically.

The development of therapeutic probiotics is a major area of IBD research. Previous attempts used engineered probiotics expressing therapeutic proteins in an uncontrolled manner, based on plasmid systems that require constant selection pressure and present the risk of horizontal transfer to other microbes[10,45]. To overcome these limitations, we applied directed evolution and CRISPR–Cas9 to engineer yeast strains with a gene circuit that produces apyrase in response to eATP levels, delivering a probiotic-based dynamic anti-inflammatory response in the inflamed tissue microenvironment. Moreover, we integrated this engineered gene circuit into the yeast genome to avoid the use of antibiotic selection markers, while maintaining uracil auxotrophy for biocontainment, in agreement with Food and Drug Administration guidelines on live biotherapeutic organisms (docket number FDA-2010-D-0500).

S. cerevisiae has not been commonly used as a probiotic. However, *S. cerevisiae* strains are a component of the healthy microbiome, which is reduced during IBD[46,47], and have been associated with physiological training of the immune system[48–51]. Indeed, supplementation with *S. cerevisiae* has been proposed as an anti-inflammatory approach based on its ability to increase IL-10 levels[47]. Notably, natural anti-inflammatory effects of *S. cerevisiae* appear to be strain dependent, as some wild *S. cerevisiae* isolates exacerbate colitis[52,53], while others ameliorate it[54]. Alternatively, *Saccharomyces boulardii* has been commonly used as a yeast probiotic[19], but the tools for its genetic manipulation have become available only very recently[55,56]. Thus, the inducible system described in this work may be implemented in *S. cerevisiae*, or it can be transferred to *S. boulardii* to increase its translational potential. However, it is important to consider that the higher survival and growth rate of *S. boulardii* in the gut, when compared to those of *S. cerevisiae*[55,56], could favor its engraftment, which is not desirable because of the potential for competition with the native gut flora and dysbiosis.

In summary, the engineered yeasts described in this work could represent a step forward in the application of directed evolution and synthetic biology to develop self-tunable anti-inflammatory probiotics. eATP promotes intestinal inflammation in other diseases aside from IBD, such as graft-versus-host disease and irradiation-induced abdominal fibrosis[57,58]. Moreover, the intestinal microbiome controls inflammation at distant body sites such as the central nervous system[59,60]. Thus, control of the intestinal pro-inflammatory–anti-inflammatory balance with engineered yeast probiotics such as the ones described in this work may provide a generalizable therapeutic approach for intestinal inflammation and also for inflammatory disorders targeting other tissues beyond the intestinal system.

Online content

Any methods, additional references, Nature Research reporting summaries, source data, extended data, supplementary information, acknowledgements, peer review information; details of author contributions and competing interests; and statements of data and code availability are available at https://doi.org/10.1038/s41591-021-01390-x.

Received: 28 October 2020; Accepted: 7 May 2021;
Published online: 28 June 2021

References

1. Huang, H. et al. Fine-mapping inflammatory bowel disease loci to single-variant resolution. *Nature* **547**, 173–178 (2017).
2. Neurath, M. F. Targeting immune cell circuits and trafficking in inflammatory bowel disease. *Nat. Immunol.* **20**, 970–979 (2019).
3. Blander, J. M., Longman, R. S., Iliev, I. D., Sonnenberg, G. F. & Artis, D. Regulation of inflammation by microbiota interactions with the host. *Nat. Immunol.* **18**, 851–860 (2017).
4. Jostins, L. et al. Host–microbe interactions have shaped the genetic architecture of inflammatory bowel disease. *Nature* **491**, 119–124 (2012).
5. Lloyd-Price, J. et al. Multi-omics of the gut microbial ecosystem in inflammatory bowel diseases. *Nature* **569**, 655–662 (2019).

6. Plichta, D. R., Graham, D. B., Subramanian, S. & Xavier, R. J. Therapeutic opportunities in inflammatory bowel disease: mechanistic dissection of host–microbiome relationships. *Cell* **178**, 1041–1056 (2019).
7. Suez, J., Zmora, N., Segal, E. & Elinav, E. The pros, cons, and many unknowns of probiotics. *Nat. Med.* **25**, 716–729 (2019).
8. Aggarwal, N., Breedon, A. M. E., Davis, C. M., Hwang, I. Y. & Chang, M. W. Engineering probiotics for therapeutic applications: recent examples and translational outlook. *Curr. Opin. Biotechnol.* **65**, 171–179 (2020).
9. Hwang, I. Y. et al. Engineered probiotic *Escherichia coli* can eliminate and prevent *Pseudomonas aeruginosa* gut infection in animal models. *Nat. Commun.* **8**, 15028 (2017).
10. McKay, R. et al. A platform of genetically engineered bacteria as vehicles for localized delivery of therapeutics: toward applications for Crohn's disease. *Bioeng. Transl. Med.* **3**, 209–221 (2018).
11. Idzko, M., Ferrari, D. & Eltzschig, H. K. Nucleotide signalling during inflammation. *Nature* **509**, 310–317 (2014).
12. Atarashi, K. et al. ATP drives lamina propria T_H17 cell differentiation. *Nature* **455**, 808–812 (2008).
13. Gulbransen, B. D. et al. Activation of neuronal P2X7 receptor–pannexin-1 mediates death of enteric neurons during colitis. *Nat. Med.* **18**, 600–604 (2012).
14. Takenaka, M. C., Robson, S. & Quintana, F. J. Regulation of the T cell response by CD39. *Trends Immunol.* **37**, 427–439 (2016).
15. Mascanfroni, I. D. et al. IL-27 acts on DCs to suppress the T cell response and autoimmunity by inducing expression of the immunoregulatory molecule CD39. *Nat. Immunol.* **14**, 1054–1063 (2013).
16. Takenaka, M. C. et al. Control of tumor-associated macrophages and T cells in glioblastoma via AHR and CD39. *Nat. Neurosci.* **22**, 729–740 (2019).
17. Cekic, C. & Linden, J. Purinergic regulation of the immune system. *Nat. Rev. Immunol.* **16**, 177–192 (2016).
18. Vuerich, M., Robson, S. C. & Longhi, M. S. Ectonucleotidases in intestinal and hepatic inflammation. *Front. Immunol.* **10**, 507 (2019).
19. Sen, S. & Mansell, T. J. Yeasts as probiotics: mechanisms, outcomes, and future potential. *Fungal Genet. Biol.* **137**, 103333 (2020).
20. Brown, A. J. et al. Functional coupling of mammalian receptors to the yeast mating pathway using novel yeast/mammalian G protein α-subunit chimeras. *Yeast* **16**, 11–22 (2000).
21. Shaw, W. M. et al. Engineering a model cell for rational tuning of GPCR signaling. *Cell* **177**, 782–796 (2019).
22. Lazarowski, E. R. & Harden, T. K. Quantitation of extracellular UTP using a sensitive enzymatic assay. *Br. J. Pharmacol.* **127**, 1272–1278 (1999).
23. Wan, P. et al. Extracellular ATP mediates inflammatory responses in colitis via P2 × 7 receptor signaling. *Sci. Rep.* **6**, 19108 (2016).
24. Di Virgilio, F., Pinton, P. & Falzoni, S. Assessing extracellular ATP as danger signal in vivo: the pmeLuc system. *Methods Mol. Biol.* **1417**, 115–129 (2016).
25. Hillmann, P. et al. Key determinants of nucleotide-activated G protein-coupled $P2Y_2$ receptor function revealed by chemical and pharmacological experiments, mutagenesis and homology modeling. *J. Med. Chem.* **52**, 2762–2775 (2009).
26. Schutz, M. et al. Directed evolution of G protein-coupled receptors in yeast for higher functional production in eukaryotic expression hosts. *Sci. Rep.* **6**, 21508 (2016).
27. Montaner, S., Kufareva, I., Abagyan, R. & Gutkind, J. S. Molecular mechanisms deployed by virally encoded G protein-coupled receptors in human diseases. *Annu. Rev. Pharmacol. Toxicol.* **53**, 331–354 (2013).
28. Venkatakrishnan, A. J. et al. Diverse activation pathways in class A GPCRs converge near the G-protein-coupling region. *Nature* **536**, 484–487 (2016).
29. Komoszynski, M. A. Comparative studies on animal and plant apyrases (ATP diphosphohydrolase EC 3.6.1.5) with application of immunological techniques and various ATPase inhibitors. *Comp. Biochem. Physiol. B Biochem. Mol. Biol.* **113**, 581–591 (1996).
30. Nourizad, N., Ehn, M., Gharizadeh, B., Hober, S. & Nyren, P. Methylotrophic yeast *Pichia pastoris* as a host for production of ATP-diphosphohydrolase (apyrase) from potato tubers (*Solanum tuberosum*). *Protein Expr. Purif.* **27**, 229–237 (2003).
31. Derkx, B. et al. Tumour-necrosis-factor antibody treatment in Crohn's disease. *Lancet* **342**, 173–174 (1993).
32. Dotan, I. et al. The role of integrins in the pathogenesis of inflammatory bowel disease: approved and investigational anti-integrin therapies. *Med. Res. Rev.* **40**, 245–262 (2020).
33. Shen, C. et al. Remission-inducing effect of anti-TNF monoclonal antibody in TNBS colitis: mechanisms beyond neutralization? *Inflamm. Bowel Dis.* **13**, 308–316 (2007).
34. Goettel, J. A. et al. AHR activation is protective against colitis driven by T cells in humanized mice. *Cell Rep.* **17**, 1318–1329 (2016).
35. Nowarski, R., Jackson, R. & Flavell, R. A. The stromal intervention: regulation of immunity and inflammation at the epithelial–mesenchymal barrier. *Cell* **168**, 362–375 (2017).
36. Sonnenberg, G. F., Fouser, L. A. & Artis, D. Border patrol: regulation of immunity, inflammation and tissue homeostasis at barrier surfaces by IL-22. *Nat. Immunol.* **12**, 383–390 (2011).
37. Trivedi, P. P. & Jena, G. B. Dextran sulfate sodium-induced ulcerative colitis leads to increased hematopoiesis and induces both local as well as systemic genotoxicity in mice. *Mutat. Res.* **744**, 172–183 (2012).
38. Musch, M. W. et al. T cell activation causes diarrhea by increasing intestinal permeability and inhibiting epithelial Na^+/K^+-ATPase. *J. Clin. Invest.* **110**, 1739–1747 (2002).
39. Ueno, N. et al. TU-100 (Daikenchuto) and ginger ameliorate anti-CD3 antibody induced T cell-mediated murine enteritis: microbe-independent effects involving Akt and NF-κB suppression. *PLoS ONE* **9**, e97456 (2014).
40. Goretsky, T. et al. p53 mediates TNF-induced epithelial cell apoptosis in IBD. *Am. J. Pathol.* **181**, 1306–1315 (2012).
41. He, Q. et al. Dysbiosis of the fecal microbiota in the TNBS-induced Crohn's disease mouse model. *Appl. Microbiol. Biotechnol.* **100**, 4485–4494 (2016).
42. Frank, D. N. et al. Molecular–phylogenetic characterization of microbial community imbalances in human inflammatory bowel diseases. *Proc. Natl Acad. Sci. USA* **104**, 13780–13785 (2007).
43. Machiels, K. et al. A decrease of the butyrate-producing species *Roseburia hominis* and *Faecalibacterium prausnitzii* defines dysbiosis in patients with ulcerative colitis. *Gut* **63**, 1275–1283 (2014).
44. Chen, Y. et al. Genetic circuit design automation for yeast. *Nat. Microbiol.* **5**, 1349–1360 (2020).
45. Braat, H. et al. A phase I trial with transgenic bacteria expressing interleukin-10 in Crohn's disease. *Clin. Gastroenterol. Hepatol.* **4**, 754–759 (2006).
46. Nash, A. K. et al. The gut mycobiome of the Human Microbiome Project healthy cohort. *Microbiome* **5**, 153 (2017).
47. Sokol, H. et al. Fungal microbiota dysbiosis in IBD. *Gut* **66**, 1039–1048 (2017).
48. Enaud, R. et al. The mycobiome: a neglected component in the microbiota–gut–brain axis. *Microorganisms* **6**, 22 (2018).
49. Martins, F. S. et al. Oral treatment with *Saccharomyces cerevisiae* strain UFMG 905 modulates immune responses and interferes with signal pathways involved in the activation of inflammation in a murine model of typhoid fever. *Int. J. Med. Microbiol.* **301**, 359–364 (2011).
50. Rizzetto, L. et al. Fungal chitin induces trained immunity in human monocytes during cross-talk of the host with *Saccharomyces cerevisiae*. *J. Biol. Chem.* **291**, 7961–7972 (2016).
51. Zanello, G. et al. *Saccharomyces cerevisiae* modulates immune gene expressions and inhibits ETEC-mediated ERK1/2 and p38 signaling pathways in intestinal epithelial cells. *PLoS ONE* **6**, e18573 (2011).
52. Chiaro, T. R. et al. A member of the gut mycobiota modulates host purine metabolism exacerbating colitis in mice. *Sci. Transl. Med.* **9**, eaaf9044 (2017).
53. Rinaldi, M., Perricone, R., Blank, M., Perricone, C. & Shoenfeld, Y. Anti-*Saccharomyces cerevisiae* autoantibodies in autoimmune diseases: from bread baking to autoimmunity. *Clin. Rev. Allergy Immunol.* **45**, 152–161 (2013).
54. Tiago, F. C. et al. Effect of *Saccharomyces cerevisiae* strain UFMG A-905 in experimental model of inflammatory bowel disease. *Benef. Microbes* **6**, 807–815 (2015).
55. Hudson, L. E. et al. Functional heterologous protein expression by genetically engineered probiotic yeast *Saccharomyces boulardii*. *PLoS ONE* **9**, e112660 (2014).
56. Durmusoglu, D. et al. In situ biomanufacturing of small molecules in the mammalian gut by probiotic *Saccharomyces boulardii*. *ACS Synth. Biol.* **10**, 1039–1105 (2021).
57. Takemura, N. et al. Eosinophil depletion suppresses radiation-induced small intestinal fibrosis. *Sci. Transl. Med.* **10**, eaan0333 (2018).
58. Wilhelm, K. et al. Graft-versus-host disease is enhanced by extracellular ATP activating P2X7R. *Nat. Med.* **16**, 1434–1438 (2010).
59. Berer, K. et al. Commensal microbiota and myelin autoantigen cooperate to trigger autoimmune demyelination. *Nature* **479**, 538–541 (2011).
60. Rothhammer, V. et al. Microglial control of astrocytes in response to microbial metabolites. *Nature* **557**, 724–728 (2018).

Methods

Reporter yeast strains. All genome modifications of initial yeast strains were conducted using homologous recombination of selectable markers and transformed using a standard lithium acetate transformation method with at least 1 µg linear insert DNA. The parent strain was either CB008 (Ctrl), for constitutive overexpression of fluorescent reporter genes[61], or BS004, for the P2Y2–mCherry or P2Y2–apyrase gene circuit[62] (see Supplementary Table 1 for detailed strain genotypes, which were all derived from a laboratory-domesticated haploid strain). p*FUS1*-mCherry was integrated at the *MFA2* locus using plasmid pJW609 containing the KanR marker. p*FUS1* was defined as the 1,636 bp immediately upstream of the *Fus1* start codon, and ~1-kb homology regions were used. *STE2* and *SST2* were targeted for deletion using TRP1 and HygB selectable markers respectively, each with 180 bp of flanking homology regions identical to the sequences flanking the ORF. The five C-terminal amino acids of Gpa1 (KIGII) were replaced with a Gpa1–Gα chimera containing the C-terminal amino acids from the indicated human Gα protein, using plasmid pBS600 containing the selectable marker LEU2 and 800-bp homology regions. The *Candida albicans Adh* terminator was used for gene knock-ins to express p*FUS1*-mCherry and Gpa1–Gα. To create a strain that constitutively expressed mCherry, the integration plasmid pJW609 was modified to replace the KanMX marker with *HIS3* from *Candida glabrata*, and sequence coding for p*TDH3*-mCherry was inserted at PspOMI and BamHI sites. The linearized *HIS3*-p*TDH3*-mCherry cassette was transformed into strain Ctrl, and integrations were selected by plating on SC-HIS. To create strains that contained the KanMX selectable marker and constitutively expressed GFP, an integration plasmid was constructed using the MoClo Yeast Toolkit. The resulting plasmid pBS211 contained *HO* locus homology regions, the KanMX marker and a yeast codon-optimized gene coding for sfGFP downstream of p*TDH3* (ref. [21]). The linearized KanMX-p*TDH3* sfGFP cassette was transformed into strains described in Supplementary Table 1, and integrations were selected by plating on yeast extract peptone dextrose (YPD)–G418 sulfate (200 µg ml^{-1}). All strains were confirmed by PCR and flow cytometry.

Yeast microscopy. Yeast strain BS016 expressing the endogenous yeast GPCR Ste2 or a yeast codon-optimized sequence coding for human P2Y2 (obtained from ATUM) C-terminally tagged with GFP were grown to log phase in SC-URA medium. The centromere plasmid pRS316 was used, containing the endogenous p*STE2* promoter for Ste2 expression or p*TDH3* for P2Y2 expression. Restriction enzyme sites were introduced into the sequence coding for an amino acid linker (GGERGS) between the final GPCR residue and first GFP residue. Cells were plated on glass-bottomed dishes (Greiner Bio-One) that had been treated with concanavalin A (Sigma-Aldrich) and then covered with 1 ml SC-URA medium. Cells were imaged using a Leica TCS SP8 confocal microscope and processed using Leica LAS X version 3.1.5.16308 software.

Flow cytometry evaluation of response to ATP and UTP. Yeast strain BS016 transformed with a human *P2Y2* gene in the pRS316 p*TDH3* vector was grown in SC-URA liquid medium overnight. The same strain transformed with a plasmid not containing a *P2Y2* sequence (vector) was used as a negative control. Cells were diluted to an optical density at 600 nm (OD_{600}) of 0.05 in 600 µl SC-URA containing ATP (0–25.6 mM; pH 7.0, Bio Basic) or UTP (0–3.2 mM; pH 7.0, Sigma-Aldrich) and incubated for 6 h at 30 °C with shaking (225 r.p.m.). Cells were then treated with cycloheximide at a final concentration of 10 µg ml^{-1}. The mCherry signal from at least 10,000 cells was measured for each sample with a Miltenyi Biotec MACSQuant VYB flow cytometer. The mean mCherry fluorescence was determined using FlowJo. For dose–response assays, data were fitted with the 'log(agonist) vs. response – Variable slope (four parameters)' model in Prism (GraphPad). After subtracting the mCherry fluorescence signal of the vector control, fluorescence values were normalized to those from the WT P2Y2 control used in the same experiment to allow comparisons between experiments performed on different days. The flow cytometry gating strategy is shown in Supplementary Fig. 2a. Data were collected using MACSQuantify version 2.11, and analysis was performed using FlowJo software.

Directed evolution of the human P2Y2 receptor. Error-prone PCR mutagenesis was performed using the Agilent GeneMorph II Random Mutagenesis kit with yeast codon-optimized human *P2Y2* as a template. The desired mutation rate of approximately three mutations per *P2Y2* gene, determined by sequencing 12 randomly selected plasmids (Supplementary Table 2), was achieved by using template DNA (150 ng) and 30 cycles. The randomly mutated sequences were inserted into pRS316 p*TDH3* using AarI-based cloning and transformed into NEB 5-alpha competent *Escherichia coli* cells (New England Biolabs), generating >15,000 individual colonies. Cells were scraped off agar plates and mixed together, and plasmid DNA was extracted (QIAquick Spin Miniprep kit, Qiagen) to create the final plasmid library. The library was transformed into the yeast strain BS016 using a high-efficiency lithium acetate-based method, yielding at least tenfold the number of colonies as the total library size, so that each mutant would be screened multiple times. Transformed cells were incubated overnight and then diluted to an OD_{600} of 0.05 in 100 ml fresh SC-URA liquid medium containing 100 µM ATP (pH 7.0, Bio Basic) and incubated for either 18 or 6 h at 30 °C with shaking (225 r.p.m.) (Extended Data Fig. 2). After brief sonication, 10^6–10^7 cells were gated by side and forward scatter and sorted for the highest ~1% of mCherry signal using a BD Influx cell sorter (gating strategy is shown in Supplementary Fig. 2b). A total of 174 yeast colonies recovered from various sorting experiments were individually screened for their response to 100 µM UTP or 100 µM ATP or screened with no ligand after a 6-h incubation. Of these colonies, 128 colonies exhibited a response to eATP stronger than the one detected using the WT human P2Y2 receptor; 163 colonies showed a stronger response to eUTP. Plasmids were isolated from selected colonies by first incubating with zymolyase (BioShop Canada) and then extracting plasmid DNA (QIAquick Spin Miniprep kit, Qiagen). Plasmid DNA was amplified using NEB 5-alpha competent *E. coli* cells (New England Biolabs), plasmid DNA was sequenced, and fresh BS016 yeast cells were transformed for dose–response experiments. Targeted mutations were introduced via PCR following the QuikChange site-directed mutagenesis protocol (Agilent) and using PfuUltra II Fusion HS DNA Polymerase (Agilent).

Homology modeling of P2Y2. Modeling was conducted as described by Rafehi et al.[63] using the crystal structure of the human P2Y1 receptor (PDB, 4XNW) bound to the nucleotide antagonist MRS2500 as a template. The sequences of human P2Y1 and P2Y2 were aligned using Clustal Omega. As only residues S38–F331 of P2Y1 were visible in the crystal structure, these were used as the template to generate 500 models of the corresponding P2Y2 residues L20–L313. Standard MODELLER 9.18 settings were used, maintaining MRS2500 in the models. The generated models were first analyzed based on DOPE and GA341 scores, and the top five models were manually inspected to ensure the natural disulfide bonds were maintained (C25–C278, C106–C183). Next, models were evaluated by ProSA-web[64] and Ramachandran plots[65], and the final model was selected. ATP was docked to the WT P2Y2 homology model using the Galaxy7TM web server[66], which generated ten docked models. The lowest energy model in which the adenine ring of ATP was oriented toward the key Y114 and F261 residues was selected[63]. Publication-quality images were generated with PyMOL (Schrödinger). In addition to residue numbers, in the text we also provide Ballesteros–Weinstein numbering, in which the first number is the transmembrane helix followed by a conserved position across all class A GPCRs[67].

Integration of P2Y2 mutants with CRISPR. The pCAS plasmid was obtained from Addgene, which expresses Cas9 and a yeast-optimized guide RNA (gRNA)[68]. The gRNA sequence was replaced with an AarI-based multiple cloning site to generate the pCAS AarI plasmid (Extended Data Fig. 5). This enabled the use of AarI, a type IIS restriction enzyme, to insert any gRNA sequence (20 bp) without modifying the required nuclear localization signal or 3′ tail of the gRNA. gRNA sequences were designed with CRISPR MultiTargeter[69] and Off-Spotter web servers[70] (Supplementary Table 6). A gene cassette containing an engineered *P2Y2* mutant sequence downstream of the p*TDH3* promoter was assembled in the plasmid pBS600, flanked by 800-bp homology arms for the *SST2* locus. The cassettes were amplified by PCR and transformed into strain BS021 along with plasmid pCAS AarI HygB 1143 as described previously[68]. Colonies were screened for mCherry expression in response to ATP, and *P2Y2* integration was confirmed by sequencing.

Apyrase genome mining. Apyrase isolated from the potato species *S. tuberosum* (RROP1; GenBank accession U58597.1) has the highest ATPase activity reported[71]. The BlastPhyMe tool was employed for genome mining of homologous genes, using *RROP1* as the initial input sequence. Apyrase from wild einkorn wheat *T. urartu* (named 'TUAP1' in our study; GenBank accession KD039156.1) was selected as it had conserved domains known to be required for apyrase function[71] and based on previous reports of wheat apyrase activity[29]. Yeast codon-optimized RROP1 and TUAP1 were modified to contain an N-terminal α-factor signal peptide (first 85 amino acids of yeast MFα1, lacking the Ste13 cut site) and a C-terminal HA tag (gene synthesis was performed by ATUM).

Integration of genes encoding apyrases into the genome of P2Y2 strains. A gene cassette containing one of the genes encoding apyrase downstream of the p*FUS1* promoter was assembled in the plasmid pBS600. Cassettes were amplified by PCR and transformed into a strain in which *P2Y2* had previously been integrated, along with plasmid pCAS AarI mCherry g664 as described previously[68]. The promoter and terminator of the cassette functioned as homology arms, as sequence coding for mCherry had previously been inserted with p*FUS1* and the *C. albicans Adh* terminator at the *MFA2* locus. Colonies were screened for mCherry expression in response to ATP, and integration of the gene encoding apyrase was confirmed by sequencing colonies that did not express mCherry. A second group of gene cassettes was assembled using plasmid pBS603 (pBS600 containing a HIS3 selection marker) with one of the genes encoding apyrase downstream of the p*TDH3* promoter, flanked by 1-kb homology arms for the *MFA2* locus. Cassettes were amplified by PCR and transformed into strain CB008 (Ctrl) before plating on selective medium to create strains BS029, referred to as conAP (p*TDH3*-RROP1) and BS030 (p*TDH3*-TUAP1).

Western blot. Overnight cultures were diluted to an OD_{600} of 0.05 in 50 ml YPD. All cultures were incubated for 24 h at 30 °C with shaking (225 r.p.m.). Samples

of lysed cells were resolved on a 10% SDS–PAGE gel (Bio-Rad) and transferred to a PVDF membrane using a Bio-Rad Trans-Blot Turbo transfer system. Membranes were blocked overnight with Odyssey Blocking Buffer (TBS) (LI-COR Biosciences). The following primary antibodies were used: rabbit anti-HA tag (C29F4, Cell Signaling Technology, 1:1,000), mouse anti-PGK (459250, Invitrogen, 1:5,000). After washing, the following secondary antibodies were used: IRDye 680LT Goat anti-Mouse IgG (926-68020, LI-COR Biosciences, 1:5,000), IRDye 800CW Goat anti-Rabbit IgG (926-32211, LI-COR Biosciences, 1:5,000). Bands were visualized with a LI-COR Odyssey CLx infrared imaging system (LI-COR Biosciences) using LI-COR Image Studio version 5.0 software.

Induction of apyrase secretion with ATP. Yeast strains containing a *P2Y2* mutant gene and p*FUS1* regulating the expression of RROP1 apyrase were incubated overnight in YPD medium. Cells were diluted to an OD_{600} of 0.05 in 2 ml fresh YPD, with 0–500 µM ATP (pH 7.0) added. After incubation for 16 h (overnight) at 30 °C with shaking (225 r.p.m.) until an OD_{600} of 3.5 was reached, 500-µl samples were pipetted into 1.5-ml tubes and centrifuged at 2,000*g* for 5 min to pellet cells. Culture supernatants were then evaluated for ATPase activity.

Quantification of secreted ATPase activity. The amount of ATP remaining following incubation with apyrase was determined by Kinase-Glo Plus luminescence (V3771, Promega). In a white 96-well microplate (655075, Greiner Bio-One) 5 µl raw supernatant from yeast cultures at an OD_{600} of 3.5, to which ATP had been added at the start of culturing to induce expression of apyrase, was mixed with 50 µM ATP (pH 7.0) in assay buffer (60 mM HEPES, pH 6.0, 2 mM $MgCl_2$, 2 mM $CaCl_2$, 1 mM dithiothreitol, 0.1 mg ml^{-1} BSA, 0.1 mM EDTA and 0.01% Tween-20) to a final volume of 50 µl. The reaction was incubated for 30 min at 30 °C and quenched by adding 50 µl Kinase-Glo Plus (V3771, Promega). Luminescence was measured with a Fluoroskan Ascent FL microplate reader (Thermo Fisher Scientific) using Ascent software version 2.6. ATPase activity was compared to that of commercial potato apyrase (A6410, Sigma-Aldrich) incubated with ATP under the same conditions. 'Percent ATP degraded' was calculated by comparing ATP levels to 50 µM ATP incubated in YPD medium and assay buffer under the same conditions.

Yeast cultures for in vivo testing. Yeast strains were cultured in 550 ml or 1 l YPD medium (BioShop Canada) at 30 °C with shaking (225 r.p.m.). G418 sulfate antibiotic (200 µg ml^{-1}, BioShop Canada) was added to the medium when culturing strains containing the KanMX resistance marker. After 24 h, cultures were centrifuged and yeast were resuspended in fresh YPD to a density of approximately 2×10^9 colony-forming units (CFU) ml^{-1} (~25-fold concentrated culture), and colony density was confirmed by plating. Yeast were stored as 800-µl aliquots at −80 °C for up to 1 year.

Mice. Mice were kept in an SPF facility at the Hale Building of Transformative Medicine at the Brigham and Women's Hospital in accordance with Institutional Animal Care and Use Committee guidelines. Two to five mice were housed per cage under a standard light cycle (12 h:12 h light:dark) at 20–23 °C and ~50% humidity with ad libitum access to water and food. C57BL/6J (Jackson Laboratory, 000664) adult female (for the DSS model and the anti-CD3 antibody enteritis model) or male (for the TNBS model) mice between 8 and 10 weeks of age were used throughout the study. Upon receipt, mice were kept for 1 month in our facility for acclimatation and homogenization of microbiome and then were randomly allocated to the different treatment groups without co-housing of mice treated with different probiotic strains to avoid transfer between mice. All experiments were carried out in accordance with guidelines prescribed by the Institutional Animal Care and Use Committee at Brigham and Women's Hospital and Harvard Medical School.

Trinitrobenzenesulfonic acid-induced mouse colitis model. To induce colitis with TNBS in C57BL/6J mice, males were presensitized 1 week before colitis induction by applying 150 µl presensitization TNBS solution (64% acetone (179124, Sigma-Aldrich), 16% olive oil (Sigma-Aldrich, O1514), 20% 50 mg ml^{-1} TNBS (picrylsulfonic acid solution, 5%, Sigma-Aldrich, P2297)) to their preshaved backs. One week after, presensitized mice were fasted for 4 h, and, subsequently, 100 µl TNBS induction solution (50% ethanol, 50% 50 mg ml^{-1} TNBS) was administered rectally. The control group was treated only with 50% ethanol. Mouse weight was monitored daily until the day of the euthanasia 72 h after colitis induction, at the peak of the disease.

Dextran sodium sulfate-induced mouse colitis model. IBD was induced by adding 4% DSS salt (DSS colitis grade, MP Biomedicals) to the drinking water. Treatment was maintained for 7 d, and two cycles were performed with a week without treatment in between. After the second cycle of DSS, DSS was removed, and mice were killed. Animal body weight was evaluated daily throughout the study. In some studies, treatment was maintained for 7 d, and mice were killed at day 10 when we were only aiming to analyze the first cycle.

Anti-CD3 antibody-induced enteritis. C57BL/6J mice were injected intraperitoneally with 200 µg anti-CD3 monoclonal antibody (InVivoPlus anti-mouse CD3ε; BP0001-1, Bio X Cell) and killed at the stated time points. For enteropooling, mice were fasted overnight but allowed to drink water ad libitum before injection with anti-CD3 antibody and sacrificed 3 h after injection. The jejunum was then excised and carefully isolated after ligation at both ends, adherent mesentery was cut off, and jejunum segments were then weighed, their lengths were measured, and weight/length ratios were determined.

Mouse treatment with yeasts. Mice treated with either DSS or TNBS were given 2×10^8 CFU (100 µl of 2×10^9 CFU ml^{-1}) of the corresponding yeast strain by oral gavage for the whole length of the experiment, meaning from day 0 for mice treated with DSS and from the day of presensitization for mice treated with TNBS. Alternatively, to test a preventive schedule in the DSS model, mice were given the same amount starting 3 d before inducing the disease. The same schedule was followed for anti-CD3 antibody-induced enteritis. For studying yeast culture from feces, mice were gavaged once. For mCherry- and ATP-measurement studies, mice were gavaged for 3 d before the study with 2×10^8 CFU of the corresponding yeasts.

Mouse treatment with monoclonal antibodies. When stated, mice were injected intraperitoneally with 100 µg monoclonal antibodies anti-mouse TNF (BE0244, Bio X Cell) or anti-mouse α4β7 (BE0034, Bio X Cell) or the pertinent isotype controls (BE0089, BE0091, Bio X Cell).

Yeast culture from mouse feces. Ctrl, conAP and indAP yeasts expressing the gene conferring resistance to the antibiotic G418 were administered by oral gavage as described above. Feces were collected 6, 24 or 48 h after the gavage, weighed, homogenized in PBS and cultured at 30 °C in YPD agar (Y1500, Sigma-Aldrich) containing 500 µg ml^{-1} G418 (A1720, Sigma-Aldrich). CFU were quantified after 72 h.

ATP measurement in fecal content. To evaluate the amount of ATP in the fecal content, feces from the duodenum, jejunum, ileum, cecum and colon of TNBS-treated mice treated with the corresponding yeast strain were collect 72 h after TNBS induction, 2 h after the last gavage with the yeasts. The fecal content of the corresponding part of the gut was homogenized in PBS, and ATP measurements were performed using the ATP Determination kit (A22066, Molecular Probes) following the manufacturer's instructions. Data were normalized to the weight of the fecal content and to values from the control sample.

Detection of mCherry reporter yeast strains in vivo. To confirm the response of our engineered P2Y2 mutant to ATP in vivo, reporter yeasts expressing mCherry under control of the TM-3 P2Y2 mutant or WT P2Y2 and constitutively expressing GFP were administered as described above to mice with TNBS-induced colitis at the peak of the disease when we expect more ATP to be present in the gut. Content from the specified section of the gut was collected 2 h after the gavage, homogenized in YPD medium (Y1375, Sigma-Aldrich) and cultured overnight. GFP and mCherry expression was measured by flow cytometry in a Fortessa flow cytometer (BD Biosciences), and data analysis was performed using FlowJo 10.7 software.

Microbiome (16S) sequencing and analysis. Fecal samples were collected from control mice and mice with TNBS-induced colitis from each respective yeast treatment at the end of the study. DNA was extracted using the DNeasy PowerLyzer PowerSoil kit (12855, Qiagen) following the manufacturer's instructions. The 16S rRNA gene V4 region was amplified and barcoded by PCR using HotMaster Taq DNA Polymerase and HotMasterMix (10847-708, VWR) and a primer library that contained adaptors for MiSeq sequencing and dual-index barcodes so that PCR products could be pooled. DNA was then quantified using the Quant-iT PicoGreen dsDNA Assay kit (P11496, Thermo Scientific), and 100 ng of each sample was pooled and cleaned up using the QIAquick PCR Purification kit (28104, Qiagen). DNA was requantified after cleanup with the Qubit Fluorometric Quantification kit (Thermo Scientific) and submitted for paired-end 151-bp read sequencing on the Illumina MiSeq instrument at the Harvard Medical School Biopolymers Facility as previously described[72]. Quantitative insights into microbial ecology software 2 (QIIME2) was used for quality filtering and downstream analysis for α- and β-diversity and for compositional analysis following standardized protocols[73]. Dada2 was used to denoise and filter sequences for quality, to join reads and to dereplicate the reads into amplicon sequence variants. Taxonomic assignment was performed using the RDP classifier built into QIIME2, which was trained on the 16S rRNA V4 region database from the EZBioCloud database[74]. Distances between samples (β-diversity) were calculated using the unweighted UniFrac distance metric that evaluates qualitative differences of microbial taxa, taking into account their phylogenetic relationship[75]. Statistical testing for differential clustering of samples on principal-coordinate analysis plots was performed using the PERMANOVA test using 999 permutations. Significant differences in taxa modulated by control or active yeast treatment were determined by linear discriminant analysis effect size[76].

Histological evaluation. Colonic or jejunal tissue was removed and assessed for histological evaluation blindly upon fixation with Bouin's solution (HT10132, Sigma-Aldrich). Paraffin-embedded tissues were sectioned, stained with H&E and examined for evidence of colitis or inflammation with a Zeiss Axioskop2 Plus

microscope with AxioCam HRC and AxioVision software. Colitis histology scores (range, 0–6) were calculated based on the presence of lymphomononuclear cell infiltrate (0, absence of inflammatory foci; 1, mild presence of inflammatory foci in mucosa; 2, presence of multiple inflammatory foci in mucosa and submucosa; 3, evidence of transmural infiltration) and intestinal architecture disruption (0, normal architecture; 1, presence of focal erosions; 2, erosions and focal ulcerations; 3, extended ulceration, granulation of tissue and/or pseudopolyps) as previously described[77]. For evaluation of enteritis, the length of villi and depth of crypts were measured, and the villus length/crypt depth ratio was calculated. For analysis of fibrosis, Masson's trichrome staining was performed. The TUNEL assay was used to identify apoptotic cells in the jejunal tissue. Briefly, jejunal samples previously fixed in Bouin's solution and then embedded in paraffin were deparaffinized and rehydrated by subsequent incubations with xylene, 100% ethanol, 96% ethanol, 70% ethanol and PBS. TUNEL staining was performed following the manufacturer's instructions (11684795910, Sigma-Aldrich). Sections were analyzed in a Leica DMi8 fluorescent microscope, and positive cells were quantified using ImageJ software[78].

Flow cytometry staining and acquisition. For jejunal intraepithelial lymphocyte extraction, tissues were excised, cleaned and cut in 1-cm pieces. Pieces were incubated subsequently in PBS with 1 mM dithiothreitol (646563, Sigma-Aldrich), 2.5 mM EDTA (E177, VWR) and 2.5% FBS; PBS with 5 mM EDTA and 5% FBS; and finally digested in RPMI with 5% FBS, 1 mg ml^{-1} collagenase VIII (C2139, Sigma-Aldrich) and 10 U ml^{-1} DNase (90083, Thermo Fisher Scientific). Samples were then filtered through a 40-µm cell strainer to obtain single-cell suspensions. Cell suspensions were prepared from mesenteric lymph nodes by smashing lymph nodes through a 70-µm cell strainer. Single-cell suspensions were stimulated with 50 ng ml^{-1} phorbol 12-myristate 13-acetate (P1585, Sigma-Aldrich), 1 µM ionomycin (I9657, Sigma-Aldrich), GolgiStop (554724, BD Biosciences, 1:1,500) and GolgiPlug (555029, BD Biosciences, 1:1,500) in RPMI 1640 medium (11875119, Life Technologies) containing 10% FBS (10438026, Gibco) and penicillin–streptomycin (15140122, Gibco, 1:100) for 4 h at 37 °C in a 5% CO_2 incubator. Antibodies for flow cytometry were BUV395 anti-mouse CD45 (BD Biosciences, 564279, 30-Fll, 1:100), APC anti-mouse IFN-γ (BD Biosciences, 554413, XMGl.2, 1:100), PE anti-mouse IL-17a (eBioscience, 12-7177-81, TC11-18H10.1, 1:100), BV421 anti-mouse CD4 (BD Biosciences, 562891, GKl.5, 1:100), BV650 anti-mouse CD3 (BD Biosciences, 740530, 17A2, 1:100), FITC anti-mouse FOXP3 (eBioscience, 11-5773-82, FJK-16s, 1:100) and PE/Dazzle594 anti-mouse IL-10 (BioLegend, 505034, JES5-16E3, 1:100). Cells were then analyzed on a Fortessa flow cytometer (BD Biosciences). CD4$^+$FOXP3$^+$ cells were defined as CD3$^+$CD4$^+$IFN-γ$^-$IL-17$^-$IL-10$^-$FOXP3$^+$; CD4$^+$IFN-γ$^+$ cells were defined as CD3$^+$CD4$^+$IFN-γ$^+$IL-17$^-$IL-10$^-$FOXP3$^-$; CD4$^+$IL-17$^+$ cells were defined as CD3$^+$CD4$^+$IFN-γ$^-$IL-17$^+$IL-10$^-$FOXP3$^-$; CD4$^+$IL-10$^+$ cells were defined as CD3$^+$CD4$^+$IFN-γ$^-$IL-17$^-$IL-10$^-$FOXP3$^-$IL-10$^+$.

Enzyme-linked immunosorbent assay. Jejunal tissue (1 cm) was excised and mechanically disrupted into RIPA buffer (89900, Thermo Scientific) supplemented with Halt protease inhibitor (78441, Thermo Scientific). Supernatants were stored at −80 °C. Levels of the IL-10 cytokine were measured by ELISA (88-7105-88, Invitrogen) following the manufacturer's instructions. Data were normalized to protein content in the supernatants measured by BCA (23235, Thermo Scientific).

RNA extraction and quantitative PCR. Twenty mg of the distal colon or from the medial jejunum was flash frozen and later disrupted in TRIzol (Invitrogen). RNA was extracted following the manufacturer's instructions for the miRNeasy kit (Qiagen). When needed to remove DSS from RNA, we further purified mRNA using the Oligotex kit (Qiagen). cDNA was prepared using the High-Capacity RT kit (Applied Biosystems) and used for qPCR. Results were normalized to expression levels of *Gapdh*. All primers and probes were from Applied Biosystems: *Gapdh*, Mm99999915_gl; *Il17a*, Mm00439618_m1; *Ifng*, Mm00801778_m1; *Foxp3*, Mm00475162_m1; *Ccl2*, Mm00441242_m1; *Nos2*, Mm00440502_m1; *Il1b*, Mm00434228_m1.

Gene-expression analysis by NanoString. Total RNA (100 ng) from colon tissue obtained from mice 21 d after the start of DSS administration was analyzed using nCounter Mouse Immunology Panel expression code sets according to the manufacturer's instructions (NanoString Technologies). Data were analyzed using nSolver Analysis software and plotted with Heatmapper[79]. Functional pathway enrichment analysis was conducted using Enrichr. The combined score was calculated as $c = \ln(P) \times z$, where P is the P value computed using Fisher's exact test and z is the rank score or z score computed using a modification to Fisher's exact test in which a z score for deviation from an expected rank is computed[80].

Gene-expression analysis by RNA sequencing. Total RNA (5 ng) from colon tissue was sent for SMART-seq by the Broad Technology Labs and the Broad Genomics Platform. Processed RNA-seq data were filtered, removing genes with low read counts. Read counts were normalized using TMM normalization, and counts per million were calculated to create a matrix of normalized expression values. The fastq files of each RNA-seq data sample were aligned to the *Mus musculus* GRCm38 transcriptome using Kallisto (version 0.46.1), and the same software was used to quantify alignment results. Differential expression analysis was conducted using DESeq2, and $\log_2$ fold change values were adjusted using apeglm for downstream analysis. The Benjamini–Hochberg method was used for multiple-hypothesis-testing correction. The GSEA analysis was performed using apeglm-adjusted differential expression analysis results. Genes that were differentially expressed with adjusted P values < 0.05 were analyzed with the Ingenuity Pathway Analysis tool to determine significantly regulated pathways.

Reporting Summary. Further information on research design is available in the Nature Research Reporting Summary linked to this article.

Data availability

RNA-seq data were deposited in the GEO database under the accession number GSE152869. Sequencing data from microbiota 16S rRNA were submitted to the NCBI short-read archive under BioProject number PRJNA641709. Source data are provided with this paper.

References

61. Bashor, C. J., Helman, N. C., Yan, S. & Lim, W. A. Using engineered scaffold interactions to reshape MAP kinase pathway signaling dynamics. *Science* **319**, 1539–1543 (2008).
62. Scott, B. M. et al. Coupling of human rhodopsin to a yeast signaling pathway enables characterization of mutations associated with retinal disease. *Genetics* **211**, 597–615 (2019).
63. Rafehi, M. et al. Molecular recognition of agonists and antagonists by the nucleotide-activated G protein-coupled P2Y2 receptor. *J. Med. Chem.* **60**, 8425–8440 (2017).
64. Wiederstein, M. & Sippl, M. J. ProSA-web: interactive web service for the recognition of errors in three-dimensional structures of proteins. *Nucleic Acids Res.* **35**, W407–W410 (2007).
65. Lovell, S. C. et al. Structure validation by Cα geometry: ϕ,ψ and Cβ deviation. *Proteins* **50**, 437–450 (2003).
66. Lee, G. R. & Seok, C. Galaxy7TM: flexible GPCR–ligand docking by structure refinement. *Nucleic Acids Res.* **44**, W502–W506 (2016).
67. Ballesteros, J. A. & Weinstein, H. Integrated methods for the construction of three-dimensional models and computational probing of structure–function relations in G protein-coupled receptors. In *Methods in Neurosciences* **25** (ed. Stuart, C. S.), 366–428 (Academic Press, 1995).
68. Ryan, O. W. et al. Selection of chromosomal DNA libraries using a multiplex CRISPR system. *eLife* **3**, e03703 (2014).
69. Prykhozhij, S. V., Rajan, V., Gaston, D. & Berman, J. N. CRISPR multitargeter: a web tool to find common and unique CRISPR single guide RNA targets in a set of similar sequences. *PLoS ONE* **10**, e0119372 (2015).
70. Pliatsika, V. & Rigoutsos, I. 'Off-Spotter': very fast and exhaustive enumeration of genomic lookalikes for designing CRISPR/Cas guide RNAs. *Biol. Direct* **10**, 4 (2015).
71. Knowles, A. F. The GDA1_CD39 superfamily: NTPDases with diverse functions. *Purinergic Signal.* **7**, 21–45 (2011).
72. Cox, L. M. et al. Calorie restriction slows age-related microbiota changes in an Alzheimer's disease model in female mice. *Sci. Rep.* **9**, 17904 (2019).
73. Caporaso, J. G. et al. QIIME allows analysis of high-throughput community sequencing data. *Nat. Methods* **7**, 335–336 (2010).
74. Yoon, S. H. et al. Introducing EzBioCloud: a taxonomically united database of 16S rRNA gene sequences and whole-genome assemblies. *Int. J. Syst. Evol. Microbiol.* **67**, 1613–1617 (2017).
75. Lozupone, C., Lladser, M. E., Knights, D., Stombaugh, J. & Knight, R. UniFrac: an effective distance metric for microbial community comparison. *ISME J.* **5**, 169–172 (2011).
76. Segata, N. et al. Metagenomic biomarker discovery and explanation. *Genome Biol.* **12**, R60 (2011).
77. Erben, U. et al. A guide to histomorphological evaluation of intestinal inflammation in mouse models. *Int. J. Clin. Exp. Pathol.* **7**, 4557–4576 (2014).
78. Schneider, C. A., Rasband, W. S. & Eliceiri, K. W. NIH Image to ImageJ: 25 years of image analysis. *Nat. Methods* **9**, 671–675 (2012).
79. Babicki, S. et al. Heatmapper: web-enabled heat mapping for all. *Nucleic Acids Res.* **44**, W147–W153 (2016).
80. Kuleshov, M. V. et al. Enrichr: a comprehensive gene set enrichment analysis web server 2016 update. *Nucleic Acids Res.* **44**, W90–W97 (2016).

Acknowledgements

This work was supported by grants NS102807, ES02530, ES029136 and AI126880 from the NIH; RG4111A1 from the National MS Society; PA-1604-08459 from the International Progressive MS Alliance; and NSERC 492911 from the Natural Sciences Engineering Research Council of Canada. B.M.S. was supported by an Ontario Graduate Scholarship and by the Professional Research Experience Program agreement between the National Institute of Standards and Technology (NIST) and the University of Maryland. C.G.-V. was supported by an Alfonso Martín Escudero Foundation

postdoctoral fellowship and by postdoctoral fellowship ALTF 610-2017 from the European Molecular Biology Organization. J.P. was supported by grant 2019/04780-7 from the São Paulo Research Foundation (FAPESP). This paper is dedicated to the memory of Dan S. Tawfik. We thank Z. Kelman and J. Marino of the University of Maryland Institute for Bioscience and Biotechnology Research for use of their incubators and W. Shaw of Imperial College London for providing yeast codon-optimized sfGFP. We thank the Harvard Medical School Rodent Histopathology Core, which provided histopathology service. We thank the NeuroTechnology Studio at Brigham and Women's Hospital for providing access to the Leica DMi8 fluorescent microscope and consultation on data acquisition and data analysis. B.M.S. is an International Associate of the NIST. The NIST notes that certain commercial equipment, instruments and materials are identified in this paper to describe an experimental procedure as completely as possible. In no case does this identification imply a recommendation or endorsement by the NIST, nor does it imply that the materials, instruments or equipment are necessarily the best available for the purpose. The opinions expressed in this article are the authors' own and do not necessarily represent the views of the NIST.

Author contributions

B.M.S., C.G.-V., L.M.S., J.A.d.S.P., A.P., P.H., M.O'.B. and S.K.C. performed in vitro and in vivo experiments; Z.L., L.M.C. and C.G.-V. performed bioinformatic analysis; P.M.M.-V. discussed and interpreted findings; B.M.S., C.G.-V. and F.J.Q. wrote the manuscript with input from co-authors; and B.S.W.C., S.G.P. and F.J.Q. contributed equally to the design and supervision of the study and editing the manuscript.

Competing interests

B.M.S., C.G.-V., B.S.W.C., S.G.P. and F.J.Q. filed a patent for the use of engineered yeast to treat inflammation. All other authors declare no competing interests.

Additional information

Extended data is available for this paper at https://doi.org/10.1038/s41591-021-01390-x.

Supplementary information The online version contains supplementary material available at https://doi.org/10.1038/s41591-021-01390-x.

Correspondence and requests for materials should be addressed to F.J.Q.

Peer review information *Nature Medicine* thanks Cathryn Nagler and the other, anonymous, reviewer(s) for their contribution to the peer review of this work. Saheli Sadanand was the primary editor on this article and managed its editorial process and peer review in collaboration with the rest of the editorial team.

Reprints and permissions information is available at www.nature.com/reprints.

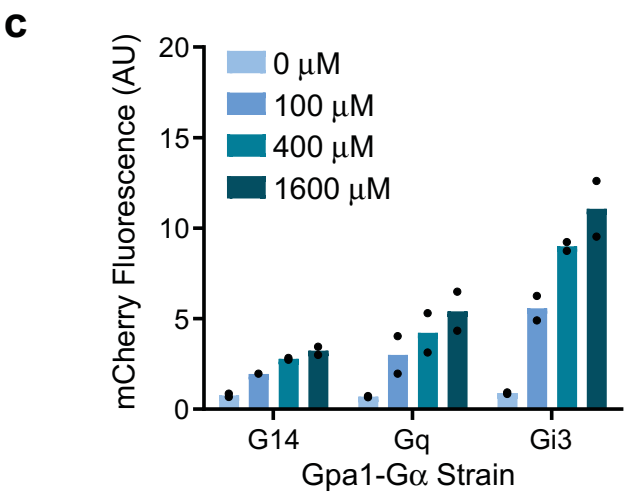

Extended Data Fig. 1 | Response to eATP over time of engineered mating pathway. a,b, Yeasts from the BS016 strain transformed with plasmid pRS316 pTDH3 P2Y2 (WT human P2Y2 receptor) were incubated with 100 µM ATP in 300 µL **(a)** or 5 mL SC-URA media **(b);** and mCherry fluorescence was quantified. Data points represent the mean of 2 colonies. **c,** Engineered mating pathway response to UTP using the wild-type (WT) human P2Y2 receptor and various yeast strains with integrated Gpa1-Gα chimeras as follows: BS019 (G14), BS020 (Gq), BS016 (Gi3). Following incubation for 6h with the indicated UTP concentration, the activation of the mating pathway was monitored by quantifying mCherry fluorescence by flow cytometry. Data points represent the mean of 2 colonies.

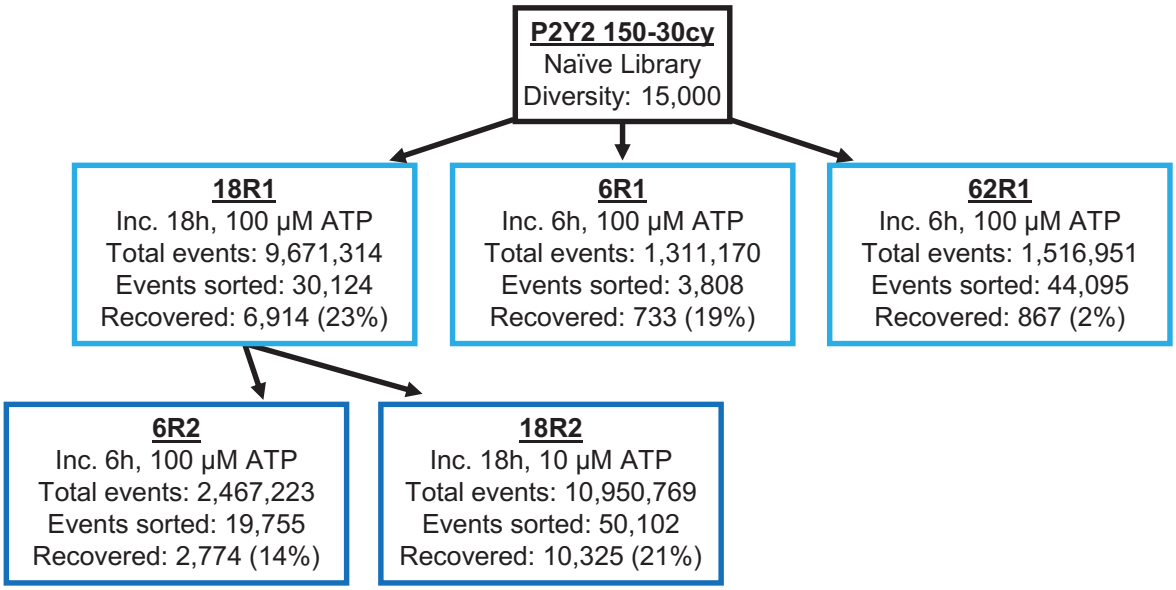

Extended Data Fig. 2 | Strategy for directed evolution of human P2Y2 receptor. During each FACS sort the top ~1% of mCherry fluorescence was collected. 'Recovered' refers to the number of yeast colonies obtained after plating sorted cells on selective media.

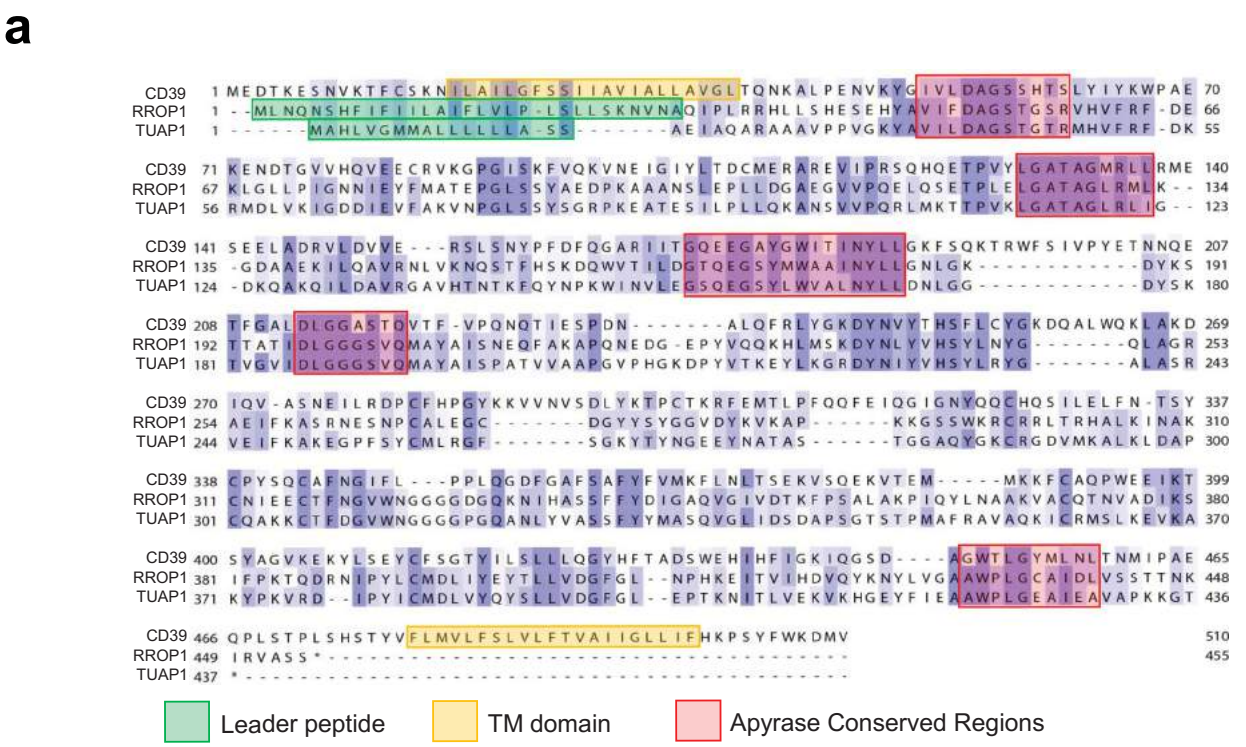

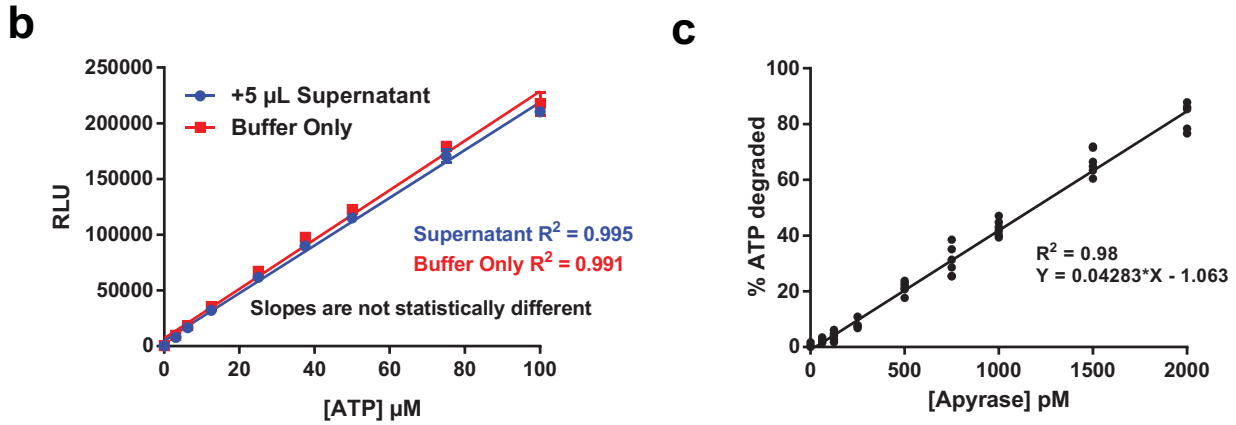

Extended Data Fig. 3 | Apyrase Genes and ATP concentration in yeast supernatants. a, Sequence Alignment of Apyrase Genes. Human ENTPD1 (CD39), potato apyrase (RROP1) and wheat apyrase (TUAP1) were aligned using MUSCLE, in the MEGA6 alignment explorer. **b,** Measurement of a known ATP concentration in the presence of 5 µL yeast supernatant from strain CB008 (blue) or reaction buffer only (red). Yeast supernatant did not affect the measurement readout. n = 3 samples, error bars represent SD. **c,** To estimate the amount of active apyrase secreted by yeast, 50 µM ATP was incubated with the indicated concentration of commercial apyrase for 30 minutes at 30oC, with 5 µL supernatant from a culture of strain Ctrl, in a 50 µL reaction volume and residual ATP was quantified. No apyrase activity was observed when 31.3 pM commercial apyrase was added. n = 6 samples.

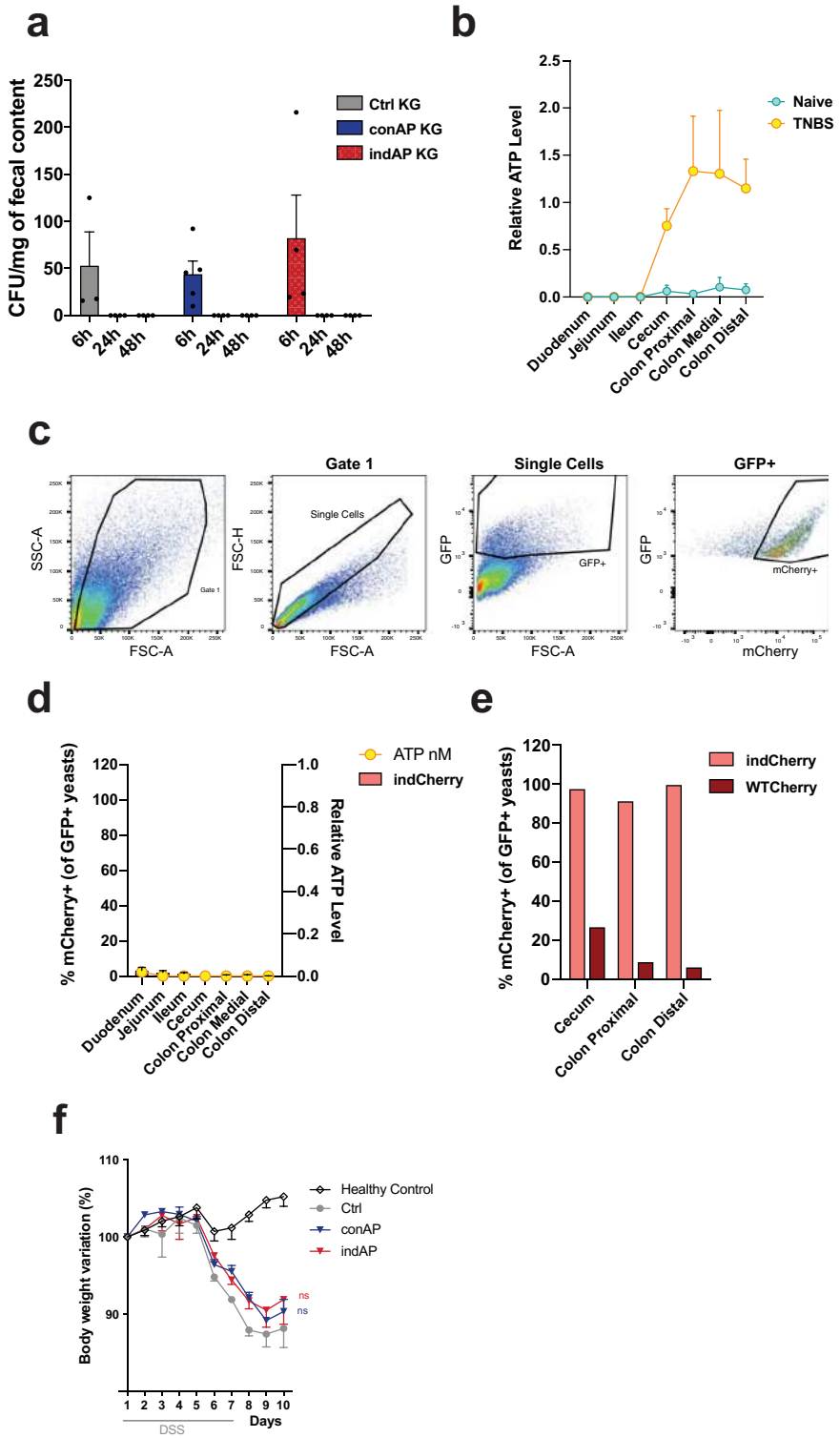

Extended Data Fig. 4 | Engineered yeasts probiotics are viable in the mouse gut. a, Colony forming units per mg of stool collected 6, 24 and 48h after oral gavage to the mice with either Ctrl KG, conAP KG or indAP KG yeast strains. n = 3 Ctrl, n = 5 conAP and n = 4 indAP samples per group. **b,** ATP relative levels in the specified portions of the gut of naïve and TNBS induced mice. n = 4 naïve, n = 6 TNBS mice per group. **c,** Gating strategy to measure mCherry positive yeasts in the fecal content. **d,** mCherry positive yeasts (% of total GFP yeast) measured by flow cytometry in the fecal content of the specified portion of the gut after 2h from oral gavage to naïve mice with ATP inducible strain indCherry KG. ATP levels were measured in the same portions of the gut. n = 3 samples for cytometry and n = 8 for eATP levels. **e,** mCherry positive yeasts (% of total GFP yeast) quantified by flow cytometry in the fecal content of the specified portion of the gut from TNBS treated mice 2 hours after oral gavage with indCherry KG or WTCherry KG yeast strains. **f,** Changes in body weight during the course of DSS-induced colitis in mice treated with engineered yeasts starting 3 days before DSS administration. n = 4 mice Healthy control and n = 3 otherwise. Two-way ANOVA followed by Tukey's post-hoc test, ns = not significant.

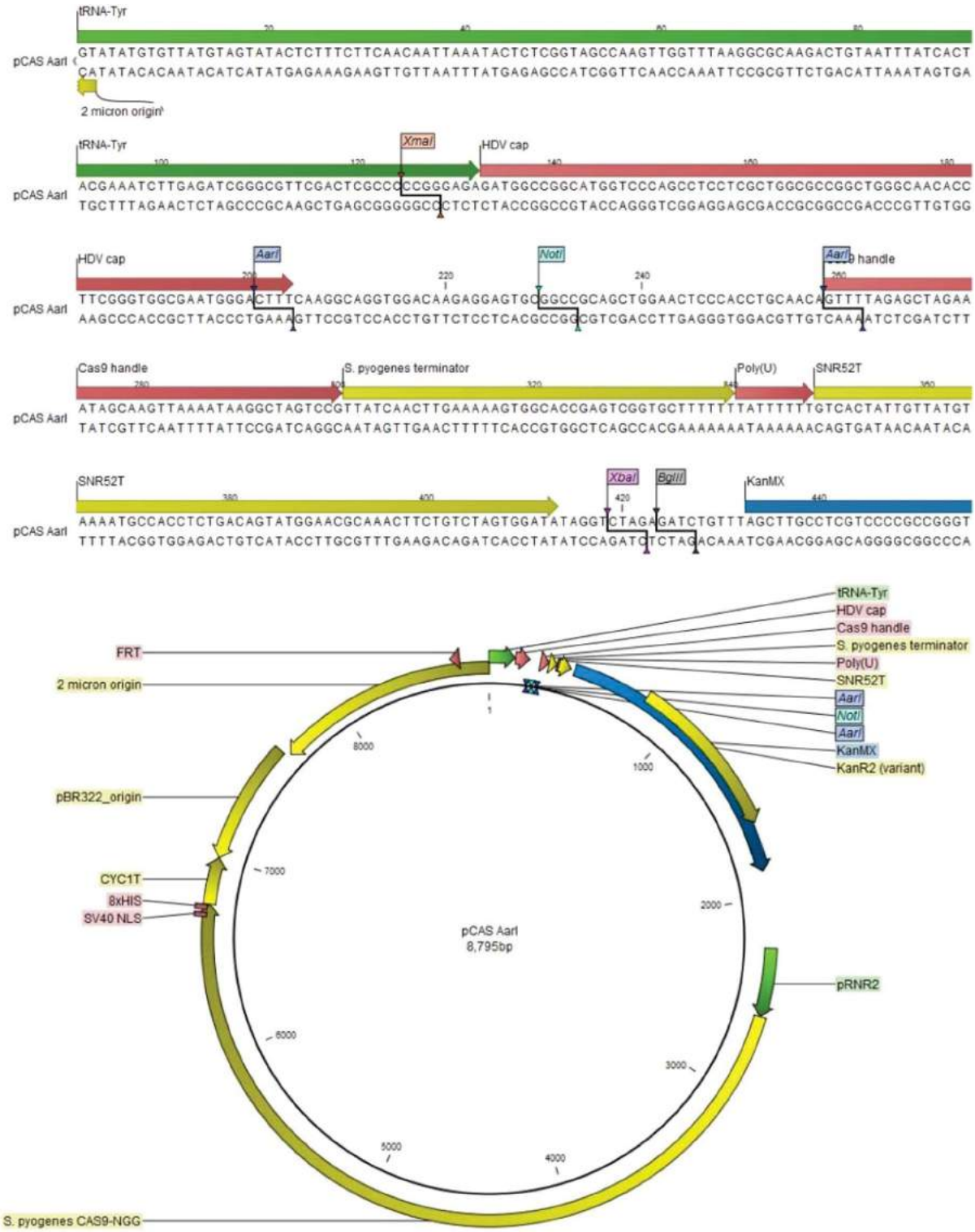

Extended Data Fig. 5 | Integration of P2Y2 mutants with CRISPR STAR Method. Plasmid pCAS AarI. Custom multiple cloning site inserted at the XmaI and BglII sites in the pCAS plasmid, obtained from AddGene[68]. Image generated with CLC Sequence Viewer.

nature research

Corresponding author(s): Francisco J. Quintana

Last updated by author(s): May 5,2021

Reporting Summary

Nature Research wishes to improve the reproducibility of the work that we publish. This form provides structure for consistency and transparency in reporting. For further information on Nature Research policies, see Authors & Referees and the Editorial Policy Checklist.

Statistics

For all statistical analyses, confirm that the following items are present in the figure legend, table legend, main text, or Methods section.

n/a	Confirmed	
☐	☒	The exact sample size (*n*) for each experimental group/condition, given as a discrete number and unit of measurement
☐	☒	A statement on whether measurements were taken from distinct samples or whether the same sample was measured repeatedly
☐	☒	The statistical test(s) used AND whether they are one- or two-sided *Only common tests should be described solely by name; describe more complex techniques in the Methods section.*
☐	☒	A description of all covariates tested
☐	☒	A description of any assumptions or corrections, such as tests of normality and adjustment for multiple comparisons
☐	☒	A full description of the statistical parameters including central tendency (e.g. means) or other basic estimates (e.g. regression coefficient) AND variation (e.g. standard deviation) or associated estimates of uncertainty (e.g. confidence intervals)
☐	☒	For null hypothesis testing, the test statistic (e.g. *F*, *t*, *r*) with confidence intervals, effect sizes, degrees of freedom and *P* value noted *Give P values as exact values whenever suitable.*
☒	☐	For Bayesian analysis, information on the choice of priors and Markov chain Monte Carlo settings
☒	☐	For hierarchical and complex designs, identification of the appropriate level for tests and full reporting of outcomes
☒	☐	Estimates of effect sizes (e.g. Cohen's *d*, Pearson's *r*), indicating how they were calculated

Our web collection on statistics for biologists contains articles on many of the points above.

Software and code

Policy information about availability of computer code

Data collection	BD FACSDIVA (v.8.0.1); MACSQuantify (v2.11); BD FACS (v1.2.0.142); Li-Cor Image Studio (v5.0); Leica LAS X (v3.1.5.16308); MODELLER (v9.18); Ascent Software (v2.6); AxioVision v4.8.2.0; Promega Glomax Explorer v3.1.0
Data analysis	FlowJo v10.7; nSolver v4.0; QUIME2; Prism v8.4.3; FIJI-ImageJ v2.0; R (v3.4.0); ggplot2 (v3.1.0); FASTQC (v0.11.5);Kallisto (v0.46.1); DESeq2 (1.20.0); STAR v2.7.3; RSEM (v1.3);

For manuscripts utilizing custom algorithms or software that are central to the research but not yet described in published literature, software must be made available to editors/reviewers. We strongly encourage code deposition in a community repository (e.g. GitHub). See the Nature Research guidelines for submitting code & software for further information.

Data

Policy information about availability of data

All manuscripts must include a data availability statement. This statement should provide the following information, where applicable:

- Accession codes, unique identifiers, or web links for publicly available datasets
- A list of figures that have associated raw data
- A description of any restrictions on data availability

Raw data are presented in Source Data files for all Figures and Extended Data Figures 1, 3 and 4. RNA-seq sequencing data have been deposited in GEO under the accession code GSE152869. Sequencing data from the microbiota 16S rRNA is submitted in the NCBI short-read archive under Bioproject number PRJNA641709. Readers are welcome to comment on the online version of the paper. Correspondence and request for materials should be addressed to F.J.Q.

Field-specific reporting

Please select the one below that is the best fit for your research. If you are not sure, read the appropriate sections before making your selection.

☒ Life sciences ☐ Behavioural & social sciences ☐ Ecological, evolutionary & environmental sciences

For a reference copy of the document with all sections, see nature.com/documents/nr-reporting-summary-flat.pdf

Life sciences study design

All studies must disclose on these points even when the disclosure is negative.

Sample size	No statistical methods were used to predetermine sample sizes. Sample sizes are similar to those used in the field, as previously reported: Sanmarco et al. Nature 2021, Wheeler et al. Nature 2020, Rothhammer et al Nature 2018, Rothhammer etl al Nature Medicine 2016, Mayo et al. Nature Medicine 2014
Data exclusions	Data were only formally excluded by formal outlier tests in Prism.
Replication	To ensure replication, all deep sequencing data were repeated in 3-6 mice per group For in vitro and in vivo experiments, experiments were repeated multiple times, at least twice independently as stated in figure legends. All attempts at replication were successful.
Randomization	Samples and mice were randomly allocated into treatment groups.
Blinding	Experimenters were blinded to treatment during colitis disease. Similarly, during data processing of all sequencing data, experimenters were blinded to condition. Otherwise, blinding was not performed, such as during in vitro experiments, where experimenters were required to know the conditions of each well.

Reporting for specific materials, systems and methods

We require information from authors about some types of materials, experimental systems and methods used in many studies. Here, indicate whether each material, system or method listed is relevant to your study. If you are not sure if a list item applies to your research, read the appropriate section before selecting a response.

Materials & experimental systems

n/a	Involved in the study
☐	☒ Antibodies
☒	☐ Eukaryotic cell lines
☒	☐ Palaeontology
☐	☒ Animals and other organisms
☒	☐ Human research participants
☒	☐ Clinical data

Methods

n/a	Involved in the study
☒	☐ ChIP-seq
☐	☒ Flow cytometry
☒	☐ MRI-based neuroimaging

Antibodies

Antibodies used	BUV395 anti-mouse CD45 (BD Biosciences, #564279, 30-Fll, 1:100); APC anti-mouse IFNg (BD Biosciences, #554413, XMGl.2, 1:100); PE anti-mouse IL-17a (eBioscience, #12-7177-81, TC11-18H10.1, 1:100); BV421 anti-mouse CD4 (BD Biosciences, #562891, GKl.5, 1:100); BV650 anti-mouse CD3 (BD Biosciences #740530, 17A2, 1:100); FITC anti-mouse Foxp3 (eBioscience, #11-5773-82, FJK-16s, 1:100); PE/Dazzle594 anti-mouse IL-10 (Biolegend, #505034, JES5-16E3, 1:100); rabbit anti-HA tag (Cell Signaling Technology, #C29F4, 1:1000); mouse anti-PGK (Invitrogen, #459250, 1:5000); IRDye® 680LT Goat anti-Mouse lgG (LI-COR Biosciences, 926-68020, 1:5000); IRDye® 800CW Goat anti-Rabbit lgG (LICOR Biosciences, 926-32211, 1:5000); anti-mouse CD3ε monoclonal Ab (#BP0001-1 Bio X Cell, 10 mg/kg); Armenian Hamster anti-mouse TNF (#BE0244 Bio X Cell, 5mg/kg); Armenian Hamster IgG # BE0091 Bio X Cell,5mg/kg); Rat anti-mouse LPAM-1 or integrin apha4beta7 (#BE0034 Bio X Cell, 5mg/kg); Rat IgG2a (#BE0089 Bio X Cell, 5mg/kg). All additional information is readily available on the manufacturer's web site for each antibody
Validation	All antibodies were commercial in origin and validated by the company. Specifically, Flow cytometry antibodies from BD Bioscience, eBioscience/Invitrogen (https://www.thermofisher.com/us/en/home/life-science/antibodies/invitrogen-antibody-validation.html) and Biolegend (https://www.biolegend.com/nl-nl/reproducibility) and western blot antibodies from Invitrogen and LI-COR were purified from cell line supernatant using affinity chromatography followed by validation using proper negative and positive controls in functional assays as well as for their mouse reactivity. Western Blot antibody #C29F4 from Cell Signaling Technology (https://www.cellsignal.com/about-us/cst-antibody-validation-principles) were purified from serum from animals immunized with a synthetic peptide containing the HA epitope using affinity chromatography followed by validation using proper negative and positive controls in functional assays. Antibodies used in vivo from BioXCell (https://bxcell.com/the-bio-x-cell-advantage/) were also originated in cell line cultures and each lot validated with a library of recombinant proteins and bioassay to ensure they binds strongly and specifically to their target antigen. Additional information for each specific antibody listed above can be found by entering the antibody product number listed above on the company's web site.

Animals and other organisms

Policy information about studies involving animals; ARRIVE guidelines recommended for reporting animal research

Laboratory animals	WT C57BL/6J (The Jackson Laboratory, #000664). Male and female mice were used. Experiments were initiated in 8-12 week old mice.
Wild animals	The study did not involve wild animals.
Field-collected samples	The study did not involve samples collected from the field.

Ethics oversight	Brigham and Women's Hospital Institutional Animal Care and Use Committee (IACUC) (https://animal.bwh.harvard.edu).

Note that full information on the approval of the study protocol must also be provided in the manuscript.

Flow Cytometry

Plots

Confirm that:

☒ The axis labels state the marker and fluorochrome used (e.g. CD4-FITC).

☒ The axis scales are clearly visible. Include numbers along axes only for bottom left plot of group (a 'group' is an analysis of identical markers).

☒ All plots are contour plots with outliers or pseudocolor plots.

☒ A numerical value for number of cells or percentage (with statistics) is provided.

Methodology

Sample preparation	For dose-response measurements, yeast cells were incubated overnight, then diluted to OD600 0.05 in 600 µL SC-URA media (BioShop Canada, DOM007 with YNB406) containing ATP (0-25.6 mM pH 7.0; Bio Basic, AB0020) or UTP (0-3.2 mM pH 7.0; Sigma-Aldrich, U6625) and incubated for 6 hours at 30°C with shaking (225 rpm). Cells were then treated with cycloheximide (BioShop Canada, CYC003) to a final concentration of 10 µg/mL. The mCherry signal of at least 10,000 cells was measured for each sample with a MACSQuant VYB (Miltenyi Biotec). For cell sorting experiments, yeast cells were incubated overnight, then diluted to OD600 0.05 in 600 µL SC-URA media (BioShop Canada, DOM007 with YNB406) containing ATP (0-25.6 mM pH 7.0; Bio Basic, AB0020), and incubated for either 18 or 6 hours at 30°C with shaking (225 rpm). Cells were then treated with cycloheximide (BioShop Canada, CYC003) to a final concentration of 10 µg/mL. After brief sonication (two pulses, minimum amplitude), cells were filtered into a sterile tube (35 µm filter, Falcon, 352235). One million to ten million cells were then sorted for the highest ~1% of mCherry signal using a BD Influx cell sorter (BD Biosciences). For Cell suspensions preparation from mesenteric lymph nodes: Animals were euthanized and mesenteric lymph nodes extracted after surgical excision in the abdomen. Tissue was mechanically dissociated and filtered through at 70 µm cell strainer (Fisher Scientific, #22363548) into a fresh 50 mL conical. Cell suspension was centrifuged at 300g for 5 minutes and stimulated with 50 ng/mL phorbol 12-myristate 13-acetate (PMA, #P1585, Sigma-Aldrich), 1 µM ionomycin (#I9657, Sigma-Aldrich), GolgiSTOP and (#554724, BD Biosciences, 1:1500) GolgiPLUG (#555029, BD Biosciences, 1:1500) in RPMI 1640 medium (#11875119, Life Technologies) containing 10% FBS (#10438026, GIBCO), penicillin/streptomycin (#15140122, GIBCO, 1:100) for 4 h at 37°C in a 5% CO2 incubator. Following stimulation, T cells were stained with antibodies against surface markers, and thereafter fixed and stained with antibody against intracellular target protein with an intracellular antibody labeling kit following its instructions (#00-5523, eBioscience). Antibodies for flow cytometry were purchased from eBioscience, Biolegend or BD Biosciences and used at a concentration of 1:100. Cells were then analyzed on a Fortessa flow cytometer (BD Biosciences). Treg cells were defined as CD3+CD4+IFN-γ−IL-17−IL-10−FOXP3+. For mCherry/GFP detection in the fecal contents: Content from the specified section of the gut was collected 2 hours after the gavage, homogenized in YPD media (#Y1375, Sigma-Aldrich) and cultured overnight. GFP and mCherry expression was measured by flow cytometry in a Fortessa flow cytometer (BD Biosciences)
Instrument	Fortessa Flow Cytometer (BD Bioscience); MACSQuant VYB (Miltenyi Biotec); BD Influx cell sorter (BD Bioscience)
Software	BD FACSDIVA; MACSQuantify; BD FACS
Cell population abundance	Abundance is reported in figures and methods where relevant.
Gating strategy	Gating strategies are specified within the text or figure legend for relevant flow cytometry experiments. For dose-response assays, yeast were gated from background events by side scatter vs forward scatter (SSC vs FSC) For cell sorting of yeast, yeast were gated from background events by side scatter vs forward scatter (SSC vs FSC), singlets were then gated from doublets by trigger pulse width vs SSC, and the top ~1% of mCherry expressing cells were then sorted based on FSC vs mCherry signal.

☒ Tick this box to confirm that a figure exemplifying the gating strategy is provided in the Supplementary Information.